Intramuscular gene transfer of Apolipoprotein E (ApoE) to reverse hyperlipidaemia and atherosclerosis in ApoE-deficient mice

By Vanessa Evans

A thesis submitted in partial fulfilment of the requirements for the Degree of Doctor of Philosophy

Royal Free and University College Medical School,
Department of Medicine, University College London

2007

ProQuest LLC
789 East Eisenhower Parkway
P.O. Box 1346
Ann Arbor, MI 48106-1346

ABSTRACT

Intramuscular gene transfer of Apolipoprotein E (ApoE) to reverse hyperlipidaemia and atherosclerosis in ApoE-deficient mice

Plasma ApoE has multiple atheroprotective actions, including clearance of cholesterol-rich remnant lipoproteins, and is an attractive gene therapy candidate to treat atherosclerosis. Here, I focus on the single intramuscular injection of an ApoE-expressing vector, non-viral DNA (plasmid) or adeno-associated virus (AAV), as a safe and effective treatment to alleviate hypercholesterolaemia and atherosclerosis in ApoE-deficient ($ApoE^{-/-}$) mice. Firstly, I constructed expression plasmids harbouring human ApoE3 cDNA, driven by two muscle-specific (CK6 and C512) and one ubiquitous (CAG) promoter. The CAG-driven plasmid was injected into tibialis anterior muscles, pre-treated with hyaluronidase, of young $ApoE^{-/-}$ mice and, provided the injection site was electropulsed, gave strong local expression of ApoE3 protein at 1 week (13.38±7.46μg ApoE3 per muscle). This amount was much greater than the CK6- and C512-driven plasmids (0.61±0.38 and 0.45±0.38μg, respectively), but in all mice plasma ApoE3 levels were below the detection limit (<15ng/ml) and did not ameliorate the hyperlipidaemia. Next, I generated both single-stranded (ss) and self-complementary (sc) AAV2/7 vectors. At 1, 2 and 4 weeks, ApoE was readily measured in the plasma of $ApoE^{-/-}$ mice injected with the ssAAV2/7.CAG vector, reaching levels of 1.4μg/ml, whereas plasma ApoE was again undetected after administration of the CAG-driven plasmid . By contrast, both ssAAV2/7 and scAAV2/7 vectors driven by the muscle-specific promoters performed poorly and ApoE could not be detected in plasma. Therefore, for my final experiment I pseudotyped the ssAAV2.CAG.ApoE3 vector with the robust serotypes 8 and 9, and directly compared their efficiency with ssAAV2/7.CAG.ApoE3 in $ApoE^{-/-}$ mice. After 1 week plasma ApoE had reached 2μg/ml in ssAAV2/7 and ssAAV2/8-treated animals, and persisted at 1-2μg/ml throughout the 13 week study, whereas the ssAAV2/9 vector was less effective and gave only 0.5μg ApoE/ml. Disappointingly, however, these concentrations of plasma ApoE were still insufficient to have hypolipidaemic effects or to inhibit plaque development in the brachiocephalic artery. In conclusion, although electropulsation enhanced plasmid-mediated transgene expression from skeletal muscle, rAAV was a more efficient gene transfer vector and modest additional optimisation should provide therapeutic levels of ApoE3 in plasma.

Declaration

I, Vanessa Evans, confirm that the work presented in this thesis is my own and where information has been derived from other sources, I confirm that this has been indicated in the thesis. No portion of the work referred to in this thesis has been submitted in support of an application for another degree or qualification of this or any other university or institute of learning.

Vanessa C Evans

Acknowledgements

I would firstly like to thank the British Heart Foundation for supporting this PhD project over the last three years. The task of undertaking this PhD has been made easier due to the considerable help received in the process. I have benefited enormously from the help of my supervisor Professor Jim Owen, whom has provided vast scientific knowledge, direction and inspiration throughout. My secondary supervisor, Dr Paul Simons, has also given valuable scientific advice and guidance during my studies.

I am greatly indebted for the help received from Helen Foster, Keith Foster, Ian Graham and Takis Athanasopoulos, from the Royal Holloway University, whom performed the animal work and provided excellent technical expertise and knowledge in viral gene therapy. I would also like to thank Dr Christopher Jackson and Deb Watkins, from the Bristol University for helping with the specialised analysis of brachiocephalic artery tissue. Dr Amit Nathwani and Jenny McIntosh, from the Haematology department at UCL provided the scAAV plasmids and gave valuable guidance for the development of rAAV vectors. I would also like to thank the other members of my group, Petra Disterer, Eyman Osman and Ioannis Papaioannou for their technical expertise and scientific advice.

Finally, for forgiving my weekends at work, for his support and providing endless cups of tea while writing this thesis, I would like to thank my lovely husband John.

Vanessa Evans, June 2007

ABBREVIATIONS

AAV	Adeno-associated virus
ABCA1	ATP-binding cassette transporter A1
APCs	Antigen presenting cells
ApoAI	Apolipoproteins AI
ApoB100	Apolipoprotein B100
ApoE $^{-/-}$	ApoE knockout
ApoE	Apolipoprotein E
ApoER2	ApoE receptor 2
BSA	Bovine serum albumin
CAG	CMV enhancer/chicken β-actin
cAMP	Cyclic AMP
CETP	Cholesteryl ester transfer protein
CHD	Coronary heart disease
CIP	Calf intestinal alkaline phosphatase
CMV	Cytomegalovirus
CVD	Cardiovascular disease
DMEM	Dulbecco's modified Eagle's medium
DMSO	Dimethylsulphoxide
EF-1α	Cellular elongation factor 1α
ELISA	Enzyme-linked immunosorbent assay
EPO	Erythropoietin
FBS	Fetal bovine serum
FCH	Familial combined hyperlipidaemia
FDB	Familial defective ApoB100
FGFR1	Fibroblast growth factor receptor 1
FH	Familial hypercholesterolaemia
HD-Ads	Helper-dependent adenoviruses
HDL	High-density lipoprotein
HDL-C	HDL-cholesterol
HEK	Human Embryonic Kidney
HIV	Human immunodeficiency virus
HL	Hepatic lipase
HLP	Hyperlipoproteinaemia
HRP	Horse radish peroxidase
HSCs	Hematopoietic stem cells
HSPG	Heparin-sulphate proteoglycans
HSV-1	Herpes simplex-1 virus
HUVECs	Human umbilical vein endothelial cells
ICAM-1	Intracellular adhesion molecule-1
IDL	Intermediate density lipoproteins
IFN-γ	Interferon-gamma
IL-10	Interleukin-10
IL-12	Interleukin-12
IL-1Ra	Interleukin-1 receptor antagonist
im	Intramuscular
ITR	Inverted terminal repeat
Lam-R	Laminin receptor
LB	Luria Bertani
LCAT	Lecithin-cholesterol acyltransferase

LDL	Low density lipoprotein
LDL-R	Low density lipoprotein receptor
$LDLR^{-/-}$	LDL receptor deficient
Lp(a)	Lipoprotein(a)
LPL	Lipoprotein lipase
LRP	Low density lipoprotein receptor related protein
LSP	Liver-specific promoter
MCK	Muscle creatine kinase
MCP-1	Monocyte chemotactic protein-1
M-CSF	Macrophage colony-stimulating factor
ME	Multi-enhancer
MLV	Murine leukaemia virus
mmLDL	Minimally oxidised LDL
MMPs	Matrix metalloproteinases
OD	Optical density
OVA	Ovalbumin
Ox-LDL	Oxidised low density lipoprotein
PBS	Phosphate-buffered saline
PDGF	Platelet-derived growth factor
Q-PCR	Quantitative PCR
rAAV	Recombinant AAV
rAd	Recombinant adenoviruses
RBE	Rep binding element
RCT	Reverse cholesterol transport
RV	Retroviral
SCIDX1	X-linked severe combined immunodeficiency
SMC	Smooth muscle cells
SR-BI	Scavenger receptor B1
SV40	Simian virus 40
TA	Tibialis anterior
TBE	Tris-borate EDTA
TGF-β	Transforming growth factor β
TIMP	Tissue inhibitor of metalloproteinase
TMB	Tetra-methylbenzidine
TNF-α	Tumour necrosis factor-α
TRL	Triglyceride-rich lipoprotein
TRS	Terminal resolution site
UV	Ultraviolet
VCAM-1	Vascular cell adhesion molecule-1
VLDL	Very low density lipoproteins
WHHL	Watanabe heritable hyperlipidaemic
wtAAV	Wild type AAV

LIST OF CONTENTS

LIST OF FIGURES

LIST OF TABLES

Chapter 1:

General Introduction

1 GENERAL INTRODUCTION

1.1 Epidemiology of cardiovascular disease

The prevalence of cardiovascular disease (CVD) is increasing in developing countries and Eastern Europe and the incidence of obesity and diabetes is rising in the Western world; CVD has, therefore, been predicted to be the leading cause of death globally within the next 15 years [1]. In the UK, CVD accounted for around 216,000 deaths in 2004, half of which were caused by coronary heart disease (CHD) and a quarter from stroke, making it the main cause of mortality. Although death rates from CHD and stroke have been falling since the late 1970s, the decline has not been as fast as that in other Western countries and the UK has, thus, one of the highest CVD death rates among developed countries (Coronary Heart Disease statistics, BHF, 2006).

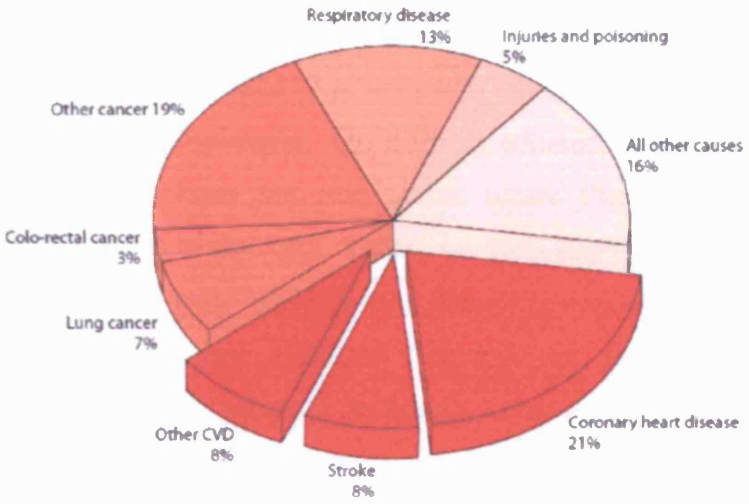

Figure 1-1. Causes of death in men in 2004 (Coronary Heart Disease statistics, BHF, 2006)

1.2 Atherosclerosis

Atherosclerosis, the principle cause of CHD and stroke in the Western world, has multiple genetic and environmental contributions, such as age, gender, smoking, hypertension, diabetes, stress and high cholesterol. These risk factors cause injury to the endothelial lining of the arterial wall and what follows is an inflammatory response involving T lymphocytes, monocytes, cytokines and chemokines. The normal homeostatic properties of the endothelium are altered leading to changes in the

permeability of the arterial wall and increased expression of cell surface adhesion molecules and cytokine production [2].

Adhesion of circulating leukocytes to the endothelium is one of the earliest steps in atherogenesis, suggesting the involvement of an immune process [3]. Low-density lipoprotein (LDL) undergoes oxidative modifications in the intima which stimulates endothelial cells to produce proinflammatory molecules, including adhesion molecules and growth factors and these in turn trigger the entry of T-lymphocytes and monocytes into the arterial wall [4]. Adhesion molecules, such as vascular cell adhesion molecule-1 (VCAM-1) and P-selectin, on the surface of the endothelial cells interact with their counterligands on leukocytes [5]. Chemotactic molecules, such as monocyte chemotactic protein-1 (MCP-1), are also induced by endothelial cells and Apolipoprotein (Apo) E deficient mice ($ApoE^{-/-}$) mice with a disruption in the *MCP-1* gene, or its receptor *CCR2* show a marked reduction in atherosclerotic lesions [6]. This suggests that the interaction of the *MCP-1* protein with the *CCR2* receptor contributes to monocyte recruitment in atherosclerosis. Once firmly adhered, the leukocytes migrate across the endothelial monolayer into the intima where they proliferate and the monocytes differentiate into macrophages. This is a critical step in atherosclerosis and a study involving osteopetrotic mice which have a natural mutation in their macrophage colony-stimulating (*M-CSF*) gene confirms the role of macrophage in lesion development; these mice were significantly resistant to atherosclerosis [7].

Extensive oxidation of LDL leads to fragmentation of the Apolipoprotein B (ApoB) component, which renders the particle unable to bind to the LDL receptor (LDL-R). Oxidised LDL (Ox-LDL), instead, binds to the scavenger receptors, SR-A and CD36, expressed on macrophages and smooth muscle cells [8]. It has been reported that transgenic mice deficient in CD36 and SR-A, do not accumulate cholesteryl esters from modified lipoproteins in macrophages [9]. The cholesteryl ester-engorged macrophages eventually become foam cells [10] and it is this accumulation of lipids and foam cells in the intima that form the earliest lesions of atherosclerosis, termed fatty streaks. Macrophages also undergo apoptosis throughout all stages of atherosclerosis and an *in vivo* study has demonstrated that in early lesions macrophage death is beneficial as both lesion size and macrophage load are reduced [11]. Conversely, it has recently been reported that an early form of Ox-LDL, minimally oxidised LDL (mmLDL), may offset

the apoptotic effect of extensively Ox-LDL on macrophages, thus, prolonging their survival in lesions [12].

As the atherosclerotic process continues additional monocytes and T-lymphocytes are attracted to the lesion by pro-inflammatory cytokines, such as tumour necrosis factor-α (TNF-α) and interleukin-1β (IL-1β) [13]. TNF-α is upregulated in atherosclerotic plaques and when the activity of this gene is blocked in ApoE-deficient mice, lesion size and expression of intracellular adhesion molecule-1 (ICAM-1), VCAM-1 and MCP-1 are reduced [14]. Other cytokines, interleukin-10 (IL-10) and transforming growth factor β (TGF-β), are thought to have a protective, anti-inflammatory role in atherosclerosis. Overexpression of IL-10 in LDL-R deficient mice significantly reduces lesion size [15] and in a mouse model where TGF-β signalling is blocked in T-cells, the disease process is accelerated [16].

The inflammatory response also stimulates the migration and recruitment of smooth muscle cells (SMCs) from the media into the intima resulting in a fibro-fatty lesion [17]. Following further enlargement and restructuring, combined with continued lipid accumulation, an advanced, complex plaque develops which is characterised by a central lipid–rich necrotic core bounded on its lumen side by a fibrous cap containing SMCs and connective tissue. Eventual rupture and destabilisation of the plaque is initiated by the activation of macrophage, T-cells and mast cells, which release inflammatory cytokines, proteases, coagulation factors, free radicals and vasoactive molecules. Matrix metalloproteinases (MMPs) released from macrophage are implicated in the rupture of plaques due to their ability to degrade extracellular matrix proteins and their increased expression in vulnerable plaques [18]. A recent study has demonstrated that overexpression of tissue inhibitor of metalloproteinase (TIMP)-2 attenuates plaque development and destabilisation [19]. Other studies, however, have added controversy to the role of MMPs and have shown that some enhance plaque cap growth and stability [20]. Plaque rupture and thrombosis subsequently leads to major clinical complications such as myocardial infarction and stroke [10]

1.3 Lipoproteins and their metabolism

Initially α- and β-migrating lipids were discovered by electrophoresis of human plasma [21] and this was followed, in 1945, by the isolation of β-migrating lipoproteins using

an ultracentrifugal flotation technique [22]. Lipoproteins were further classified into 5 sub-fractions based on their flotation densities and were named, chylomicrons, very low density (VLDL), intermediate density (IDL), low density (LDL) and high density (HDL) lipoproteins [23]. The general lipoprotein structure comprises a core of triglycerides and cholesteryl esters, which are surrounded by a single layer of phospholipids, free cholesterol and apolipoproteins. The latter family of proteins includes Apo(a), AI, AII, AIV, AV, B48, B100, CI, CII, CIII and E and has a major function in lipid transport and metabolism.

1.3.1 Metabolism of triglyceride rich lipoproteins

Apolipoprotein B100 and E (ApoB100, ApoE) are synthesised in the liver and are important mediators in the binding of lipoproteins to their receptors; ApoB100 binds only to the LDL-R, while ApoE binds to both the LDL-R and LDL-receptor related proteins (LRP) [24;25]. ApoB48, in contrast, is synthesised in the intestine and has a major role in chylomicron metabolism. Chylomicrons are large triglyceride rich-dietary lipids that are secreted by intestinal mucosal cells into the lymph and then rapidly lipolysed by lipoprotein lipase (LPL). The resulting free fatty acids are delivered to peripheral tissues, while the remnant particles are taken up by the liver, first via attachment to the cell surface molecules, heparan sulphate proteoglycans (HSPGs), ApoE and hepatic lipase (HL), followed by transfer to the LDL-R and LRP [26] (Figure 1-2). Triglycerides and cholesterol are synthesised by the liver and secreted as VLDL, which are large due to their high triglyceride content. Once in the circulation they undergo lipolysis and are reduced to IDL, half of which are subsequently taken up by the liver and the remainder are degradated further into LDL. LDL have a rich cholesteryl ester core surrounded only by ApoB100 and remain in the circulation for much longer than VLDL or IDL. As discussed in section 1.2 LDL deposits cholesterol within cells of the arterial wall and, therefore, elevated plasma levels are correlated with atherosclerosis. Lipoprotein(a) (Lp(a)) is a variant of LDL and has the same structure, but contains an additional apo(a) polypeptide. The concentration of Lp(a) in the circulation is also highly variable among individuals and studies have shown that elevated levels are an independent risk factor for cardiovascular disease [27;28].

1.3.2 HDL metabolism and Reverse Cholesterol Transport (RCT)

HDL is secreted as nascent HDL into the circulation by the liver or intestine, or formed from VLDL and chylomicron surface remnants. The mature HDL particle is predominantly comprised of cholesteryl esters and surrounded by Apolipoproteins AI and AII (ApoAI and AII), which provide structure and confer receptor binding activity [29]. Epidemiological studies have shown that both HDL-cholesterol (HDL-C) and ApoA-I plasma levels are inversely correlated with the risk of CHD [30] and transgenic animal studies have further demonstrated their anti-atherosclerotic properties [31]. Although the mechanisms by which they inhibit the progression of atherosclerosis is not fully understood, they are thought to have several atheroprotective functions. These include anti-inflammatory and anti-oxidant effects [32;33] and, more importantly, they are essential for reverse cholesterol transport (RCT). RCT involves the efflux of excess, unesterified cholesterol from peripheral tissues and macrophages and its delivery to the liver for removal. The process is initiated by the interaction of lipid-free ApoA-I with the adenosine triphosphate (ATP) binding cassette transporter (ABC) AI, which results in the formation of pre-β HDL. This nascent HDL is subsequently converted to HDL_2 and HDL_3 by the enzyme lecithin-cholesterol acyltransferase (LCAT) which esterifies the cholesterol. These modified HDL particles can then bind to ABCG1 transporters which mediate a second cholesterol efflux pathway predominantly in macrophage [34]. HDL-C is either transferred to ApoB containing lipoproteins by the cholesteryl ester transfer protein (CETP), or taken up by the liver via the scavenger receptor B1 (SR-BI) and deposited into the bile. Interestingly, in a recent report using an ApoA-I deficient mouse model, the specific contribution of ApoA-I in the prevention and regression of atherosclerosis was elucidated. ApoA-I exerts an anti-atherosclerotic effect predominantly through macrophage RCT and the HDL anti-inflammatory function, both of which were discovered to be independent of the plasma levels of HDL-C [35]. Macrophage RCT is a term more appropriately used when this process is discussed in relation to atherosclerosis, as it is these cells in the arterial wall that become overloaded with cholesterol and from which efflux occurs.

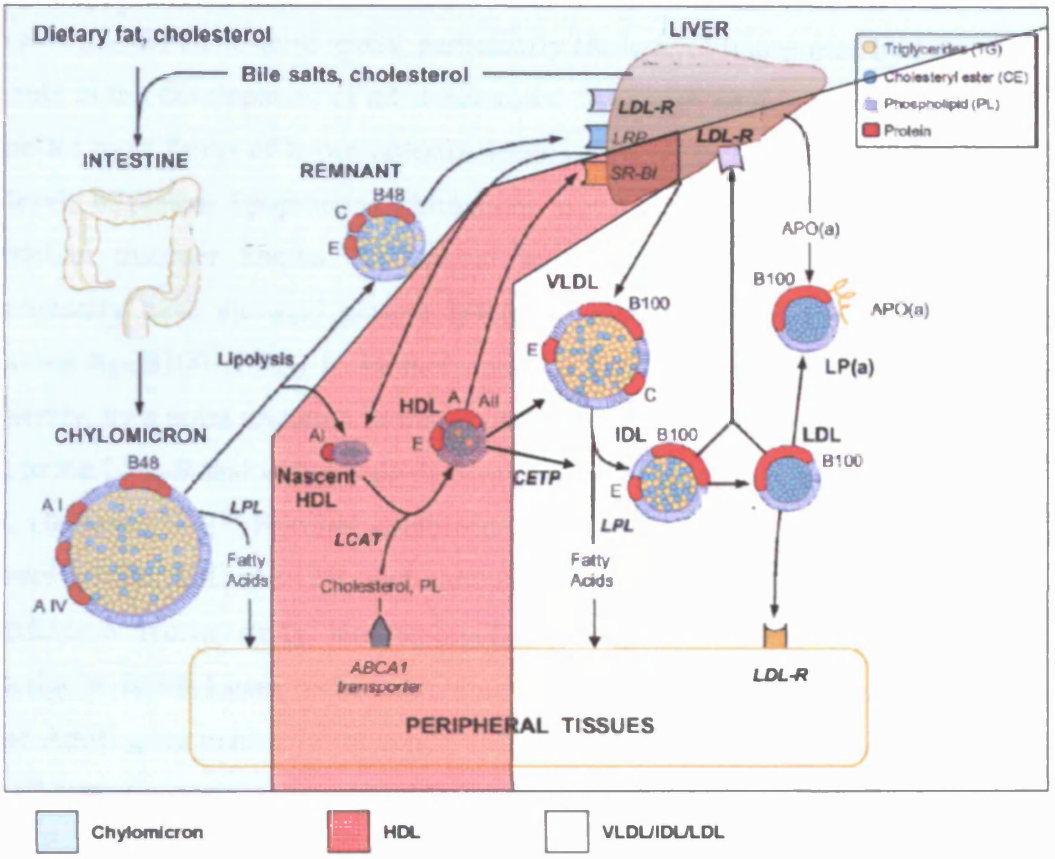

Figure 1-2. An overview of lipoprotein metabolism [10]
Lipoprotein metabolism can be divided into three sections: chylomicron (blue section), HDL (pink section) and VLDL/IDL/LDL metabolism (white section). All lipoproteins are composed of triglycerides (TG), cholesteryl ester (CE), phospholipid (PL) and protein (ApoE, ApoC, ApoB100, ApoB48, ApoAI, ApoAII, ApoAIV) at different relative proportions. Chylomicrons are secreted by the intestine into the lymph and lipolysed by LPL. The resulting free fatty acids are delivered to peripheral tissues, while the remnant particles are taken up by the liver. Triglycerides and cholesterol are synthesised by the liver and secreted as VLDL, which undergo lipolysis and are reduced to IDL. Half the IDL is taken up by the liver and the remainder are degradated further into LDL, which have a rich cholesteryl ester core surrounded only by ApoB100. HDL is secreted as nascent HDL into the circulation by the liver or intestine, or formed from VLDL and chylomicron surface remnants. The mature HDL particle is predominantly comprised of cholesteryl esters and surrounded by ApoAI and AII.

1.3.3 Lipoprotein related disorders

Elevated plasma cholesterol levels, particularly cholesterol transported by LDL, plays a key role in the development of atherosclerosis. Although environmental aspects are to blame for most forms of hypercholesterolaemia, genetic factors also strongly influence the levels of plasma lipoproteins. Mutations in the LDL-R gene results in a dominant Mendelian disorder known as familial hypercholesterolaemia (FH) and patients consequently have elevated plasma levels of cholesterol and LDL [36]. Familial defective ApoB100 (FDB) is another common lipid disorder which is caused, most frequently, by a point mutation in the ApoB100 gene; mutant forms are, thus, unable to bind to the LDL-R and individuals demonstrate high cholesterol levels due to defective LDL clearance [37]. Familial combined hyperlipidaemia (FCH) is characterised by elevated VLDL, IDL and LDL and although the primary causative gene has yet to be identified, a recent study has reported a strong association with the upstream transcription factor 1 gene on human chromosome 1q21 [38]. Finally, common variants of the ApoE gene markedly influence plasma cholesterol levels and are the cause of type III hyperlipoproteinaemia [39] (discussed in more detail in section 1.4.4).

1.4 Apolipoprotein E

As discussed in section 1.3 ApoE was first discovered in the early 1970s as a protein constituent of VLDL [40]. Further research identified ApoE as an important component of several classes of plasma lipoproteins and it is now viewed as a key molecule in the maintenance of plasma cholesterol homeostasis.

1.4.1 ApoE synthesis and expression

ApoE is most abundant in the liver, however, it is also expressed in the brain, spleen, lung, ovary, adrenal gland, kidney and muscles. Plasma ApoE is largely secreted by the liver (~90%) and a small amount is derived from extra-hepatic sources, such as macrophages [41]. The normal human plasma ApoE level ranges from 50 to 80μg/ml and increases in hypercholesterolaemic patients.

The human ApoE gene has been mapped to chromosome 19 [42] and contains four exons separated by three introns. ApoE is a secretory protein and is synthesised and released via the classical secretory pathway. The translated product is 317 amino acids in length and contains a signal peptide of 18 amino acids at the amino-terminal end,

which directs the polypeptide chain to the endoplasmic reticulum. From there the ApoE protein precursor is transferred to the Golgi where it undergoes intracellular proteolysis and *O*-glycosylation at Thr^{194}, prior to being secreted into the plasma as a 34-kDa glycoprotein. Newly secreted ApoE from the liver is highly sialylated and in plasma it exists, predominantly, in a non-sialylated form [43]. ApoE sialylation, however, is not essential for the synthesis or the secretion of the protein [44]; thus, the functional relevance of this process remains unclear.

1.4.2 ApoE gene regulation

ApoE gene expression is regulated in a tissue-dependent manner and in response to changes in cell morphology and various extracellular/intracellular factors. Studies have demonstrated enhanced transcriptional activation of the ApoE gene during the differentiation of monocytes into macrophages [45], and the proximal promoter region of the gene is thought to be implicated [46]. In macrophages, ApoE gene expression is upregulated by cholesterol loading [47] and by inflammatory mediators, such as TNF-α [48] and TGF-β [49]. Interferon-gamma (IFN-γ), interleukin-1 and granulocyte colony-stimulating factor, in contrast, inhibit the production of ApoE by macrophages [49-51]. ApoE expression is also modulated by cyclic AMP (cAMP); in HepG2 cells it has been shown to downregulate transcription via elements within a specific region of the promoter [52].

Several polymorphisms in the proximal promoter region of ApoE have been identified which are associated with variations in transcriptional activity due to differential binding of nuclear proteins [53]. Interestingly, an association between the -219G/T polymorphism with decreased plasma ApoE levels and an increased risk of myocardial infarction has been discovered [54]. Despite evidence demonstrating the role of the proximal promoter in the regulation of ApoE expression, this region of the gene requires distal enhancers to direct transcription in all cells of the transgenic mouse. ApoE expression is mediated by hepatic control regions 1 and 2 in the liver [55] and by multi-enhancers (ME) 1 and 2 in adipocytes and macrophages [56]. Furthermore, ME1 and ME2 contain a conserved liver-X receptor responsive element which mediates lipid-inducible expression of ApoE in macrophage [57].

At the post-translational level, newly synthesised ApoE in macrophages is either secreted or directed along the lysosomal pathway for degradation [58] and this has been

shown to be regulated by artificial phospholipid vesicles and lipoproteins [59]. ApoE secretion from cells is reported to be stimulated by cholesterol enrichment [60], acceptors involved in cholesterol efflux (ApoAI, HDL) [61;62] and the cholesterol transporters ABCA1 and ABCG1 [60]. More recently, oleic acid was found to modulate the glycosylation of ApoE in macrophage and thereby stimulate its secretion [63].

Interestingly, it has been discovered that ApoE can avoid degradation and instead undergo recycling and subsequently re-secretion [64]. Reports have demonstrated the presence of triglyceride-rich lipoprotein (TRL) derived ApoE in the peripheral recycling endosomes of the cell rather than the lysosomal compartments [65]. Not all TRL constituents, however, follow the same intracellular fate; TRL lipids and ApoB, for example, are targeted along the classical degradative pathway, in common with LDL. A study has also reported an association between recycled ApoE and HDL in macrophages; HDL-derived ApoAI is thought to be internalised and targeted to endosomes containing ApoE in order to promote ApoE recycling and cholesterol efflux [66].

1.4.3 ApoE structure

In a lipid-free state ApoE consists of two independently folded α-helical domains, which are separated by a protease-sensitive, loop (Figure 1-3). The amino-terminal (N) domain (residues 1-191), made up of four amphipathic α-helices, is the functional domain, which contains the recognition site for the LDL-R and LRP [67]. This receptor binding site is localised to an arginine and lysine rich section on helix 4 which, in addition, binds with high-affinity to HSPG [68]. This domain also contains the binding site for scavenger receptor class B type I (SR-B1) [69]. In a lipid-free state, however, ApoE cannot firmly bind to either phospholipids or lipoproteins. The carboxyl-terminal (C) domain (residues 216-299), which is highly α-helical [70], contains the major lipid binding site (residues 244-272) and facilitates helix-helix interactions to encourage ApoE self-association and helix-lipid interactions [71].

1.4.4 ApoE polymorphisms and functional consequences

ApoE is a polymorphic glycoprotein coded by three alleles (ε2, ε3, ε4) that result from a single gene locus. ApoE3 is the most common and is considered the "wild-type"

isoform as it contributes little to the normal variation of plasma lipids. The rarest form, ApoE2, differs from ApoE3 by an Arg158Cys substitution and ApoE4 varies by a Cys112Arg substitution [72]. The functional consequence of the substitution in ApoE2 is a reduced ability of this isoform to bind to the LDL-R [73]. The salt bridge between Arg158 and Asp154 is eliminated which subsequently alters the conformation of the domain and its ability to interact with the receptor. Furthermore, the isoforms differ in their lipoprotein binding preferences: ApoE4 has a high affinity for VLDL and LDL, whereas, ApoE3 and ApoE2 preferentially associate with HDL [74]. The interaction between the N- and C-terminal domains in ApoE4 is thought to govern this difference. The arginine at position 112 changes the orientation of the side chain of Arg61, allowing interaction with an acidic residue in the C-terminal domain and consequently altering the lipoprotein preference [75]. The ApoE isoforms also have a varying effect on their own plasma level and on ApoB, triglycerides, total cholesterol and LDL-cholesterol. ApoE2 is, most often, associated with raised levels of ApoE and triglyceride and decreased levels of ApoB and cholesterol; ApoE4, in contrast, is linked to a decrease in ApoE and an increase in ApoB and cholesterol levels [76].

The ApoE variants associate with CVD as a result of these functional consequences. ApoE2 is well documented as a risk factor for recessive, type III hyperlipoproteinaemia (HLP) which is characterised by increased plasma cholesterol and triglyceride. The majority of patients with type III HLP are homozygous for apoE2, although not all ε2/ε2 carriers develop this disease, as more than 90% are normolipidaemic. Due to the receptor-binding defect of ApoE2, the main metabolic abnormality in type III HLP is delayed clearance of remnant lipoproteins; this alone, however, is not sufficient to cause the disease. ApoE2 binds more efficiently with HSPG/LRP, suggesting that hormonal, environmental and/or genetic factors are required to develop overt type III HLP. Interestingly, dominant inheritance of this condition occurs with several rare ApoE variants, for example $ApoE3_{Leiden}$; like ApoE2, this variant has a receptor-binding defect, but only a single mutant allele is required for development of the disease. ApoE4 is also associated with dominant hyperlipoproteinaemia [76] and several studies link ApoE4 with greater risk for CVD. It was reported that male carriers of the ε4 allele from nine populations had a 40% greater risk of mortality from CHD compared with ε2 or ε3/ε3 carriers [77]. Furthermore, a recent meta-analysis has verified the ε4 allele as a significant risk factor for CHD [78]. ApoE4, in addition, has a pronounced association with neurodegenerative disorders, such as Alzheimer's disease [79].

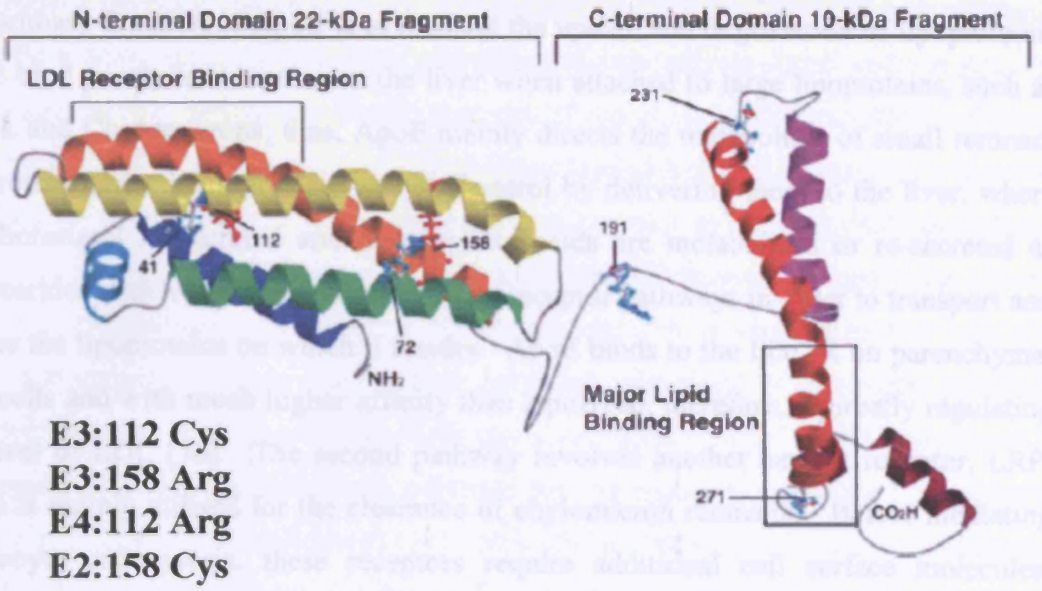

Figure 1-3. Structure of human ApoE

The model illustrates the structural regions and the polymorphic sites (residues 112 and 158) that distinguish ApoE3 from ApoE4 and ApoE2 [80].

1.4.5 The role of ApoE in lipoprotein metabolism and transport

The primary function of ApoE is to mediate the uptake and degradation of lipoproteins. ApoE bind poorly to receptors on the liver when attached to large lipoproteins, such as VLDL and Chylomicrons; thus, ApoE mainly directs the metabolism of small remnant lipoprotein-derived triglycerides and cholesterol by delivering them to the liver, where the cholesterol is excreted and dietary fatty acids are metabolised or re-secreted as triglycerides with VLDL. ApoE utilises two receptor pathways in order to transport and deliver the lipoproteins on which it resides. ApoE binds to the LDL-R on parenchymal liver cells and with much higher affinity than ApoB100, therefore, indirectly regulating the level of LDL [76]. The second pathway involves another hepatic receptor, LRP, which is mainly utilised for the clearance of chylomicron remnants. Before mediating hepatocyte endocytosis, these receptors require additional cell surface molecules, including HSPGs and hepatic lipase (HL), which function to capture and rapidly sequester the ApoE bound lipoproteins from the plasma [81].

ApoE utilises several other means, unrelated to receptor-mediated endocytosis, to regulate the metabolism of lipoproteins. Firstly, increased synthesis and secretion of ApoE by the liver and its accumulation in the plasma has been shown to stimulate hepatic VLDL and triglyceride production [82]. Secondly, ApoE activates enzymes such as HL, CETP and LCAT which all promote the maturation of HDL [83-85]. Most importantly, however, ApoE has a contributory role in RCT [86] and there is now a considerable amount of evidence suggesting that ApoE can directly influence macrophage lipid efflux. It was reported that ApoE-depleted HDL from human or ApoE-deficient mice had a decreased ability to promote cholesterol efflux from mouse peritoneal macrophage, but its function was restored by the addition of exogenous ApoE [87]. Interestingly, more efficient cholesterol efflux was observed in fibroblasts stimulated with "lipid-poor" ApoE (γ-LpE) from ε3/ε3 carriers in comparison to that from both ε2/ε2 and ε4/ε4 individuals [88]. Cholesterol efflux from macrophages is also enhanced by endogenously expressed ApoE [89], although the mechanism by which it achieves this remains unclear. One possibility is that the interaction of secreted ApoE with proteoglycans on the cell surface facilitates passive desorption of lipid from the plasma membrane via ABCA1 [90;91]. Alternatively, stimulation of cholesterol efflux by endogenous ApoE could depend on its intracellular synthesis and transport through internal cellular membranes before secretion. Indeed, studies have shown that ApoE potentially mediates lipid efflux independent of ABCA1 expression [92];

furthermore, a recent report provides evidence for the existence of an ABCA1-independent pathway that requires the intracellular synthesis and/or transport of ApoE [93]. At atherosclerotic lesion sites, macrophages only secrete ApoE and not ApoAI, the latter, instead stimulates ApoE secretion from these cells and this has been demonstrated to be independent of ABCAI-mediated cholesterol efflux [62]. It could therefore be assumed that ApoE is the dominant acceptor in clearing cholesterol from arteries, however, a mechanism for ApoAI-mediated removal of cholesterol from macrophage foam cells has recently been proposed. It is speculated that proteins secreted from macrophages, for example lipid and cholesteryl ester transfer proteins, remodel spherical HDL, which results in the dissociation of stable, lipid-poor ApoAI. This renders ApoAI available as a substrate for the macrophage ABCAI transporter which can efflux excess cholesterol [94]. Nevertheless, the maintenance of cholesterol homeostasis in macrophages is crucial in preventing foam cell formation, which ultimately re-enforces the anti-atherosclerotic properties of ApoE (discussed in more detail in section 1.6).

1.4.6 ApoE and non-lipid lowering functions

Initial evidence that ApoE has anti-atherogenic properties that are independent of its action on cholesterol transport and metabolism came from a study that used transgenic mice expressing high levels of human ApoE in the arterial wall. Significant reduction in atherosclerotic lesions was reported without observing any difference in the plasma cholesterol level and lipoprotein profile [95]. Later, Thorngate et al. [96] found that ApoE expression in the adrenal glands of ApoE-null mice, at levels too low to correct hypercholesterolaemia, was sufficient to provide atheroprotection in these mice. Most importantly, a recent study has directly demonstrated, for the first time, that physiological levels of ApoE can induce the regression of atherosclerosis independently of lowering plasma cholesterol levels [97]. Here the authors used hypomorphic $ApoE^{h/h}$Mx1-Cre mice, which express very low levels of an ApoE4-like form of mouse ApoE at 2-5% of normal levels in plasma. These mice are normolipidaemic and develop hypercholesterolaemia on a high-fat diet, which can be reversed when a chow diet is resumed. Induction of physiological levels of plasma ApoE in these mice was discovered to enhance removal of neutral lipids from the fibrotic core; their plasma cholesterol level, however, remained comparable to a control group. This new finding facilitates further research into the mechanisms responsible for the non-lipid, anti-atherosclerotic effect of ApoE.

Indeed, several biological functions of ApoE have been identified that are unrelated to lipid transport and metabolism and which contribute to its anti-atherogenic activity. Although absent in normal vessels, ApoE is highly expressed in atherosclerotic plaques and research has shown that it is largely macrophage derived [98]. Furthermore, this macrophage-synthesised ApoE has been discovered to exert local affects on the surrounding cells of the vessel wall. Firstly, ApoE inhibits platelet aggregation [99;100] by stimulating the release of NO, apparently via a signal transduction pathway involving an initial interaction with ApoE receptor 2 (ApoER2) [101;102]. Many of the anti-atherosclerotic mechanisms used by ApoE involve suppression of different stages of the inflammatory response. ApoE has been shown to inhibit the expression of VCAM-1 on TNF-α stimulated human umbilical vein endothelial cells (HUVECs) again via interaction with ApoER2 and induction of endothelial NO production [103]. Other anti-inflammatory properties of ApoE include modulation of the T-helper-type-I immune response by regulation of interleukin-12 (IL-12) [104], and ApoE has recently been implicated in CD1-mediated presentation of exogenous lipid antigens [105]. Additional, non-lipid lowering actions of ApoE involve the inhibition of smooth muscle cell migration and proliferation. LRP was identified as the receptor that mediates ApoE inhibition of smooth muscle cell migration [106] and the process was demonstrated to occur via activation of cAMP/protein kinase A [107]. In contrast, ApoE inhibition of smooth muscle cell proliferation was found to be mediated via its binding to HSPG [108] and the resulting activation of inducible nitric oxide synthase (iNOS) [109]. Reports have also exhibited evidence that ApoE has anti-oxidant properties [110] with the responsible region of ApoE being identified as the receptor-binding domain [111]. Inhibition of lipid oxidation could, thus, prevent the accumulation of oxidised LDL and ultimately help protect against atherosclerosis.

ApoE also plays a modulatory role in macrophage phagocytosis of apoptotic cells; *in vitro*, ingestion of apoptotic cells by ApoE-deficient macrophages was attenuated and in ApoE-knockout mice they accumulate in a range of tissues. Interestingly, the increased number of apoptotic bodies in these tissues resulted in a higher population of macrophage and this was in turn associated with a systemic increase in pro-inflammatory markers, such as TNF-α [112]. The involvement of ApoE in apoptosis, although in a different facet, has been further observed in a study, which identified ApoE as a potential tumour-associated marker in ovarian cancer. Inhibition of ApoE

expression led to G_2 cell cycle arrest and apoptosis in an ApoE-expressing ovarian cancer cell line and it was hypothesised that the downstream proliferative and anti-apoptotic signals activated by ApoE, through its binding to the LDL-R, are used by tumour cells to maintain cell growth [113]. Finally, ApoE has been reported to impede subendothelial retention of LDL, which is thought to be an initial step in atherogenesis. An early study discovered that ApoE impairs the lipase-mediated retention of LDL [114] and more recently ApoE was found to restore the decreased atherosclerotic potential of proteoglycan-binding-defective LDL which depends on its lower affinity for artery-wall proteoglycans [115].

1.5 Transgenic mouse models for hyperlipidaemia and atherosclerosis

Mice have become the most valuable experimental animals due to their small size, easy maintenance, short breeding time and their potential for use in transgenesis and gene targeting studies. However, mice exhibit important differences in their lipoprotein profile compared with humans; they bear relatively low steady-state concentrations of VLDL and LDL and their plasma cholesterol is mainly found in the HDL fraction. Notwithstanding these differences, mice and humans largely carry the same set of genes to control lipoprotein metabolism [116]. In the absence of atherogenic plasma lipoproteins, mice naturally resist the development of atherosclerosis. A change in the balance of the VLDL and LDL fractions and a general increase in ApoB containing lipoproteins is needed to promote this disease in mice, via either genetic or dietary means. The C57BL/6J mouse is the most atherosclerosis susceptible strain, but even on a pro-atherogenic/high-fat diet, they only develop small immature fatty streak lesions with largely lipid-laden foam cells. It is therefore, not surprising that prior to the advent of genetically modified animals, the use of mice in atherosclerosis research remained limited.

1.5.1 The ApoE-deficient mouse model

In 1992, two separate research groups created the ApoE-deficient ($ApoE^{-/-}$) mouse through targeted gene inactivation [117;118]. On a normal chow diet, these mice develop atherosclerotic lesions and have a plasma total cholesterol ranging from 500mg/dL to 800mg/dL; this is due to a severe defect in the clearance of remnant lipoproteins from plasma. When fed a Western-type diet, cholesterol-rich VLDL further accumulate and a subsequent doubling in plasma cholesterol is observed. In

fact, their lipid distribution resembles that found in patients with type III hyperlipidaemia, although the VLDL composition differs [119]. Atherosclerotic lesions in $ApoE^{-/-}$ mice increase in size and complexity with age. In young mice, the lesions are mainly centred in the aortic sinus but become widely distributed throughout the arterial tree when the mice reach 8 to 9 months of age. As early as 10 weeks, foam cell deposits are apparent and by 5 months, moderate lesions additionally containing free cholesterol and smooth muscle cells are observed. Beyond 8 and 9 months of age the lesions are much more complex and start to resemble a fibrous plaque [120].

When the animals are fed a Western-type diet, the progression of atherosclerosis is advanced by at least 6 weeks with lesions developing more rapidly throughout the vascular tree. This type of diet also renders the lesions more lipid-rich [121]. Interestingly, heterozygous ApoE-deficient mice ($ApoE^{+/-}$) develop atherosclerosis on a high-fat diet, even though their plasma lipid levels remain comparable to those of wild-type mice; suggesting that mice lacking one allele of ApoE are susceptible to diet-induced atherosclerosis [121]. Advanced fibrous plaques are observed in $ApoE^{-/-}$ mice after only 6 months on a high-fat diet; these plaques are characterised by a fibrous cap containing smooth muscle cells surrounded by connective tissue matrix which covers a central lipid-rich necrotic core [122]. Several studies have reported that these advanced lesions can spontaneously become unstable and rupture [123;124]. The brachiocephalic artery, which is the first branch from the aortic arch, is a well-defined area in which to study plaque stability and rupture. $ApoE^{-/-}$ mice, when fed a high-fat diet, exhibit a high frequency of plaque rupture in these arteries; these ruptured plaques also show many of the characteristics of vulnerable plaques in humans [125]. Furthermore, it has recently been reported that $ApoE^{-/-}$ mice on a high-fat diet for a period as short as 8 weeks, develop unstable atherosclerotic plaques in the brachiocephalic artery which are prone to rupture [126]. Mouse models of plaque rupture are continually being developed, with the purpose to help our understanding of plaque development, destabilisation and rupture. There has been a considerable amount of discussion, however, over the phenotype of the unstable lesion and it is disputed how closely ruptured plaques in the mouse model resemble vulnerable plaques in humans.

In humans, ApoB100 is the principal structural protein of liver-derived lipoproteins, whereas, in mice, two-thirds of the lipoproteins metabolised by the liver contain ApoB48. ApoB100 and ApoB48 are the translated protein products of the same gene,

however, the latter isoform is a truncated version due to ApoB mRNA editing and as a consequence lacks the receptor-binding domain [127]. Editing of ApoB mRNA only occurs in the intestine of humans which, in contrast to mice, renders ApoB48 exclusively involved in chylomicron formation [128]. In $ApoE^{-/-}$ mice, ApoB100 naturally becomes the principle ligand mediating hepatic remnant clearance through the LDL-R; as a result the plasma from these mice is normally absent in ApoB100-VLDL, but contains very high levels of the binding defective ApoB48-VLDL [129]. LDL receptor deficient mice ($LDLR^{-/-}$), in contrast, have a disproportionate increase in ApoB100 in their plasma and on a chow diet have low cholesterol levels with only slight atherosclerotic lesions. It would therefore, be logical to infer that ApoB48 is more atherogenic than ApoB100. However, on a high-fat diet, $LDLR^{-/-}$ mice develop severe atherosclerosis [121], while modification of the ApoB gene in $ApoE^{-/-}$ mice to promote the exclusive expression of either ApoB48 or ApoB100 failed to have an effect on susceptibility to atherosclerosis [130].

Histological methods are routinely used to assess atherosclerotic plaques in $ApoE^{-/-}$ mice, which obviously requires euthanizing the animals. Non-invasive imaging techniques that are normally used for patients are now being investigated as an alternative means to evaluate lesion progression. One study applied a non-invasive magnetic resonance microscopy technique to live $ApoE^{-/-}$ mice fed a Western diet; here they were able to accurately quantify aortic root lesions and even characterise lesion components [131].

The $ApoE^{-/-}$ mouse has ultimately revolutionised the study of mechanisms of atherosclerosis and understandably, it has become the most popular and convenient mouse model used by researchers around the world. It has recently proved its versatility in a study undertaking gene expression profiling during plaque progression [132] and for proteomic/metabolomic analyses of atherosclerotic vessels [133].

1.5.2 The $ApoE3_{Leiden}$ transgenic mouse model

Transgenic mouse models expressing mutant forms of ApoE have also been generated in order to further our understanding of hyperlipidaemia and atherosclerosis. The $ApoE3_{Leiden}$ transgenic mouse carries a gene construct consisting of the $ApoE3_{Leiden}$ gene from a human carrier, ApoC1 and hepatic regulatory elements. Although endogenous ApoE is still present in these mice, they develop a hyperlipidaemic

phenotype, which resembles that of the dominant trait observed in humans. When fed a normal chow diet, the mice exhibit an increase in plasma total cholesterol and triglyceride, which dramatically increases when the animals are transferred to a high-fat diet; the increase was mainly observed in the VLDL and LDL fractions. Interestingly, on the high-fat diet the $ApoE3_{Leiden}$ protein was equally distributed between VLDL, LDL and HDL, whereas on normal chow the protein was predominantly in the HDL fraction [134]. A further study reported atherosclerotic lesion development in $ApoE3_{Leiden}$ mice fed a high cholesterol/cholate diet; moreover, atherogenesis was positively correlated with serum cholesterol levels [135]. Although this mouse model is less susceptible to atherosclerosis than the $ApoE^{-/-}$ mouse, the fact that the mice carry the human $ApoE3_{Leiden}$ gene allows a clearer insight into the nature of the disease in humans.

1.5.3 Mouse models containing common human ApoE alleles

Knock-in mouse models containing the most common human ApoE alleles, i.e., E2, E3 and E4, have been generated [136-138]. In these models, the endogenous mouse ApoE gene is replaced by the corresponding human gene using homologous recombination in embryonic stem cells. Mice expressing human ApoE2 exhibit many characteristics of Type III HLP on a normal chow diet; their plasma total cholesterol and triglyceride levels are raised, predominantly in the VLDL fraction and they develop atherosclerotic lesions [138]. It is believed, however, that there must be an additional underlying cause for the pronounced phenotype observed in these mice as humans homozygous for ApoE2 rarely develop HLP. Furthermore, the genetic factors that trigger Type III HLP in humans must already be present in mice. It was proposed that the reduced availability of ApoB100 in mice, due to ApoB mRNA editing, could be responsible, since they, consequently, become more dependent on ApoE2-mediated lipoprotein clearance which has a reduced ability to bind to the LDL-R. A study, however, demonstrated that sole expression of binding-competent ApoB100 in ApoE2 knock-in mice was not sufficient to reverse the hyperlipidaemic phenotype [139]. These results indicate that the complete penetrance of the type III HLP phenotype in this mouse model is not entirely dependent on the difference in ApoB editing between humans and mice. Another possible explanation is the reduced expression of the LDL-R in mice as over-expression of the human LDL-R in ApoE2 knock-in mice was discovered to ameliorate the plasma lipoprotein profile [140].

The ApoE3 and ApoE4 knock-in mice exhibit very similar phenotypes, although they differ slightly in lipoprotein distribution as mice homozygous for ApoE4 have increased steady-state levels of non-HDL lipoproteins due mainly to reduced plasma VLDL clearance. On normal chow diets, plasma lipid levels in both these mouse models are significantly lower than the levels in ApoE2 knock-in mice. On high cholesterol diets, the ApoE4 knock-in mouse develops larger atherosclerotic plaques than the ApoE3 knock-in mouse, however, these comparative observations demonstrate that a difference in ApoE structure alone is sufficient to alter VLDL metabolism and atherosclerosis risk in mice [136]. Interestingly, in ApoE4 transgenic mice, which also over express the LDL-R, the rate at which triglyceride-rich lipoproteins are cleared was not increased and instead lipoprotein remnants were found to accumulate. It was, subsequently, hypothesised that ApoE4 becomes trapped in the liver due to its greater affinity for the LDL-R, rendering lipoproteins unable to bind to LRP and, ultimately, slowing their rate of clearance [141].

1.6 Evidence for the therapeutic potential of ApoE to treat atherosclerosis and hyperlipidemia

As discussed in the previous sections, ApoE is generally considered anti-atherogenic due to its main function in lipoprotein metabolism and transport and the fact that $ApoE^{-/-}$ mice are grossly hypercholesterolaemic and develop spontaneous atherosclerotic lesions. There is now a significant amount of evidence endorsing the human ApoE gene as a strong candidate for therapeutic manipulation to treat atherosclerosis and hyperlipidaemia. One study demonstrated that intravenous injection of plasma-purified ApoE into Watanabe heritable hyperlipidaemic (WHHL) rabbits could markedly reduce plasma cholesterol and significantly regress atherosclerotic lesions in these animals over a period of eight months [142]. Similarly, overexpression of ApoE in the liver of transgenic mice was found to reduce plasma cholesterol and triglyceride and prevent diet-induced hypercholesterolaemia [143]. Moreover, the same protection was conferred in transgenic mice with diabetic hyperlipidaemia [144]. Interestingly, when a synthetic peptide representing the ApoE binding site was intravenously injected into $ApoE^{-/-}$ mice, a 30% reduction in total plasma cholesterol was observed; the peptide selectively associated with cholesterol-rich lipoproteins and mediated their clearance [145]. Similarly, when an ApoE mimetic peptide consisting of the ApoE receptor binding domain, covalently linked to a well-characterised class A

amphipathic helical peptide 18A, was intravenously injected into WHHL rabbits, plasma cholesterol levels were reduced and endothelial functions were improved [146].

Several studies have also assessed whether ApoE produced in the arterial wall by macrophage and other cell types could have an effect on the development of atherosclerosis. In one study, human ApoE expression was directed only to the macrophage of $ApoE^{-/-}$ mice and was discovered to prevent arterial wall lipid accumulation and to markedly reduce atherosclerosis [147]. Linton et al. [148] transplanted bone marrow from wild-type mice into $ApoE^{-/-}$ mice, thereby reconstituting the expression of murine ApoE by macrophages. ApoE was, subsequently, detected in the plasma, which normalised plasma lipid levels and, importantly, protected the animals against the development of atherosclerosis. Later, in a similar study, $ApoE^{-/-}$ mice were transplanted with $ApoE^{+/+}$ bone marrow and assessed for regression of established atherosclerotic lesions. Although macrophage-derived ApoE, which provides approximately 10% of plasma ApoE in normal mice, was sufficient to eliminate hypercholesterolaemia and protect against the progression of aortic lesions, it failed to induce significant regression of established atherosclerosis [149].

Despite the above evidence, which lends support to the therapeutic potential of ApoE to treat hyperlipidaemia and atherosclerosis, reports have shown that overexpression and accumulation of ApoE can, in fact, cause hypertriglyceridaemia. Huang and colleagues [150] found that expressing supraphysiological levels of human ApoE3 in transgenic mice lacking endogenous ApoE caused a three-fold increase in plasma triglyceride with a concomitant increase in VLDL and a decrease in HDL. This hypertriglyceridaemic effect of ApoE overexpression in $ApoE^{-/-}$ mice is thought to be caused by both stimulation of VLDL-triglyceride production and impaired VLDL lipolysis and can be eliminated by deletion of the carboxyl-terminal lipid-binding domain. Injection of a high dose of an adenovirus vector expressing a truncated form of ApoE2, lacking its lipid binding domain, did not increase plasma triglyceride levels in these mice and, moreover, normalised the hypercholesterolaemia [151]. The results from a recent study further indicate that residues 261, 264, 265, 268 and 269 in the C-terminal domain of ApoE are responsible for the hypertriglyceridaemic effect and, in addition, were found to displace ApoA-I from HDL, resulting in a reduction in plasma ApoA-I and HDL levels. Most importantly, these findings have allowed a recombinant ApoE variant with improved function to be generated [152]. Interestingly, the sensitivity and severity of

ApoE-induced hypertriglyceridaemia is intensified by, either bolus injection of purified ApoE in $ApoE^{-/-}$× $LDL\text{-}R^{-/-}$ mice or injection of an adenovirus expressing a LDL-R binding-defective form of ApoE4 in $ApoE^{-/-}$ mice. Their data suggests that the LDL-R may represent the only physiological route for clearance of ApoE bound lipoproteins in mice [153].

1.7 Gene Therapy

Somatic gene therapy typically involves the delivery of a functional gene into the nucleus of a target cell with the aim to treat disease-causing, loss-of-function mutations. Although gene therapy was initially intended to be a treatment and cure for inherited genetic disorders, the majority of clinical trials now target acquired disorders such as cancer, vascular disease and degenerative neurological conditions. Difficulties, however, in achieving sustained gene expression in host cells and in developing safe and efficient gene-delivery methods have greatly impeded the progress of these clinical trials. The main problem is the vehicles that are being used to deliver the therapeutic genes to the target tissue. Research efforts are now focusing on understanding the molecular basis of how viruses and viral vectors interact with the host. Vectors with improved efficiency, specificity and safety are currently being developed; this, however, is a substantial challenge, which needs to be overcome before gene therapy can fully achieve all of its promises.

1.7.1 Viral vectors

Viruses are employed as a gene therapy tool essentially because they can efficiently gain access to host cells, which they then use for their survival and replication. The viral life cycle is divided into two distinct phases: infection and replication. The viral genome is introduced into the cell following infection and this subsequently leads to the expression of early phase genes involved in viral regulation. A late phase then follows, in which structural genes are expressed and new viral particles are assembled [154]. In most gene therapy applications today, viral vectors are constructed in such a way that makes them as safe as possible. While genes controlling the viral infection pathway and those that are required for *in cis* functions, such as packaging the vector genome into the virus capsid, are left intact, viral genes that lead to replication and toxicity are deleted. An expression cassette, consisting of a promoter and transgene of interest, is then cloned into a modified viral backbone, in which unwanted genes are deleted. A separate

helper construct, however, is provided *in trans* which contains genes that are involved in replication and encapsidation; this is co-transfected along with the vector genome into packaging cells to produce the recombinant vector particle [155] (Figure 1-4, A). The vector particles are then ready to be transduced into the target cell; they enter the cell through a receptor-mediated process and then undergo uncoating. Once in the nucleus the vector genome forms transcriptionally active dsDNA molecules, and either persists as an episome or becomes integrated into the host genome itself (Figure 1-4, B).

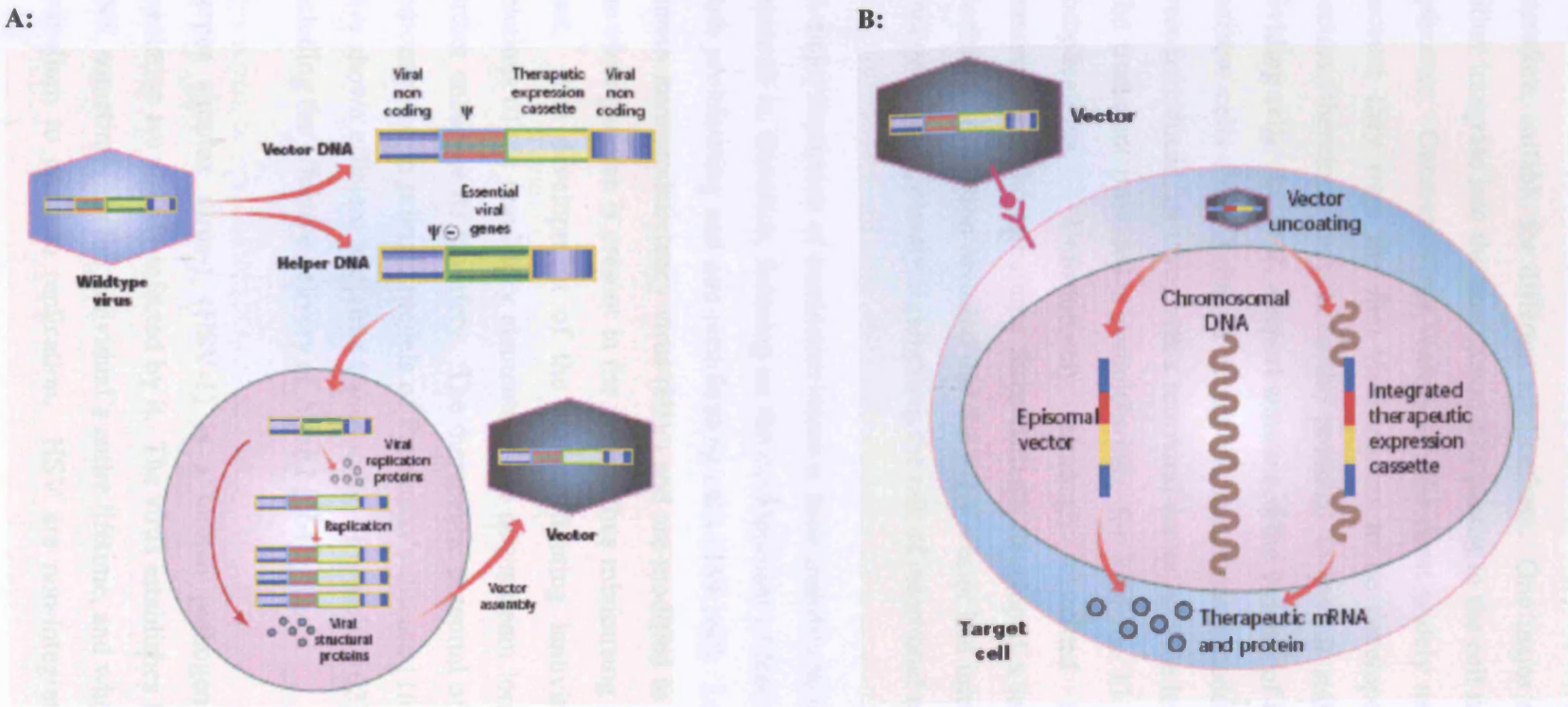

Figure 1-4. The production of a viral vector and its transduction into the target cell [154]
(A) *The helper plasmid contains genes essential for viral replication and encapsidation, and this is co-transfected along with the vector DNA, carrying the expression cassette, into packaging cells. Viral proteins are produced which initiate replication of the vector DNA, leading to the production of multiple copies. The vector genomes are then packaged into viral particles by structural proteins, which recognise vector but not helper DNA.* ***(B)*** *The viral particles enter the cell through a receptor-mediated process and then undergo uncoating. Once in the nucleus the vector genome forms transcriptionally active dsDNA molecules and, depending on the vector, can persist as an episome or become integrated into the host genome. This is followed by the production of the therapeutic mRNA and protein.*

1.7.1.1 Classes of viral vectors

There are currently five main classes of viruses from which viral vectors are derived, which include oncoretrovirus, lentivirus, adenovirus (Ad), adeno-associated virus (AAV) and herpes simplex-1 virus (HSV-1). They all have varying properties and are, therefore, suitable for different applications. One major distinction is their ability to either integrate into the host genome or persist in the cell nucleus as extrachromosomal episomes. Oncoretrovirus vectors are the most widely used in clinical trials, mainly because they were the first viral vectors to be developed and they are integrating vectors, therefore, they have the potential to permit stable transgene expression in dividing cells. In 2002, a report announced the success of a clinical trial in which bone marrow cells from X-linked severe combined immunodeficiency (SCIDX1) patients were transduced, ex vivo, with a retroviral vector, murine leukaemia virus (MLV) [156]. The treatment provided a complete cure for 8 of the 11 patients whom suffered no complications. Unfortunately, although sustained transgene expression was demonstrated, the remaining three patients developed a leukaemia-like disease [157]. Further investigation revealed that the MLV vector had integrated near and activated an oncogene [158], clearly highlighting the risk of insertional mutagenesis.

A major limitation of oncoretroviruses is their inability to transduce non-dividing cells; research is, therefore, focusing on the development of lentiviruses which can transduce both proliferating and non-proliferating cells [159;160]. Lentiviruses are derived from human immunodeficiency virus (HIV) and are modified to the extent that very little of the virus genome is present in the vector, thus minimising its ability to replicate in the host. The development of the self-inactivating lentivirus vector, which contains deletions of the regulatory elements in the downstream long-terminal repeat sequence, further enhances its biosafety. The therapeutic potential of lentivirus vectors has been demonstrated in primate models of Parkinson's disease [161] and other *in vivo* studies have shown efficient lentivirus transduction of muscle [162], liver [163] and also brain; including the effective delivery of ApoE2 [164].

Herpes simplex virus-1 (HSV-1) is a human pathogen and around 80% of the population are already infected by it. The virus establishes latency as an episome in the CNS, sometimes for the individual's entire lifetime, and when re-activated travels to the epithelium to undergo replication. HSV are non-integrative and contain a double-

stranded DNA molecule. The vectors are made replication defective by deleting the immediate-early genes required for lytic infection and expression of all other viral proteins. Replication-defective HSV vectors have been widely applied in animal models for the treatment of cancer [165] and neurological diseases [166]. Long-term transgene expression has been achieved in the CNS with the use of a HSV vector containing a neuron-specific latency-activated promoter [167]. The main drawback, however, with these vectors is the immune response and cytotoxicity that develops upon their administration [168;169].

Adenoviruses consist of a non-enveloped, icosahedral capsid containing a linear double-stranded DNA genome that exists and propagates as extrachromosomal episomes. Although recombinant adenoviral vectors (rAd) are the most efficient gene transfer system in a broad range of tissues and infect both dividing and non-dividing cells, they preferentially transduce the mammalian liver following systemic delivery. Unfortunately, the rAd vector has had to be extensively modified to reduce its immunogenicity; only two viral early genes were deleted from the 1st generation vectors, which induced strong cytotoxic and host immune responses, culminating in only transient transgene expression. Reduced toxicity and prolonged transgene expression, however, has been demonstrated in animal studies with the use of a 2nd generation vector, lacking additional early genes [170;171]. Furthermore, the introduction of a helper-dependent rAd (HD-Ads) vector [172], in which all viral genes are deleted, has shown the most significant reduction in rAd vector-related toxicity and immunogenicity *in vivo* [173-175].

1.7.2 Adeno-associated viruses (AAV)

AAVs are human parvoviruses that were first discovered as contaminants in adenovirus cultures. This single-stranded DNA-containing nonenveloped virus has the best safety profile among all viral vectors as wild-type AAV (wtAAV) infection has never been associated with human disease, making it an ideal candidate for gene therapy. AAV has also been classified as a dependovirus because it requires a helper virus, such as adenovirus, for productive infection *in vitro*, which further endorses its safety. wtAAV has the ability to establish latent infection *in vitro* and integrates into the AAVS1 site of human chromosome 19 [176]. Recombinant AAV (rAAV), in contrast, rarely integrates and forms extrachromosomal, intermolecular concatemers in the target cell. Interestingly, this circular structure is thought to be responsible for rAAVs long-term

episomal persistence and ability to direct stable transgene expression in muscle tissue [177]. Although reports have shown that, within the liver, rAAV can integrate into the host's chromosomal DNA, it is only a small fraction and extrachromosomal forms are the primary source of rAAV mediated gene expression [178]. The worrying issue, however, is that the small percentage that does integrate, preferentially integrates into active gene and accompanies chromosomal deletions, which may lead to loss-of-function insertional mutagenesis [179]. A recent study has further highlighted hot spots for integration in the liver, which, disconcertingly, include gene regulatory sequences [180]. This issue, ultimately, has important implications for future clinical trials and further research is needed, especially since only AAV serotype 2 has been examined for its potential to integrate, other serotypes may not behave in the same manner. Interestingly, rAAV integrants could not be detected following transduction of skeletal muscle [181], which perhaps reinforces the safety of muscle compared with liver.

1.7.2.1 AAV structure/biology

The wild-type AAV genome is only 4.7 kb and is composed of two genes, *rep* and *cap*, which encode four replication proteins and three capsid proteins respectively. Preferential integration into the AAVS1 site requires the nicking activity of two large replication proteins, Rep 78 and 68 [182], which also have additional roles in AAV transcription and replication. DNA packaging into the preformed capsid within the nucleus of the cell involves the smaller proteins, Rep 40 and 52. The icosahedral virion shell is made up of three capsid proteins Vp1, Vp2 and Vp3 in proportions of 1:1:10 respectively. Vp3 is used in receptor recognition at the surface of cells and the N-terminus of Vp1 contains a phospholipase domain essential for viral infectivity [183]. The AAV genome is flanked by two inverted terminal repeats (ITRs) which have a T-shaped hairpin structure containing a terminal resolution site (trs) and a rep binding element (RBE) that play essential roles in replication and encapsidation (Figure 1-5). The ITR is the only required cis-acting viral component necessary for genome replication, integration and packaging into the capsid. The *rep* and *cap* genes in the rAAV vector therefore, can be replaced with an expression cassette, consisting of the promoter, transgene and polyadenylation signal (Figure 1-5). The *rep* and *cap* genes are, instead, provided in *trans* from a different plasmid along with a helper construct containing the Ad early region genes, E1A, E1B, E4 and E2A and Ad virus-associated RNAs. E1A is responsible for transactivation of AAV gene expression and E4 and E1B help the transport of mRNA to the cytoplasm, thereby regulating AAV gene expression.

Transcription from the vector promoter is initiated by the help of the E2A DNA binding protein, which is additionally involved in AAV DNA replication. The Ad virus-associated RNAs helps in initiating AAV protein synthesis by inhibiting the host cell shutoff mechanism of translation induced by interferons [184].

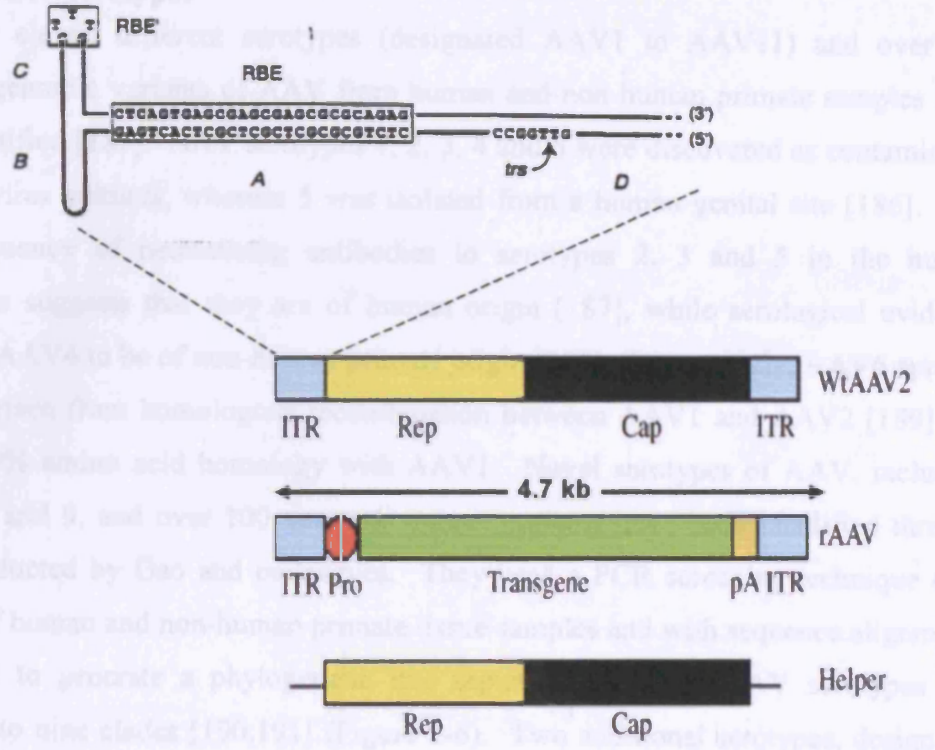

Figure 1-5. WtAAV genome and rAAV transgene cassette

This figure illustrates the structure of the wtAAV genome, which contains rep and cap genes that are flanked by two ITRs. The ITR has a T-shaped structure resulting from the palindromic sequence folded on itself to optimise potential base pairing. The positions of the Terminal Resolution Site (TRS), the Rep Binding Element (RBE) and a portion of the small internal palindromes within the terminal hairpin (RBE') are indicated. The rAAV transgene cassette consists of a promoter (Pro), the gene of interest and a polyadenylation site (pA). Below this is the helper plasmid, which contains essential genes for viral replication and encapsidation.

1.7.2.2 AAV serotypes

Currently eleven different serotypes (designated AAV1 to AAV11) and over one hundred genomic variants of AAV from human and non-human primate samples have been identified [185]. AAV serotypes 1, 2, 3, 4 and 6 were discovered as contaminants of adenovirus cultures, whereas 5 was isolated from a human genital site [186]. The high frequency of neutralising antibodies to serotypes 2, 3 and 5 in the human population suggests that they are of human origin [187], while serological evidence indicates AAV4 to be of non-human primate origin [188]. Interestingly, AAV6 appears to have arisen from homologous recombination between AAV1 and AAV2 [189] and has a >99% amino acid homology with AAV1. Novel serotypes of AAV, including AAV7, 8 and 9, and over 100 new and unique variants have been identified through work conducted by Gao and colleagues. They used a PCR screening technique on a number of human and non-human primate tissue samples and with sequence alignments were able to generate a phylogenetic tree separating the new AAV serotypes and isolates into nine clades [190;191] (Figure 1-6). Two additional serotypes, designated AAV10 and AAV11, have recently been identified in cynomolgus monkey tissue. Phylogenetic analysis of their capsid proteins showed that they resembled most AAV8 and AAV4 respectively [192].

All serotypes, apart from AAV6, exhibit a significantly different amino-acid sequence of the capsid proteins, with the most divergent region located in VP3 [193]. Table 1-1 shows the capsid amino acid homology between AAV serotypes 1-9 and it is clear that AAV4 and AAV5 share the least homology with other serotypes.

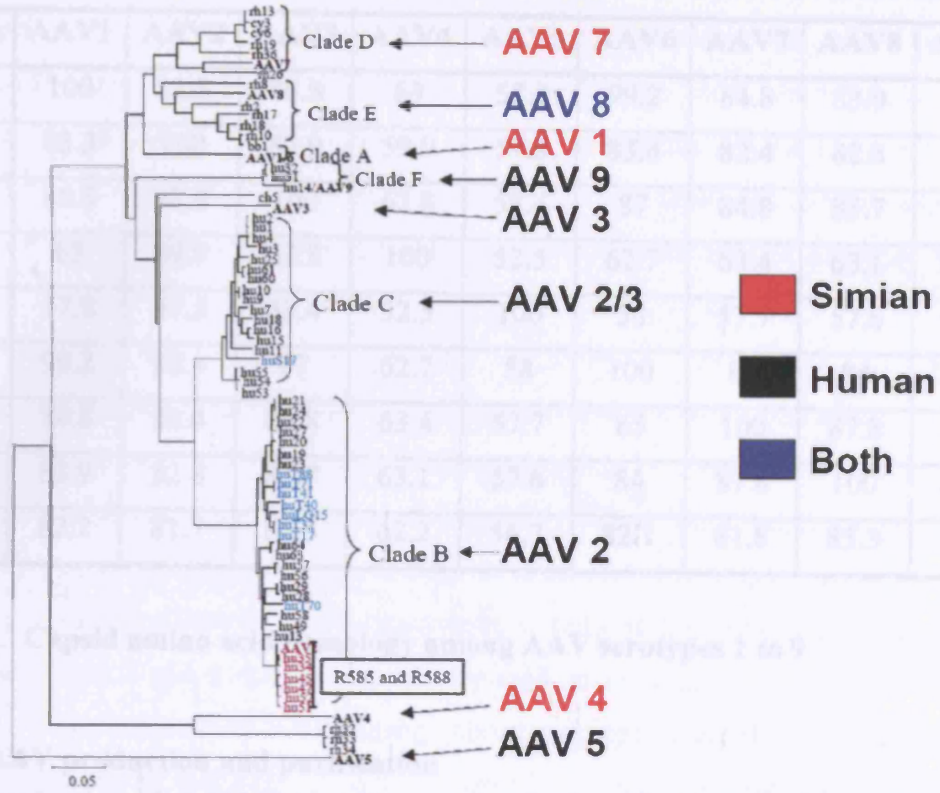

Figure 1-6. A phylogenetic tree separating the AAV serotypes and isolates into clades

Gao and colleagues used a PCR screening technique on a number of human and non-human primate tissue samples and with sequence alignments were able to generate a phylogenetic tree separating the new AAV serotypes and isolates into nine clades [190;194]. The origin of each AAV serotype is indicated.

Serotype	AAV1	AAV2	AAV3	AAV4	AAV5	AAV6	AAV7	AAV8	AAV9
AAV1	100	83.3	86.8	63	57.9	99.2	84.8	83.9	82.2
AAV2	83.3	100	87.9	59.9	57.3	83.4	82.4	82.8	81.7
AAV3	86.8	87.9	100	62.8	58.4	87	84.8	85.7	83.6
AAV4	63	59.9	62.8	100	52.5	62.7	63.4	63.1	62.2
AAV5	57.9	57.3	58.4	52.5	100	58	57.7	57.6	56.7
AAV6	99.2	83.4	87	62.7	58	100	85	84	82.1
AAV7	84.8	82.4	84.8	63.4	57.7	85	100	87.8	81.8
AAV8	83.9	82.8	85.7	63.1	57.6	84	87.8	100	85.3
AAV9	82.2	81.7	83.6	62.2	56.7	82.1	81.8	85.3	100

Table 1-1. Capsid amino acid homology among AAV serotypes 1 to 9

1.7.2.3 AAV production and purification

Initially, production of rAAV involved the co-transfection of cells with vector DNA and a packaging plasmid followed by infection with Ad [195]. Concerns, however, were raised over the safety of this method as AAV stocks were often contaminated with adenoviral capsids. Significant improvements have since been made and currently the method of choice requires a triple transfection of vector DNA, containing the transgene cassette, a packaging plasmid to supply Rep and Cap proteins, and a helper plasmid carrying Ad genes [196]. It is also now possible to scale-up AAV production by the use of cell lines that stably express the desired vector DNA and the essential Rep and Cap genes; infection with Ad is all that is needed to generate rAAV [197]. Furthermore, Urabe and colleagues have developed a baculovirus expression vector system for large-scale rAAV production in SF9 insect cells [198]. Their method involves the co-infection of SF9 cells with a Rep-baculovirus, a VP-baculovirus and an AAV vector genome baculovirus; the rAAV particles produced are identical to those generated in mammalian cells in both physiological properties and biological activities. The baculovirus helpers, however, were discovered to be prone to passage-dependent, loss-of-function deletions, which resulted in a decrease in rAAV titer. The system has since been modified to alleviate the instability and a much more efficient and convenient method has now been generated for the large-scale production of AAV [199].

Another significant development in the production of AAV has been the generation of pseudotyped AAV vectors. It is now possible to cross-package the AAV2 vector genome with capsid proteins of a different serotype [200]. To achieve this, a triple transfection is carried out with a helper plasmid containing AAV2 ITRs and rep proteins, but with cap proteins from an alternative serotype. Unbiased comparisons can therefore, be made between different serotypes, since they all contain identical AAV genomes.

Caesium chloride density gradient ultracentrifugation was the conventional method for the purification of AAV, however, this technique resulted in a significant loss in viral titer and vector preparations often varied in quality. Non-ionic iodixanol gradients followed by ion-exchange or heparin-affinity column chromatography are now more routinely used [201]. Heparin-affinity columns can only be applied to the purification of AAV-serotypes 2 and 6 due to their ability to bind to heparin sulphate; however, alternative protocols based on ion-exchange chromatography have been developed for serotypes 1, 2, 5 and 8 [202;203].

1.7.2.4 AAV and tissue tropism

Early studies were based on AAV2 as it was the first serotype to be fully characterised and demonstrated high transduction efficiency in a broad range of tissues and cells *in vitro*. Unfortunately, rAAV2 is less efficient *in vivo* and clinical trials have shown little progress. For example, in a study with haemophilia B patients, intramuscular transfer and transient expression of factor IX was evident, although persistence of the gene was not sufficient for long-term efficacy [204]. Fortunately, the alternative serotypes have been evaluated and show strikingly improved transduction efficiencies in a variety of tissue types. AAV1, AAV6 and AAV7 show high levels of transduction in skeletal muscle [191;205-208], whereas, AAV8 has a higher tropism for the liver and in a murine model was found to have 10-100 fold higher transduction than AAV2 [191;209;210]. Unlike other serotypes, AAV8 can transduce multiple organs and disseminate throughout the body; Nakai *et al.* found that intravascular administration of a rAAV8 vector at a high dose could transduce all the skeletal muscles throughout the body [211]. Furthermore, a recent study demonstrated systemic gene transfer in skeletal and cardiac muscle following intravenous injection of AAV8 [212]. It can therefore be considered as a robust vector for gene transfer, albeit caution is required as spillover and undesirable transduction could have adverse consequences. Inagaki and colleagues

have recently discovered that AAV9 is as robust as AAV8 and can also cross vascular endothelial cell barriers very efficiently and transduce many nonhepatic tissues following systemic administration [213]. This study and two others have also shown that serotype 9 preferentially transduces the myocardium and, in terms of gene delivery efficiency to this tissue, outperforms AAV8 [214;215].

Interestingly, one study has shown that the primary barrier to transduction of the liver with AAV2 is slow uncoating of its vector genome in the nucleus. Conversely, vector genomes packaged inside AAV6 and AAV8 do not persist as encapsidated molecules, but uncoat rapidly and are, therefore, able to convert to stable, biologically active double-stranded molecular forms more efficiently [216]. Furthermore, a recent study has helped to elucidate the transduction mechanisms of AAV8. Here, they screened a mouse liver complementary DNA library for cellular proteins capable of interacting with the viral capsid proteins. The researchers identified two endosomal proteases, cathepsins B and L, which act as uncoating factors for a number of other viruses and, in the report, they demonstrate the ability of these cathepsins to bind to and cleave the capsids of both AAV8 and AAV2. Interestingly, AAV2 and AAV8 were found to be processed differently by the proteases and AAV8 exhibited a quicker rate of cleavage; these differences were thought to account for the more rapid uncoating and higher transduction efficiency of AAV8 [217].

1.7.2.5 AAV and cell surface receptors

The diverse tissue tropisms of different AAV serotypes is partly due to their binding to alternate cellular receptors. AAV2 has been shown to bind to various receptors including HSPG [218], human fibroblast growth factor receptor 1 (FGFR1) [219], hepatocyte growth factor receptor [220] and integrins $\alpha_v\beta_5/\alpha_v\beta_1$ [221]. Furthermore, the amino acids within the capsid of AAV2 that contribute to HSPG binding have been identified [222]. These amino acids are not present in the capsids of AAV1, AAV3 and AAV6, yet serotypes 3 and 6 still have the ability to bind HSPG [200;206]; other residues must, therefore, be responsible for heparin binding. In a similar manner to that of AAV2, AAV3 also binds to FGFR1 [223]. In contrast to the aforementioned serotypes, AAV4 uses sialic acid, and AAV5 both sialic acid and platelet-derived growth factor (PDGF) receptors, for binding [224;225]. Recent reports have also shown that in certain cell types, sialic acid is used by both AAV1 and AAV6 [226;227], and a further study has established that they use N-linked and not O-linked sialic acids [228].

The laminin receptor (Lam-R) has recently been identified as the receptor for AAV8 and, in addition, was found to play an important role in the transduction of serotypes 2, 3 and 9. The Lam-R is constitutively expressed in several tissues, which may explain the broad tissue tropism of AAV8 [229].

1.7.2.6 AAV and immunity

Unlike adenoviruses, little or no innate immunity is induced following AAV vector transfer *in vivo*. An adaptive immune response, however, does occur which can eliminate the vector and the transfected cells, thus limiting sustained transgene expression. Adaptive immunity includes a humoral response, characterised by the production of neutralising antibodies specific for the vector or transgene antigen, and a cell-mediated response involving T-cells and N-K cells. The adaptive cell-mediated response, however, is far weaker with AAV vectors than with other viral vectors due to the inability of AAV to efficiently transduce or activate antigen presenting cells (APCs).

The prevalence of anti-AAV2 antibodies in the human population ranges from 35 to 80% according to the age group and geographic location [187]. Pre-existing immunity to AAV2 ultimately creates an additional barrier to effective gene delivery by an AAV2 vector and reduces the efficiency of repeated administration. Neutralising antibodies to other AAV serotypes have also been identified in the human population. Xiao et al. screened a cohort of 77 normal human volunteers for the presence of neutralising antibodies to AAV serotypes 1 and 2 and found that 20% had anti-AAV1 antibodies and 27% had anti-AAV2 antibodies [230]. The prevalence of neutralising anti-AAV5 and 6 antibodies has also been assessed in 37 normal individuals; only 10-20% were seropositive for AAV5 and 20-30% seropositive for AAV6 [231]. Neutralising anti-AAV5 antibodies are clearly uncommon and, in fact, one study reported that they were consistently negative in 85 healthy human subjects [232]. Several studies carried out in animals have shown that neutralising antibodies eliminate or greatly reduce the levels of transgene expression of the re-administered vector. Repeated administration of AAV2, in particular, was found to inhibit transgene expression in both the lung [233] and liver [234]. Fortunately, the alternative AAV serotypes offer more benefit in terms of evading the host immune response [235;236]. The cross-reactivity between neutralising antibodies of different serotypes has been assessed. For example, Halbert and colleagues re-administered various AAV vectors in mouse lung and discovered that serum from mice pre-immunised with AAV2 did not neutralise AAV6 infection, and

vice-versa, indicating that neutralising anti-AAV2 and 6 antibodies do not cross-react in mice [237]. Another study found that AAV1, 2 and 5 could be cross-administered in immunocompetent mice without causing any significant change in gene expression [208].

One of the main advantages of using the non-human primate isolates AAV7, 8, 10 and 11 is their ability to evade the human immune system; neutralising antibodies to these serotypes are rare in human serum and when present are low in activity [192;194;207]. For example, haemophilia B dogs receiving intraportal injections of an AAV2/8 vector, expressing factor IX, did not develop vector-related toxicity and antibodies against the transgene [238]. There is also a lack of cross-reactivity between mouse antisera against AAV2, AAV10 and AAV11 capsids [239]. Furthermore, intrapleural administration of an AAV10 vector, expressing alpha1-antitrypsin, provided long-term transgene expression in mice pre-immunised with AAV5 [240]. AAV serotype 9, although isolated from human tissue, also has the ability to circumvent the neutralising effect of pre-existing AAV antibodies. Recently, an AAV9 vector was found to efficiently transduce murine alveolar and nasal epithelia and, most importantly, could be re-administered without diminution [241].

1.7.2.6.1 Factors influencing immune responses against the AAV vector

Both cell-mediated and humoral responses to components of the AAV vector and the delivered transgene depend on a number of factors; these include the nature of the transgene, the promoter used, the route of administration, vector dose and host factors. The route of administration and promoters are the two factors more relevant to the work carried out in this thesis, which are therefore discussed in more detail below.

Route of administration

Several studies have shown that the extent of the immune response varies greatly with the route of administration. Mice that were given AAV-ovalbumin (OVA) injections intraperitoneally, intravenously or subcutaneously all developed antibodies against OVA and cytotoxic T-cells specific to OVA. A much weaker cytotoxic cell-mediated response, however, was generated in mice injected via the muscle [242]. Conversely, in a later study using muscle directed AAV2 gene transfer, OVA expression was completely eliminated by a local immune response, involving cytotoxic T-cells [243]. Interestingly, a cell-mediated response to human factor IX was observed in mice after

intramuscular administration, but a much weaker immune response was elicited following hepatic gene transfer [244]. One explanation for this is that immune tolerance has, previously, been found to favour the high expression of factor IX and the associated antibody suppressive $CD4^+$ T-cells produced following liver directed gene transfer [245]. Another report, however, has further complicated the issue of anti-AAV immunity; in this study an autoimmune response in nonhuman primates resulted from AAV vector transfer of erythropoietin injected into the muscle and aerosolised in the lung. This immune response could not be restricted to specific serotypes as it was observed in 3 of the 4 serotypes tested and was not due to intramuscular administration as it was also seen in macaques where the AAV vector was administered via the lung [246].

Promoters

Interactions between transgene promoters and the host immune system have been well documented. Cytokines present at the site of injection can either inhibit or activate promoters. For example, IFN-γ and IL-10 were discovered to down-regulate the activity of the cytomegalovirus (CMV) promoter in endothelial cells, whereas, TNF-α, IL-1β and IL-4 increased promoter activity [247]. Mouse strain-specific differences in the induction of these cytokines has also been hypothesised to influence CMV shut-down [248]. In addition, the CMV promoter is subject to transcriptional silencing in some tissues, by methylation of the CpG dinucleotides [249]. The hybrid version of this promoter, CMV enhancer/chicken β-actin (CAG), however, is not susceptible to silencing and has been reported to show 137-fold higher transgene expression compared with the CMV promoter in the liver [250]. The CAG promoter was also found to be more active than the CMV promoter in the lung [251] and has exhibited efficient transgene expression in muscle [252]. Although both CMV and CAG drive high levels of transgene expression in many different types of cells and tissues, expression from these promoters is often only temporary and inactivation by the host immune system is likely instigated.

One approach that is now being used in an attempt to evade the host immune system is the incorporation of a promoter in the vector that constrains expression to the tissue being transduced. Several reports have shown that tissue-specific promoters significantly eliminate host immune reactions to the vector and transgene. A recent

study directly compared the efficiency of two AAV vectors driven by a liver-specific promoter (LSP) and a CAG promoter. No antibodies against the transgene were detected in response to the AAV-LSP vector, whereas the CAG-driven vector provoked an escalating cellular immune response resulting in a much lower level of transgene expression [253]. The importance of using tissue-specific promoters in skeletal muscle has also been documented. The muscle creatine kinase (MCK) promoter, which was first used by Cordier et al. [254] has been reported in several studies to evade the host immune response. In one study, a MCK promoter/enhancer directed a high level of muscle-restricted transgene expression and provoked only a humoral (not cellular) immune response [255]. Similarly, a recent study found that a hybrid promoter containing the MCK enhancer and simian virus 40 (SV40) promoter yielded long-term expression of a reporter gene following electrotransfer of the plasmid into mice; expression using the CMV and CAG promoters, however, diminished within a few weeks [256]. Tissue specificity has also been achieved with the use of a small, MCK regulatory element, CK6 [257] and a synthetic C512 promoter, consisting of a combination of several myogenic regulatory elements (TEF-1, MEF-1, MEF-2 and TEF-1) [258]. One study demonstrated therapeutic levels of F.IX transgene expression from the C512 promoter *in vivo*, however, it failed to eliminate antibody formation in response to F.IX [259]. In another report the CK6 promoter, although only 10% as active as the ubiquitous CMV promoter *in vivo*, regulated microdystrophin gene expression and was readily tolerated by mice for at least 8 weeks [260].

1.7.2.7 Skeletal muscle as a target tissue for AAV transduction

Skeletal muscle is an important target for gene delivery and it is now viewed as an attractive alternative to the liver. Muscle is easily accessible for delivery of vectors, highly vascularised and actively secretory and a stable tissue with little nuclear turnover, which allows it to function as a reservoir for heterologous expression of recombinant proteins [261;262]. Indeed, the transduction of skeletal muscle with rAAV has been extensively applied to animal models for the treatment of various genetic diseases. AAV has a natural tropism for muscle fibres and several studies have shown that when rAAV vectors are injected into muscle transgene expression reaches a plateau and is sustained for weeks [263;264]. In fact, Xiao et al. [264] observed maintained expression of *LacZ* following muscle transduction for 1.5 years without elicitation of an immune response.

In 1999, Chao et al. administered a rAAV2 vector expressing FIX into the skeletal muscle of haemophilic B dogs and demonstrated circulating FIX at levels of 1-2% of normal for a year post-injection, albeit plasma infusions were still required [265]. Improvements, however, were reported a year later using a CMV-driven rAAV2 vector; sustained therapeutic levels of FIX and partial correction of whole blood clotting and activated thromboplastin time were achieved in treated dogs [266]. AAV-mediated gene transfer to skeletal muscle has also been assessed for its potential to treat muscle wasting diseases such as limb-girdle muscular dystrophy [267-269]. In a recent report, Pacak et al. intramuscularly injected sarcoglycan-deficient mice with a creatine kinase promoter-driven AAV serotype 1 vector expressing the human sarcoglycan gene. Expression was localised to the sarcolemma and reduced muscle fibre damage was apparent; moreover, animals showed continued tissue correction for 6 months post-administration of vector [268]. In a canine model of Duchenne muscular dystrophy, prolonged AAV6-mediated microdystrophin expression in the skeletal muscle was achieved using a short course of immunosupression. Canine microdystrophin was still present in the muscle 30 weeks post-injection and its expression restored localisation of components of the dystrophin-associated protein complex at the muscle membrane [270].

1.7.2.8 AAV vector improvements

1.7.2.8.1 Hybrid AAV vector engineering from different AAV serotypes

Despite the fact that AAV has enjoyed some success in human clinical trials, several challenges remain. For example, the prevalence of pre-existing neutralising antibodies in humans previously exposed to AAV significantly attenuates the efficacy of AAV vectors [233;234]. Additional problems with AAV vectors include their limited packaging capacity [271], poor infection of refractory cells [272] and achieving targeted delivery of therapeutic transgenes to specific tissue types. These challenges have therefore, prompted the generation of new AAV vectors with selective features from different serotypes that synergistically enhance transgene expression.

Hauck et al. developed a strategy to generate mosaic vectors, which have a capsid structure composed of a mixture of capsid proteins from different serotypes. By mixing helper plasmids encoding the capsid proteins of AAV1 and AAV2 in the transfection process, he was able to combine the strong affinity of AAV1 for muscle and the high

heparin binding activity of AAV2 into one hybrid vector [273]. Using a similar approach, Rabinowitz et al. generated mosaic vectors by the transfection of pairwise combinations of helper constructs for AAV serotypes 1 to 5 at different ratios. Some of the properties of the two serotypes were shared, some were masked and some were dominant depending on the ratio of the helper plasmid used. Furthermore, additive properties, found in neither of the parental serotypes were observed in the new mosaic vectors. Another interesting observation was the differing mosaic AAV titers; high titers were obtained from mosaic vectors involving a combination of either serotypes 1, 2 or 3, whereas intermediate AAV titers were obtained from serotype 5 mixtures [274].

Chimeric vectors differ from mosaic vectors in that they contain capsid proteins that have been modified by amino acid or domain swapping between different serotypes. Samulski and colleagues have recently shown that it is possible to transfer the muscle binding characteristics of AAV1 to AAV2 by swapping only five amino acid residues. The same group have produced a chimeric AAV3 vector, exhibiting higher transduction efficiency in mouse heart compared with the parental AAV3; this was achieved by substituting similar amino acid residues [239]. Another study has reported the characterisation of a chimeric vector, named AAV-221-IV, for its effectiveness in the treatment of haemophilia B in mice. Here they replaced amino acids 350 to 430 of AAV2 VP1 with the corresponding amino acids from VP1 of AAV1 and discovered that intramuscular injection of this hybrid vector produced 4-10 fold higher human factor IX expression in the plasma compared with the AAV2 vector [275].

Directed evolution has been used in a number of facets, for example to generate enzymes with novel catalytic qualities [276] and retroviruses with new properties [277]. Directed evolution can be brought about by strategies such as DNA shuffling and error-prone PCR, which generate diversity by recombination and combining useful mutations from individual genes. Maheshri et al. have developed an efficient and high-throughput method to generate AAV vectors with improved capabilities. They produced a large AAV2 library with randomly distributed capsid mutations and selected for AAV variants that had altered receptor-binding properties and with the ability to evade neutralising antibodies [278].

1.7.2.8.2 Other new technologies for AAV vector improvements

Short peptide sequences that encode specific receptor ligands have been engineered into the AAV capsid open reading frame as a way to alter vector tropism. These changes can result in vectors with expanded or more selective tropism. The success of the introduction of receptor-targeting peptides into AAV capsid proteins depends on proper surface display and presentation of the ligand to its receptor. Extended work has therefore, been carried out to identify the best position for insertion in the AAV2 capsid. Girod et al. inserted a peptide containing an RGD motif into the surface loop position (residue 587) of AAV2. The modified vector was capable of transducing a cell line normally refractory to AAV2 infection [279]. Phage display methods of randomised peptide sequences have also been used to select peptides with cell-specific binding properties. For example, AAV2, normally has a relatively poor tropism for endothelial cells, however, insertion of a phage display-derived peptide increased the efficiency and selectivity of AAV2 endothelial cell transduction following intravenous injection [280]. Caution, however, is required with these techniques since the genetic insertion of foreign sequences can often result in loss of function or loss of virion integrity. A novel approach to AAV vector targeting has, thus been described which involves engineering AAV vectors to be metabolically biotinylated during production in mammalian cells. These biotinylated vectors can be easily purified by affinity chromatography on an avidin resin and also efficiently targeted to cells engineered to express the avidin-biotin receptor [281].

Several techniques have been used to overcome the packaging constraint of AAV (Figure 1-5); for example "mini-genes" have been generated which fit into a single AAV virion [282] and large genes have been split into small fragments which are then packaged into separate AAV viruses. The key issue, however, with the latter approach is the ability of the fragments to reassemble into a functional expression unit within the cell. One approach has been to split the gene into two overlapping fragments, which then re-assemble in the cell through homologous recombination between the two fragments. AAV6 has demonstrated the highest efficiency for overlapping vector-mediated muscle gene therapy [283].

1.7.3 Self-complementary AAV vectors

A major limiting factor in the efficiency of ssAAV vectors is their requirement for either host-cell mediated synthesis of the complementary-strand or annealing of the plus and minus strands from two separate viral particles co-infected into the same cell.

Samulski et al. (2001), however, have found a way to circumvent this problem by packaging both strands as a single DNA molecule. By utilising the knowledge that rAAV DNA of half or less than the wtAAV genome length can be packaged as a dimer [284] they have developed a self-complementary vector [285]. In this construct the terminal resolution site (trs), from which replication initiates, is deleted from one of the ITR regions and the effect is that replication initiates from the wild-type ITR, proceeds through the mutant end without terminal resolution and continues back across the genome, using the opposite strand as a template to create the dimer. The result is a linear self-complementary genome with two wild-type ITRs at either end and a mutated ITR in the middle (Figure 1-7). After uncoating in the cell nucleus, the vector rapidly undergoes base pairing to form a double-stranded molecule without the help of the host, thus, bypassing the rate-limiting step. In one study, transduction of mouse liver, muscle and brain with the scAAV vector demonstrated faster onset of gene expression and higher transduction efficiency when compared with the conventional ssAAV [286]. A later study also reported stable and rapid transgene expression following intramuscular injection of a scAAV vector, but, in addition, discovered that transgene expression from scAAV was balanced over time by the ssAAV vector [287]. Molecular rearrangement of the ssAAV vector genome into either circular or linear concatemers is an essential event for stable persistence of the transgene *in vivo* [177;178]. A double stranded structural intermediate is required for such molecular rearrangements to occur, and since this event does not occur immediately after transduction, a rapid disintegration of linear single-stranded vector genome follows. In contrast, delivery of the double-stranded scAAV genome may account for stable persistence early after transduction. Recently, Nathwani et al. reported a 20-fold improvement in human FIX expression in mice, following transduction of the liver with an AAV8 pseudotyped scAAV vector. Furthermore, they found that an AAV5 pseudotyped scAAV vector mediated efficient transduction in non-human primates with pre-existing immunity to AAV8 [288].

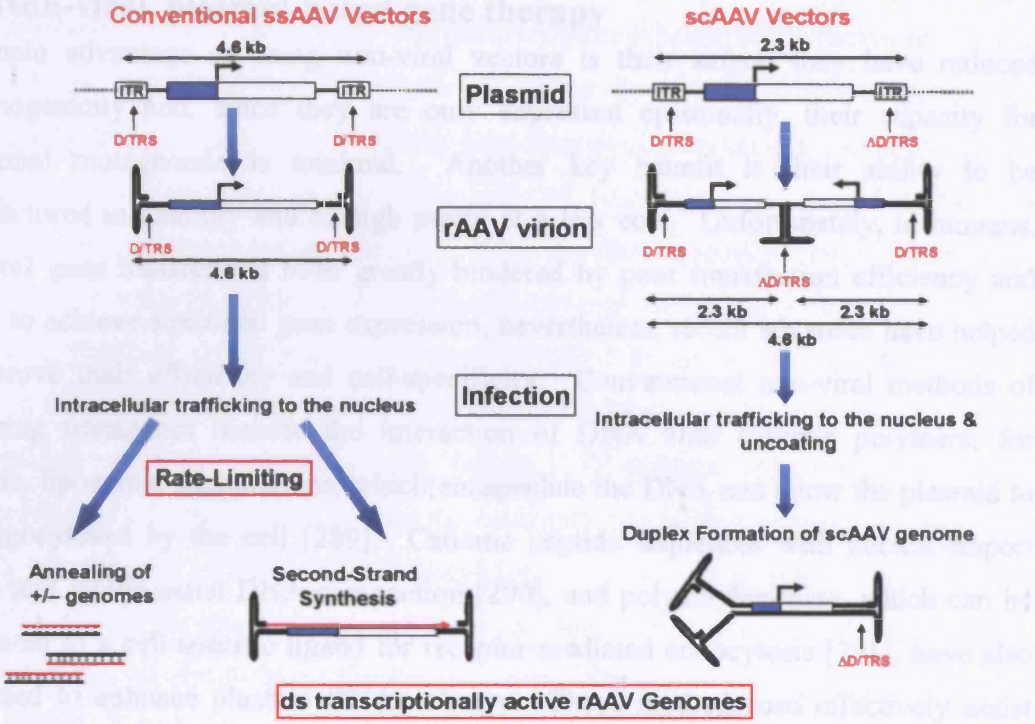

Figure 1-7. Conventional ssAAV vs scAAV vectors

This diagram illustrates how ssAAV and scAAV vectors differ in the size of their transgene cassette, their replication and generation into viral particles and their infection and formation of transcriptionally active rAAV genomes. Both vectors are flanked by ITRs, however, the right-hand ITR of scAAV vectors is mutated by deleting the terminal resolution site (TRS) within the D sequence (ΔD/TRS). The effect is that replication initiates from the wild-type ITR, proceeds through the mutant end without terminal resolution and continues back across the genome, using the opposite strand as a template to create the dimer. The result is a linear self-complementary genome with two wild-type ITRs at either end and a mutated ITR in the middle. The scAAV transgene cassette, however, must be half the size of the conventional ssAAV vector, which is achieved by using truncated promoters [288] and/or removing non-coding sequences. After uncoating in the cell nucleus, the vector genomes are converted into double-stranded transcriptionally active DNA. For ssAAV-mediated transduction, annealing of plus and minus genomes, and perhaps second-strand synthesis is required, both of which are considered rate limiting steps. For scAAV vectors, the complementary sequences rapidly hybridise to form stable DNA duplexes.

1.8 Non-viral, plasmid-based gene therapy

The main advantage of using non-viral vectors is their safety; they have reduced immunogenicity and, since they are only expressed episomally, their capacity for insertional mutagenesis is minimal. Another key benefit is their ability to be manufactured in quantity and to high purity at a low cost. Unfortunately, in humans, non-viral gene transfer has been greatly hindered by poor transfection efficiency and failure to achieve sustained gene expression, nevertheless, recent advances have helped to improve their efficiency and cell-specificity. Conventional non-viral methods of delivering transgenes include the interaction of DNA with cationic polymers; for example, liposomal formulations, which encapsulate the DNA and allow the plasmid to be phagocytosed by the cell [289]. Cationic peptide sequences with nuclear-import signals and which assist DNA compaction [290], and polyethylenimine, which can be conjugated to a cell-specific ligand for receptor-mediated endocytosis [291], have also been used to enhance plasmid DNA delivery. These methods can effectively assist DNA entry into the cell *in vitro*; however, *in vivo* the transfection efficiency is poor and only transient gene expression is achieved. Barriers to efficient *in vivo* transfection include blood plasma proteins, binding to a broad variety of non-target cell types and the extracellular matrix. Transfection complexes must, therefore, be soluble, small enough to allow passage through physiological barriers and have target cell specificity. Once inside the cell, the passage of the transgene to the nucleus is also hampered by obstacles such as cytoplasmic degradative enzymes and the double-membrane structure of the nuclear envelope.

The most important improvements in plasmid delivery, however, have been achieved with the use of physical methods such as hydrodynamic pressure [292], microinjection of DNA into individual cells [293] and electroporation [294]. Electroporation or electrotransfer involves the application of an electrical field to the cells or tissue, which increases cell membrane permeability and facilitates the transport of plasmid DNA into and through the cell. Electroporation was originally developed for *in vitro* transfection [295] and has now become a standard laboratory method. Skeletal muscle has been the most investigated target tissue for gene therapy by *in vivo* electroporation due to its ready access and ability to sustain long-term expression of the episomal plasmid. Intramuscular electroporation has, therefore, been tested therapeutically with many gene types in numerous disease models. This technique resulted in highly efficient transfer

of the β-galactosidase reporter gene in dystrophic muscle with limited muscle damage. Approximately 40% of muscle fibre was efficiently transfected over a period of 1 week, with both the superficial and deep portions of the dystrophic muscle displaying β-galactosidase expression [296]. In cancer gene therapy, intramuscular electrotransfer of IL-12 resulted in significant levels of plasma IL-12, which persisted for at least 60 days and completely regressed murine tumours [297]. Another success in cancer therapeutics was reported with electroporation-mediated intramuscular injection of a plasmid expressing TIMP-4. Here, sustained plasma TIMP-4 levels were demonstrated for a period of 14 days and accompanied by significant tumour suppression [298]. The direct electrotransfer of a plasmid expressing human IL-1 receptor antagonist (IL-1Ra) to skeletal muscle was reported to reduce the incidence of collagen-induced arthritis with the effect lasting for 20 days. The investigators demonstrated a peak on day 10 in the level of IL-1Ra in the injected area and in serum, followed by a gradual decrease [299]. In most studies, electroporation significantly enhanced and resulted in long-term gene expression compared with injection of plasmid DNA alone. The means, however, by which electroporation enhances gene expression in skeletal muscle is debatable. It is widely believed that the electric pulses create pores in the membrane through which the plasmids move by an electrophoretic effect [300]. Another study proposed a mechanism of DNA uptake by receptor-mediated endocytosis [301]. Neither of these mechanisms, however, explain how prolonged transgene expression is achieved in muscles after electroporation, although one recent report suggests that activation and transfection of myogenic satellite cells, which develop into regenerated muscle fibres, could be involved [302].

Extra-chromosomal replication and stability is another hurdle for plasmid-mediated gene delivery. Plasmid DNA that is delivered to the nucleus is generally not replicated and is lost during the breakdown of the nuclear envelope at mitosis. A plasmid, however, has been generated that contains an SV40-ori sequence and the scaffold/matrix attachment region (S/MAR) from the human β-interferon gene cluster [303]. This plasmid, designated "pEPI", does not require viral genes for episomal maintenance and is stably propagated over several cell generations in culture without selection [304]. The S/MAR element in pEPI has been found to interact with components of the nuclear matrix [305]. Interestingly, one study reported that the CMV promoter, in a vector construct containing S/MAR, was not subject to silencing by cytosine methylation and, thus, long-term gene expression was observed. Whether this

was due to the S/MAR present in this construct, the episomal status of the vector or a combination of both, is still uncertain [306]. The bacterial backbone of plasmid DNA also seems to be a factor in transgene silencing. Recently the use of DNA vectors devoid of bacterial sequences gave robust and persistent transgene expression [307].

The methods discussed above all rely on the host cell machinery to achieve long-term nuclear gene expression, but at the same time avoid disrupting host gene expression or signalling pathways. This factor makes non-viral gene transfer preferable over the currently used viral-based methods. Furthermore, these advances in non-viral gene transfer now make the potential to mimic viral mechanisms, such as nuclear maintenance and replication, more realistic.

1.9 Gene therapy and ApoE

1.9.1 Viral

Recombinant adenoviruses (rAd) were used for the first gene transfer studies with ApoE in 1995; they reported a lowering in plasma cholesterol in $ApoE^{-/-}$ mice and a deceleration in aortic atherogenesis following intravenous injection [308]. Unfortunately, further research using this first generation rAd vector was hindered due to a strong cytotoxic T-cell immunological response directed against both the transgene and the rAd proteins. Transduced hepatocytes were cleared and repeat vector administration was precluded as a result of this immune response. Significant progress, however, was seen 5 years later in a study where $ApoE^{-/-}$ and immunodeficient mice were cross-bred and injected with rAd.ApoE3; a complete regression in advanced plaques at 6 months was demonstrated [309].

Prolonged ApoE transgene expression and reduced toxicity was observed with a 2^{nd} generation rAd vector, which had additional viral genome sequences deleted or inactivated in other early genes (E2 and/ or E4). One study used this new rAd vector to compare hepatic expression of different human ApoE isoforms in $ApoE^{-/-}$ mice with established atherosclerotic lesions. ApoE4 was found to be less effective in reducing regression and, most importantly, liver-secreted ApoE gained access to the arterial intima, where it is believed to sequester excess cellular cholesterol [310]. A subsequent study using this 2^{nd} generation rAd vector expressing ApoE3 further demonstrated the non-lipid lowering effect of ApoE. Here they found that liver-derived ApoE could

induce regression of pre-existing atherosclerotic plaques in $LDLR^{-/-}$ mice without lowering plasma cholesterol levels and altering the lipoprotein profile. Furthermore, the expressed ApoE markedly reduced isoprostane levels, a marker of oxidative stress, highlighting that the anti-oxidant property of ApoE contributes to its atheroprotective actions [311].

An improved rAd.ApoE3 vector, with E1, E3 and DNA polymerase deleted, exhibited high levels of plasma ApoE and normalised the hyperlipidaemia in $ApoE^{-/-}$ mice. Inhibition of early aortic lesions in these mice as well as regression of advanced atheroma in older animals was also observed, however, the effect was transient due to cellular shutdown of the CMV promoter [312]. Nevertheless, sustained ApoE transgene expression was achieved with the use of a (E1-, E3-, polymerase-, pTP-) rAd vector containing either a liver-specific promoter [313] or a promoter for cellular elongation factor 1α (EF-1α) [314]. Although plasma ApoE levels were low, significant retardation of atherosclerosis was demonstrated. An alternative rAd vector, known as the helper-dependent rAd (HD-rAd), has also been used for ApoE mediated gene transfer. A single intravenous injection of this vector carrying the mouse ApoE genomic locus into $ApoE^{-/-}$ mice provided lifelong correction of hypercholesterolaemia. Interestingly, the same vector expressing ApoE cDNA did not perform as well; ApoE levels slowly declined over time resulting in a partial return of the hypercholesterolaemic phenotype [315].

Replication-defective rAAV are attractive candidate vectors for gene transfer as, unlike rAd vectors, they are non-pathogenic and devoid of all viral structural genes, which diminishes the potential for a host immune response. For these reasons, rAAV vectors have also been used to mediate ApoE gene transfer. An AAV vector expressing human ApoE3 was used to transduce the tibialis anterior (TA) muscle of young $ApoE^{-/-}$ mice and although hyperlipidaemia was not reversed, as the levels of ApoE secreted were low, there was a 29% reduction of plaque formation up to 3 months later [316]. This study utilised a rAAV vector derived from AAV serotype 2, which is now well documented to be inefficient *in vivo* compared with other serotypes and could explain the disappointing outcome. Indeed, liver-directed administration of a pseudotyped AAV2/8 vector, expressing ApoE, into $ApoE^{-/-}$ mice produced normal human levels (50 to 80μg/ml) in the plasma [317]. More recently, intravenous injection of AAV2/7 and AAV2/8 vectors expressing human ApoE3 produced sustained therapeutic levels of

ApoE3 in plasma and cholesterol levels were lowered for up to 1 year. Furthermore, at termination atherosclerosis in these mice was completely prevented [318].

1.9.2 Non-viral

Transplantation of normal ($ApoE^{+/+}$) bone marrow cells into $ApoE^{-/-}$ mice successfully restores ApoE expression and, consequently, results in the reversal of hypercholesterolaemia and prevention of atherosclerosis progression in these animals [148;149]. One study has determined the minimal concentration of plasma ApoE required to reduce plasma cholesterol completely. By mixing $ApoE^{+/+}$ bone marrow with $ApoE^{-/-}$ bone marrow in increasing amounts and transplanting it into $ApoE^{-/-}$ recipient mice, it was deduced that only approximately 1μg ApoE/ml plasma (2.5% of normal levels) was required [319]. A novel gene therapy approach for the treatment of atherosclerosis in $ApoE^{-/-}$ mice has been the transplantation of homologous bone marrow cells, transduced with ApoE-expressing retroviral (RV) vectors. Initial studies using this technique observed ApoE expression from arterial macrophages and protection from early atherosclerosis in treated animals [320;321]. Later, a self-inactivating retroviral vector with macrophage-restricted expression was developed and which was reported to reverse both hypercholesterolaemia and atherosclerotic lesion development [322].

1.9.2.1 Plasmid-mediated

Although muscle does not normally secrete ApoE, non-hepatic, non-macrophage-derived ApoE is known to be atheroprotective [96;323]. For example, Rinaldi et al. injected naked plasmid DNA expressing human ApoE3 into the skeletal muscle of $ApoE^{-/-}$ mice and observed a sustained lowering in plasma cholesterol [324]. Another study, in contrast, reported that plasmid injections of ApoE into the muscle of $ApoE^{-/-}$ mice was not effective in reducing hyperlipidaemia, although, atherosclerotic lesion and xanthoma formation were significantly reduced after 9 months [325].

1.9.2.2 Cell-based therapies

A cell-based gene therapy approach utilising endothelial cells secreting ApoE has also been developed. The investigators delivered the endothelial cells intradermaly into $ApoE^{-/-}$ mice and found a significant lowering in plasma cholesterol, which was concomitant with a reduction in atherosclerotic lesion size [326]. Further refinement of

the cell-based gene-therapy approach for ApoE gene transfer has been investigated by Tagalakis et al. Here, Chinese hamster ovary (CHO) cells expressing human ApoE3 were encapsulated into alginate-based microspheres and implanted into the peritoneal cavity of $ApoE^{-/-}$ mice. ApoE3 was successfully secreted into the plasma, which lowered total cholesterol levels and increased atheroprotective HDL. Unfortunately, by day 14 both ApoE and total cholesterol levels had rebounded, which was believed to be due to the emergence of anti-ApoE antibodies, perhaps exacerbated by a non-specific host inflammatory reaction to capsule constituents [327].

Vector/expression plasmid	Animal model	Target tissue	Plasma total cholesterol	Lipoprotein profile	Plaque development and regression	Duration of expression	Ref.
rAd.CMV.ApoE3 (1st generation)	ApoE$^{-/-}$ mice	Liver	84% ↓	↓ VLDL/IDL/LDL and ↑ in HDL	↓ in aortic lesion development	1 month	[308]
rAd.CMV.ApoE3 (1st generation)	ApoE$^{-/-}$ nude mice	Liver	84% ↓	↓ VLDL/IDL/LDL and ↑ in HDL	87% ↓ in advanced aortic lesions	6 months	[309]
rAd.CMV.ApoE2/E3/ E4 (2nd generation)	ApoE$^{-/-}$ mice	Liver	E2 = 50% ↓ E3 and E4 = 70% ↓	↓ VLDL/IDL/LDL and ↑ in HDL	E2/E3/E4 ⇒ ↓ in progression, and E3 ⇒ regression	6 weeks	[310]
rAd.CMV.ApoE3 (2nd generation)	LDLR$^{-/-}$ mice	Liver	No ↓	No change	53% regression of advanced lesions	6 weeks	[311]
rAd.CMV.ApoE3 (2nd generation Pol^{-} vector)	ApoE$^{-/-}$ mice	Liver and muscle	Liver-directed = ↓	Liver-directed = ↓ VLDL/IDL/LDL and ↑ in HDL	Liver-directed = 38% ↓ in progression and 40% regression	Gradual decline after 7 days	[312]
rAd.LSP.ApoE3 (2nd generation)	ApoE$^{-/-}$ mice	Liver	No ↓	No change	30% ↓ aortic lesion development	Very low plasma levels over 28 weeks	[313]
rAd.EF-1α.ApoE3 (2nd generation)	ApoE$^{-/-}$ mice	Liver	No ↓	No change	15% ↓ aortic lesion development	Very low plasma levels over 37 weeks	[314]
HD-rAd.ApoE3	ApoE$^{-/-}$ mice	Liver	50% ↓	↓ VLDL/IDL/LDL and ↑ in HDL	Lesion-free aortas after 2.5 years	Detectable levels for >4 months	[315]
rAAV2.CMV.ApoE2/ E3	ApoE$^{-/-}$ mice	Muscle	No ↓	No change	E3 ⇒ 29% ↓ aortic lesion development	Undetectable levels	[316]
rAAV2/7.LSP.ApoE3 and rAAV2/8.LSP.ApoE3	ApoE$^{-/-}$ mice	Liver	92% ↓	↓ VLDL/IDL/LDL and ↑ in HDL	Lesion-free aortas after 1 year	Stable expression for 128 days and gradual decline thereafter	[318]
RV.CMV.ApoE3	ApoE$^{-/-}$ mice	Ex-vivo bone marrow cells	No ↓	No change	Significant ↓ aortic lesion development	Expression for 5.5 months	[320]
Self-inactivating RV.CMV.ApoE3	ApoE$^{-/-}$ mice	Ex-vivo bone marrow cells	66% ↓	No data	74% ↓ aortic lesion development	59% the level of wt mice 12 weeks post-transplantation	[322]
p.CMV.ApoE3	ApoE$^{-/-}$ mice	Muscle	42% ↓	↓ VLDL/IDL/LDL and ↑ in HDL	No data	Very low plasma levels 4 weeks post-injection	[324]
p.CMV.ApoE2/E3	ApoE$^{-/-}$ mice	Muscle	No ↓	No change	E2 ⇒ 20-30% ↓ aortic lesion development	E2 ⇒ detectable levels, E3 ⇒ undetectable levels	[325]

Table 1-2 Viral and non-viral gene therapy approaches for the delivery of ApoE

1.10 Aims of thesis

The main aim of this thesis is to identify and evaluate a potentially safe and effective rAAV vector(s) for reversing hypercholesterolaemia and regressing atherosclerotic plaques, namely muscle-based expression of human ApoE3 using rAAV to provide sustained systemic delivery. The work/steps carried out to achieve this aim are as follows:

- To construct ssAAV2 and scAAV2 plasmids all expressing human ApoE3, but driven by three different promoters, including two muscle specific (C512 and CK6) and one constitutive promoter (CAG). Cultured C2C12 myoblasts were then transiently transfected with all plasmids to check their ability to express ApoE3 *in vitro*.
- To directly inject these plasmids into skeletal muscle of $ApoE^{-/-}$ mice via electro-transfer and assess their efficiency *in vivo*.
- To generate pseudotyped ssAAV and scAAV vectors by packaging the AAV2 vector genome with the capsid from AAV serotype 7.
- The ssAAV and scAAV vectors, expressing ApoE3 were directly injected into skeletal muscle of $ApoE^{-/-}$ mice to form stable transgenic myofibres secreting ApoE.
- To evaluate the ability of these gene therapeutics to reverse hyperlipidaemia in this murine preclinical model of human heart disease. These studies will allow direct comparison of ssAAV and scAAV as gene therapy vectors and determine the most efficient promoter to drive ApoE3 expression.
- The ssAAV2/7.CAG.ApoE3 vector performed significantly better than the muscle-specific promoter-driven AAV vectors. We, therefore, decided to pseudotype the ssAAV2.CAG.ApoE3 vector with additional serotypes 8 and 9, which were directly injected into the skeletal muscle of young $ApoE^{-/-}$ mice. These serotypes were selected as both are reported to transduce various tissues efficiently and globally through systemic vector administration. Furthermore, there are no studies to date that have assessed transgene expression following direct injection of AAV9 into skeletal muscle.
- This study will allow the direct comparison of serotypes 7, 8 and 9 and determine which is most efficient for AAV transduction into skeletal muscle, with the ultimate goal to reverse hyperlipidaemia and inhibit the progression of atherosclerosis.

Chapter 2:

Materials and Methods

2 MATERIALS AND METHODS

2.1 Materials

2.1.1 Plasmid vectors and DNA resources

The ssAAV2.CAG plasmid was kindly given to us by Dongsheng Duan (University of Missouri, Columbia, MO USA), while Jeffrey S. Chamberlain (University of Washington, Seattle, Washington USA) and George Dickson (Royal Holloway University of London, Egham, Surrey) provided the CK6 and C512 promoters respectively. The scAAV2 plasmid was from Amit C. Nathwani (Department of Haematology, University College London, London, U.K). The p.CMV.DsRed2-C1 plasmid (p.CMV.RFP) was purchased from BD Clontech.

2.1.2 Animals

C57BL/6 ApoE$^{-/-}$ mice were bred and housed at The Royal Holloway University of London, and had originally been generated by inactivation of the mouse *ApoE* locus through homologous recombination [328].

2.1.3 Cell culture reagents

Dulbecco's modified Eagle's medium (DMEM, Sigma, Gillingham, Dorset, UK)

Heat-inactivated fetal bovine serum (FBS, Sigma)

Heat-inactivated horse serum (Sigma)

L-glutamine (Sigma)

Streptomycin (10mg/ml) and penicillin (10,000 units/ml) solution (Sigma)

Phosphate-buffered saline (PBS; 138mM NaCl, 10mM Na_2HPO_4, 1.75mM KH_2PO_4, 7.2mM KCL)

Trypsin-EDTA (0.25% trypsin and 0.2g EDTA) (Sigma)

Dimethylsulphoxide (DMSO; Sigma)

Trypan blue (Sigma)

Lipofectamine™ 2000 (Invitrogen, Paisley, UK)

2.1.4 Molecular Biology reagents

Bovine serum albumin (BSA; Sigma)

NuPAGE® LDS sample buffer (4×) (Invitrogen)

β-mercaptoethanol (Sigma)

MagicMark™ XP (Invitrogen)

NuPAGE® Novex 4-12% Bis-Tris polyacrylamide gels (Invitrogen)

NuPAGE® MES SDS running buffer (20×) (Invitrogen; 50mM MES, 50mM Tris base, 0.1% SDS, 1mM EDTA)

NuPAGE® Antioxidant (Invitrogen)

Hybond ECL nitrocellulose membrane (Amersham Biosciences, Piscataway, USA)

Hybond-N$^+$ nitrocellulose membrane (Amersham Biosciences)

NuPAGE® Transfer buffer (20×) (Invitrogen; 25mM Bicine, 25mM Bis-Tris, 1mM EDTA)

Ponceau S solution (Sigma)

Tween 20 (Sigma)

ECL detection system (Amersham Biosciences)

Hyperfilm ECL (Amersham Biosciences)

Restriction endonucleases (New England BioLabs, Ipswich, MA, USA)

Calf intestinal alkaline phosphatase (CIP) (New England BioLabs)

10× DNA ligase buffer (Promega; 300mM Tris-HCl (pH 7.8 at 25°C), 100mM $MgCl_2$, 100mM DTT and 10mM ATP)

T4 DNA ligase (Promega, Southampton, UK)

S.O.C medium (Invitrogen; 2% tryptone, 0.5% yeast extract, 10mM NaCl, 2.5mM KCl, 10mM $MgCl_2$, 10mM $MgSO_4$, 20mM glucose)

LB agar (Sigma; 1% tryptone, 0.5% yeast extract, 1% NaCl, agar 15 g/L)

LB broth (Sigma; 1% tryptone, 0.5% yeast extract, 1% NaCl)

Ethidium bromide (Sigma)

Agarose (Biogene, Kimbolton, Cambs., UK)

10× BLUEJUICE Gel Loading Buffer (Invitrogen; 65% sucrose, 10mM Tris-HCl, 10mM EDTA, 0.3% bromophenol blue)

Novex TBE Hi-Density Sample Buffer (Invitrogen; 18mM Tris base, 18mM boric acid, 0.4mM EDTA, 3% Ficoll, 0.02% bromophenol blue, 0.02% Xylene Cyanol)

TBE running buffer (Invitrogen; 89mM Tris base, 89mM boric acid, 2mM EDTA)

CelLytic MT Mammalian Tissue Lysis/Extraction Reagent (Sigma)

Complete mini, EDTA-free Protease Inhibitor cocktail tablets (Roche, Welwyn Garden City, Hertfordshire, UK)

Ampicillin sodium salt (Sigma)

Kanamycin (Sigma)

Benzonase (Sigma)

Optiprep density gradient medium/ Iodixanol (Sigma)

DNase I amplification grade (Invitrogen)

Proteinase K (Sigma)

Glycogen (Invitrogen)

Infinity cholesterol liquid stable reagent (Thermo Electron Corporation, Manchester, UK)

2.1.5 Antibodies

Polyclonal goat anti-human ApoE antibody (#0650-1904, Biogenesis, Poole, UK)

Anti-goat IgG (whole molecule, peroxidase conjugate) (Sigma)

Goat polyclonal anti-human ApoE antibody (#178479, Calbiochem/Merck Biosciences)

Recombinant Apolipoprotein E (#178475, ApoE3 isoform; Calbiochem/Merck Biosciences)

2.1.6 Kits

Bio-Rad Protein Assay Kit (Bio-Rad, Hemel Hempstead, UK)

ECL Protein Biotinylation Module (Amersham Biosciences)

TMB substrate kit (Pierce, Perbio Science, Northumberland, UK)

DH5α chemically competent *E.coli* (Invitrogen)

One shot TOP10 chemically competent *E.coli* (Invitrogen)

Wizard Plus SV miniprep DNA Purification System (Promega)

QIAquick Gel Extraction Kit (Qiagen, Crawley, West Sussex, UK)

EndoFree Plasmid Maxi kit (Qiagen)

QuantiTect SYBR Green PCR Kit (Qiagen)

PureLink™ HiPure Plasmid Megaprep kit (Invitrogen)

ECL direct nucleic acid labelling and detection system (Amersham)

Hydragel Lipo + Lp(a) K20 kit (Analytical Technologies, Hampshire, UK)

The PlusOne silver staining kit (GE Healthcare, Buckinghamshire, UK)

2.1.7 Equipment

Nalgene Cryo 1°C Freezing Container (Fisher Scientific, Leicestershire, UK)

37°C incubator (Jencons Millenium CO_2 incubator, Jencons-PLC, Leighton Buzzard, UK)

Inverted phase-contrast microscope (Nikon TMS, Jencons-PLC)

Dynex plate-reader (Jencons-PLS, East Sussex, UK)

Novex Western Transfer apparatus (Invitrogen)

Compact X4 (X-ograph Imaging Systems, Wiltshire, UK)

Dynex plate washer (Dynex Technology, West Sussex, UK)

Horizon minigel apparatus (Life Technologies)

UVP Epi Chem II Darkroom (Jencons-PLC)

Image analysis software (Labworks UVP, Media Cybernetics, USA)

XCell *SureLock* Mini-Cell (Invitrogen)

UVIKON 930 spectrophotometer (Kontron Instruments, Bletchley, UK)

BTX ECM 830 electroporator and Tweezertrodes (Kramel Biotech, Cramlington, UK)

Rotor-stator homogeniser (Scientific Laboratory Supplies Ltd, Nottingham, UK)

RotorGene RG3000 (Corbett Research, Cambridge, UK)

Quick-Seal Ultra-Clear Ultracentrifuge tubes (Beckman Coulter, Buckinghamshire, UK

Biomax 100 ultrafiltration device (Millipore, Watford, UK)

96-well dot-blot manifold apparatus (Schleicher and Schuell, London, UK)

Hydragel K20 applicator carrier (Analytical Technologies)

Electrophoresis chamber (Analytical Technologies)

Hyrys 2 Hit densitometer with the Phoresis software (Analytical Technologies)

2.2 Methods

2.2.1 Molecular biology methods

2.2.1.1 Polymerase Chain Reaction (PCR)

PCR is a process by which a section of DNA can be amplified in a sequence-specific manner. The selected region of a genome can be amplified a billion-fold with the use of short oligonucleotide primers of 15–30 bases in length, which possess sequence complementarity with the target. The primers lie on opposite strands of DNA and flank the region to be amplified. Each cycle of the reaction requires a heat denaturation step to separate the double-stranded DNA and this is achieved by heating the target DNA to 94°C or more. The DNA is then cooled to allow the oligonucleotide primers to anneal specifically to complementary sequences and the primers are extended using thermostable DNA polymerase. The extension reaction creates two double-stranded target regions, which can be denatured, again ready for a second cycle of hybridisation and extension. A third cycle produces two double-stranded molecules that comprise the target region in double-stranded form. By repeated cycles of heat denaturation, primer annealing and extension, there follows a rapid exponential accumulation of the target fragment of DNA.

2.2.1.1.1 General PCR protocol

For each PCR a master mix was prepared as shown in Table 2-1.

Reaction component	Volume (μl)	Final concentration
10× PCR buffer	2.5	1×
50mM $MgCl_2$	0.75	1.5mM
10mM dNTP mix	0.5	200μM
10μM Forward primer	1.5	0.6μM
10μM Reverse primer	1.5	0.6μM
Taq polymerase (5U/μl)	0.25	1.25U
DNA template	5	50ng
Nuclease-free water	13	-
Total Volume	25	

Table 2-1. PCR master mix components

In order to minimise contamination, gloves were worn at all times, filter-protected pipette tips were used and the reactions were prepared in a designated PCR room. In addition a negative PCR control was set up which contained all the above components apart from the DNA template. The initial denaturation step at 94°C was carried out for 5 min, followed by 35 cycles of denaturation at 94°C for 30 sec, annealing at 58°C-68°C for 30 sec and polymerisation at 72°C for 30 sec. A final 'polishing off' polymerisation step at 72°C for 5min completed the PCR. A primer design tool called 'DNA calculator' on the Sigma Genosys website (http://www.sigma-genosys.com/calc/DNACalc.asp) was used to design all the primers (Table 2-2); this tool provided essential information such as melting temperature (T_m), and potential secondary structure and primer dimer formation. All PCRs were carried out in a Bio-Rad iCycler, which has a heated lid to prevent loss of sample through evaporation upon heating.

Primer	Sequence (5' to 3')	T_m (°C)
TF	TCCAAGGAGCTGCAGGCGGCGCA	83
TR	ACAGAATTCGCCCCGGCCTGGTACACTGCCA	84
BSRGIC512F	AGTCAGTGTACATAATGATTAACCCGCCATGC	73
XHOC512R	ATAATACTCGAGACCATGGTGGCGATGGATCC	77
C512NheF	ATCTTAGCTAGCCGTAGCCATGCTCTAGACAT	72
C512Acc65R	CGCGGTACCGTCGACTGCAGAATTCCT	78
CK6NheF	ATATTAGCTAGCAACCCGCCATGCTACTTATC	71
CK6BsiWIR	ATATTACGTACGTGATTCGGCCGTCTAGAGGA	74
CK6F1	TCTAGGCTGCCCATGTAAGG	64
CKR1	AGGAGCCTACAGGGTGTGA	62
ApoEQ-PCRF	AAGAACTGAGGGCGCTGATG	66.6
ApoEQ-PCRR	GTTGTTCCTCCAGTTCCGAT	62.9

Table 2-2. Primer sequences used for PCR

2.2.1.2 Agarose gel electrophoresis

Both PCR products and plasmid DNA digests were analysed using agarose gel electrophoresis. Double-stranded DNA molecules migrate through the gel matrix from the cathode to the anode area and separate according to their size. Ethidium bromide, when added to the gel, intercalates between adjacent base pairs of the DNA molecules and allows visualisation of distinct DNA bands when viewed under ultraviolet (UV) light. A DNA fragment of a given size migrates at increasing rates through gels containing lower concentrations of agarose. For efficient separation, the smaller the fragment the higher the percentage of agarose in the gel.

A minigel electrophoresis apparatus was set up as recommended by the manufacturer. For a 1% agarose gel, 0.5g of agarose was dissolved in 50ml of 1× Tris-borate EDTA (TBE) buffer (100mM Tris, pH 8.4, 90mM boric acid and 1mM EDTA) by heating in a microwave. Once the solution had cooled, ethidum bromide was added at a concentration of 0.5μg/ml and the gel solution was then poured into the minigel cassette, within the electrophoresis chamber. When the gel had set, the comb was removed and a sufficient volume of TBE buffer was added to cover the surface of the

gel. The DNA samples were mixed 4:1 with 10× BLUEJUICE Gel Loading Buffer and 10-20μl of each sample along with a DNA ladder were loaded into each well. The gel was subjected to electrophoresis at 150V for 20min or until the dye-front was ~ 1cm from the bottom of the gel. The gel was visualised on a UV transilluminator connected to a computer operated camera and image analysis software (UVP Epi Chem II Darkroom).

2.2.1.3 TBE gel electrophoresis

Pre-cast polyacrylamide TBE gels were also used in this study, as they require less sample concentration and volume have high resolution and sensitivity and give lower background staining than agarose gels. Both 20% and 6-20% TBE gels were used with the XCell *SureLock* Mini-Cell electrophoresis apparatus. DNA samples were mixed with 5× Novex TBE Hi-Density Sample Buffer (final concentration 1×) and, following the addition of 200ml of 1× TBE running buffer to the upper buffer chamber and 600ml to the lower buffer chamber, the samples along with a DNA ladder were loaded into the appropriate wells. The gel was subjected to electrophoresis at 200V for 1h and then carefully removed and stained with 0.5μg/ml of ethidium bromide for 10min on a shaker. The gel was visualised as described above.

2.2.1.4 Real-time quantitative PCR (Q-PCR)

Real-time Q-PCR allows the reaction to be monitored as it progresses and is an extension of the PCR technique which Kary Mullis and colleagues developed in the mid-1980s [329;330]. A basic PCR "run" can be separated into 3 phases, termed the exponential, linear and plateau phases. During the exponential phase, an exact doubling of product is accumulating at every cycle, while in the following linear phase, the substrates are being consumed, the reaction is slowing and products are beginning to degrade. The plateau phase is when the reaction has stopped and therefore no more products are being made. Traditional PCR results are obtained from this final end-point. The end-point, however, is variable from sample to sample and agarose gels are not able to resolve these differences in yields. In contrast, it is the highly precise exponential phase, which is monitored in Q-PCR, allowing determination of the initial copy number, or relative quantity of a particular gene as expressed within that system. Fluorescence is measured during each cycle and an increase in reported fluorescent signal is directly proportional to the amount of PCR product. At the end of a reaction, a

threshold fluorescence is defined which is measured as a function of the background fluorescence. For each reaction, it is possible to establish a cycle number at which this threshold is crossed, termed the Cycle Threshold (C_t). The CT is directly proportional to the amount of starting template in the reaction (Figure 2-1A).

PCR product can be detected using either fluorescent dyes or fluorescently labelled sequence-specific probes. In this study the SYBR® Green I fluorescent dye was used, which binds to the minor groove of all double-stranded DNA molecules, emitting a fluorescent signal of a defined wavelength on binding (Figure 2-2). The only disadvantage of using SYBR Green I is that non-specific PCR products and primer-dimers will also contribute to the fluorescent signal. The PCR conditions must therefore be altered to increase the specificity of the reaction. In addition, a melt curve can be performed immediately following the PCR, which is used to analyse the specificity of the reaction (Figure 2-1B). A melt curve is achieved by gradually increasing the thermocycler temperature from the annealing (~55-60°C) to the denaturing temperature (~99°C). The SYBR Green dye is released into the reaction mix as the amplicon denatures and this should occur at a specific temperature for each reaction product formed. More than one peak is observed on the melt curve if non-specific binding has occurred and ideally, only one peak should be present.

2.2.1.4.1 Real-time Q-PCR protocol

Real-time Q-PCR was used in this study solely for the quantification of viral titer, therefore, purified virus was the template for all reactions. The virus preparations were diluted 1:1000 with nuclease-free water and 5μl of this was used in the reaction. Primer sequences within the ApoE gene (ApoEQ-PCRF and ApoEQ-PCRR) were designed to amplify a 72bp amplicon. A reaction mix was prepared, as shown in Table 2-3, using the Quantitect kit (Qiagen), which contains a ready-prepared 2× mix of PCR buffer, dNTPs, $MgCl_2$, *Taq* polymerase and SYBR Green I dye.

Reaction component	Volume (μl)	Final concentration
2× Quantitect mix	12.5	1×
10μM Forward primer	1	0.4μM
10μM Reverse primer	1	0.4μM
DNA template	5	
Nuclease-free water	5.5	-
Total Volume	25	

Table 2-3. Real-time Q-PCR reaction mix components

The amounts listed in the table were added to 0.2ml thin-walled, flat-cap, PCR tubes and then placed in the RotorGene RG3000. The following programme was used for all reactions:

Reaction step	Temperature	Time	
Enzyme activation	95°C	10 min	
Annealing	95°C	15 sec	
Extension	60°C	15 sec	× 40 cycles
Final extension	72°C	20 sec	

The reaction was followed immediately with a melt curve analysis to give a measure of the reaction specificity. The copy number of DNA in each sample was calculated from a standard curve of known amounts of linearised vector DNA, which was serially diluted from 10^2 to 10^8.

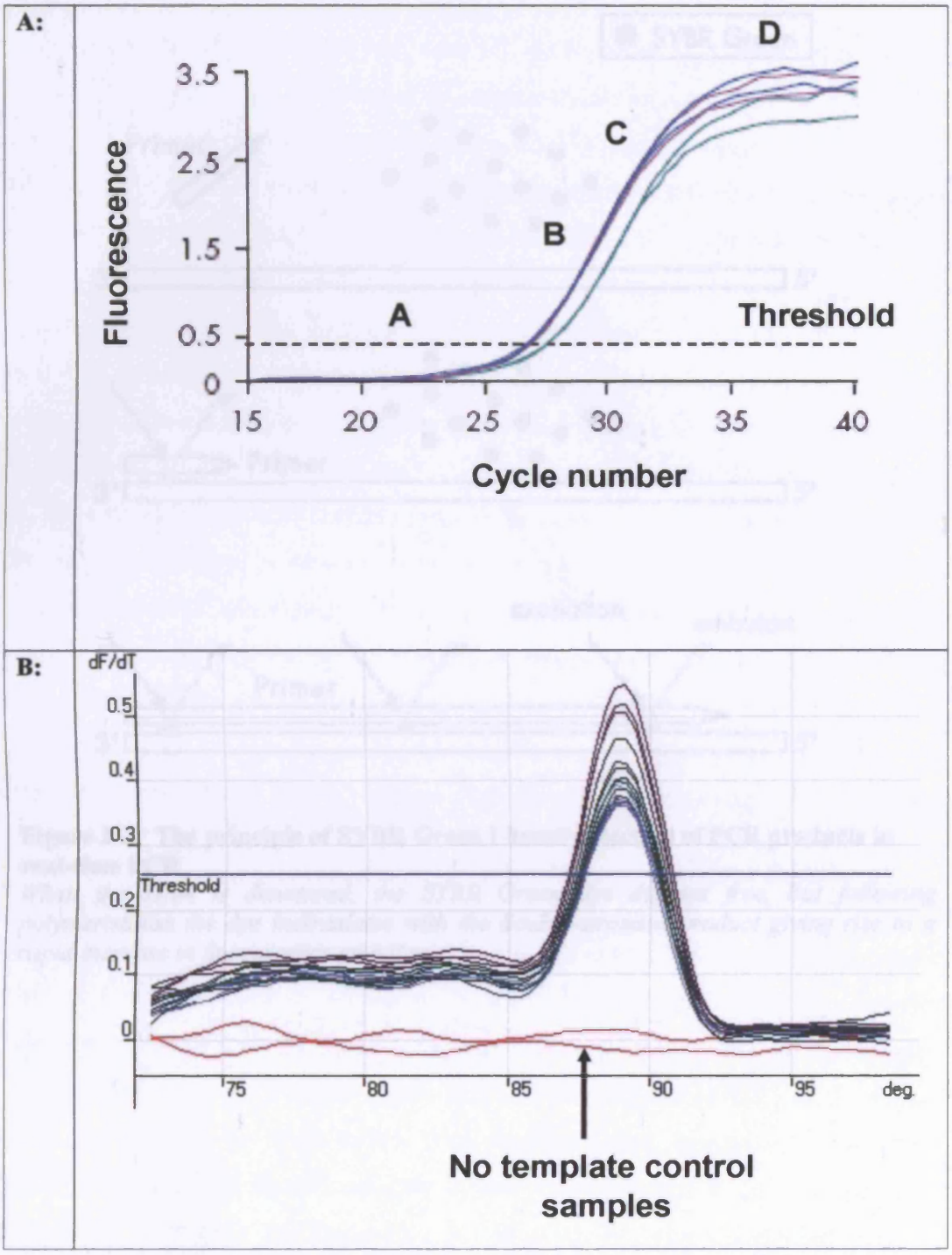

Figure 2-1. Typical amplification plot and melt curve
*(A) Different individual C_t values are obtained from the defined threshold. The graph represents the background fluorescence **A**, the exponential phase **B**, the linear phase **C**, and the plateau phase **D**. (B) A melt curve revealing only one peak in each template sample and verifying the specificity of the primers. As expected the negative control samples (without template) do not show any amplification.*

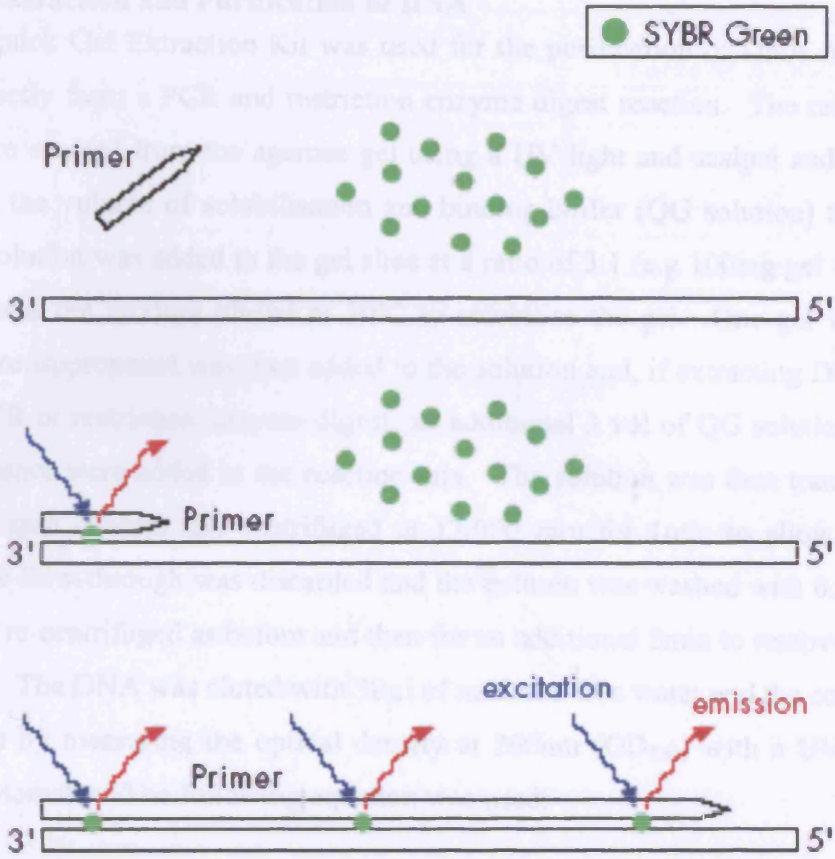

Figure 2-2. The principle of SYBR Green I based detection of PCR products in real-time PCR

When the DNA is denatured, the SYBR Green dye diffuses free, but following polymerisation the dye intercalates with the double-stranded product giving rise to a rapid increase in fluorescence emission.

2.2.1.5 Extraction and Purification of DNA

The QIAquick Gel Extraction Kit was used for the purification of DNA from agarose gel or directly from a PCR and restriction enzyme digest reaction. The relevant DNA bands were excised from the agarose gel using a UV light and scalpel and weighed to determine the volume of solubilisation and binding buffer (QG solution) to be added. The QG solution was added to the gel slice at a ratio of 3:1 (e.g 100mg gel = 300μl QG solution) and the mixture placed at 50°C to solubilise the gel. One gel vol of room temperature isopropanol was then added to the solution and, if extracting DNA directly from a PCR or restriction enzyme digest, an additional 3 vol of QG solution and 1 vol of isopropanol were added to the reaction mix. The solution was then transferred to a QIAquick spin column and centrifuged at 13,000 rpm for 1min to allow binding of DNA. The flow-through was discarded and the column was washed with 0.75ml of PE buffer and re-centrifuged as before and then for an additional 2min to remove any traces of ethanol. The DNA was eluted with 30μl of nuclease-free water and the concentration determined by measuring the optical density at 260nm (OD_{260}) with a UVIKON 930 spectrophotometer. The following equation was used:

$$DNA\ concentration\ (\mu g/ml) = OD_{260} \times 50\ (spectrophotometric\ conversion\ rate) \times dilution\ factor$$

2.2.1.6 Restriction enzyme digestion of plasmid DNA

Restriction endonucleases are enzymes purified from bacteria that recognise and cleave specific and short nucleotide sequences within DNA. Restriction sites comprise palindromes of 4, 5, 6 or more bp, each with an axis of rotational symmetry. Cleavage by a restriction enzyme produces either cohesive (having either a 5′ or 3′ single-stranded protrusion) or blunt-ended (no single-stranded protrusion) fragments. Cohesive fragments can be subsequently ligated to plasmids if their single-stranded protrusions or 'overhangs' are compatible. All blunt-ended fragments can be ligated to each other.

Manufacturer recommended buffers and instructions were used to digest up to 2μg of plasmid DNA. The reaction buffers (NEBuffers 2 to 4) contained varying concentrations of Tris-HCl (pH 7.5), NaCl, and $MgCl_2$. A restriction enzyme reaction was set up as detailed below (Table 2-4) and incubated at the optimum temperature for at least 2h.

Component	Volume (μl)	Final concentration/amount
Reaction buffer (10×)	2	1×
BSA (10×)	2	1×
Restriction enzyme (10U/μl)	1	10U
DNA	-	2μg
Nuclease-free water	-	To a total volume of 20μl

Table 2-4. The restriction enzyme reaction components

All the enzymes used in this study and their required conditions are detailed in Table 2-5. In most cases a double digest was performed where the DNA was cleaved simultaneously with two restriction enzymes and a buffer was selected that resulted in the most activity for both enzymes. However, when different incubation temperatures were needed for each enzyme, or when no single buffer was found to satisfy their buffer requirements, the reactions were carried out sequentially. Between each reaction, a purification step was necessary to remove any previously used buffer and restriction enzyme.

Restriction enzyme	Cleavage site	Reaction conditions for optimal activity
XhoI	C/TCGA G G AGCT/C	NEBuffer 2 at 37°C
SpeI	A/CTAG T T GATC/A	NEBuffer 2 at 37°C
XbaI	T/CTAG A A GATC/T	NEBuffer 2 at 37°C
SapI	GCTCTTC$(N)_1$ CGAGAAG$(N)_4$	NEBuffer 4 at 37°C
BsrGI	T/GTAC A A CATG/T	NEBuffer 2 at 37°C
Acc65I	G/GTAC C C CATG/G	NEBuffer 3 at 37°C
SnaBI	TAC/GTA ATG/CAT	NEBuffer 4 at 37°C
EcoRV	GAT/ATC CTA/TAG	NEBuffer 3 at 37°C
NheI	G/CTAG C C GATC/G	NEBuffer 2 at 37°C
BsiWI	C/GTAC G G CATG/C	NEBuffer 3 at 55°C
BssHII	G/CGCG C C GCGC/G	NEBuffer 3 at 50°C
MscI	TGG/CCA ACC/GGT	NEBuffer 4 at 37°C
SmaI	CCC/GGG GGG/CCC	NEBuffer 4 at 25°C

Table 2-5. Restriction enzyme cleavage sites and reaction conditions

2.2.1.7 Ligation reaction

During ligation *in vitro*, DNA ligase catalyses the formation of a phosphodiester bond between adjacent nucleotides only if one nucleotide carries a 5'-phosphate residue and the other carries a 3'-hydroxyl terminus. Prior to performing a ligation reaction between plasmid and insert, it is necessary to remove the 5'-phosphate residues from both termini of the plasmid DNA with alkaline phosphatase to minimise re-circularisation of plasmid DNA. The following reaction mix was prepared (Table 2-6):

Component	Volume (μl)	Final concentration/amount
Purified linear vector (eluted in 30μl)	30	1-2μg
10× NEBuffer 3	4	1×
Calf intestinal alkaline phosphatase (CIP) (1U/μl)	1	1U
Nuclease-free water	5	Total volume = 40μl

Table 2-6. Alkaline phosphatase reaction components

The reaction mix was incubated for 1h at 37°C and then purified through a Qiagen column. For all ligations a 1:3 molar ratio of vector:insert DNA was used and the following equation was used to convert molar ratios to mass ratios for a given plasmid and insert DNA fragment size:

(ng of vector × kb size of insert/ kb size of vector) × molar ratio (insert:vector) = ng of insert

The reaction mix was composed of the following (Table 2-7):

Component	Volume (μl)	Final concentration/amount
Vector	-	100ng
Insert	-	Calculated from equation
10× DNA ligase buffer	1	1×
T4 DNA ligase (2 Weiss Units/μl)	0.5	1U
Nuclease-free water	-	To a total volume of 10μl

Table 2-7. Ligation reaction components

The reaction components were then mixed and incubated at room temperature for 4h. A control reaction mix was also prepared containing every component apart from the insert DNA; this allows background level of re-circularised plasmid to be assessed.

2.2.1.8 Transformation of plasmid DNA in competent *E. coli.*

The ability of bacterial cells to take up recombinant DNA vectors is enhanced when the cells are in a 'competent' state [331]. This can be achieved by treating bacterial cultures with an ice-cold solution of 50mM calcium chloride prior to heating. DH5α and TOP10 chemically competent *E.coli* were used for the transformation reactions in this study. Firstly, 5μl of the ligation reaction was gently mixed with either 50μl of TOP10 or 100μl of DH5α cells and incubated on ice for 30min. The DH5α cells were then heat-shocked for exactly 45sec in a 37°C water bath, while the TOP10 cells were incubated for 30sec in a 42°C water bath. Both DH5α and TOP10 transformation mixes were then placed on ice for 2min, followed by the addition of 900μl and 250μl of S.O.C medium respectively and incubation at 37°C in a shaking incubator for 1h. A volume of 50μl of the transformation mix was then spread onto a pre-dried Luria Bertani (LB) agar plate containing either 100μg/ml of ampicillin or 50μg/ml of kanamycin (depending on the plasmid antibiotic resistance) and left overnight in a 37°C incubator. The ampicillin and kanamycin plates allow only transformed bacteria to grow as the vectors contain either an ampicillin or kanamycin resistance gene. The next day single colonies were picked and grown in 5ml of LB broth containing the appropriate antibiotic by overnight incubation in a 37°C shaking incubator. Recombinants were identified by PCR directly from the overnight cultures; primers were designed to amplify the insert (see results section 3.2.1.1) and the initial denaturation step was extended to 10min. The cultures were purified using the Wizard Plus SV miniprep DNA Purification System (see section 2.2.1.9) and recombinants were confirmed by restriction enzyme digestion.

2.2.1.9 Plasmid DNA mini-prep purification

The overnight culture was first centrifuged at 13,000 rpm for 2min prior to the use of the Wizard Plus SV miniprep DNA Purification System. The supernatant was removed and the cell pellet was re-suspended in 250μl of Cell Resuspension Solution (50mM Tris-HCl (pH7.5), 10mM EDTA, 100μg/ml RNAse A). This was followed by the addition of 250μl of Cell Lysis Solution (0.2M NaOH, 1% SDS), a short incubation at room temperature for 5min and then the addition of 10μl of Alkaline Protease solution to inactivate endonucleases and proteins. After 5min incubation at room temperature, 350μl of Neutralization Solution (4.09M guanidine hydrochloride, 0.759M potassium acetate, 2.12M glacial acetic acid) was added and the solution was immediately mixed by inversion and centrifuged at 13,000 rpm for 10min. The cleared lysate was transferred to a spin-column and centrifuged at 13,000 rpm for 1min, after which the

flow-through was discarded and the column washed with 750μl of Column Wash Solution (60mM potassium acetate, 10mM Tris-HCl (pH 7.5), 60% ethanol). The column was washed a second time and then the plasmid DNA eluted by adding 50μl of nuclease-free water and centrifuging at 13,000 rpm for 1min.

2.2.1.10 Plasmid DNA maxi-prep purification

Larger amounts of endotoxin-free plasmid DNA were needed for animal injections and for *in vitro* transfections to produce recombinant AAV; it was necessary, therefore, to use an EndoFree Plasmid Maxi kit to purify the plasmid DNA for these applications. Endotoxins are cell membrane components of Gram-negative bacteria (e.g, *E.coli*), which strongly decrease the transfection efficiency of DNA into cultured cells and cause fever, endotoxic shock syndrome and activation of the complement cascade in animals. It was essential, therefore, to remove any traces from the plasmid preparations and to ensure that all plastic-ware and media were free from endotoxin contamination. A starter culture was diluted 1:500 into 100ml of LB broth containing the appropriate antibiotic and grown overnight in a 37°C shaking incubator. The bacterial cells were harvested by centrifugation at 6,000× g for 15min at 4°C and then re-suspended in 10ml buffer P1. The cells were then lysed by the addition of 10ml of buffer P2 and incubated at room temperature for 5min. A volume of 10ml of chilled buffer P3 was then added to the lysate, mixed thoroughly and poured into a QIAfilter cartridge. After a 10min incubation at room temperature to allow the precipitate to float to the top of the solution, a plunger was inserted into the QIAfilter cartridge and the lysate was filtered into a 50ml tube. A volume of 2.5ml of buffer ER was added to the solution, mixed thoroughly and then incubated on ice for 30min. During this time, a QIAGEN-tip 500 was equilibrated by the addition of 10ml of buffer QBT and allowed to empty by gravity flow. The filtered lysate was applied to the column and was again allowed to enter the resin by gravity flow, after which the column was washed with 2× 30ml of buffer QC. The DNA was eluted with 15ml of buffer QN and precipitated by the addition of 10.5ml (0.7 vol) of room-temperature isopropanol and centrifuged immediately at 15,000× g for 30min at 4°C. The supernatant was carefully decanted and the DNA pellet was washed with 5ml of endotoxin-free room-temperature 70% ethanol and centrifuged as before for 10min. The pellet was air-dried for 5-10min and re-suspended in endotoxin-free TE buffer or sterile 0.9% NaCl for animal injections.

2.2.1.11 Plasmid DNA mega-prep purification

The PureLink™ HiPure Plasmid Megaprep kit was used to isolate even larger quantities of plasmid. This kit uses an anion exchange resin to purify plasmid DNA to a level equivalent to two passes through CsCl gradients and provides efficient endotoxin removal (levels are <0.1 EU/μg DNA). A starter culture was diluted 1:500 into 1.5L of LB broth containing the appropriate antibiotic and grown overnight in a 37°C shaking incubator. The bacterial cells were harvested by centrifugation at 6,000× g for 15min at 4°C and then re-suspended in 50ml of buffer R3. A 50ml volume of lysis buffer (L7) was then added to the cell suspension to lyse the bacterial cells and the tube was inverted gently until a homogeneous lysate was observed. Following 5min incubation at room temperature, 50ml of precipitation buffer (N3) was added to neutralise the lysate, which was mixed gently but thoroughly until a completely non-viscous and homogeneous mixture was obtained. A white, flocculent precipitate of proteins, cellular debris, genomic DNA and detergent is formed during this process. The bacterial lysate was then poured into a megaprep lysate filtration cartridge attached to a 500ml Duran bottle and a vacuum source. Before applying the vacuum, the lysate was left to stand for 2min without agitation, which allows the precipitate to float to the top and ensures efficient filtration without clogging. Around 125ml of clarified lysate containing plasmid DNA was drained though after the vacuum was applied and to further ensure that all lysate had passed through the cartridge, 50ml of wash buffer (W8) was added. Next, the lysate was passed over a vacuum-assisted megaprep DNA binding filter, which was pre-equilibrated with 100ml of buffer EQ. The negatively charged phosphates on the DNA backbone interact with the positive charges on the resin surface and under moderate salt conditions the plasmid DNA binds to the resin. RNA, protein, carbohydrates and other impurities are washed away by the addition of 350ml of wash buffer. The binding cartridge was then attached to a sterile (autoclaved) Duran bottle and the plasmid DNA was eluted under high salt conditions with 50ml of elution buffer (E4). The eluted DNA was finally desalted and concentrated by an alcohol precipitation step as described before in section 2.2.1.10.

2.2.2 Cell culture

Human Embryonic Kidney (HEK) 293-T cells and murine C2C12 myoblast cells were the two cell lines used in this study. C2C12 myoblasts, which are derived from normal adult C3H mouse leg muscle, divide rapidly and can differentiate into post-mitotic, multinucleate myotubes when exposed to horse serum or low-serum medium. HEK

293-T cells are a packaging cell line which constitutively express the adenovirus E1a protein and the SV40-T antigen [332] and are generally used for the production of viral vectors. This cell line is used in preference to conventional 293 cells as they show a high level of transfection efficiency and subsequently improved rAAV yields.

2.2.2.1 General culture maintenance and cryopreservation

Both cell lines mentioned above are adherent and were cultured in 75 or 175cm^2 tissue culture flasks, in DMEM, supplemented with 10% (v/v) FBS, 2mM L-glutamine, 100μg/ml streptomycin and 100IU/ml penicillin. They were maintained in an incubator at 37°C with a humidified atmosphere of 5% CO_2 and 95% air. The cells were split by trypsinisation when semi-confluent; they were first washed with warm PBS (37°C) and incubated with 0.25% (v/v) trypsin-EDTA at 37°C for 2min, which was then neutralized by the addition of pre-warmed fresh growth medium. The cells were then re-suspended and split 1:3-1:6.

For cryopreservation, the cells were first pelleted at 300g for 5min and then re-suspended in 90% FBS and 10% (v/v) DMSO; this solution lowers the freezing point and allows the cells to be slowly cooled without any damage. The cell suspension was divided into 1.8ml cryovials and initially placed in a Nalgene Cryo 1°C Freezing Container and stored at -80°C for 5-6h which reduces the temperature by 1°C per min. The cells were subsequently transferred to liquid nitrogen for long-term storage.

Trypan blue was used to count the cells and assess cell viability; it is a dye that is only retained by dead cells, therefore, differentiating them and allowing only the viable cells to be counted. Trypan blue was diluted 1:10 with cell suspension and pipetted into the chambers of a haemocytometer, which was then observed under an inverted phase-contrast microscope. The number of viable cells were counted in 8× 1mm^2 squares with a total volume of 10^{-4} cm^3. The average was then multiplied by the dilution factor and 10^4 to give the number of cells per ml.

2.2.2.2 Transient transfection of murine C2C12 myoblasts

Murine C2C12 myoblasts were seeded at a concentration of 2× 10^5 per well of a 6-well plate and left overnight to adhere. The cells were cultured in DMEM containing 10% (v/v) heat-inactivated FBS (incubated at 55°C for 30min), 2mM L-glutamine, 100μg/ml

streptomycin and 100IU/ml penicillin. For transfection the next day the cells needed to be 90-95% confluent to obtain high efficiency and expression levels, and to minimize decreased cell growth associated with high transfection activity. Lipofectamine™ 2000, which is a cationic lipid, was used for transfection of the C2C12 cells, adding plasmid DNA at a ratio of 1:2. In two separate microfuge tubes, 2μg of plasmid and 4μl of Lipofectamine™ 2000 were diluted in 50μl of DMEM without FBS and antibiotics and incubated at room temperature for 5min. The diluted plasmid and lipofectamine solutions were then gently mixed together (total volume of 100μl) and incubated at room temperature for 20min to allow the plasmid-Lipofectamine™ 2000 complexes to form. During this incubation period, the normal growth medium from the cultured myoblasts was removed and replaced with 2ml of DMEM without FBS and antibiotics. The 100μl complex solution was then added drop-wise to the cells in one well of the 6-well plate and the cultures incubated at 37°C for 5h. Following transfection, the medium was removed and replaced with fresh DMEM containing 10% FBS, glutamine and antibiotics and the cultures were left to grow under normal conditions for 24h. They were then either processed for ApoE analysis or transferred for a further 24h to DMEM containing 5% heat-inactivated horse serum to induce cell differentiation and fusion into large multinucleate myotubes.

2.2.2.3 Protein quantification

Samples of medium were transferred to pre-chilled microcentrifuge tubes, and centrifuged at 13,000 rpm for 5min at 4°C to pellet any dead cells. The supernatant was concentrated 10× using 30,000 MWCO vivaspin concentrators and total protein was quantified using the 'Bio-Rad Protein Assay Kit'. This assay is based on the Bradford dye-binding procedure [333] in which the Coomassie Brilliant Blue G-250 dye changes colour in response to various concentrations of protein.

Seven dilutions of the protein standard BSA were prepared in PBS, ranging from 160μg/ml – 2.5μg/ml. A volume of 160μl of each standard and sample was added in triplicate to appropriate wells of a 96-well plate, followed by 40μl of dye reagent concentrate. The samples were mixed thoroughly and incubated at room temperature for at least 5min. The optical density (OD) at 595nm was read using a Dynex plate-reader, allowing a standard curve of OD_{595} versus concentration to be plotted and from this the concentration of test samples was determined.

2.2.3 Recombinant AAV vector production

As described in section 1.7.2.3, AAV production has changed significantly over the years. One important improvement has been the development of plasmids containing parts of the Ad genome necessary for rAAV production, resulting in the elimination of infectious helper virus contamination. Such plasmids have been developed by Grimm et al. [334], Matsushita et al. [335] and Xiao et al. [196] and all reported good yields, if not better than those observed using infectious helper Ad virus. Grimm et al. used a two-plasmid system in which the helper Ad genes, the *Rep68/78* genes and the *Cap* genes are assembled into one plasmid and the AAV vector sequences are in another. Xiao et al. in contrast, developed a three-plasmid system in which the helper Ad genes were separated from the *Rep* and *Cap* genes and placed into two different constructs.

2.2.3.1 Triple transfection of rAAV plasmid, helper Ad plasmid and packaging plasmid into 293-T cells

In this study, the three-plamid system was used which involved the triple transfection of 293-T cells with a helper Ad plasmid (HGTI) a pAAV-based plasmid (a vector flanked by the AAV-serotype 2 ITRs and harbouring the cDNA of interest), and a packaging plasmid containing the AAV *Rep* and *Cap* genes, at a molar ratio of 3:1:1 respectively (Figure 2-3). Since the generation of pseudotyped AAV vectors was required, the packaging construct contained AAV2 *Rep* proteins, but *Cap* proteins from an alternative serotype (7, 8 or 9).

The day before transfection, 293-T cells were seeded into 40 (15cm diameter) dishes at a cell density of between 8-9.5× 10^6 cells/dish, so that the cultures were about 70% confluent the following day. On the day of transfection, the following transfection mixture was prepared for 10 dishes in a 50 ml Falcon tube:

Plasmid/reagent	Amount/volume	Final concentration
HGTI	300μg	
pAAV	100μg	
pAAV7-2	100μg	
2.5M $CaCl_2$	1.25ml	0.25M
ddH_2O	made up to 12.5ml	

Table 2-8. Components of the transfection mix

While aspirating the above mix with a 1ml pipette to create bubbles, 12.5ml 2× HEPES-buffered saline (HBS; 280mM NaCl, 10mM KCl, 1.5mM Na_2HPO_4, 12mM dextrose and 50mM HEPES; pH 7.05) was added at a steady slow rate. The transfection mix was incubated at room temperature for 2min and then the entire 25ml was transferred to 200ml of pre-warmed growth medium and mixed gently by inversion. The culture medium was removed from the 10 (15cm diameter) dishes containing the 293-T cells and 22ml of the transfection mix was carefully added without disruption of the cell monolayer. After an incubation period of 2 to 3 days, the culture medium was removed from the transfected cells leaving 2-3ml in each dish into which the cells were scraped. The scraped cells from each dish were then pooled and pelleted by centrifugation at 1000g for 10min and the cell pellet was re-suspended in 15ml cell lysis buffer (150mM NaCl, 50mM Tris-HCL; pH 8.5). The cells were then lysed by four cycles of freeze/thaw by alternately placing in ethanol/dry ice and then a 37°C water bath. Lysis of the cells results in the release of the AAV particles into the supernatant. The lysate was then treated with 3μl (100 Units) of benzonase, which is an enzyme used to dissociate aggregated rAAV particles by digesting any extraneous nucleic acid, before purification. An aggregate of virus particles would behave as a single transducing unit, therefore, it is important that these are separated to maximise the infectious virus titer. The benzonase-treated lysate was vortexed, followed by incubation at 37°C for 1h and then centrifugation at 6,500 rpm for 20min to clarify the cell lysate.

2.2.3.2 Purification of the clarified lysate by iodixanol step gradient ultracentrifugation

To isolate the rAAV particles from the clarified lysate, the latter was loaded onto a step-gradient of iodixanol. Upon ultracentrifugation the virus particles sediment into the 40% iodixanol gradient fraction. The most concentrated iodixanol fraction (60%) is the lower layer and functions as a cushion to prevent the particles pelleting at the bottom of the tube. The iodixanol fractions were prepared as shown in Table 2-9.

% Iodixanol	Iodixanol (ml)	5M NaCl (ml)	*5× PBS-MK (ml)	ddH_2O (ml)	Phenol Red (μl)
15%	12.5	10	10	17.5	-
25%	20.8	-	10	19.2	100
40%	33.3	-	10	6.7	-
60%	50	-	-	-	100

Table 2-9. Preparation of iodixanol fractions
** 5x PBS-MK (5x PBS, 5mM $MgCl_2$, 12.5mM KCL)*

The clarified lysate was transferred to a Quick-Seal Ultra-Clear Ultracentrifuge tube using a Pasteur pipette and then carefully underlayed with the iodixanol fractions in the following order (Figure 2-3):

9ml 15% iodixanol
6ml 25% iodixanol
5ml 40% iodixanol
5ml 60% iodixanol

The remaining space in the tube was filled with cell lysis buffer before heat-sealing the ultracentrifuge tube. Ultracentrifugation of the iodixanol step-gradient was performed in a Beckman Ultracentrifuge using a Type 60Ti rotor at 60,000 xg for 90min. The 40% fraction is easily distinguished owing to the presence of phenol red in the 25% and 60% iodixanol fractions. Using a 19-gauge needle and 10ml syringe, the 40% fraction was removed by carefully puncturing the tube at the 60%/40% interface and withdrawing no more than 4.5ml of the fraction. The purified virus was then loaded onto a single Biomax 100 ultrafiltration device and the volume brought up to 15ml with 1× PBS-MK. The filter device was centrifuged at 2000g at room temperature until approximately 1ml remained. The virus stock was re-diluted and re-concentrated a second time, ending with a final volume of 500μl, which could then be stored at -80°C.

2.2.3.3 Determination of virus particle titer by DNA dot-blot hybridisation analysis

To estimate the virus particle titer, rAAV vector genomes were isolated from 1μl and 5μl portions of the virus stock and transferred to a nitrocellulose membrane, together

with a serial dilution of known quantities of the corresponding pAAV vector. To extract vector genomes, the virus was treated with DNase I (1U/μl) to digest any extraneous DNA. To the 1μl and 5μl virus portions, 5μl of DNase I and 20μl of 10× DNase I reaction buffer was added and brought to 200μl with serum-free DMEM. Following incubation at 37°C for 1h, the virus was treated with 200μl of 2× proteinase K buffer (20mM Tris-HCl, 20mM EDTA and 1% (w/v) SDS) containing 100μg of proteinase K and incubated a second time at 37°C for 1.5h. The proteinase K digests the virus capsid proteins releasing the vector genome. The vector DNA was then isolated by the addition of 400μl of phenol:chloroform:isoamyl alcohol (25:24:1) and vortexed to form an emulsion, which was centrifuged at 10,000 g for 10min. The upper aqueous phase was transferred to a 1.5ml microfuge tube and 40μl 3M sodium acetate (pH 5.2) and 2μl of glycogen (20μg/μl) was added. This was vortexed and then 1ml ethanol (2.5 vol) was added, mixed and incubated at -80°C for 30min to precipitate vector genome DNA. The preparations were centrifuged at 10,000 g for 20min at room temperature to pellet the DNA, which was clearly visible due to the presence of glycogen. The supernatant was removed and the pellets washed with 800μl 70% ethanol and centrifuged at 10,000 g for 5min at 4°C. Once the supernatant had been removed, the DNA pellets were air-dried and dissolved in 400μl of 0.4M NaOH/10mM EDTA (pH 8).

For dot blot analysis, a two-fold serial dilution of the corresponding pAAV vector was prepared, ranging from 80ng to 0.3125ng. To each 5μl pAAV dilution, 400μl of 0.4M NaOH/10mM EDTA was added. While heating the viral and plasmid samples at 100°C for 5min a piece of Hybond-N^+ nitrocellulose membrane and three pieces of 3MM Whatman blotting paper were cut to the size of the dot-blot manifold and pre-wetted in ddH_2O. The manifold was set up with the membrane overlaying the three sheets of blotting paper and attached to a vacuum pump. Each well to be used in the analysis was washed with 400μl of ddH_2O and the vacuum was applied to dry. The two denatured vector genome samples and the pAAV DNAs were then added to the appropriate wells of the apparatus and the vacuum applied. Once the samples had passed through, each well was rinsed with 400μl 0.4M NaOH/10mM EDTA and the membrane was removed and air-dried for 15min.

The ECL direct nucleic acid labelling and detection system was used for labelling the DNA probe and the subsequent hybridisation and detection of the DNA dot-blot. The

membrane was first rinsed in 2× SSC (NaCl and $Na_3Citrate{\cdot}2H_2O$) and transferred to a hybridisation cylinder with 34ml ECL gold hybridisation buffer containing 1g NaCl and 1.7g ECL blocking agent pre-dissolved at 42°C for 2h. The membrane was pre-hybridised by incubation with rotation at 42°C for a minimum of 1h. Meanwhile, the DNA probe, which was 100ng of an agarose gel-purified DNA fragment derived from the pAAV vector, was diluted to 10ng/μl in ddH_2O and denatured by incubating at 100°C for 5min. The denatured DNA was cooled on ice and 10μl DNA labelling reagent was added, mixed gently, followed by the addition of 10μl of glutaraldehyde solution. The labelling mix was vortexed and incubated at 37°C for 10min. The labelled DNA probe could then be added to the cylinder containing the pre-hybridised membrane and incubated at 42°C with rotation overnight. The next day the hybridisation mix was replaced with 100ml pre-warmed primary wash buffer (1L = 2× SSC, 360g urea, 4g SDS) and incubated at 42°C with rotation for 30min. The wash procedure was repeated once more and then the membrane was removed and washed twice with 400ml of 2× SSC at room temperature for 6min with gentle agitation. Detection was carried out by chemiluminescence, with the use of an ECL system (described in section 2.2.4.1).

To calculate the number of rAAV particles present in the virus stock, the number of vector genomes present in 1ng of the pAAV plasmid vector used in the DNA dot-blot hybridisation was determined. This value could then be used to determine the number of virus particles present in the virus stock. See Figure 2-4 for details of the calculations carried out. The intensity of the signals produced by the 1μl and 5μl portions of virus stock was compared with those of the quantified pAAV serial dilution and densitometric analyses was used to estimate the number of vector genomes in ng in each dot (Figure 2-4).

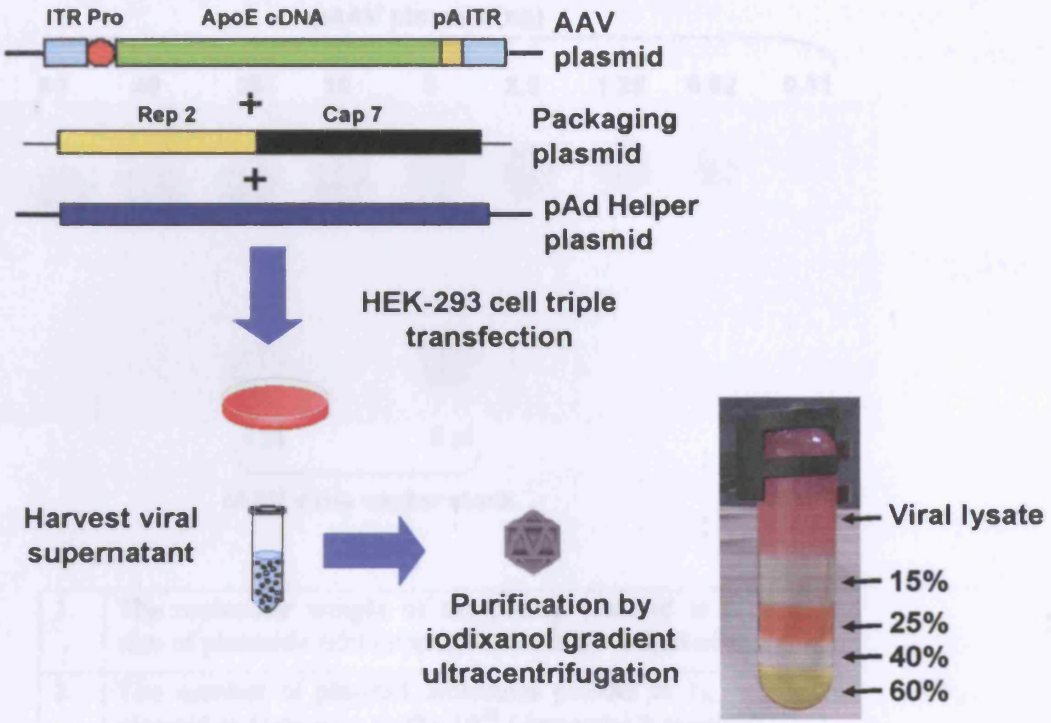

Figure 2-3. Production and purification of rAAV vector particles
The three-plamid system was used for the production of rAAV vector particles, which involved the triple transfection of 293-T cells with a helper Ad plasmid (HGTI) a pAAV-based plasmid (a vector flanked by the AAV-serotype 2 ITRs and harbouring the cDNA of interest), and a packaging plasmid containing the AAV Rep and Cap genes, at a molar ratio of 3:1:1 respectively. Cell lysates were prepared two days after transfection and rAAV particles purified by iodixanol gradient ultracentrifugation.

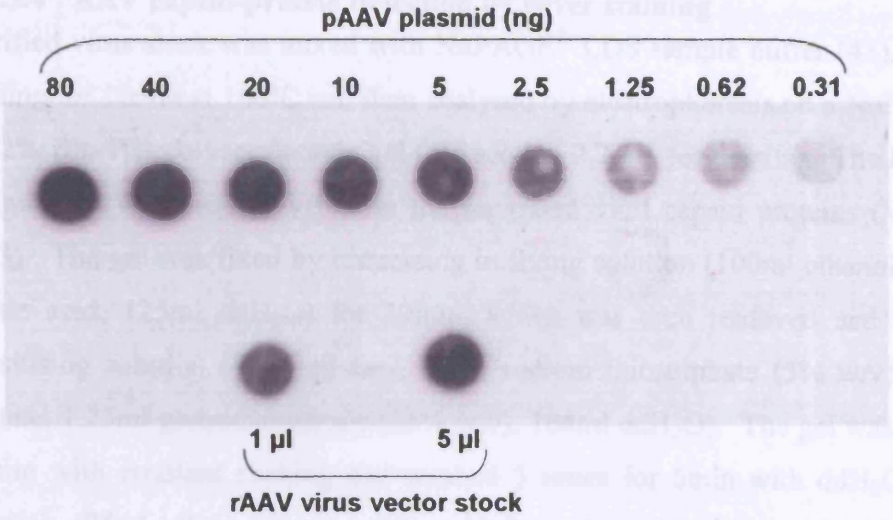

1.	The molecular weight of the pAAV plasmid in Daltons = size of plasmid× 650 (average molecular weight of 1bp)
2.	The number of plasmid molecules present in 1g = MW of plasmid in Daltons ÷ 6.02×10^{23} (Avogadro's number)
3.	To convert into molecules/ng = number of plasmid molecules in 1g× 10^{-9}

Figure 2-4. DNA dot-blot hybridisation analysis

2.2.3.4 AAV capsid-protein detection by silver staining

Purified virus stock was mixed with NuPAGE® LDS sample buffer (4×), denatured by boiling for 10min at 100°C and then analysed by electrophoresis on a NuPAGE® Novex 4-12% Bis-Tris polyacrylamide gel (see section 2.2.4.1 for details). The PlusOne silver staining kit was used to visualise the separated viral capsid proteins (VP1, VP2 and VP3). The gel was fixed by immersing in fixing solution (100ml ethanol, 25ml glacial acetic acid, 125ml ddH_2O) for 30min, which was then removed and replaced with sensitising solution (75ml ethanol, 10ml sodium thiosulphate (5% w/v), 17g sodium acetate, 1.25ml glutardialdehyde (25% w/v), 164ml ddH_2O). The gel was sensitised for 30min with constant shaking and washed 3 times for 5min with ddH_2O. The silver solution (25ml silver nitrate solution (2.5% w/v), 0.1ml formaldehyde (37% w/v), 225ml ddH_2O) was then added and left shaking for 20min. This was followed by 2 washes for 1min with ddH_2O and immersion of the gel into developing solution (6.25g sodium carbonate, 0.2ml formaldehyde (37% w/v), 250ml ddH_2O) until the bands on the gel had reached the desired intensity. The reaction was stopped by the addition of stopping solution (3.65g EDTA-Na_2•$2H_2O$ and 250ml ddH_2O) and after 5min the gel was washed a final time with ddH_2O.

2.2.4 Human ApoE expression and detection

2.2.4.1 ApoE Western blot

In Western blotting, electrophoretically separated proteins are transferred from a SDS-polyacrylamide gel to a nitrocellulose membrane and probed with antibodies that react specifically with the antigens in the target protein attached to the membrane. Western blotting is therefore, primarily used to identify and quantify a specific protein of interest in a complex mixture of proteins.

The total protein per well loaded onto the SDS-polyacrylamide gel depended on the sample; for example, 40 μg was typically used for cell culture supernatant and tissue lysate samples, whereas 2μl of plasma (80-100μg) was loaded. The protein samples were mixed with PBS, NuPAGE® LDS sample buffer (4×) and β-mercaptoethanol as follows (Table 2-10):

Component	Volume (μl)	Final concentration/amount
Protein sample	-	40μg
NuPAGE® LDS sample buffer (4×)	5	1×
β-mercaptoethanol (50×)	1	1×
PBS	-	To a total volume of 20μl

Table 2-10. Preparation of protein samples for SDS-polyacrylamide gels

The samples were boiled for 5min at 100°C and, along with a protein molecular weight standard marker (MagicMark™ XP), loaded onto a NuPAGE® Novex 4-12% Bis-Tris polyacrylamide gel with 1× NuPAGE® MES SDS running buffer. NuPAGE® Antioxidant (500μl), which keeps the protein samples in a reduced state and prevents re-oxidation, was added to the upper (cathode) buffer chamber of the elecrophoresis tank and the gel was subjected to electrophoresis at 200V for 35min.

The proteins were then transferred from the gel to Hybond ECL nitrocellulose membrane using wet blotting. Blotting pads were first soaked in 1× NuPAGE® Transfer buffer, containing 10% methanol and antioxidant (1ml per litre of transfer buffer) and placed into the cathode (-) core of the blot module. One pre-soaked sheet of 3MM absorbent paper was placed on top of the gel and used to lift the gel off the electrophoresis plate and onto the blotting pads with the gel facing upwards. Pre-soaked nitrocellulose membrane was then placed on top of the gel, followed by another piece of pre-soaked absorbent paper and 2 blotting pads. The transfer sandwich module was placed in a Novex Western Transfer apparatus and the middle blot module was filled with transfer buffer and the outer buffer chamber with deionised water. Blotting was carried out for 90min at 25V.

Following transfer, the membrane was stained with Ponceau S solution to check that protein had successfully transferred and then the membrane was blocked by incubating with PBS containing 5% Marvel milk powder and 0.1% Tween-20 for 2h at room temperature using continuous shaking. The membrane was then probed with a polyclonal goat anti-human ApoE primary antibody, which was diluted 1:1,500 with PBS/Tween (0.1%), 1% Marvel and 1% BSA. Following overnight incubation at 4°C on a rotating shaker, the membrane was washed 3 times for 10min in PBS/tween and

then stained with anti-goat IgG (whole molecule, peroxidase conjugate) secondary antibody, diluted 1:10,000 with PBS/Tween (0.1%), 1% Marvel and 1% BSA, for 1h at room temperature with continuous shaking. The membrane was then washed as before and detection was carried out by chemiluminescence, using an ECL system. This involves the oxidation of luminol by horse radish peroxidase (HRP) in the presence of a chemical enhancer such as phenol with the emitted light (438nm) detected by short exposure to blue-light sensitive autoradiograph film. The ECL substrate was added to the membrane, which was secured in a film cassette and then exposed briefly to autoradiograph film (Hyperfilm ECL). The film was subsequently developed in an automatic bench top processor.

2.2.4.2 Enzyme-Linked Immunosorbent Assay (ELISA) for measurement of ApoE concentration

ELISA is a sensitive immunodetection method that uses biotinylated capture antibodies to detect specific antigens in a complex of proteins. Antibodies against ApoE are now available from several companies and this has made it possible to develop an ELISA that can subsequently be used to measure accurately the concentration of ApoE in serum or conditioned medium. An optimised sandwich ELISA for ApoE had previously been developed in our laboratory and was used for this project. It is termed sandwich assay because an antibody-antigen-antibody complex is formed and the quantity of antigen is measured by using a biotin-labelled detecting antibody, which allows it to be conjugated to HRP. The HRP conjugated antibody-antigen complex is then exposed to the substrate tetra-methylbenzidine (TMB) to produce a visible colour change (to yellow). The colour intensity is proportional to the concentration of target antigen and can be measured in a microplate reader.

An ECL Protein Biotinylation Module was used to biotinylate the goat polyclonal anti-human ApoE detection antibody. The antibody was diluted in 2.5ml of 40mM bicarbonate buffer to give a working concentration of 1mg/ml and then 100μl of the biotinylation reagent was added. The solution was incubated for 1h at room temperature and passed through a Sephadex G25 column, eluting with 5ml PBS. The eluted fractions (200μl) were analysed by a spectrophotometer to locate the antibody and the concentration of appropriate pooled fractions measured by a Bradford assay (section 2.2.2.3) using IgG as the standard.

The following buffers were prepared prior to starting the ELISA:

- 10× Blocking buffer (50mM Tris, 150mM NaCl, 1mM $MgCl_2$, pH 7.4)
- 1× Assay buffer (0.05% gamma-globulin, 50mM Tris, 150mM NaCl, 0.01% Tween-40, pH 7.4)
- 10× Washing buffer (10mM Tris, 150mM NaCl, 0.05% Tween-20 pH 7.4)

Immediately before use, the blocking and assay buffers were supplemented with 1% and 0.5% BSA (w/v), respectively, and were filtered through a 0.22μm vacuum filter.

The ELISA plate was prepared by coating each well of a Nunc Maxisorp 96-well immunoassay plate with 100μl of goat polyclonal anti-human ApoE capture (1°) antibody at a concentration of 1.5μg/ml (diluted in PBS). The plate was covered and either incubated overnight at 4°C or for 4h at 37°C in a humidified incubator. Following incubation, the unbound capture antibody was shaken from the wells and 350μl of 1× blocking buffer was added to each well to prevent non-specific binding. After blocking for 1h at 37°C, the plate was washed using a programmed Dynex plate washer, which washed each well 5 times with 300μl of 1× washing buffer. Seven dilutions of a recombinant ApoE3 standard were prepared in assay buffer ranging from 160ng/ml – 2.5ng/ml. A vol of 50μl of each sample and standard was added in triplicates to the appropriate wells and the plate was covered and incubated overnight at 37°C in a humidified incubator. The following day the plate was washed as before and 50μl of biotinylated detection antibody, diluted to a concentration of 3μg/ml in assay buffer containing 1% (v/v) goat serum, was added to each well. The plate was covered and incubated for 1h on a shaker at room temperature and this was followed by further washing and the addition of 100μl of streptavidin-HRP (supplied with the ECL Protein Biotinylation Module) diluted 1:1000 with assay buffer. After 30min incubation at room temperature the plate was washed and 100μl of TMB substrate (equal volumes of 0.004% (v/v) H_2O_2 and TMB dye) was added to each well. The plate was wrapped in aluminium foil and incubated for 30min on a shaker at room temperature, after which the enzymatic reaction was stopped by the addition of 2M H_2SO_4 (100μl/well). The absorbance at 450nm was immediately measured using a Dynex microplate reader.

2.2.5 *In* vivo studies

2.2.5.1 Intramuscular injection of plasmid DNA

In vivo experiments were carried out on C57BL/6 ApoE$^{-/-}$ mice, which were housed in a minimal disease facility with food and water *ad libitum*. Prior to intramuscular (i.m) injection tail bleeds were taken and the mice were anaesthetised with fentanyl/fluanisone and midazolam. This was followed by the injection of the tibialis anterior (TA) muscles with 10U (25μl at 0.4U/μl) of bovine hyaluronidase which is an enzyme that breaks down components of the extracellular matrix and causes the muscle to become porous. Hyaluronidase has been shown to significantly improve transduction efficiency of plasmid DNA in skeletal muscle [336;337]. Injections were carried out using a 27-gauge needle in a proximal-to-distal direction in the TA muscle. Two hours post-hyaluronidase treatment, 25μg (1μg/μl) of plasmid DNA in sterile 0.9% NaCl was injected percutaneously in the TA muscle and this was immediately followed by the application of an electrical field. The mice were given isoflurane inhalation anaesthesia for both injection of plasmid DNA and application of the electrical pulse. The injected leg was held steady and the 7mm circular electrodes were applied to the medial and lateral sides of the lower hind limb with reasonable pressure to maintain contact with the skin surface. Electrode jelly was used on the electrode plates to ensure good electrical contact and a voltage of 175V/cm was applied in ten 20ms square wave pulses at 1Hz using a BTX ECM 830 electroporator.

2.2.5.2 Collection of blood samples

Animals were placed in an appropriate restrainer and approximately 1mm of tail was removed. Blood (~50μl) from the tail vein was collected in a capillary and transferred to citrated tubes (0.109M sodium citrate was added in 1:10 of the volume) prior to injection and at various times post-injection. At termination, animals were sacrificed in a rising concentration of CO_2. The chest cavity was opened up and 0.5 – 1ml blood harvested by direct cardiac puncture. The samples were centrifuged twice at 8,000 rpm for 10min at 4°C and the plasma stored at -80°C for further use.

2.2.5.3 Collection of tissue samples

Following exsanguination of the mice, the TA muscles were excised, snap-frozen in liquid nitrogen and stored at -80°C. For removal of the brachiocephalic arteries, the animals were first perfused in situ with 10% formalin. Brachiocephalic arteries were

excised with a piece of the aortic arch and the stump of the right subclavian artery still attached to aid orientation during histological analysis and also to avoid any trauma to the brachiocephalic artery during removal [126].

2.2.5.4 Brachiochephalic artery sectioning and staining

Brachiocephalic arteries were placed into a pellet of liquid 2.5% agarose, and orientated so that the proximal end of the artery (with part of aortic arch attached) was downward, and the brachiocephalic artery itself was vertical. Once solidified, the agarose pellets were then embedded in paraffin. Sections were cut every 30μm (starting from the proximal end) and mounted onto slides. Serial sections were stained with hematoxylin, eosin and Miller's elastin/van Gieson stain.

The sections were dried in an oven at 35°C for 24h prior to staining. The sections were then immersed for 5min in a series of pots containing Histoclear, 100% alcohol (IMS 99%), 100% alcohol and 70% alcohol. The slides were rinsed in distilled H_2O and stained with 0.5% (w/v) potassium permanganate for 10min. This was followed by a 3min wash in tap water and a 5min incubation in 1% (w/v) oxalic acid. The sections were washed as before in tap water, rinsed in 70% alcohol and stained with Miller's (BDH elastin (Miller) diluted to half strength with water) for 3h. Sections were then rinsed by immersion in 70% alcohol, washed in distilled H_2O and counterstained with van Gieson (saturated aqueous picric acid 450ml + 1% aqueous acid fusion 50ml) for 10min. The sections were finally dried in a 60°C oven for 3h and rinsed in 100% alcohol.

2.2.5.5 Plaque morphology and morphometry

Elastin-stained sections were visualised under a microscope and plaques were inspected for the presence of buried fibrous caps, which are characterised by smooth muscle cell-rich layers, containing elastin, and overlayed with foam cells. Plaque morphometry was performed with a computerised image-analysis program (Image Pro-Plus, Media Cybernetics). The internal and external elasticae perimeters were recorded and used to derive the media area, which was assumed to be the circumference of a perfect circle. The plaque area was measured and the true lumen size was determined by subtracting the plaque area from the area enclosed by the internal elastic lamina (Figure 2-5). Plaque lipid content was quantified with the Scion image analysis software program. The total number of pixels in the plaque area of the brachiocephalic artery was first

calculated, and the image was then converted into black and white, with the same colour threshold set for each image. The white area represents lipid and the black area tissue, therefore, the % lipid content could be calculated by subtracting the number of pixels in the plaque area of the black and white image from the total number of pixels originally determined.

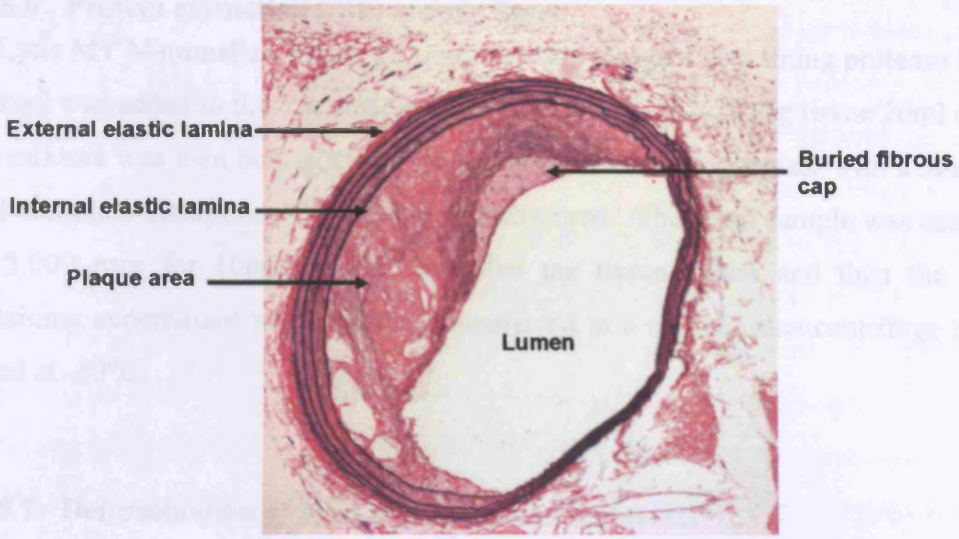

External Elastic Lamina (EEL)
Internal Elastic Lamina (IEL)
Total vessel area = perimeter of $EEL^2 \div 4\Pi$
True lumen area = (perimeter of $IEL^2 \div 4\Pi$) – plaque area
Media area = (perimeter of $EEL^2 \div 4\Pi$) – (perimeter of $IEL^2 \div 4\Pi$)

Figure 2-5. Brachiocephalic artery.
Microscope image (10×) of a 120μm section of the brachiocephalic artery stained with Miller's elastin/van Gieson. The External Elastic Lamina (EEL), Internal Elastic Lamina (IEL), plaque area, lumen and a buried cap are indicated.

2.2.5.6 Protein extraction from muscle tissue

CelLytic MT Mammalian Tissue Lysis/Extraction Reagent containing protease inhibitor cocktail was added to the TA muscle samples at a ratio of 1:20 (1g tissue/20ml reagent). The mixture was then homogenised using a rotor-stator homogeniser with a 5mm probe until complete disruption of the tissue was observed. The lysed sample was centrifuged at 13,000 rpm for 10min at 4°C to pellet the tissue debris and then the protein-containing supernatant was aspirated, transferred to a chilled microcentrifuge tube and stored at -80°C.

2.2.5.7 Determination of total plasma cholesterol levels

The use of enzymes to assay cholesterol is routinely used by many investigators. Cholesteryl esters are enzymatically hydrolysed by cholesterol esterase (CE) to cholesterol and free fatty acids. Free cholesterol, including that originally present, is then oxidised by cholesterol oxidase (CO) to cholest-4-en-3-one and hydrogen peroxide (H_2O_2). The hydrogen peroxide combines with hydroxybenzoic acid (HBA) and 4-aminoantipyrine (4AAP) to form a chromophore (quinoneimine dye) which may be quantified at 500-550 nm.

1.	Cholesteryl Esters	⟶	Cholesterol + Fatty Acids
2.	Cholesterol + O_2	⟶	Cholest-4-en-3-one + H_2O_2
3.	$2H_2O_2$ + HBA + 4AAP	⟶	Quinoneimine Dye + $4H_2O$

Individual mouse plasma from tail-vein bleeds was added at a ratio of 1:100 with infinity cholesterol liquid stable reagent, for example 2μl of plasma and 200μl of reagent. The samples and a cholesterol standard with a value of 4.29mmol/L were added in triplicate to a microtitre 96-well plate and incubated at 37°C for 5min. The absorbance at 500nm was immediately measured with a Dynex microplate reader. The relationship between cholesterol and absorbance is linear, therefore, the cholesterol values were calculated using the equation below:

Cholesterol = (Absorbance of unknown ÷ Absorbance of cholesterol standard) × cholesterol standard value

2.2.5.8 Analysis of plasma lipoprotein distribution

The Hydragel Lipo + Lp(a) K20 kit was used to determine the lipoprotein profile of pooled (10μl) and individual (10μl, diluted 1 in 5 with PBS) mouse plasma. The analysis was performed by electrophoresis on pH 7.5 buffered agarose gels and the separated lipoproteins were then stained with a lipid-specific Sudan black stain. The Hydragel K20 applicator carrier and gel were set up according to the manufacturer's instructions and 10μl of each sample was applied into the applicator wells. The sample applicator was placed into the correct position on the applicator carrier and left for 7min 30sec. The gel was then removed and placed into an electrophoresis chamber containing 300ml of Hydragel running buffer and subjected to electrophoreis for 90min at 50V. After migration, the gel was dried with hot air (80°C) for at least 45min and then immersed in Sudan black stain for 15min. The gel was de-stained for 5min in de-staining solution (45% pure ethanol and 55% ddH_2O) and immersed in wash solution for 1min. The gel was washed rapidly with ddH_2O and dried once again with hot air. The percentage of lipoprotein fractions were determined by densitometry using the Hyrys 2 Hit densitometer with the Phoresis software.

2.2.6 Statistical analysis

Values in text, tables and figures were expressed as the mean±S.D when appropriate. Statistical analysis was performed by student's t-test using Microsoft Excel (Microsoft Office XP, 2004). A $p<0.05$ was considered to be significant.

Chapter 3:

Plasmid-Mediated ApoE3 Gene Transfer

3 PLASMID-MEDIATED APOE3 GENE TRANSFER

3.1 Introduction

ApoE is considered an attractive gene transfer candidate to alleviate hypercholesterolaemia and atherosclerotic pathology. Indeed, liver-directed gene transfer of human ApoE3 by recombinant adenoviruses (rAd) in $ApoE^{-/-}$ mice lower plasma cholesterol and decelerate aortic atherogenesis [308]. The major limitation, however, with rAd vectors is their potential to induce immune and inflammatory responses, and although these can be reduced using modified vectors, levels of plasma ApoE are often compromised [312;313] (see section 1.9.1 for further details). Such considerations and also safety concerns have prompted renewed interest in non-viral gene transfer or 'naked DNA' delivery [338]. Skeletal muscle has emerged as an attractive target for gene transfer: it is highly vascularized and actively secretory, and is a stable post-mitotic tissue with little nuclear turnover [261;262]. Thus, two studies have reported systemic delivery and long-term biological effects of ApoE following intramuscular injection of plasmid DNA containing the cytomegalovirus (CMV) promoter to drive human ApoE expression. One study noted a decrease in plasma cholesterol despite very low levels of plasma ApoE [324], while the other found reduced atherosclerotic plaque and xanthoma formation after 9 months [325].

Skeletal muscle fibres are surrounded by a plasma membrane, the sarcolemma, which is in turn surrounded by an extracellular matrix (ECM). Groups of fibres are divided into fascicles by a further ECM barrier and finally the entire muscle is surrounded by the epimysium. Together these structures form the main barrier to efficient plasmid transfer into skeletal muscle. Pre-treatment of muscle with a sucrose solution has been shown to generate spaces between muscle fibres and, thus, improve the distribution of the plasmid [339] and specific enzymes, such as hyaluronidase and collagenase are reported to break down components of the ECM. Physical methods, such as electroporation and ultrasound, however, have demonstrated greater plasmid transfection efficiencies and studies have shown that when electroporation is used in conjunction with hyaluronidase treatment, plasmid transduction into skeletal muscle is significantly improved [336;337]. Electrotransfer of plasmid DNA is dependent on permeabilisation of the cell membrane and the electrophoresis of the DNA across the membrane and into the cell. Hyaluronidase helps to permeabilise components of the ECM, which could explain why

it improves electro-transfer. It is speculated that the permeabilisation of the ECM by hyaluronidase increases the effective concentration of plasmid at the membrane leading to increased uptake [296].

This chapter describes the construction and evaluation of single-stranded (ss) and self-complementary (sc) AAV expression plasmids harbouring the human ApoE3 gene, driven by the ubiquitous CMV enhancer/chicken β-actin (CAG) promoter [250] and two muscle-specific promoters, CK6 and C512. The CK6 promoter was first developed by Hauser et al. [257]; they determined the sequence of a genomic fragment of the MCK regulatory region and using oligomer-mediated site-specific mutagenesis were able to modify the enhancer, such that it significantly improved gene expression. They tested a series of small, highly active MCK regulatory cassettes, several of which contained the mutagenised MCK enhancer (2RS5) and a truncated MCK promoter region. The CK6 cassette, although less than 600bp in length, was found to be sixfold more active than the full-length 3.3kb MCK promoter, 8% as active as the CMV promoter in myocytes and 12% as active as the CAG promoter *in vivo*. Transgene expression was 600-fold higher in muscle than in liver, thus the CK6 promoter confers very high muscle specificity. More importantly, however, human dendritic cells infected *in vitro* with the CK6-driven rAd vectors, do not express significant levels of transgene; this promoter is, therefore, likely to increase the persistence of transduced muscle cells.

The C512 promoter was first described by Li et al., who designed a simple strategy to construct synthetic muscle-specific promoters [258]. The investigators, firstly, randomly assembled myogenic control elements from human α-skeletal actin (E-box, MEF-2, TEF-1 and SRE) into recombinant synthetic promoter libraries. Then, by screening the clones for their transcriptional activity *in vitro* and *in vivo*, they were able to identify promoters with enhanced activity which greatly exceeded that of natural myogenic and viral gene promoters. Multiple single elements demonstrated low activity compared with the natural skeletal α-actin promoter or clones derived from the library containing a combination of regulatory elements. In primary chicken myotubes, transgene expression from the C512 promoter was 6-fold and 10-fold greater than the CMV and skeletal α-actin promoters, respectively. The synthetic C512 promoter also demonstrated higher expression *in vivo*; transcriptional activity was reported to be 3-4-fold higher than the natural skeletal muscle promoter and 6-8-fold higher than the CMV promoter. The muscle specific activity of C512 was also confirmed in several non-

muscle cell lines and in transgenic animals; this promoter is, therefore, unlikely to drive the expression of transgenes in antigen-presenting cells. In a later study, systemic expression of FIX from the C512 promoter following intramuscular injection of an AAV1 vector was reported to be 50% of that obtained from a CMV immediate-early enhancer promoter-driven construct [259]. The small size of C512 along with its capability of directing robust levels of transgene expression make this promoter an appealing choice for our experiments.

Each plasmid construct was first tested *in vitro* in murine C2C12 myoblasts and myotubes and then injected via electrotransfer into the *T. anterior* muscles of $ApoE^{-/-}$ mice. I show that each plasmid efficiently secretes ApoE3 protein when transfected into cultured mouse C2C12 myotubes and also produces local expression, which is markedly enhanced by electropulsing the site, when injected into skeletal muscle of $ApoE^{-/-}$ mice. However, the identical assay methods failed to detect ApoE protein in plasma and the hyperlipoproteinaemia was not ameliorated, implying that a more efficient vector and delivery system is needed to achieve therapeutic levels in the circulation.

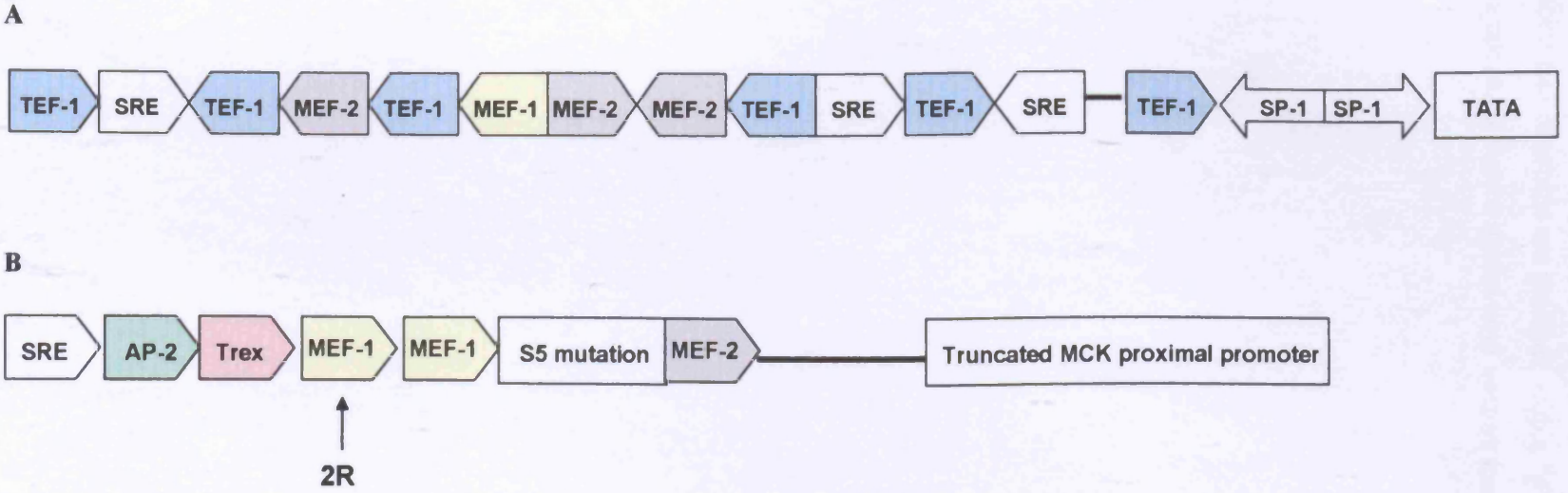

Figure 3-1. Schematic representation of the C512 and CK6 promoters

(A) The C512 promoter includes minimal muscle-specific elements of the human α-skeletal actin promoter (transcription enhancer factor 1 [TEF-1], two SP-1-binding sites and a TATA box). Additional binding sites for muscle transcription factors (TEF-1, serum response element [SRE], myocyte enhancer factor 1 [MEF-1, also known as E box], and MEF-2) were cloned upstream of the minimal promoter for optimal expression in myoctes. *(B)* The CK6 promoter contains a mutated MCK enhancer sequence (2RS5), which is composed of the transcription factor binding sites, SRE, activator protein-2 (AP-2), Trex, MEF-1 and MEF-2. The left MEF-1 is replaced with a right MEF-1 site (2R) and the sequence is mutated (S5) between the second MEF-1 and the MEF-2 sites. The S5 modification was originally created as one of a series of linker-scanner mutants, but was found to significantly increase enhancer activity. Downstream from these transcription factor binding sites is a truncated version of the MCK proximal promoter.

3.2 Results

3.2.1 Generation of ssAAV2 and scAAV2 plasmid constructs

Before explaining the construction of each plasmid, it is necessary to highlight at this point that plasmids are prefixed with a "p" rather than with "ssAAV2" or "scAAV2" so as not to confuse with the viral vectors mentioned in Chapter 4.

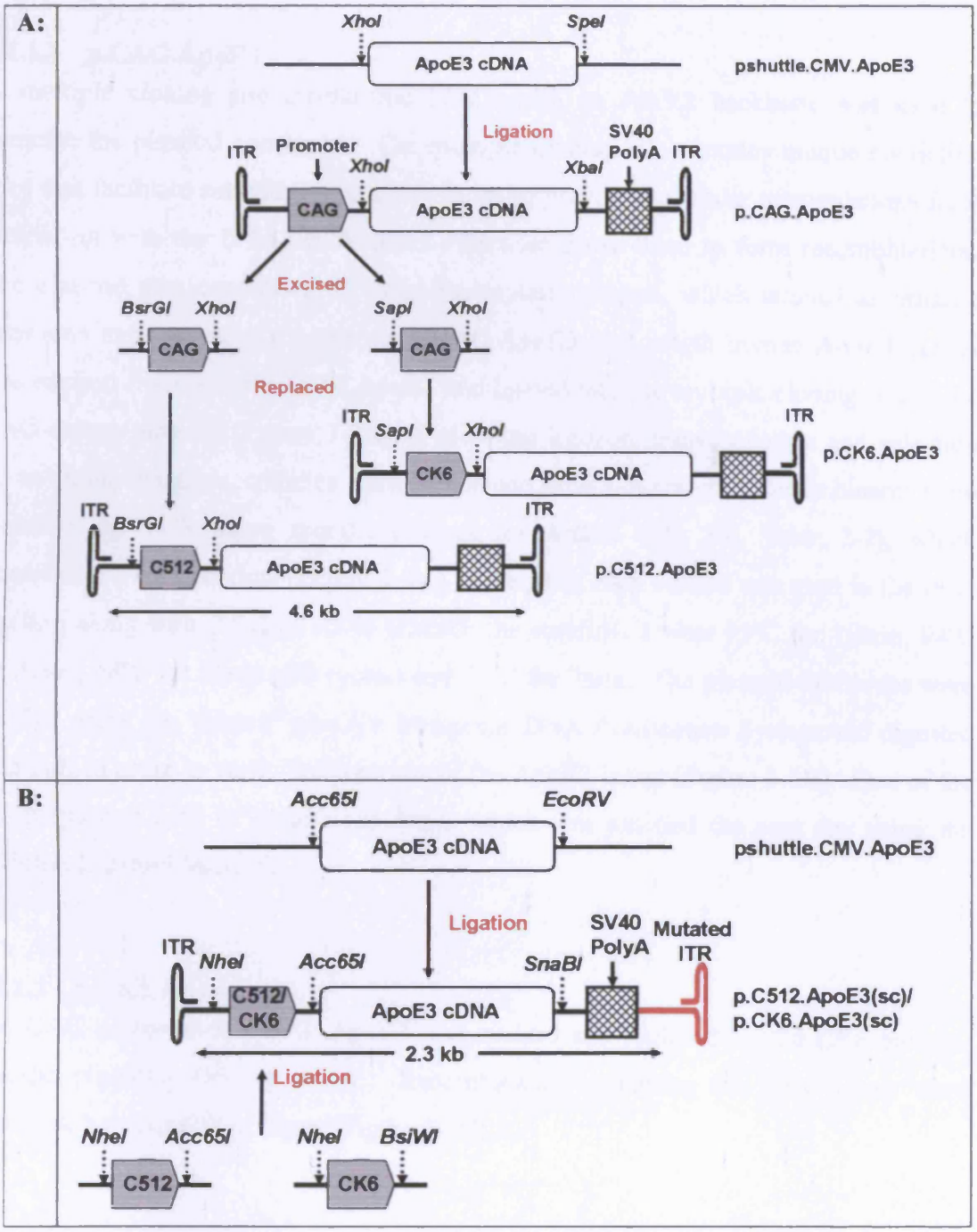

Figure 3-2. Schematic representation of the restriction digests for generation of ssAAV2 and scAAV2 plasmid constructs

Schematic representation of the restriction digests required for the generation of p.CAG.ApoE3, p.CK6.ApoE3 and p.C512.ApoE3 plasmid constructs ***(A)*** *and p.C512.ApoE3(sc) and p.CK6.ApoE3(sc) plasmid constructs* ***(B)****.*

3.2.1.1 p.CAG.ApoE3

A multiple cloning site *cis*-plasmid [252], with an AAV2 backbone was used to generate the plasmid constructs. The multiple cloning site contains unique restriction sites that facilitate sub-cloning and also helps to prevent molecular manipulations from interfering with the ITRs which could otherwise cause them to form recombinations. The plasmid also contains a SV40 polyadenylation signal, which is used to enhance transgene expression. To construct p.CAG.ApoE3, full-length human ApoE3 cDNA was excised from pshuttle.CMV.ApoE3 and ligated into the multiple cloning site of the CAG-driven plasmid (Figure 3-2A). Following ligation, transformation and selection on an ampicillin plate, colonies were picked and grown overnight. Recombinants were identified by PCR using specific primers for ApoE3 (TF, TR, Table 2-2), which amplified a 270bp product (Figure 3-3A). One μl of each culture was used in the PCR reaction along with 2.5μl of 100% DMSO; the conditions were 95°C for 10min, 94°C for 30sec, 68°C for 30sec. (25 cycles) and 72°C for 7min. The plasmid minipreps were purified using the Wizard® plus SV Minipreps DNA Purification System and digested with *SalI* in order to verify the presence of the ApoE3 insert (Figure 3-3B). One of the minipreps was used to make a maxiprep, which was purified the next day using the Endofree Plasmid Maxi kit.

3.2.1.2 p.CK6.ApoE3

The CAG promoter in p.CAG.ApoE3 was excised and replaced by the CK6 muscle-specific promoter (Figure 3-2A). Recombinants containing the CK6 insert were identified by a *SapI/XhoI* digest (Figure 3-3C).

3.2.1.3 p.C512.ApoE3

PCR primers were designed with the *BsrGI* and *XhoI* restriction sites incorporated in their 5' regions (BSRGIC512F; XHOC512R; Table 2-2). These primers were then used in PCR to amplify the C512 promoter. The amplification then generates a C512 target fragment whose termini now carry the new restriction sites. The C512 promoter insert was then purified using the Qiagen gel extraction kit and digested overnight with *BsrGI/XhoI* to generate the restriction sites. The CAG promoter in p.CAG.ApoE3 was removed and replaced with the C512 promoter (Figure 3-2A). Recombinants were identified by a *BsrGI/XhoI* digest (Figure 3-3D).

3.2.1.4 p.C512.ApoE3 (sc)

As discussed in section 1.7.3, the scAAV vector must be half the length of wild-type AAV so that it can be packaged as a dimer. The length between the two ITRs is, therefore, restricted to 2.3 kb, which makes cloning more complex when large transgenes and promoters are required. Indeed, it proved to be impossible to clone the large CAG promoter into the scAAV plasmid, thus, only scAAV vectors driven by muscle-specific promoters are assessed in this study. Full-length human ApoE3 cDNA was excised from pshuttle.CMVApoE3 and ligated into the multiple cloning site of the scAAV2 plasmid (Figure 3-2B and Figure 3-3E). Recombinants were identified by the use of PCR with specific primers for ApoE3, which amplified a 270bp product (see section 3.2.1.1 for PCR conditions). Following purification, the recombinants were verified by an *Acc65I/MfeI* digest, which produces a 1200bp fragment (Figure 3-3F). Next, it was necessary to clone the C512 promoter into the scAAV2.ApoE3 vector. *NheI/Acc65I* restriction sites were incorporated onto the ends of the C512 promoter insert by PCR amplification (C512NheF, C512Acc65R; Table 2-2) and then cloned into the scAAV2 plasmid at the 5' end of the ApoE3 insert (Figure 3-2B).

3.2.1.5 p.CK6.ApoE3 (sc)

The restriction sites *NheI* and *BsiWI* were incorporated onto the ends of the CK6 promoter insert by PCR amplification (CK6NheF; CK6BsiWIR; Table 2-2) and then cloned into the scAAV2.ApoE3 plasmid at the 5' end of the ApoE3 insert (Figure 3-2B). Recombinants were identified by the use of PCR (Figure 3-3G) with specific primers for CK6 (CK6F1, CK6R1; Table 2-2) and confirmed by a *NheI/MfeI* digest (Figure 3-3H).

A:

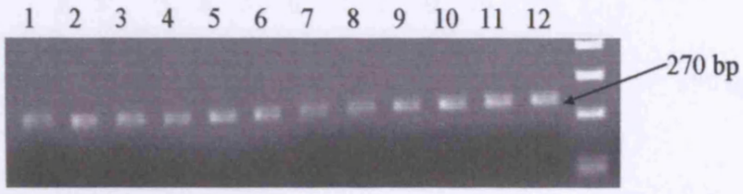
1 2 3 4 5 6 7 8 9 10 11 12
270 bp

B:

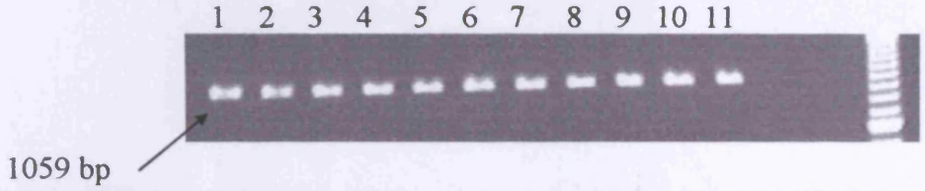
1 2 3 4 5 6 7 8 9 10 11
1059 bp

C:

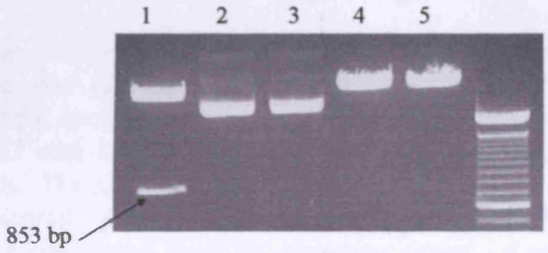
1 2 3 4 5
853 bp

D:

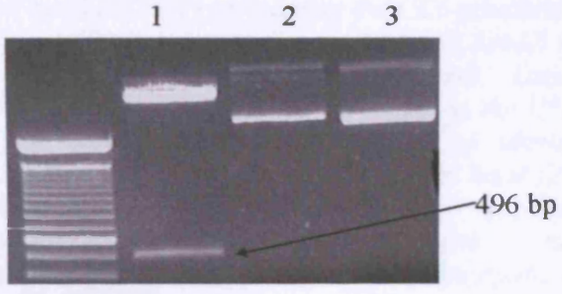
1 2 3
496 bp

E:

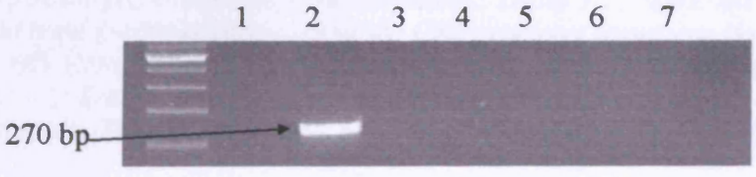
1 2 3 4 5 6 7
270 bp

F:

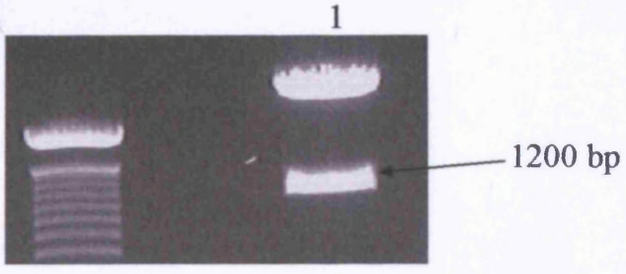
1
1200 bp

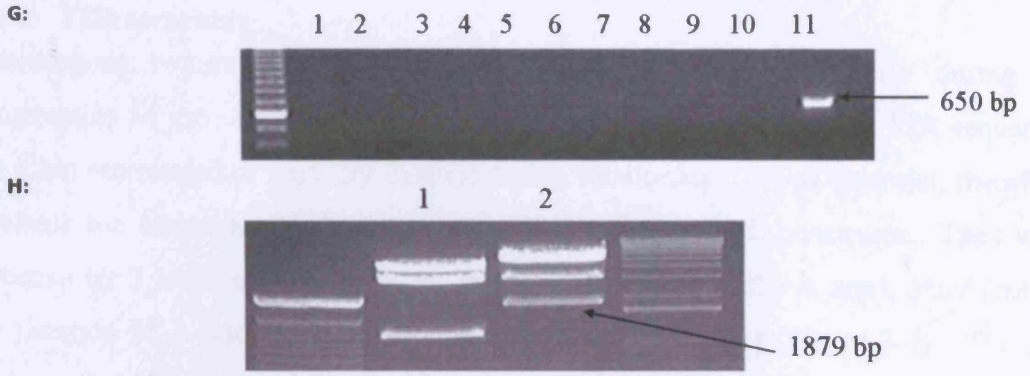

Figure 3-3. PCR and restriction enzyme digests of ssAAV2 and scAAV2 plasmid constructs

(A) PCR to identify p.CAG.ApoE3 recombinants. Lanes 1-11 represent 11 recombinants and lane 12 represents the +ve control. The expected band (270bp) representing the ApoE3 insert was amplified in all 11 colonies. ***(B)*** *Restriction digest of p.CAG.ApoE3 with SalI to verify presence of ApoE3 insert. Lanes 1-11 represent 11 recombinants. The expected band (1059bp) representing the ApoE3 insert was present in all 11 colonies.* ***(C)*** *Restriction digest of p.CK6.ApoE3 with SapI/XhoI to identify recombinants containing the CK6 promoter insert. Lanes 1-5 represent 5 separate colonies. The expected band (853bp) representing the CK6 promoter insert was present in only 1 colony (lane 1).* ***(D)*** *Restriction digest of p.C512.ApoE3 with BsrGI/XhoI to identify recombinants containing the C512 promoter insert. Lanes 1-3 represent 3 separate colonies. The expected band (496bp) representing the C512 promoter insert was present in only 1 colony (lane 1).* ***(E)*** *PCR to identify scAAV2.ApoE3 recombinants. Lane 1-7 represent 7 colonies. The expected band (270bp) representing the ApoE3 insert was present in only 1 colony (lane 2).* ***(F)*** *Restriction digest of scAAV2.ApoE3 with Acc65I/MfeI to verify the recombinant. Lane 1 represents the recombinant. The expected band (~1200bp) representing the ApoE3 insert was present.* ***(G)*** *PCR to identify p.CK6.ApoE3(sc) recombinants. Lanes 1-11 represent 11 colonies. The expected band (~650bp) representing the CK6 promoter insert was present in only 1 colony.* ***(H)*** *Restriction digest of p.CK6.ApoE3(sc) with NheI/MfeI to verify the recombinant. Lane 1 represents scAAV2.ApoE3 and lane 2 represents p.CK6.ApoE3(sc). The expected band (~1879bp) representing the CK6/ApoE3 insert was present.*

3.2.2 ITR screening

Homologous recombination can occur between the ITRs in *E.coli* during the construction of the rAAV plasmids. As a result of this recombination, ITR sequences are often rearranged or partially deleted during subcloning. It was essential, therefore, to check the intactness of the 5' and 3' ITR sequences in all constructs. They were screened by 3 restriction enzymes including *BssHII* (cuts at the A arm), *MscI* (cuts at the junction of A and D arms) and *SmaI* (cuts at the B arm) (Figure 3-4). The ITR regions were also sequenced to verify the absence of any mutation.

All the ss and sc plasmid constructs produced the correct size bands when digested with the three screening restriction enzymes (Figure 3-5 and Figure 3-8), suggesting that both the 3' and 5' ITRs were intact. Sequencing helped to further verify that there were no mutations (Figure 3-6A, B, C, D), although the ITR regions proved to be very difficult to sequence due to their hairpin structure and high guanine and cytosine content. This occasionally resulted in the loss of sequence and regions that could not be read (Figure 3-6E).

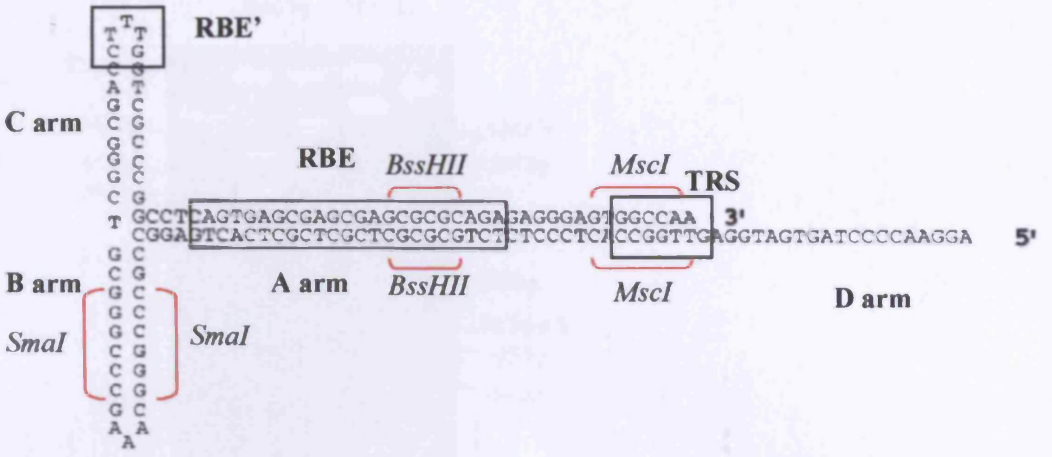

Figure 3-4. Structure and sequence of a ssAAV2 vector ITR.
The diagram includes the positions of the Terminal Resolution Site (TRS), the Rep Binding Element (RBE) and a portion of the small internal palindromes within the terminal hairpin (RBE'). The diagnostic restriction sites, MscI, BssHII and SmaI are also indicated

A:

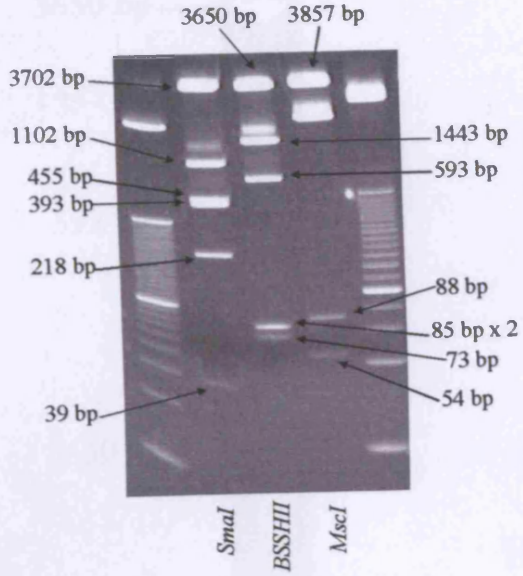
3650 bp
3857 bp
3702 bp
1102 bp
455 bp
393 bp
218 bp
39 bp
1443 bp
593 bp
88 bp
85 bp x 2
73 bp
54 bp
SmaI
BSSHII
MscI

B:

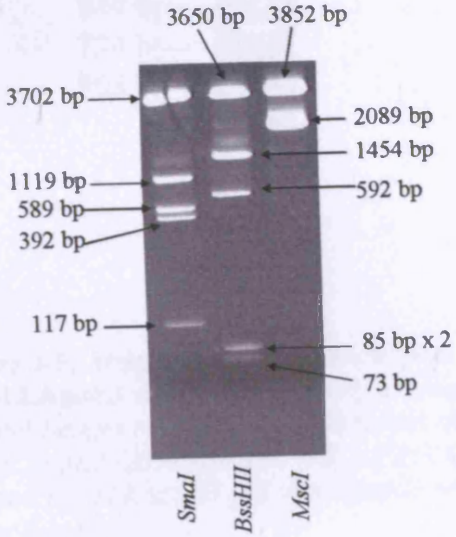
3650 bp
3852 bp
3702 bp
1119 bp
589 bp
392 bp
117 bp
2089 bp
1454 bp
592 bp
85 bp x 2
73 bp
SmaI
BssHII
MscI

C:

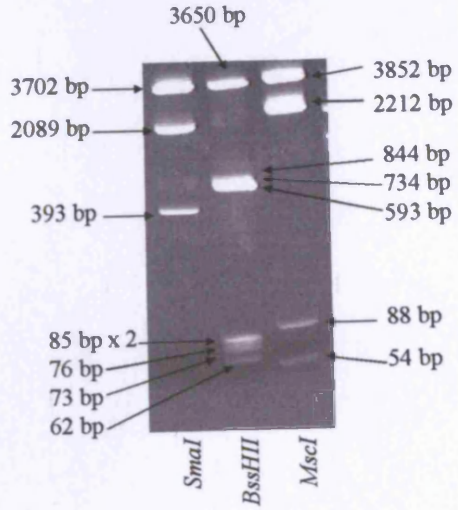
3650 bp
3702 bp
2089 bp
393 bp
85 bp x 2
76 bp
73 bp
62 bp
3852 bp
2212 bp
844 bp
734 bp
593 bp
88 bp
54 bp
SmaI
BssHII
MscI

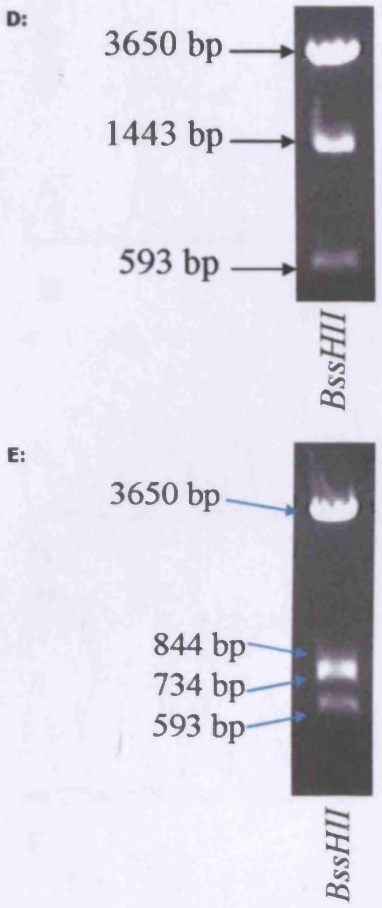

Figure 3-5. Diagnostic restriction digests of p.CAG.ApoE3, p.CK6.ApoE3 and p.C512.ApoE3 with *BssHII*, *MscI*, and *SmaI*.

The gel images represent the restriction digests of p.C512.ApoE3 (20% TBE gel) ***(A)****, p.CK6.ApoE3 (20% TBE gel)* ***(B)****, p.CAG.ApoE3 (20% TBE gel)* ***(C)****, and p.CAG.ApoE3* ***(D)*** *and p.C512.ApoE3* ***(E)*** *with BssHII only, on a 1% agarose gel to help resolve the larger bands.*

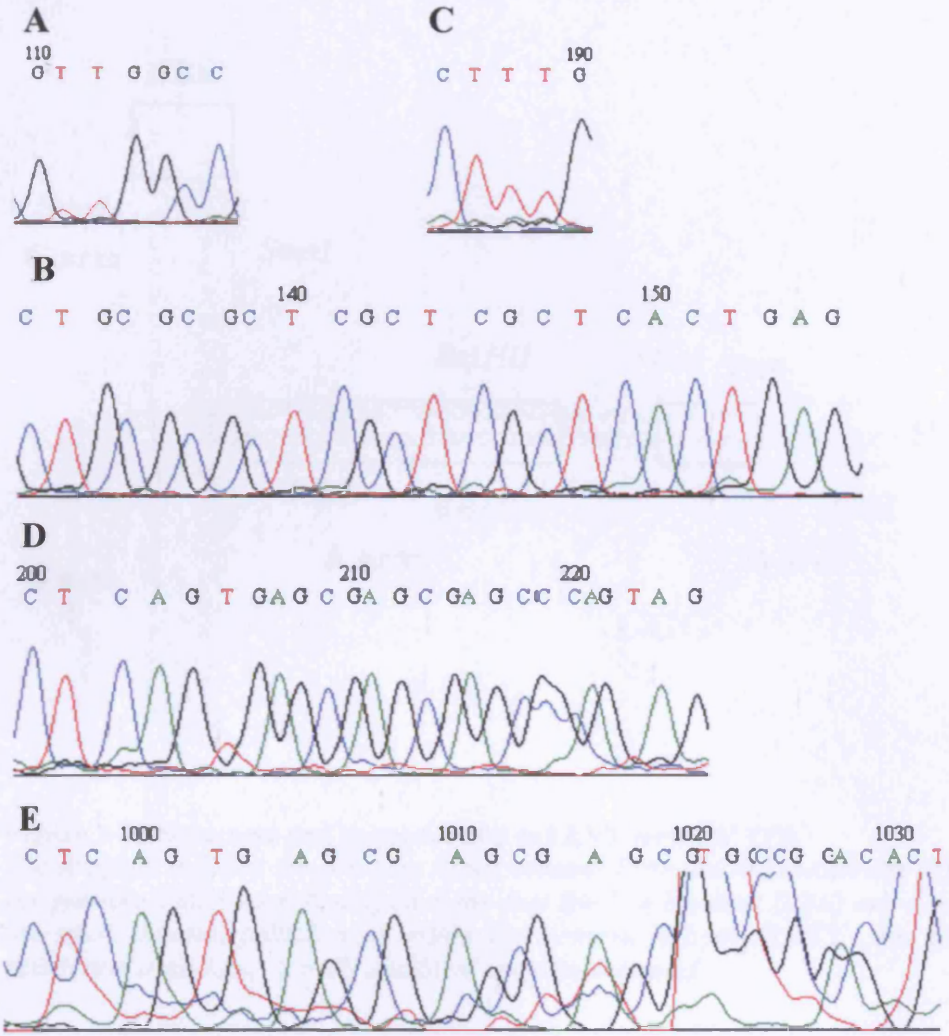

Figure 3-6. Sequencing of p.CAG.ApoE3 ITR

This figure represents the terminal resolution site (trs) ***(A)****, the Rep binding element (RBE) of the 5' ITR* ***(B)****, a portion of the small internal palindromes within the terminal hairpin (RBE') of the 5' ITR* ***(C)****, the complementary strand of the RBE of the 5'ITR* ***(D)****, and the RBE of the 3' ITR which has high background and is difficult to read* ***(E)****.*

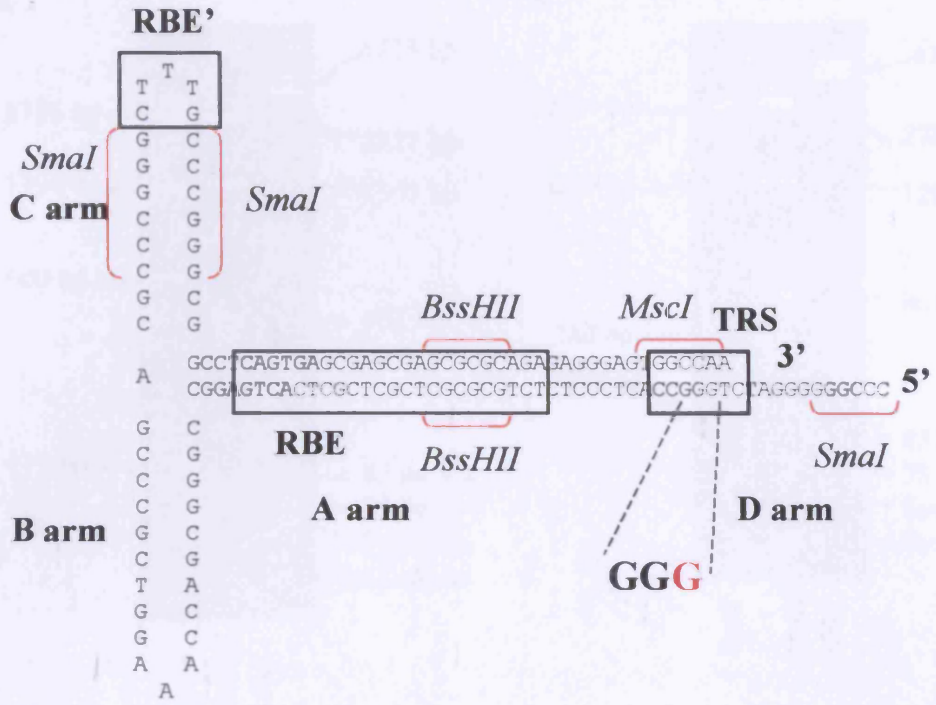

Figure 3-7. Structure and sequence of a scAAV2 vector 5' ITR
The diagram includes the positions of the mutated Terminal Resolution Site (TRS), with the guanine substitution highlighted, the Rep Binding Element (RBE) and a portion of the small internal palindromes within the terminal hairpin (RBE'). The diagnostic restriction sites, MscI, BssHII and SmaI are also indicated.

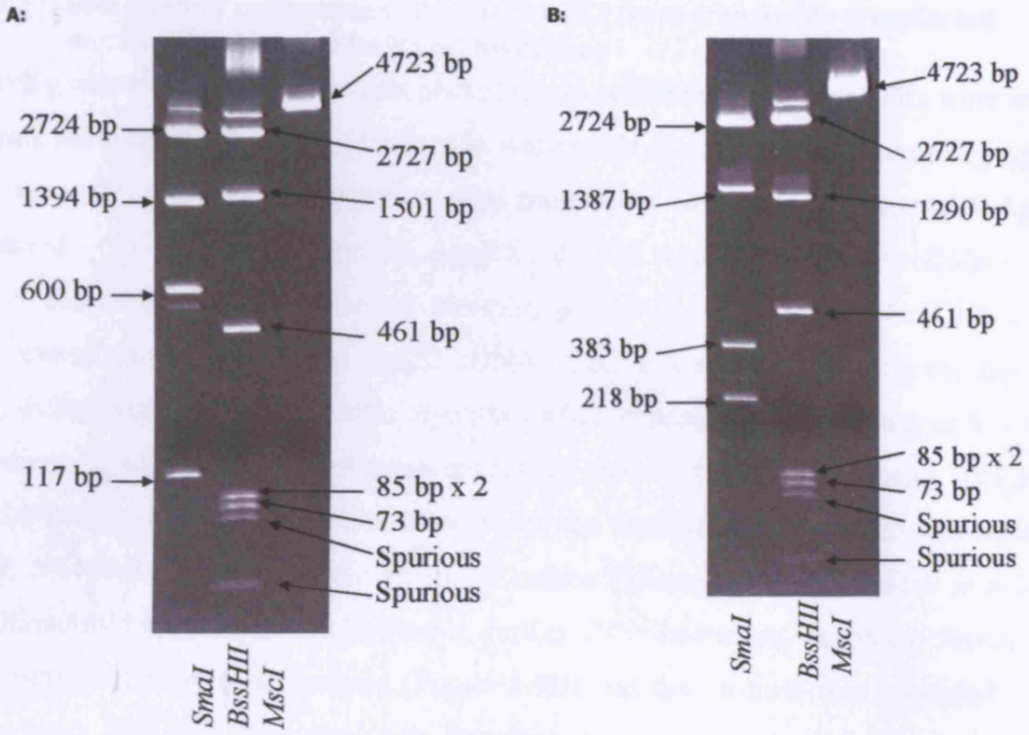

Figure 3-8. A 4-20% TBE gel showing the restriction digests of p.C512.ApoE3(sc) and p.CK6.ApoE3(sc) with *BssHII*, *MscI* and *SmaI* to screen the ITR regions
The gel images represent the restriction digests of p.CK6.ApoE3(sc) ***(A)****, and p.C512.ApoE3(sc)* ***(B)****.*

3.2.3 Secretion of recombinant human ApoE3 from transiently transfected murine C2C12 myoblasts and myotubes

Having constructed the expression plasmids and established that their ITRs were intact, it was necessary to check that the vectors were working efficiently and secreting ApoE3 *in vitro*. Murine C2C12 myoblasts were transfected with 2μg of each rAAV.ApoE3 plasmid (p.CAG.ApoE3, p.CK6.ApoE3, p.C512.ApoE3, p.CK6.ApoE3(sc) and p.C512.ApoE3(sc)) and a control plasmid, p.CK6 (-), identical to the CK6-driven expression vector, but lacking ApoE3 cDNA. C2C12 is a rapidly dividing cell line that can differentiate into post-mitotic myotubes when exposed to horse serum or low-FBS medium. The transfected cultures were left to grow in DMEM containing 10% FBS, under normal conditions for 24h, after which the medium was harvested and replaced with 5% heat-inactivated horse serum to induce differentiation and fusion into large multinucleate myotubes. Following a further 24h incubation, myoblast fusion and myotube formation was observed (Figure 3-9B) and the medium was harvested. The cells were cultured for a final 24h, at which point mature myotube formation was apparent (Figure 3-9C). ApoE3 secretion in the aspired medium was analysed by Western Blot and quantified by an ELISA. Western blot analysis (Figure 3-10) revealed that p.CAG.ApoE3 transfected cells had secreted ApoE3 at all collection-points, whereas cells transfected with plasmids driven by the muscle-specific promoters, CK6 and C512, failed to produce ApoE3 until the 24-48h collection, the time-interval in which myoblasts start to differentiate into myotubes. An ELISA (Figure 3-11) yielded values of up to 714ng/ml of ApoE3 in the medium of cells transfected with p.CAG.ApoE3. The ApoE3 content in medium from cells transfected with p.CK6.ApoE3 or p.C512.ApoE3 and their respective sc plasmids was lower, ranging from 10–80ng/ml for the 48–72h time period. Secreted ApoE3 reached optimum levels at 48h and decreased slightly at 72h, which was a trend seen in the majority of the plasmids.

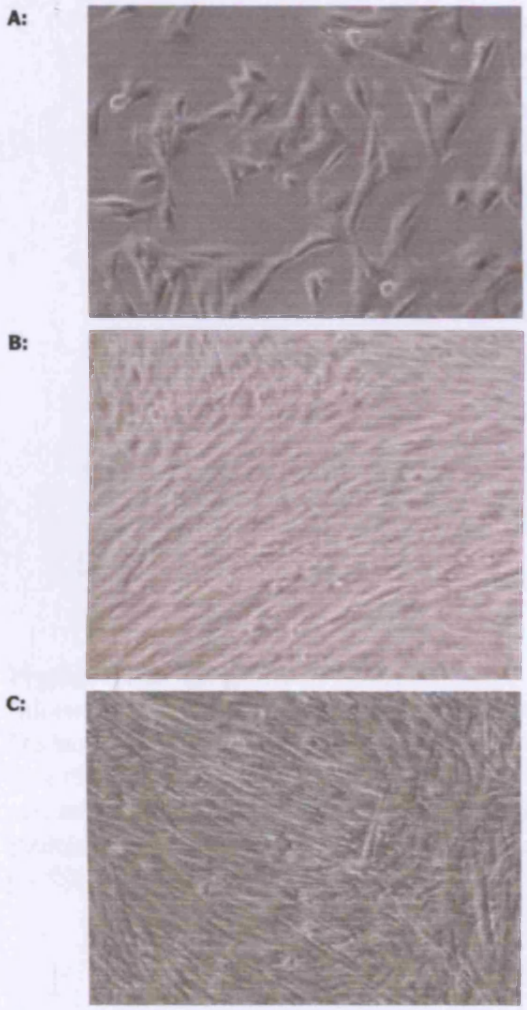

Figure 3-9. Phase microscope images (10× field) of murine C2C12 myoblast differentiation into multinucleate myotubes
(A) myoblasts after 24h incubation (seeded at 1×10^5 cells/ml); (B) myoblast fusion and myotube formation after 48h incubation; (C) mature myotubes after 72h incubation.

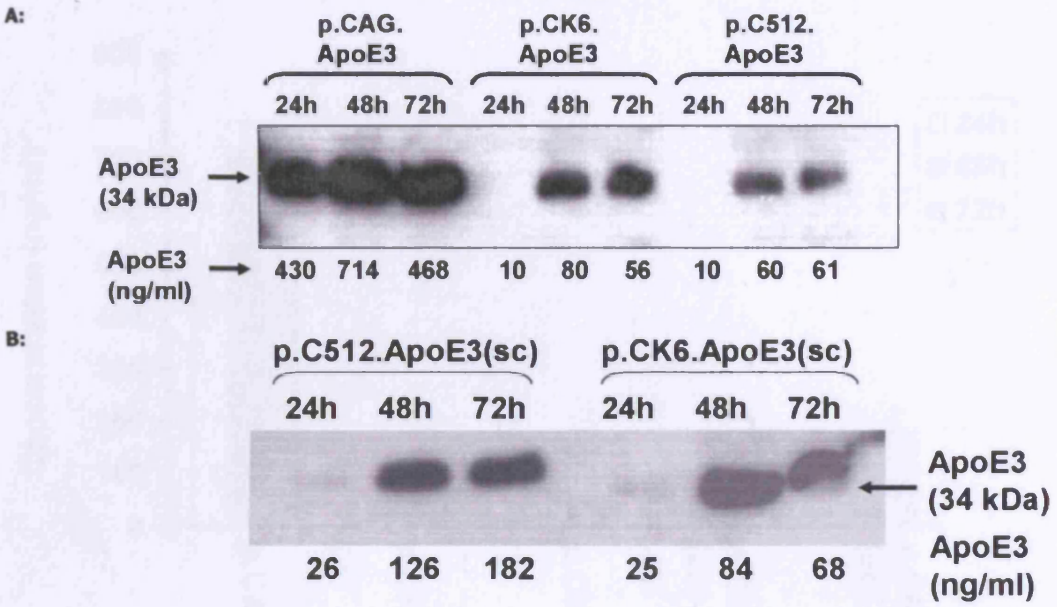

Figure 3-10. Secretion of human ApoE3 by C2C12 myoblasts and myotubes following transfection with the ApoE3 expression plasmids.
Dishes of C2C12 myoblasts were transfected with p.CAG.ApoE3 and the muscle-specific plasmids, p.CK6.ApoE3 and p.C512.ApoE3 ***(A)*** *and their respective sc plasmids* ***(B)****. Culture supernatants were probed for ApoE3 (34 kDa) by Western blotting 24, 48 and 72h after transfection, while concentrations were measured by ELISA (ng/ml).*

A:

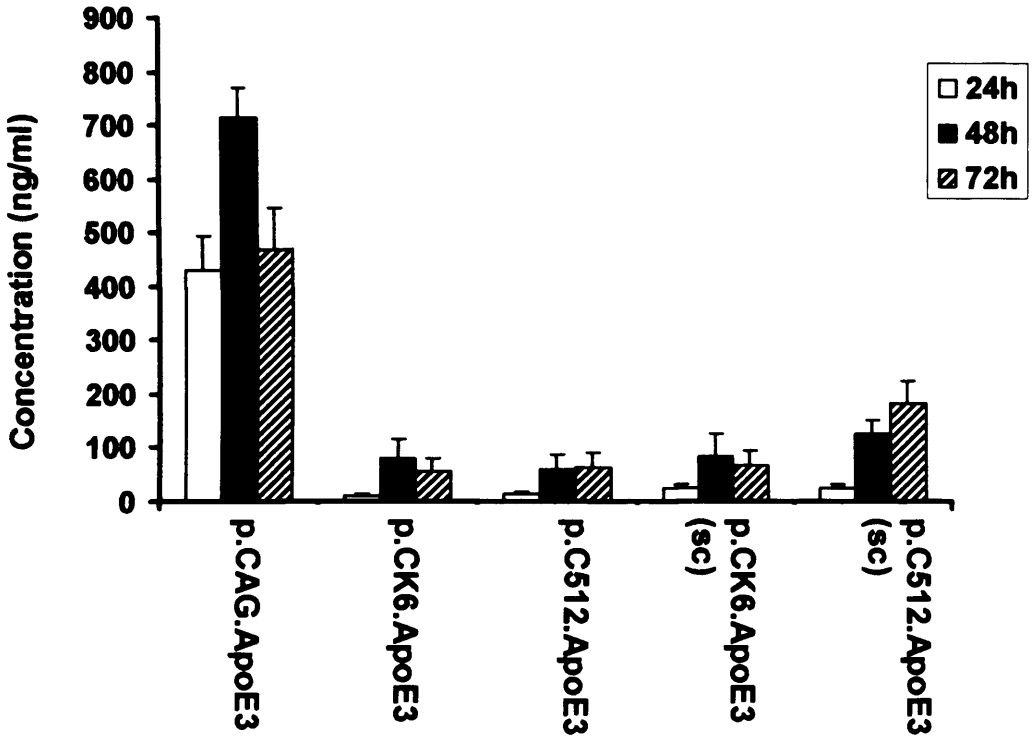

B:

	ApoE3 (ng/ml)		
Plasmid	**24h**	**48h**	**72h**
p.CAG.ApoE3	432±60.8	714±57.4	468±79.1
p.CK6.ApoE3	10±4.4	80 ±34.3	56±24.9
p.C512.ApoE3	10±3.8	60±29	61±29.4
p.CK6.ApoE3(sc)	25±7.9	84±42.8	68±27.7
p.C512.ApoE3(sc)	26±4.9	126±23.1	182±42.3

Figure 3-11. ELISA quantification of human ApoE3 secretion from transfected murine C2C12 myoblasts.

A graph (A) and a table (B) showing the concentration (ng/ml) with ± standard deviation (n = 3) of ApoE3 secreted from C2C12 myoblasts transfected with ss/scAAV2.ApoE3 plasmids.

3.2.4 Transient co-transfection of C2C12 myoblasts with p.C512.GFP and p.CMV.RFP

The transient transfection study (section 3.2.3) suggests that muscle-specific promoter activity is only switched on in differentiated myotubes. To confirm this, C2C12 myoblasts were co-transfected with 2μg of plasmids expressing fluorescent reporter genes, one driven by the muscle-specific promoter, C512 (green fluorescent protein (GFP)) and the other by the ubiquitous CMV promoter (red fluorescent protein (RFP)). As before, cells were incubated in DMEM containing 10% FBS for 24h and then switched to medium containing 5% heat-inactivated horse serum for a further 48h. At each 24h interval, cells were visualised under a phase-contrast light or fluorescent microscope to assess expression levels. Between 24-48h, myoblast fusion and myotube formation was observed, while at 72h mature myotube formation was apparent. As predicted, RFP was readily detected at all time-intervals, including the 0-24h collection when only myoblasts were present, whereas GFP was not detected until later when myotube formation was evident (Figure 3-12).

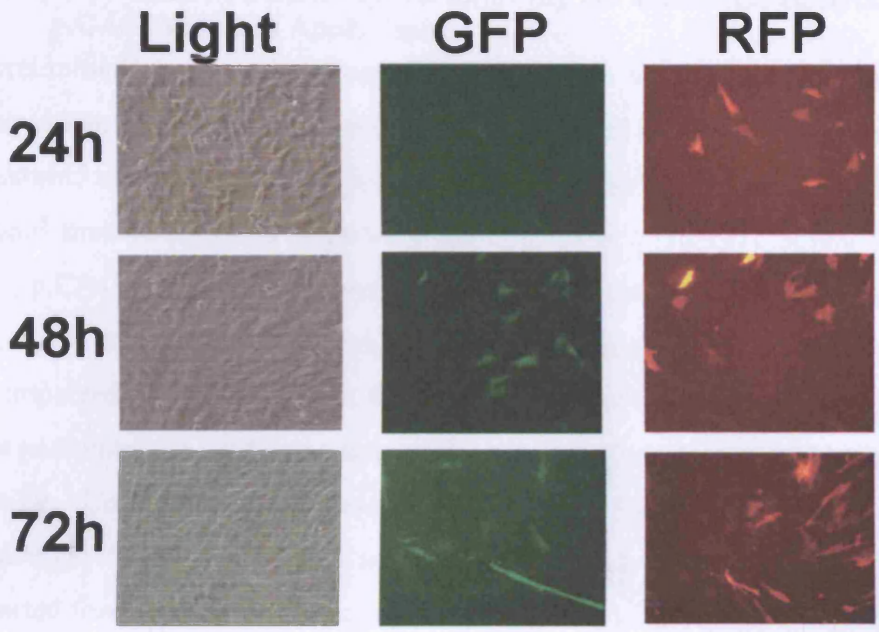

Figure 3-12. Phase and fluorescent microscope images (20× field) of murine C2C12 myoblasts co-transfected with p.C512.GFP and p.CMV.RFP
Cells were observed 24, 48 and 72h after transfection to assess relative expression levels.

3.2.5 Expression of human ApoE3 following intramuscular electrotransfer of p.CAG.ApoE3 in ApoE$^{-/-}$ mice

A preliminary *in vivo* experiment was undertaken to assess electroporation-mediated plasmid transfection. Eight ApoE$^{-/-}$ mice were given intramuscular injections of bovine hyaluronidase, an enzyme that breaks down extracellular matrix and connective tissue in skeletal muscle fibres to improve plasmid transfer [336;337], followed, 2h later, by 25μg p.CAG.ApoE3. For 5 mice an electrical field was applied immediately to the single TA muscle injection site, whereas the muscles of the other 3 mice were not electropulsed. Plasma samples were collected prior to injection and at termination, 7 days post-injection, and were assayed for ApoE3 expression by ELISA and by Western blotting. Unfortunately, the levels of plasma ApoE3 in all eight mice fell below the reliable detection limit (~15 ng/ml for the ELISA; data not shown). However, protein extracted from excised muscle clearly demonstrated local ApoE3 expression by Western blotting, though only in those electropulsed (Figure 3-13A). ELISA quantification of ApoE3 expressed in these muscles demonstrated levels between 4.8–20 μg/TA muscle, indicating high variability between each mouse, and much lower amounts in non-electroporated muscle (Figure 3-13A).

Individual total plasma cholesterol was measured at day 7, but was not significantly lower than the day 0 sample for either electroporated or non-electroporated animals (Figure 3-13B). The lipoprotein profile of pooled plasma from each group was also analysed. Very-low-density lipoprotein (VLDL), intermediate-density lipoprotein (IDL) and low-density lipoprotein (LDL) migrated as a heavily-stained broad preβ-band in the plasma of ApoE$^{-/-}$ mice, whereas, high-density lipoprotein (HDL) ran as a fast α-migrating minor fraction (Figure 3-13C). In contrast, plasma from wild-type (wt) C57BL/6 mice has high levels of HDL and a relatively low proportion of clearly separated VLDL and LDL. Densitometry of the lipoprotein profiles did not reveal any difference between day 0 and day 7 samples, either in absolute amounts or in the HDL to total lipoprotein ratio (Figure 3-13D), which can serve as a sensitive indicator of effective ApoE gene transfer [312;327].

A:

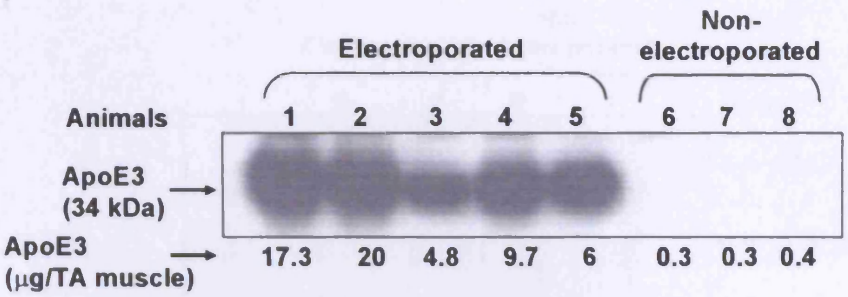
Electroporated
Non-electroporated
Animals
1 2 3 4 5 6 7 8
ApoE3 (34 kDa)
ApoE3 (μg/TA muscle)
17.3 20 4.8 9.7 6 0.3 0.3 0.4

B:

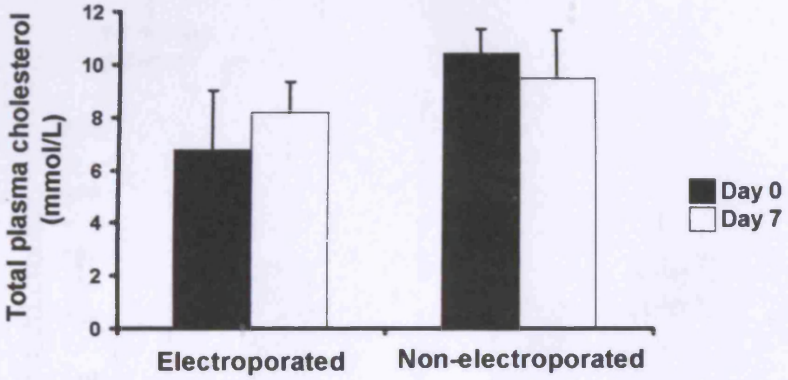
Total plasma cholesterol (mmol/L)
12
10
8
6
4
2
0
Day 0
Day 7
Electroporated
Non-electroporated

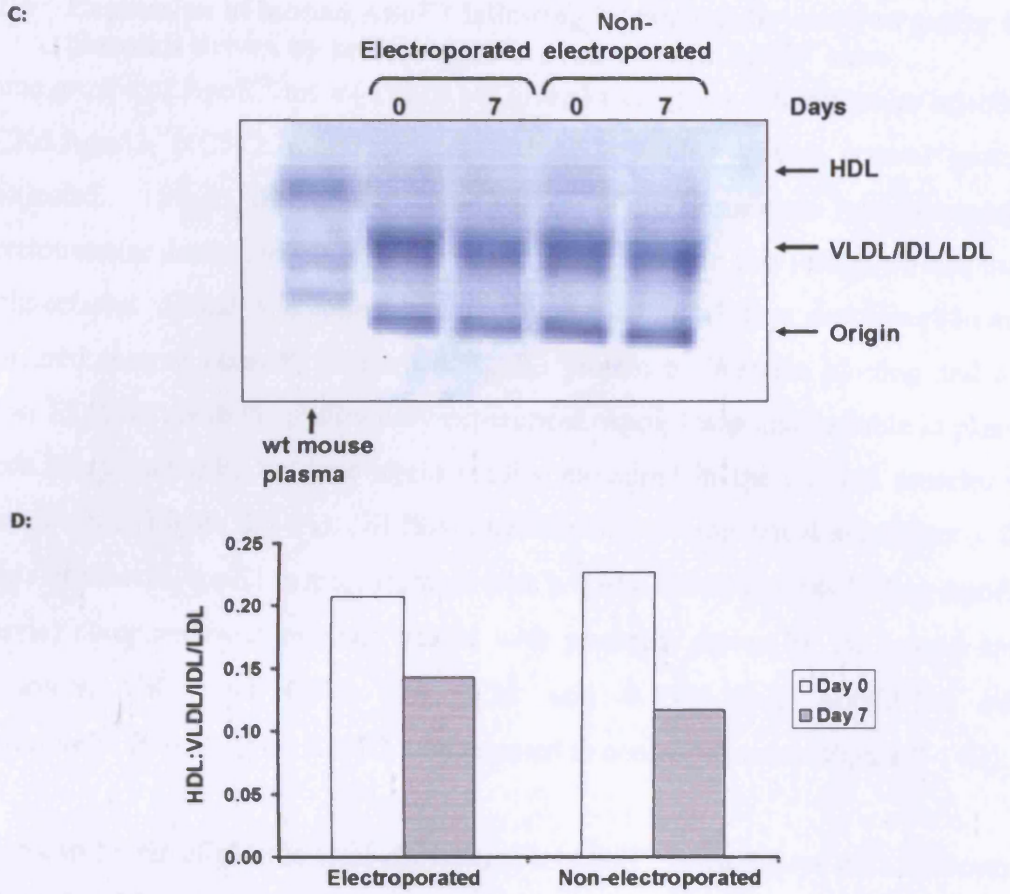

Figure 3-13. Electroporation enhances local expression of ApoE3 following intramuscular injection of the p.CAG.ApoE3 expression plasmid in ApoE$^{-/-}$ mice. *Tibialis anterior (TA) muscles of young ApoE$^{-/-}$ mice were injected with p.CAG.ApoE3 and, when required, immediately electropulsed.* ***(A)*** *Western blot analysis of ApoE3 expression after 7 days in excised TA muscle from electroporated mice (animals 1-5) and non-electroporated mice (animals 6-8); ApoE3 concentrations (μg/TA muscle) were quantified by an ELISA.* ***(B)*** *Total plasma cholesterol levels were determined for individual animals in each group before and 7 days post injection of p.CAG.ApoE3.* ***(C)*** *Pooled plasma samples at day 0 and day 7 were subjected to agarose gel electrophesis and the separated lipoproteins stained with Sudan black.* ***(D)*** *Graphical representation of the HDL:VLDL/IDL/LDL ratio.*

3.2.6 Expression of human ApoE3 following intramuscular electrotransfer of plasmids driven by muscle-specific promoters in ApoE$^{-/-}$ mice

Three groups of ApoE$^{-/-}$ mice (6 mice per group) were given intramuscular injections of p.CK6.ApoE3, p.C512.ApoE3 or p.CAG.ApoE3, while a fourth control group was uninjected. Since the above combination of hyaluronidase pre-treatment and electrotransfer demonstrated enhanced plasmid transfection this technique was used for all injections. Blood was collected prior to injection and 7 days post-injection and the separated plasma assayed for human ApoE3 protein by Western blotting and our in-house ELISA. As in the preliminary experiment, ApoE3 was undetectable in plasma by these assay methods, but was again readily measured in the excised muscles of all treated mice (Figure 3-14A). ELISA quantification demonstrated significantly higher levels of muscle ApoE3 in mice injected with p.CAG.ApoE3 (13.38±7.46μg ApoE3/TA muscle) compared with animals treated with plasmids driven by the muscle-specific promoters, CK6 and C512 (0.61±0.38 and 0.45±0.38μg ApoE3/TA muscle, respectively; $P<0.001$); no ApoE3 was detected in control muscles (Figure 3-14B).

The mean levels of plasma total cholesterol in ApoE$^{-/-}$ mice 7 days post-injection with p.CAG.ApoE3, p.CK6.ApoE3 and p.C512.ApoE3, were not significantly reduced compared with the negative control group. Furthermore, the lipoprotein profiles in the three treatment groups did not obviously differ from the control group at 7 days (Figure 3-14C), and this was confirmed by densitometric analysis.

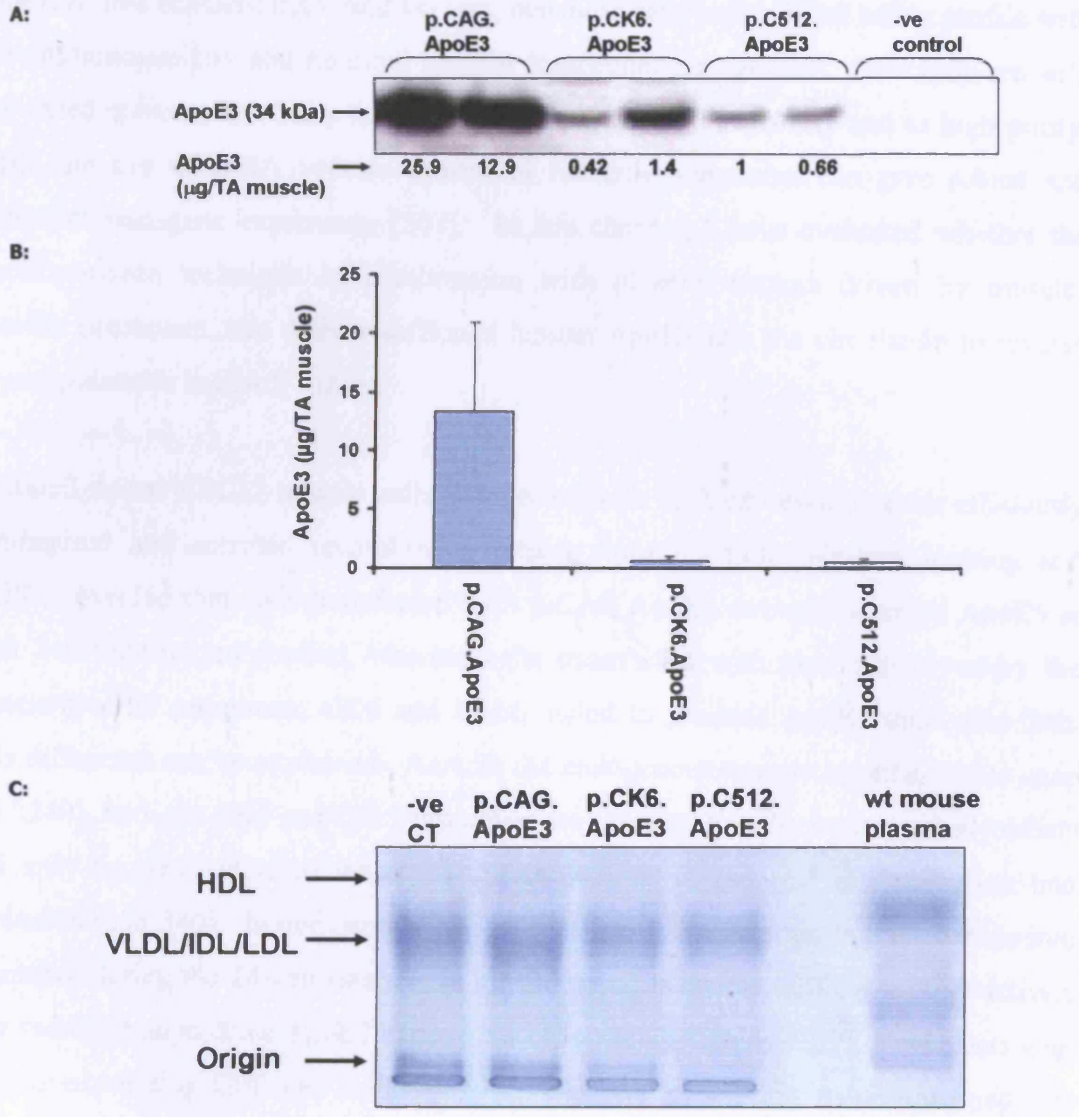

Figure 3-14. Muscle ApoE3 levels and plasma lipoprotein distribution in ApoE-deficient mice following intramuscular electrotransfer of plasmids driven by muscle-specific promoters expressing ApoE3.

Three groups of ApoE$^{-/-}$ mice were injected intramuscularly with p.CAG.ApoE3, p.CK6.ApoE3 or p.C512.ApoE3, while a fourth negative control group received no injection. ***(A)*** *Representative Western blots (2 mice per group) of ApoE3 expression in excised TA muscle; ApoE3 concentrations (µg/TA muscle) were quantified by ELISA.* ***(B)****. Graphical representation of the average ApoE3 concentration (µg/TA muscle) from each group.* ***(C)*** *Pooled plasma samples at day 7 were subjected to agarose gel electrophoresis and the separated lipoproteins stained with Sudan black.*

3.3 Discussion

Although less efficient than viral vectors, plasmids have an excellent safety profile with low immunogenicity and minimal risk for insertional mutagenesis, since they are only expressed episomally. They may also be manufactured in quantity and to high purity, while the use of DNA vectors devoid of bacterial sequences can give robust and persistent transgene expression [307]. In this chapter, I have evaluated whether the electroporation technique in combination with plasmid vectors driven by muscle-specific promoters, can deliver sufficient human ApoE3 into the circulation to reverse hyperlipidaemia in $ApoE^{-/-}$ mice.

Cultured mouse C2C12 muscle cells transfected with each expression vector efficiently synthesised and secreted recombinant human ApoE3. Both Western blotting and ELISA revealed that cells transfected with p.CAG.ApoE3 strongly secreted ApoE3 at each 24h time-period studied, whereas cells transfected with plasmids driven by the muscle-specific promoters, CK6 and C512, failed to produce ApoE3 until after 24h. This difference can be explained. As with the endogenous muscle creatine kinase gene [257;340], both the CK6 and C512 promoters are transcriptionally inactive in myoblasts and only become activated when myoblasts commit to terminal differentiation into myotubes [258;340]. In our experiments, C2C12 myoblasts started to differentiate into myotubes during the 24-48h interval, in which period muscle-specific promoter activity was switched on to drive ApoE3 expression. Co-transfection of C2C12 myoblasts with p.C512 expressing GFP and a CMV-driven plasmid expressing RFP confirmed this explanation; as expected, GFP was not detected at the early 0-24h time-interval, whereas RFP was readily observed. Although the amount of ApoE3 protein expressed from both muscle-specific promoters in terminally differentiated myotubes was 8-times less than from the CAG promoter (Figure 3-11; 48-72h collections), the latter was most probably still producing a significant proportion from myoblasts as this was evident for p.CMV.RFP (Figure 3-12; 48-72h). Nevertheless, Hauser et al. reported that CK6 had only 8% the activity of the ubiquitous CMV promoter in myocytes *in vitro*, and 12% of the CAG promoter *in vivo* [257]. On the other hand, the synthetic C512 promoter was generally very comparable to the CMV promoter in a series of *in vitro* and *in vivo* studies, and often proved superior [258;259].

$ApoE^{-/-}$ mice were used for my preliminary *in vivo* experiments since they become grossly hypercholesterolaemic on normal chow [117;133]. My experiments were

designed to evaluate hypolipidaemic effects of nonviral ApoE3 gene transfer and hence were confined to a study period of 7 days. If sufficient ApoE3 was secreted into plasma, it was predicted that there would be a rapid reduction in total cholesterol and a shift towards an atheroprotective lipoprotein profile, namely decreases in VLDL and LDL, and a rise in HDL. These changes were noted, for example, in $ApoE^{-/-}$ mice 5 days after intravenous injection (liver-directed) administration of a rAd expressing human ApoE3 [312].

In my preliminary *in vivo* experiment hyaluronidase and electrotransfer-mediated plasmid transduction was assessed in 5 mice, with the remaining 3 mice only receiving hyaluronidase treatment to enhance plasmid uptake. Unfortunately, our assay methods did not detect ApoE3 in plasma of mice injected with p.CAG.ApoE3. In agreement, I found no evidence for reduced total cholesterol or for normalisation of the lipoprotein profile in mice 7 days after treatment. Though disappointing, these results were consistent with studies in $ApoE^{-/-}$ mice [325] and Yoshida Wistar rats [341] receiving non-electroporated intramuscular injections of naked plasmids expressing human ApoE2 or ApoE3. In both of these studies, only the receptor binding-defective ApoE2, and not wild-type ApoE3, was detected in plasma, although local expression of recombinant ApoE3 was measurable in the muscle. A subsequent study did report detectable ApoE3 in plasma after an intramuscular injection of DNA, but the level was very low (0.6ng/ml, well below the range of our own ELISA) [324]. We were also able to detect local expression of human ApoE3 in excised muscles and this was markedly increased (50-fold) by electroporation, confirming previous reports that this technique significantly enhances plasmid transfer [342].

As with the preliminary *in vivo* experiment, ApoE3 was not detected in the plasma, but readily expressed in the excised muscle of mice injected with the CK6- and C512-driven plasmids. In agreement with the findings *in vitro* (Figure 3-11), the total amount of ApoE3 expressed in the muscle (~0.5μg) was much lower compared with that observed in mice treated with p.CAG.ApoE3 (6-25μg). As expected, plasma total cholesterol had not reduced and the lipoprotein profile was not normalised in the mice after 7 days of treatment with these ApoE3 expression plasmids.

Interestingly, the levels of ApoE3 expression in excised, electroporated muscle varied from one mouse to another. There are a number of factors that are likely to cause this variation; TA muscles vary in size, therefore, adjustment of the voltage applied for each

animal may be important. The distribution of transduced fibres may be affected depending on where the needle is placed within the muscle in relation to the central tendon and a precise orientation of the electrical field is necessary for efficient electropermeabilisation [343].

How can we explain this discrepancy between ample local expression of ApoE3 and very low plasma levels? One possibility is that secreted ApoE3 is promptly sequestered by the excess of remnant lipoproteins in the plasma of $ApoE^{-/-}$ mice and, unlike binding-defective ApoE2, is rapidly cleared by the liver via interaction with the LDL-R or LRP [76;153;344]. Such rapid removal has been reported following injection of ApoE3 protein [327;345]. Note too that mouse ApoB-containing lipoproteins (VLDL, IDL and LDL) are almost entirely dependent on ApoE for clearance; unlike their human counterparts, they contain a very high proportion of ApoB48, a truncated structural protein which lacks the receptor-binding domain present in fully-functional ApoB100 [128]. Hence, in our plasmid-treated $ApoE^{-/-}$ mice any lipoprotein particles sequestering ApoE3 would be rapidly targeted for hepatic clearance. An alternative explanation is that recombinant ApoE3 is successfully expressed by muscle, but the protein is inefficiently secreted. An initial appraisal would suggest this possibility is unlikely as we readily measured ApoE3 protein in myotube culture medium following *in vitro* transfections, while *in vivo* skeletal muscle transduced with an ApoE3-expressing rAd vector secreted ApoE3 into plasma [312]. However, in the latter study high-dose intramuscular injections of rAd vector were needed to measure ApoE3 in plasma 3 and 7 days post-injection; low-dose injections did not produce detectable plasma ApoE3. As ApoE interacts strongly with glycosaminoglycans (GAGs) in cell-surface membranes and extracellular matrix [346], it is conceivable that a threshold level of ApoE3 expression is needed to saturate such binding sites before efficient secretion occurs. This possibility merits further investigation.

In summary, we have shown that hyaluronidase pre-treatment and electroporation significantly enhance ApoE3 transgene expression following injection of naked DNA (plasmids) into skeletal muscle. Our original hope was that these techniques in combination with plasmid vectors driven by muscle-specific promoters would produce sustained physiological levels of ApoE3 protein in plasma. Unfortunately, measurable levels of circulating ApoE3 were not attained and consequently hyperlipidaemia was not reversed. This does not exclude, however, long-term therapeutic benefits, as

previous deliveries of ApoE3 by intramuscular plasmid injection [325] or by a cell-based platform [326] have demonstrated reductions in atherosclerotic aortic plaques despite a failure to detect ApoE3 in plasma. Notwithstanding, we conclude that a more efficient delivery vehicle is needed to fully exploit the benefits of ApoE3 gene therapeutics and that although non-viral gene therapy has made substantial progress it still struggles to mimic the efficiency of recombinant viruses.

Chapter 4:

rAAV-mediated ApoE3 Gene Transfer

4 rAAV-MEDIATED APOE3 GENE TRANSFER

4.1 Introduction

Early liver-directed gene transfer studies with ApoE utilised recombinant adenoviruses (rAd) and were initially reported to be a success as a lowering in plasma cholesterol and a deceleration in aortic atherogenesis was observed in $ApoE^{-/-}$ mice [308]. However, the therapeutic effect of these 1st generation vectors was shown only to be transient due to an immune response directed against both the transgene and the rAd proteins. Nevertheless significant progress has since been made with improved 2nd generation rAd vectors which have their E1, E3 and DNA polymerase genes deleted to reduce hepatotoxicity [312] and which contain mammalian promoters, for example cellular elongation factor 1α (EF-1α), to prolong ApoE transgene expression [314]. However, with the addition of the EF-1α promoter, ApoE levels in the plasma and normalisation of the lipoprotein profile were compromised, suggesting that further vectors are needed.

Recombinant adeno-associated virus (AAV) vectors fortunately offer more hope for improvement and have emerged as attractive alternatives for achieving stable and safe transgene expression *in vivo*. They are non-pathogenic and require a helper virus for productive infection, which ultimately enhances their safety profile. In the first report, 5 years ago, an AAV2 vector expressing ApoE was used to transduce skeletal muscle of young $ApoE^{-/-}$ mice and although hyperlipidaemia was not reversed, as the levels of ApoE secreted were low, there was a 29% reduction in plaque formation up to 3 months later [316]. Since then AAV technology has undergone several advances, the first of which involved the cloning of additional serotypes (AAV1-AAV11) that have been critically evaluated for their tissue tropism. AAV serotype-2, now well-documented to be the least efficient *in vivo*, can be pseudotyped by packaging with capsids from other serotypes [200] to achieve the most efficient transduction efficiency in a desired tissue. Indeed, intravenous injection of AAV2/7 and AAV2/8 vectors expressing human ApoE3 produced sustained therapeutic levels of ApoE3 in plasma and cholesterol levels were lowered for up to 1 year. Furthermore, atherosclerosis in these mice had been completely prevented [318]. Another major development in AAV technology has been the discovery of the self-complementary AAV (scAAV) vector. Conventional single-stranded AAV (ssAAV) vectors are limited by their requirement for either host-cell mediated synthesis of the complementary-strand or annealing of the plus and minus

strands from two separate viral particles co-infected into the same cell. Molecular rearrangement of the ssAAV vector genome into either circular or linear concatemers is an essential event for stable persistence of the transgene *in vivo* [177;178]. A double stranded structural intermediate is required for such molecular rearrangements to occur, and since this event does not occur immediately after transduction, a rapid disintegration of linear ss vector genome follows. However, it has now been demonstrated that when the rAAV genome length is half the wild-type size, two copies can be packaged as a dimeric inverted repeat DNA molecule (scAAV). Such scAAV molecules should spontaneously re-anneal, bypassing the rate-limiting step of second-strand synthesis and allowing rapid formation of a transcriptionally active molecule. This phenomenon was discovered by Hirata and Russell [284] and manipulated further by McCarty *et al.* [285;286].

In 1996, Kessler et al. first demonstrated the ability of rAAV vectors to transduce skeletal muscle and achieve sustained expression and systemic delivery of a therapeutic protein following a single intramuscular administration [347]. Several studies have since used skeletal muscle as a platform for rAAV-mediated gene transfer and their success has given us impetus for our study [263;348-350].

This chapter describes the generation of pseudotyped ssAAV2/7 and scAAV2/7 vectors harbouring the human ApoE3 gene, which are driven by the ubiquitous CMV enhancer/chicken β-actin (CAG) promoter [250] and two muscle-specific promoters, CK6 [257] and C512 [258]. The three-plasmid system was used, which involved the triple transfection of 293-T cells with an Ad helper plasmid, a pAAV expression plasmid (see section 3.2.1), and a packaging plasmid containing the AAV-serotype 2 *Rep* and AAV-serotype 7 *Cap* genes. AAV7 is reported to have a high transduction efficiency in muscle *in vivo* [194;207] and was, therefore, selected for this study. The AAV vectors were first evaluated *in vitro* and then injected into the TA muscles of $ApoE^{-/-}$ mice to assess their ability to ameliorate hypercholesterolaemia.

4.2 Results

4.2.1 Construction and characterisation of ssAAV2/7 and scAAV2/7 vectors expressing the human ApoE3 transgene

As described in the introduction, when the rAAV genome length is half the wild-type size, two copies can be packaged as a dimeric inverted repeat DNA molecule (scAAV). Here we have used specialised scAAV plasmids, which have a mutation in their 5' ITR (see section 1.7.3) and are, therefore, able to form dimeric inverted repeat forms of the genome efficiently. Initially it was thought that only scAAV2/7 vectors driven by the two muscle-specific promoters could be constructed due to the large size of the CAG promoter (see section 3.2.1.4). The replicon size of the ssAAV2/7.CAG.ApoE3 vector, however, is 2499bp, which is just over half the length of the wild-type genome (2340bp). The predicted size of the dimeric replicative form of this vector is 4853bp, which is 103.7% of the wild-type genome and within the optimal size range for efficient packaging. It is possible, therefore, that the ssAAV2/7.CAG.ApoE3 vector could package either two monomeric copies or dimeric inverted repeat DNA molecules (scAAV) (Figure 4-1A). The replicon size of the ssAAV2/7.CK6.ApoE3 vector is 2367bp, which is again close to half the length of the wild-type genome and has, thus, the potential to form a scAAV molecule. The predicted dimeric size of this vector is 4589bp, which is 98% of the wt AAV genome length (Figure 4-1B). Both the scAAV2/7.CK6.ApoE3 and scAAV2/7.C512.ApoE3 vectors have dimeric sizes of 4271bp and 3869bp respectively (Figure 4-1C), the latter, however, is below 4.1kb, which is the minimal level for efficient functional packaging [351].

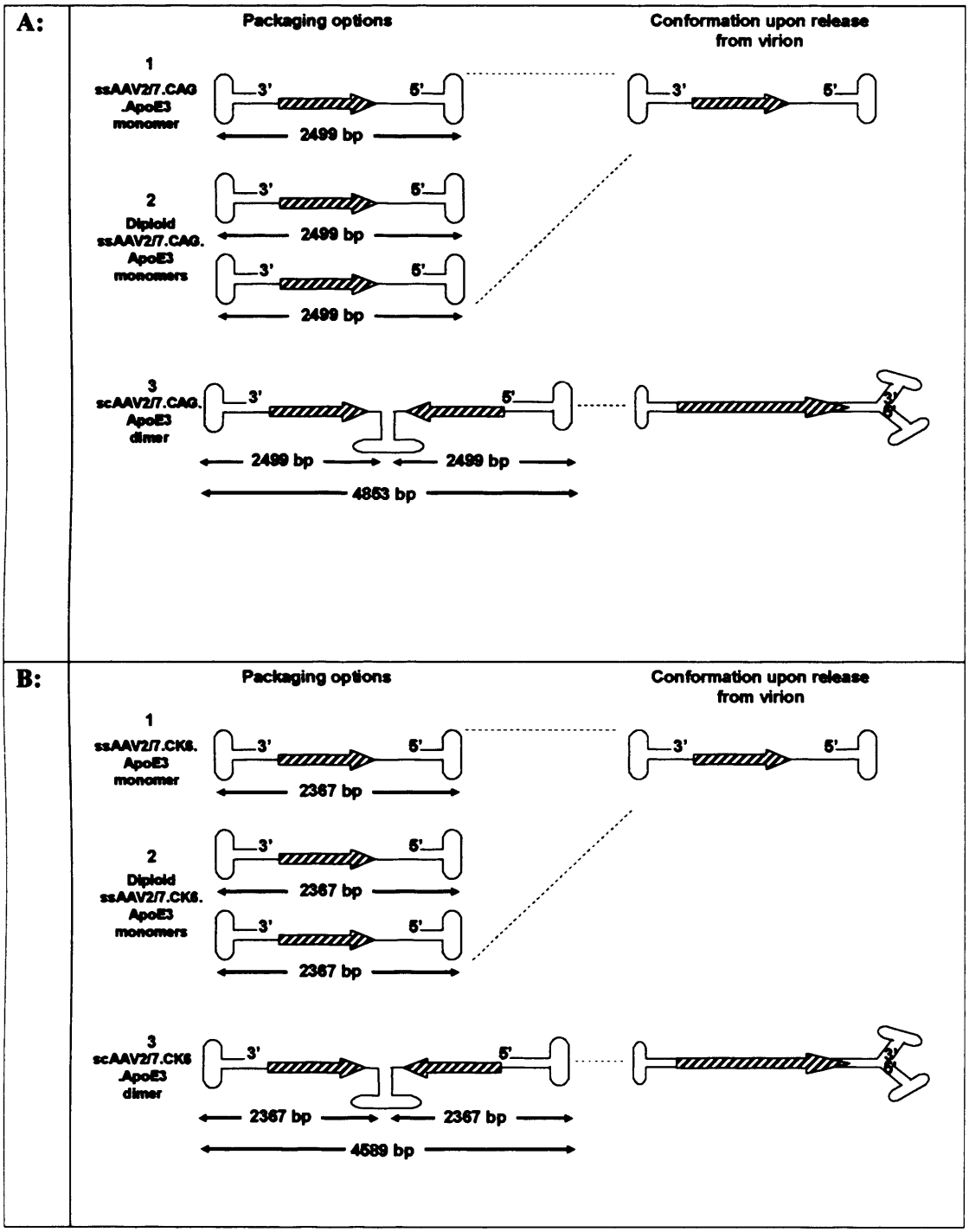
A:
Packaging options
Conformation upon release from virion
1
ssAAV2/7.CAG .ApoE3 monomer
3'
5'
2499 bp
2
Diploid ssAAV2/7.CAG. ApoE3 monomers
3'
5'
2499 bp
3'
5'
2499 bp
3
scAAV2/7.CAG. ApoE3 dimer
3'
5'
2499 bp
2499 bp
4853 bp
B:
Packaging options
Conformation upon release from virion
1
ssAAV2/7.CK8. ApoE3 monomer
3'
5'
2367 bp
2
Diploid ssAAV2/7.CK8. ApoE3 monomers
3'
5'
2367 bp
3'
5'
2367 bp
3
scAAV2/7.CK8 .ApoE3 dimer
3'
5'
2367 bp
2367 bp
4589 bp

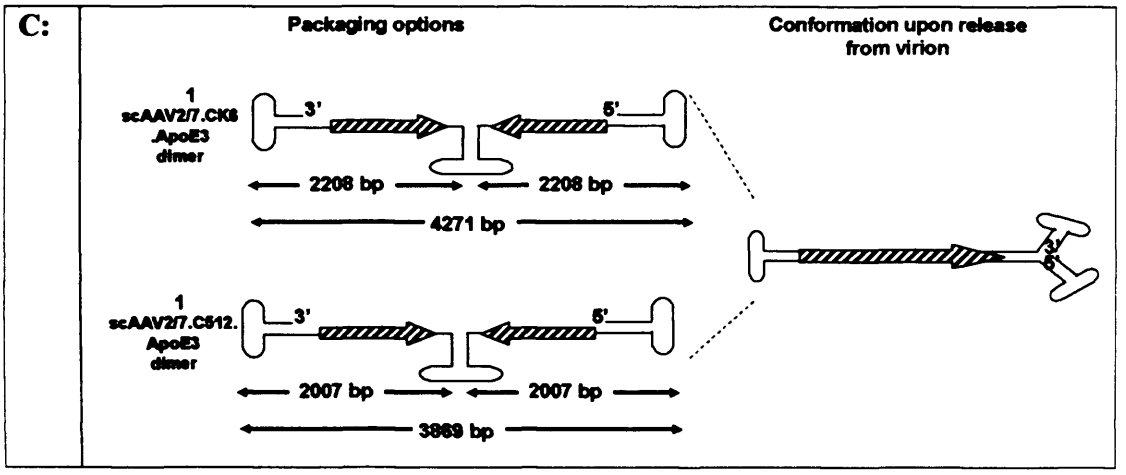

Figure 4-1. The structure of ss- and scAAV genomes during packaging and their conformation upon uncoating

When the length of the AAV genome is half the wild-type size, two copies can be packaged as a dimeric inverted repeat DNA molecule (scAAV) or as diploid monomers. Such scAAV molecules should spontaneously re-anneal, bypassing the rate-limiting step of second-strand synthesis [285]. The predicted conformation that the rAAV vectors used in this study adopt upon release from the virion is schematically illustrated. ***(A)*** *Due to the size of ssAAV2/7.CAG.ApoE3 (2499bp), this vector can be packaged as a single monomer, diploid monomers or a scAAV dimer.* ***(B)*** *As with ssAAV2/7.CAG.ApoE3, ssAAV2/7.CK6.ApoE3 (2208bp) can be packaged as a single monomer, dipoloid monomers or a scAAV dimer.* ***(C)*** *Both scAAV2/7.CK6.ApoE3 and scAAV2/7.C512.ApoE3 are packaged as scAAV dimers and re-fold and form double-stranded transcriptionally active molecules upon release from the virion.*

A triple-transfection method was used to produce the virus particles (see section **2.2.3.1** for details), followed by purification by iodixanol step-gradient ultracentrifugation (section **2.2.3.2**). The virus particle titer was determined by DNA dot-blot hybridisation analysis (section **2.2.3.3**) and verified by real-time quantitative PCR (Q-PCR) (section **2.2.1.4**). The two quantitative methods produced similar values for each viral preparation tested, giving us a high confidence that the titers were accurate. DNA dot-blot and Q-PCR estimated viral titers ranged from 1.92×10^{11} to 5.96×10^{12} and 9.9×10^{10} to 1.4×10^{12} vector genomes (vg) respectively (Table 4-1). Of the two methods, the DNA dot-blot is the most routinely used and the more reliable for viral titer quantification; I decided, therefore, to use the estimated values from this method for future experiments.

The rAAV stocks were also assessed for their quality and purity by electrophoresis of 1×10^{9}vg of each rAAV preparation on a NuPAGE® Novex 4-12% Bis-Tris polyacrylamide gel (see section **2.2.4.1** for details). The viral capsid proteins, VP1, VP2 and VP3, which are present in proportions of 1:1:10 respectively, were readily detected in the scAAV2/7.C512.ApoE3 preparation after staining the gel with silver nitrate using the PlusOne silver staining kit (see section **2.2.3.4**) (Figure 4-2). The viral capsid proteins of the other ssAAV and scAAV preparations were also seen, however, the relative proportions were less clear. Unlike scAAV2/7.C512.ApoE3, these viral preparations also exhibited the presence of additional protein bands and were, thus impure in comparison.

AAV vector	Dot-blot concentration (vg/ml)	Total yield (vg)	Q-PCR concentration (vg/ml)	Total yield (vg)
ssAAV2/7.CAG.ApoE3	5.96×10^{11}	7.15×10^{11}	1.45×10^{11}	1.74×10^{11}
ssAAV2/7.CK6.ApoE3	7.7×10^{11}	1.54×10^{12}	7×10^{11}	1.4×10^{12}
scAAV2/7.CK6.ApoE3	9.6×10^{10}	1.92×10^{11}	4.96×10^{10}	9.9×10^{10}
scAAV2/7.C512.ApoE3	2.46×10^{11}	2.46×10^{11}	1.51×10^{11}	1.51×10^{11}

Table 4-1. A comparison of viral titers obtained by DNA dot-blot hybridisation analysis and real-time Q-PCR
NB – the ssAAV2/7.C512.ApoE3 vector was made but not purified.

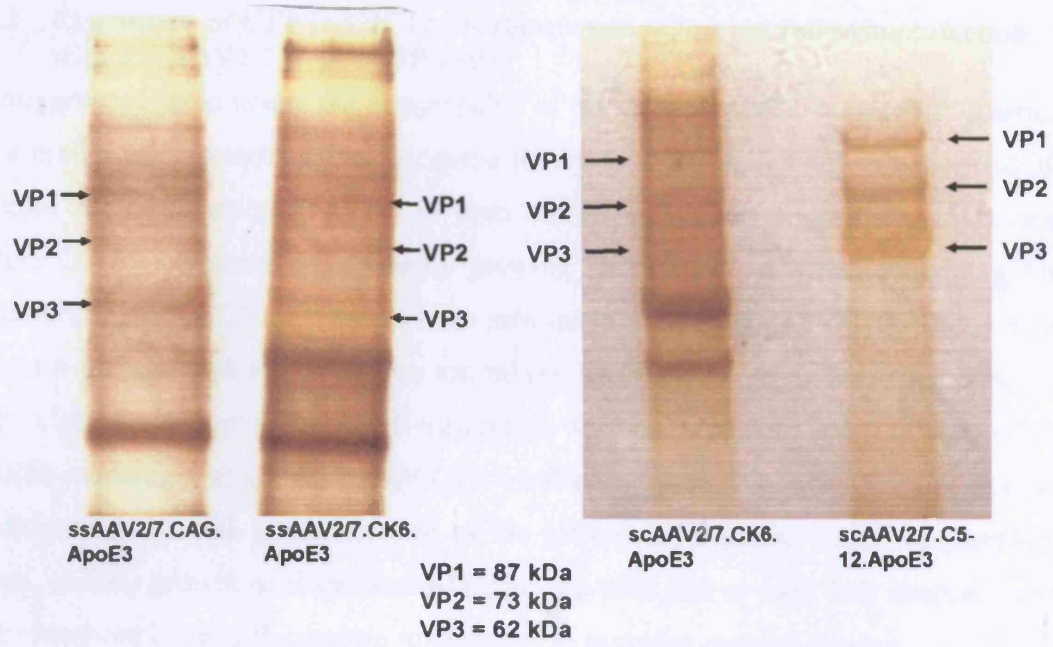

Figure 4-2. The purity profiles of the ss- and scAAV2/7 vectors isolated by iodixanol-step gradient ultracentrifugation

The volume equivalent to 1× 10^9vg of each viral preparation was loaded onto a 4-12% Bis-Tris polyacrylamide gel and, following electrophoresis, was stained with silver nitrate. The positions of the viral capsid proteins, VP1, VP2 and VP3, are indicated.

4.2.2 Expression of GFP in C2C12 myoblasts and myotubes following infection with a scAAV2/7.CMV.GFP vector

Before proceeding to assess the functionality of my viral preparations *in vitro*, I carried out a preliminary experiment to determine the optimal multiplicity of infection (MOI) required for efficient transduction in both murine C2C12 myoblasts and myotubes. Mature C2C12 myotubes, prepared by growing for 6 days in DMEM containing 5% horse serum, and C2C12 myoblasts were infected with increasing MOI (8×10^4 to 3.2×10^5) of a pseudotyped scAAV2/7 vector, driven by the CMV promoter and expressing GFP. Cell culture supernatants in 6-well plates were replaced with 700μl of serum-free DMEM containing scAAV2/7.CMV.GFP viral particles and incubated under normal conditions for 3h with gentle rotation of the plate every 20mins. After the infection period, normal growth medium was added to the cells and at each 24h interval, cells were visualised under a fluorescent microscope to assess expression levels.

GFP expression levels, in both infected myoblasts and myotubes, increased with an increase in MOI and over time, thus, high fluorescence was observed in cell cultures infected with a MOI of 3.2×10^5 after 72h. Interestingly, after the first 24h interval, GFP was only expressed in myoblasts and not in myotubes, indicating that myoblasts were more easily infected by scAAV2/7.CMV.GFP. By 48h expression levels in myotubes and myoblasts was equal, however, by 72h the GFP intensity in mature myotubes appeared greater (Figure 4-3A). It would seem that the scAAV vector takes 72h to become transcriptionally active in myotubes, whereas, in myoblasts this process occurs earlier.

4.2.3 Secretion of recombinant human ApoE3 from cultured myotubes following infection with ssAAV2/7 and scAAV2/7 vectors

Having determined the feasibility of infection of both C2C12 myoblasts and mature myotubes with a scAAV2/7 vector, I next went on to test the functionality of the four viral preparations that I had produced. As before, myoblasts were seeded at a concentration of 2×10^5 per well of a 6-well plate and grown for 6 days in DMEM containing 5% horse serum. Mature myotubes, were then infected with ssAAV2/7.CAG.ApoE3, ssAAV2/7.CK6.ApoE3, scAAV2/7.CK6.ApoE3 and scAAV2/7.C512.ApoE3 at a MOI of 3.2×10^5 (see section 4.2.2 for details of infection protocol). After 24, 48 and 72h, culture supernatant was removed and analysed for secretion of human ApoE3. Western blot analysis demonstrated secretion of ApoE3 in

myotubes infected with all viral preparations, although ApoE3 expression was much higher following infection of cells with the CAG-driven ssAAV2/7 vector (Figure 4-3B).

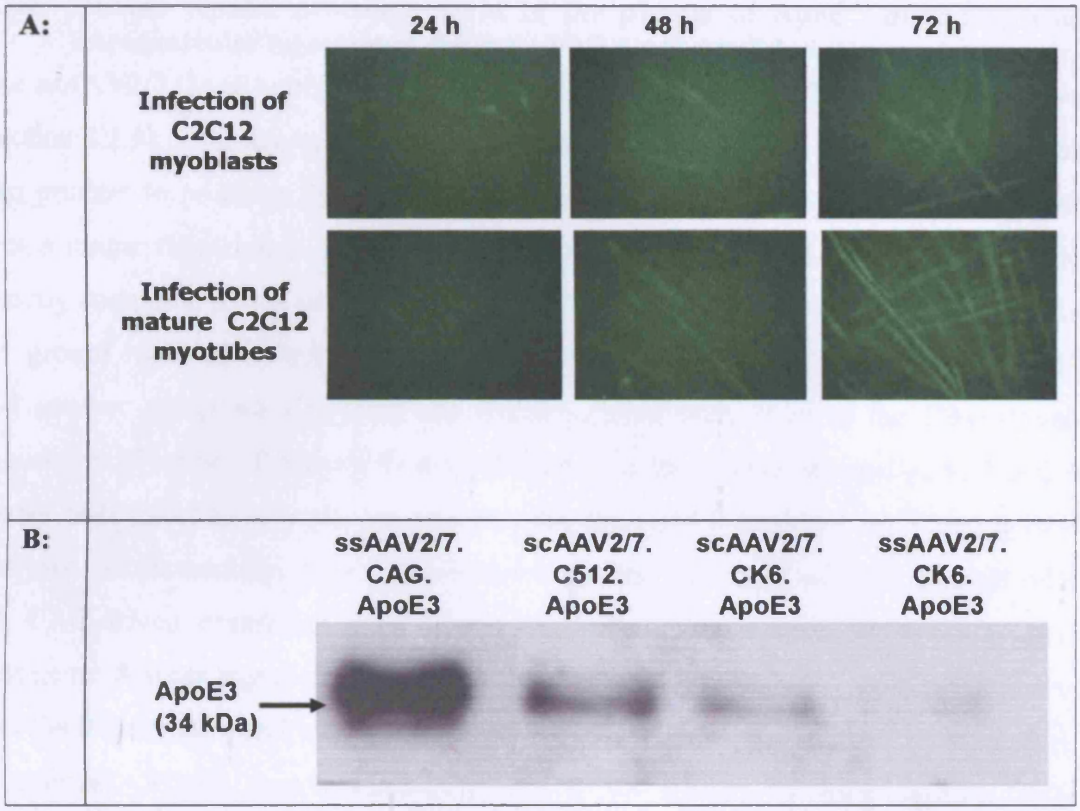

Figure 4-3. Transduction of C2C12 myoblasts and myotubes with scAAV2/7 and ssAAV2/7 vectors

(A) *Fluorescent microscope images (20× field) of murine C2C12 myoblasts and myotubes infected with scAAV2/7.CMV.GFP at a MOI of 3.2× 10^5. Cells were observed 24, 48 and 72h after infection to assess relative GFP expression levels.* ***(B)*** *Human ApoE3 secretion from mature myotubes 48h after infection with ssAAV2/7.CAG.ApoE3, scAAV2/7.C512.ApoE3, scAAV2/7.CK6.ApoE3 and ssAAV2/7.CK6.ApoE3 at a MOI of 3.2× 10^5.*

4.2.4 Human ApoE3 protein present in the plasma of ApoE$^{-/-}$ mice following intramuscular injection of the ssAAV2/7.CAG.ApoE3 vector

The ssAAV2/7.CAG.ApoE3 vector was clearly demonstrated to be functional *in vitro* (section 4.2.3), I, therefore, proceeded to test this vector *in vivo* in ApoE$^{-/-}$ mice. It was also prudent to re-assess the ApoE3 expression plasmid driven by the CAG promoter over a longer time-course, thus, both ssAAV2/7.CAG.ApoE3 and p.CAG.ApoE3 were directly compared in this *in vivo* experiment. One group of young ApoE$^{-/-}$ mice (3 mice per group) received intramuscular injections of 1×10^{10}vg of ssAAV2/7.CAG.ApoE3 and another group were injected via electroporation with 25μg of the CAG-driven expression plasmid. Tail vein bleeds were taken prior to injection and at 1, 2 and 4 weeks post injection and plasma was assayed for ApoE3 secretion by Western Blot analysis. Unfortunately, ApoE3 protein levels in the plasma of all mice injected with the CAG-driven expression plasmid remained undetectable, even at 4 weeks post treatment. A weak signal can be seen at 1, 2 and 4 weeks, however, this is not greater than the 0 time-point and was, therefore, considered as background only (Figure 4-4A). In contrast, ApoE3 was readily detected in the plasma of mice injected with ssAAV2/7.CAG.ApoE3 as early as 1 week and the total amount secreted increased over time (Figure 4-4A). The concentration of circulating ApoE3 at each time-point was semi-quantified by Western blot analysis; human plasma was serially diluted 1:30, 1:60 and 1:120 and loaded onto the 4-12% Bis-Tris polyacrylamide gel along side the mouse plasma samples for direct densitometric comparison. The level of ApoE3 in the plasma of all mice injected with the ssAAV2/7.CAG.ApoE3 vector reached an average of 1.4±0.35μg/ml at the 4 week time-point (Figure 4-4B).

The TA muscles from all animals in each group were excised at 4 weeks termination and protein was extracted for the analysis of local ApoE3 expression. Interestingly, Western blot analysis demonstrated markedly higher levels of ApoE3 protein in the muscles of mice injected with p.CAG.ApoE3. The total amount of ApoE3 attained per TA muscle from these mice ranged from 1.80 – 4.05μg, while only 0.17 – 0.52μg of ApoE3 was present in muscle from mice injected with the ssAAV2/7.CAG.ApoE3 vector (Figure 4-4C). In addition, I directly compared the level of ApoE3 expression in 1 week (obtained from our first *in vivo* experiment chapter 3, section 3.2.6) and 4 week muscle tissue from animals treated with p.CAG.ApoE3. Western blot analysis and an ELISA clearly demonstrated a decline in the total amount of ApoE3 in the muscle over

time, with an average of 7.67±3.96μg/TA muscle and 2.42±0.69 μg/TA muscle in the 1 and 4 week samples respectively (Figure 4-4D).

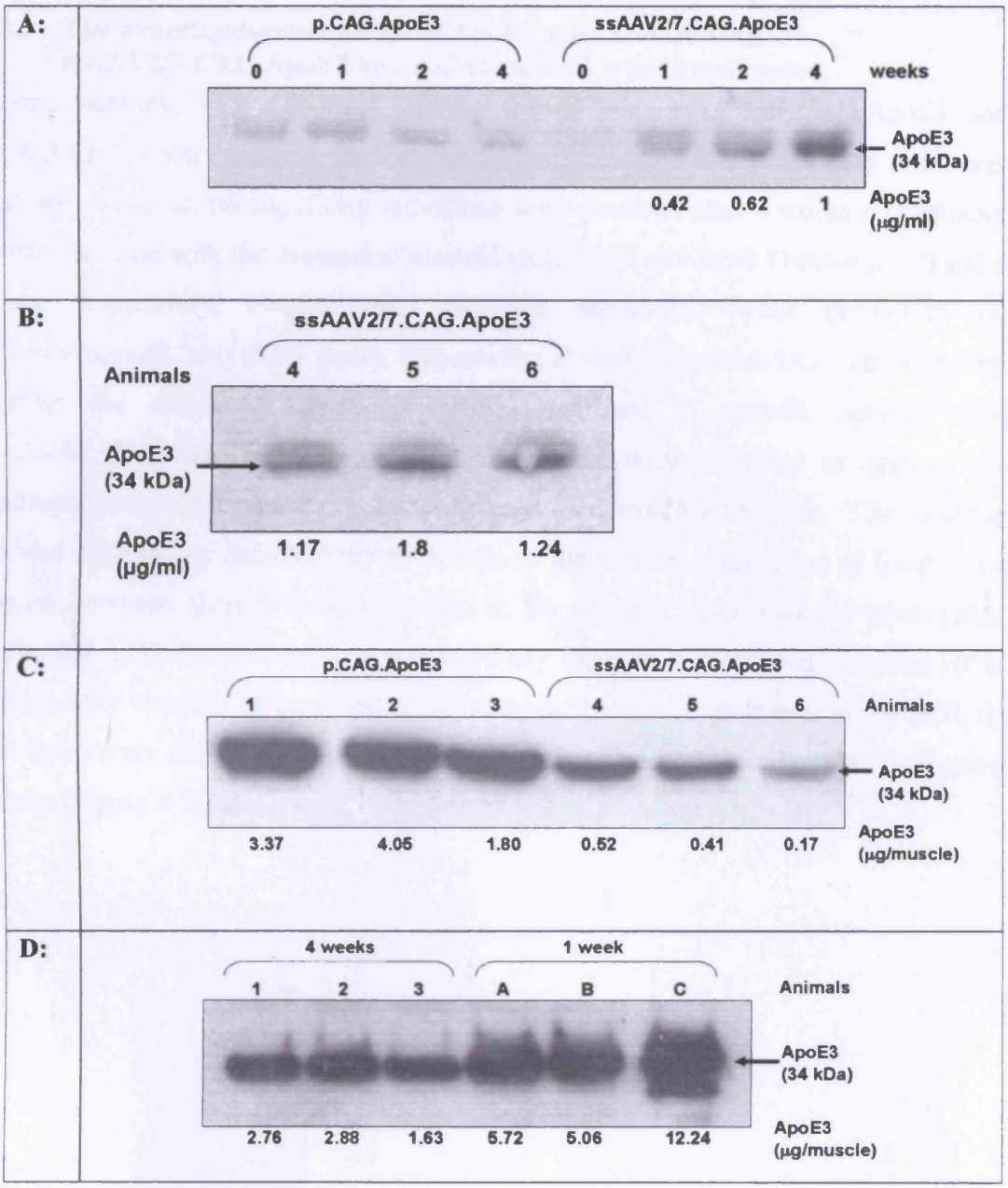

Figure 4-4. Plasma and muscle ApoE3 levels in ApoE$^{-/-}$ mice following injection of both TA muscles with ssAAV2/7.CAG.ApoE3 and p.CAG.ApoE3.

Mice were injected with 1× 10^{10}vg of ssAAV2/7.CAG.ApoE3 or 25µg of the CAG-driven ApoE3 expression plasmid and tail vein bleeds were taken before treatment (0 weeks) and 1, 2 and 4 weeks post-treatment. ***(A)*** *Representative Western blot of plasma ApoE3 levels at each time-point in individual mice from each group.* ***(B)*** *Semi-quantification by Western blot analysis of ApoE3 levels in the 4 week plasma samples of all three mice injected with ssAAV2/7.CAG.ApoE3.* ***(C)*** *Immunodetection of ApoE3 by Western blot analysis in muscle lysate from animals treated with either p.CAG.ApoE3 (animals 1, 2 and 3) or ssAAV2/7.CAG.ApoE3 (animals 4, 5 and 6).* ***(D)*** *A Western blot comparing ApoE3 levels in 1 week (A, B, and C) and 4 week (1, 2 and 3) muscle tissue from animals injected with p.CAG.ApoE3.*

4.2.5 The hyperlipidaemic profile of ApoE$^{-/-}$ mice treated with ssAAV2/7.CAG.ApoE3 and p.CAG.ApoE3 is not ameliorated

Plasma samples from individual animals treated with ssAAV2/7.CAG.ApoE3 and p.CAG.ApoE3 were assayed for total cholesterol. Plasma from each time-point was analysed, however, no significant reductions were observed after 4 weeks of treatment in mice injected with the expression plasmid (9.58±0.99 *vs* 9.44±0.71mmol/L at 0 and 4 weeks, respectively; $P>0.05$) and with the ssAAV2/7 vector (9.54±1.10 *vs.* 9.63±0.97mmol/L at 0 and 4 weeks, respectively; $P>0.05$) (Figure 4-5A). To determine whether the abnormal lipoprotein profile improved in animals injected with ssAAV2/7.CAG.ApoE3, individual plasma samples were subjected to agarose gel electrophoresis and the separated lipoproteins stained with Sudan black. The resulting gel was analysed by densitometry to determine the relative proportions of lipoprotein classes, however, there was no reduction in the absolute amount of the atherogenic VLDL/IDL/LDL lipoproteins, nor was there any increase in the anti-atherogenic HDL fraction after 4 weeks of treatment. Furthermore, there was no change in the HDL to total lipoprotein ratio, which can serve as a sensitive indicator of effective ApoE gene transfer (Figure 4-5B and C).

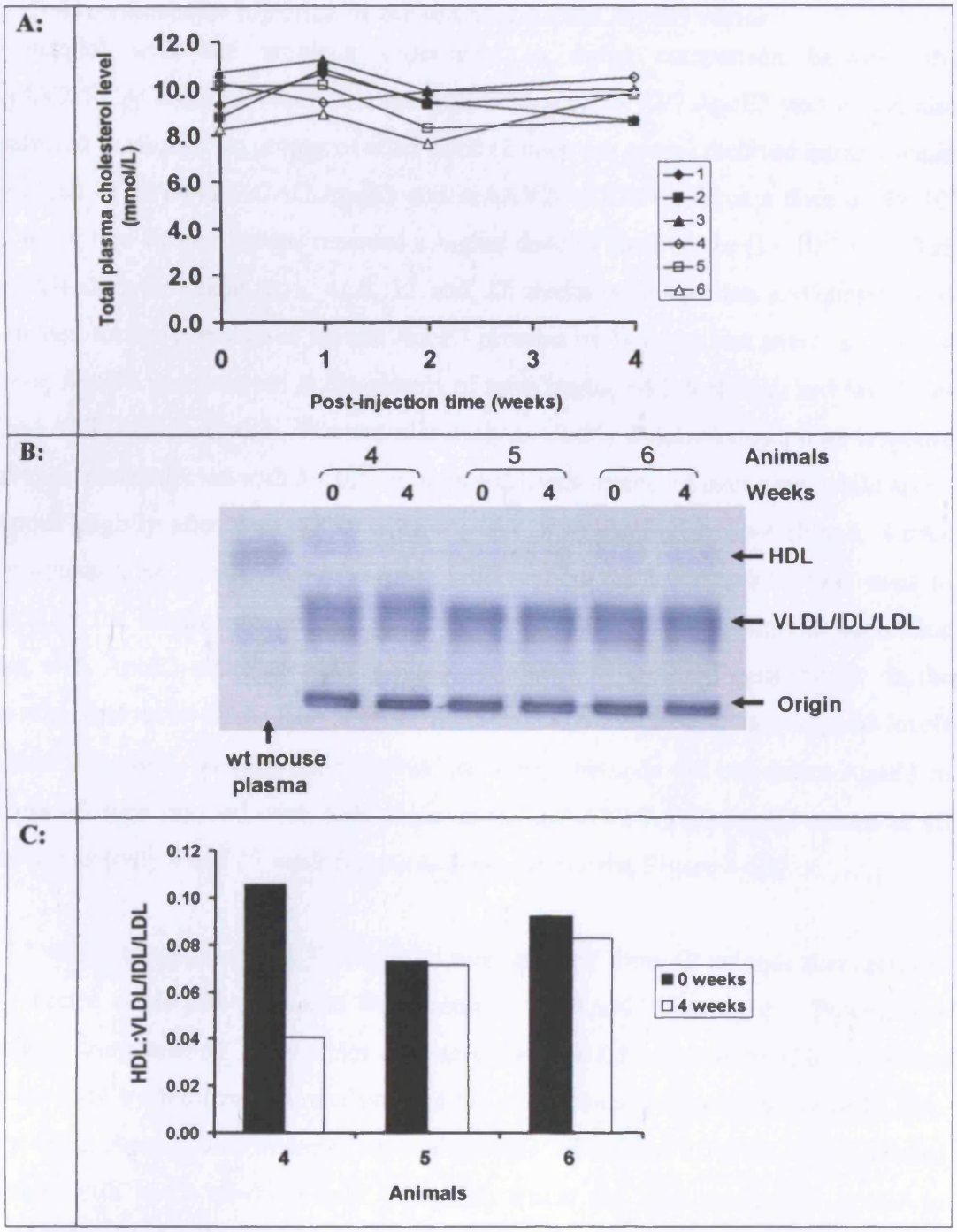

Figure 4-5. Effect of human ApoE3 expression on the total plasma cholesterol level and lipoprotein profile in ApoE$^{-/-}$ mice

(A) *Total plasma cholesterol levels (mmol/L) were determined for individual animals after intramuscular injection of either p.CAG.ApoE3 (animals 1, 2 and 3) or ssAAV2/7.CAG.ApoE3 (animals 4, 5 and 6).* ***(B)*** *The lipoprotein profiles of individual mice injected with ssAAV2/7.CAG.ApoE3 (animals 4, 5 and 6), prior to treatment and 4 weeks post-treatment.* ***(C)*** *Determination of HDL:total lipoprotein ratios by densitometry of Sudan black stained lipoprotein fractions (animals 4, 5 and 6).*

4.2.6 Undetectable levels of ApoE3 in the plasma of ApoE$^{-/-}$ mice following intramuscular injection of the scAAV2/7.CK6.ApoE3 vector

In parallel with the previous experiment, a direct comparison between the ssAAV2/7.CAG.ApoE3 vector and the CK6-driven scAAV2/7.ApoE3 vector was also conducted *in vivo*. Two groups of older mice (2 mice per group) received intramuscular injections of ssAAV2/7.CAG.ApoE3 and scAAV2/7.CK6.ApoE3 at a dose of 5×10^9 vg, while two further groups received a higher dose of each vector (1×10^{10} vg). Tail vein bleeds were taken at 1, 4, 8, 12 and 27 weeks post injection and plasma was evaluated for the presence of human ApoE3 proteins by Western blot analysis. From 4 weeks, ApoE3 was detected in the plasma of mice treated with both high and low doses of ssAAV2/7.CAG.ApoE3. Western blot analysis clearly demonstrated a dose response and in animals injected with 5×10^9 vg, secreted levels increased over time, while levels dropped slightly after 8 weeks in mice injected with the higher dose (Figure 4-6A). Semi-quantitative Western blot analysis (see section 4.2.4 for details) was used to determine the relative concentrations of ApoE3 attained in the plasma at each time point, with ApoE3 still detectable in the plasma after 27 weeks (Figure 4-6B). In the two mice that received the high dose of ssAAV2/7.CAG.ApoE3, plasma ApoE3 levels reached 1.6μg/ml. In contrast, however, our assay methods did not detect ApoE3 in plasma of mice injected with both doses of the scAAV2/7.CK6.ApoE3 vector at all time-points (only 4 and 27 week plasma samples are shown, Figure 4-6B).

At 27 weeks termination, the TA muscles were excised from all animals that received high vector doses and processed for evaluation of ApoE3 expression. Protein was extracted from excised TA muscles as before (section **2.2.5.6**) and ApoE3 expression was assessed by Western Blot analysis and the concentration determined by an ELISA. Very little ApoE3 was detected in the muscle of scAAV2/7.CK6.ApoE3-treated animals, with levels reaching only 0.1μg/TA, whilst the total amount of ApoE3 in ssAAV2/7.CAG.ApoE3-injected muscle was 13 fold higher (1.3μg) (Figure 4-6C).

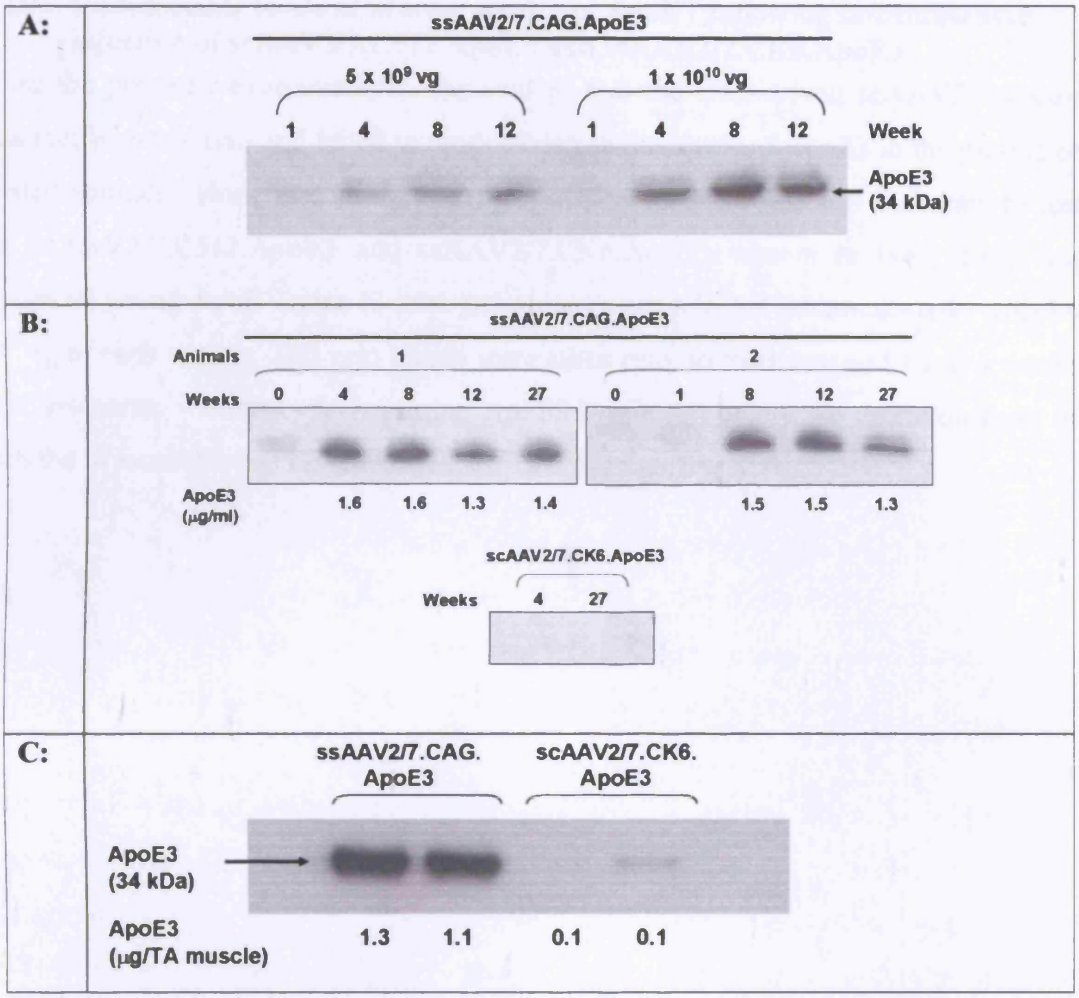

Figure 4-6. Secretion of human ApoE3 in the plasma of ApoE$^{-/-}$ mice following intramuscular injection of the ssAAV2/7.CAG.ApoE3 vector

Tibialis anterior (TA) muscles of ApoE$^{-/-}$ mice were injected with ssAAV2/7.CAG.ApoE3 and scAAV2/7.CK6.ApoE3 vectors (2 mice per group) at doses of 5× 10^9 and 1× 10^{10} vg. ***(A)*** *Western blot analysis of 1, 4, 8 and 12 week plasma samples of two individual mice injected with either 5× 10^9vg or 1× 10^{10}vg of the ssAAV2/7.CAG.ApoE3 vector.* ***(B)*** *The top two Western blots represent 1, 4, 8, 12 and 27 week plasma samples from the two mice injected with 1× 10^{10}vg of ssAAV2/7.CAG.ApoE3 and the Western below shows the 4 and 27 week plasma samples from an individual mouse treated with 1× 10^{10}vg of scAAV2/7.CK6.ApoE3.* ***(C)*** *Western blot analysis of local ApoE3 expression in the 27 week TA muscles of animals injected with ssAAV2/7.CAG.ApoE3 and scAAV2/7.CK6.ApoE3.*

4.2.7 Undetectable levels of plasma ApoE3 in ApoE$^{-/-}$ following intramuscular injection of scAAV2/7.C512.ApoE3 and ssAAV2/7.CK6.ApoE3

From the previous experiment, it was evident that the CK6-driven scAAV2/7 vector was inefficient *in vivo* and failed to produce detectable levels of ApoE3 in the plasma of treated animals. Notwithstanding this disappointing result, it was still necessary to test the scAAV2/7.C512.ApoE3 and ssAAV2/7.CK6.ApoE3 vectors *in vivo*, thus, two groups of young ApoE$^{-/-}$ mice (2 mice per group) were injected intramuscularly with 1×10^{10}vg of each vector. Tail vein bleeds were taken prior to treatment and 1 and 4 weeks post treatment. Unfortunately, plasma ApoE3 levels fell below the detection limit of both the Western blot and ELISA assay (data not shown).

4.3 Discussion

It was clear from the previous chapter that measurable levels of circulating ApoE3 with a concomitant reversal in hypercholesterolaemia were unattainable with plasmid-mediated gene transfer. It was therefore, concluded that that a more efficient delivery vehicle is needed to achieve sustainable and therapeutic levels of ApoE3. AAV has been chosen for this study primarily because it has the best safety profile among all viral vectors and with the new technological developments, it now reaps even more appeal as a gene transfer vehicle. We have taken advantage of the availability of additional serotypes with improved transduction efficiencies and also utilised the scAAV vector which has been shown to accelerate and enhance transgene expression [286-288]. It is anticipated that these factors, in combination, will improve ApoE3 gene transfer from skeletal muscle, with the ultimate goal to reverse hypercholesterolaemia and atherosclerosis. This chapter describes the construction, characterisation and the *in vitro* and *in vivo* evaluation of both ssAAV2/7 and scAAV2/7 vectors.

Dong et al. previously demonstrated that the optimal size of the ssAAV vector is between 4.1 and 4.9 kb. They discovered that, although it was possible for AAV to package a vector up to 5.2kb in size, which is larger than its genome, the packaging efficiency of this vector was markedly reduced [351]. A more recent study reported the capability of AAV to package and protect recombinant genomes as large as 6.0 kb, however, these large genome-containing virions were found to be more susceptible to degradation by the proteasome [352]. Whilst evidently improving AAV-mediated transduction efficiency, the scAAV vector has proven to be problematic for the expression of large transgenes, since its packaging capacity (~ 2.4 kb) is significantly smaller than that of the conventional ssAAV vector. A recent report, however, demonstrated the feasibility of encapsidating a double-stranded (ds) 3.3kb genome into the scAAV vector and found that it could still transduce cells with high efficiency [353]. With the exception of scAAV2/7.C512.ApoE3, all the AAV vectors generated for this study were within the optimal size range for efficient packaging. Although, scAAV2/7.C512.ApoE3 was below the minimal level, subsequent *in vitro* evaluation clearly demonstrated it to be a packageable and functional virion. The size of the vector also has a significant impact on the conformation of the AAV genome upon release from the virion. For example, previous studies have found that rAAV DNA of less than half the wtAAV genome length can be packaged either as a dimer or a diploid monomer [284;285]. The dimeric DNA molecules are encapsidated in the inverted repeat

configuration (scAAV) and have the ability to re-fold into ds DNA templates upon uncoating. Both the ssAAV2/7.CAG.ApoE3 and ssAAV2/7.CK6.ApoE3 vectors have replicative genome lengths that are close to half the length of the wt genome. Thus, it is possible that these AAV preparations had a mixed population of virions containing either monomeric (ss) or dimeric (sc) DNA vectors. Alkaline gel electrophoresis of the viral preparations would in fact confirm whether the genomes had been packaged as dimers or not [288]. The conformational constraints, however, of DNA packaging in parvoviruses [354] most likely precludes the encapsidation of double-stranded structures. Furthermore, the packaging of AAV DNA is dependent on the function of an active viral helicase, which also suggests that the DNA is single-stranded as it enters the capsid [355]. The propensity of the virion to consist of either one or two (either +/- stands, +/+ strands or -/- strands) copies of a monomeric genome is also under debate and merits further investigation. The packaging of a single copy of the viral genome, however, corroborates the current model of AAV DNA encapsidation, in which a single pore in the capsid takes up the viral genome, before a conformational change prevents further DNA packaging. Interestingly, it has been discovered that when the transgene cassette of the scAAV vector is bigger than 3492bp it can be packaged efficiently, but only in single-stranded form. The ssAAV genomes that were generated, however, were not a consequence of repair of the terminal resolution site (trs), but due to high levels of Rep proteins provided by the helper plasmid [353].

Assessment of the integrity and purity of each viral stock generated for this study was essential before any further *in vivo* experiments could be carried out. It remains unclear as to how pure a viral preparation needs to be before it is deemed "safe" for both pre-clinical and clinical work, but it is thought that contaminating cellular debris may incite an inflammatory response, which could eliminate the vector and the transfected cells, thus, limiting sustained transgene expression. Furthermore, cellular proteins can mimic true vector-mediated transduction events and produce artifactual results [356]. The electrophoresis of AAV preparations on a SDS polyacrylamide gel, followed by silver staining is a technique routinely used to assess the purity and integrity of viral stocks. Unfortunately, all the AAV preparations generated for this study, with the exception of scAAV2/7.C512.ApoE3 were less pure than anticipated. Although it was re-assuring that the viral capsid proteins, VP1, VP2 and VP3, of each ss and scAAV preparation were visible (Figure 4-2), contaminating protein bands were also present. The relative staining intensity of the viral capsid profile also varied between the four viral stocks,

which may indicate differences in the efficiency of encapsidation of the AAV2 genome into the serotype-7 capsid. Additional purification steps, however, have the effect of reducing the biological potency of viral preparations, thus, it was decided that since this is not a clinical trial, but merely a series of preliminary experiments to test the efficiency of rAAV in mice, the viral preparations would be satisfactory for our means.

Before proceeding to assess the efficiency of the scAAV2/7 and ssAAV2/7 vectors *in vivo*, it was first necessary to test their functionality *in vitro*. From our preliminary experiment, in which murine C2C12 myoblasts and myotubes were infected with a CMV-driven scAAV2/7 vector expressing GFP, we were able to determine the optimal MOI required for efficient transduction. Interestingly, we also discovered that whilst the onset of transgene expression was earlier in myoblasts, a much higher level of GFP expression was observed following infection of differentiated, mature myotubes (Figure 4-3). The transduction efficiency of the scAAV2/7.CMV.GFP vector was clearly affected by the cellular state of differentiation in C2C12 cells. When proliferating myoblasts are deprived of growth factors they enter a terminal differentiation stage and expression of various differentiation factors (myogenin and p21/WAF1) and contractile proteins (myosin and troponin) are induced [357]. It is, thus, possible that these factors are linked to the high transgene expression observed in differentiated cells. Previous studies have also demonstrated that the influence of myoblast differentiation on transduction efficiency is dependent on the AAV serotype. Duan et al. found that a pseudotyped rAAV2/5 vector performed better in differentiated C2C12 cells compared with those that were undifferentiated, while the complete opposite was found for a rAAV-serotype 2 vector [358]. Another study also reported enhanced transgene expression from a rAAV-serotype 2 vector in undifferentiated myoblasts, whereas this was not the case with pseudotyped AAV2/10 and 11 vectors which were found to transduce differentiated cell with a higher efficiency [192]. Differentiation associated changes in cell surface receptor expression may contribute to increased binding of the serotype-7 capsid in mature myotubes, although this is difficult to infer since the receptor for AAV7 is still unknown. Duan et al. hypothesised, however, that differentiation-induced changes in the intracellular processing and/or uncoating of virions might have more of an influence on the increased transduction efficiency observed with pseudotyped vectors [358].

Having established that AAV serotype-7 transduces differentiated C2C12 cells with a much higher efficiency, we proceeded to infect mature myotubes, grown for 6 days, with each of the ss and scAAV2/7 vectors. Western blot analysis demonstrated secretion of human ApoE3 into the medium of cultured myotubes infected with all viral preparations, thus verifying their functionality. It was also evident that the ssAAV2/7.CAG.ApoE3 vector was more efficient *in vitro* than both ss- and scAAV2/7 vectors driven by the muscle-specific promoters. This corroborates our previous findings (chapter 3) for the C512 and CK6-driven plasmids; both of which produced markedly less ApoE3 *in vitro* and *in vivo*. With the exception of the C512 promoter, which is reported to be as active in skeletal muscle and cell cultures as the natural myogenic and viral gene promoters [258;259], previous studies have also shown CK6 to perform less efficiently than the ubiquitous promoters [257]. The scAAV vector, which obviates the need for viral second-strand DNA synthesis, has been reported to perform equally as efficient *in vitro* as *in vivo*. Studies have used this vector as a helper virus to improve the transduction efficiency of the conventional ssAAV vectors in various human cell lines *in vitro* [359;360]. It was therefore, anticipated that the scAAV vector would enhance transgene expression from our less active muscle-specific promoters, however, our findings clearly suggest otherwise.

Although it was conclusive from chapter 3, that measurable levels of plasma ApoE3 could not be achieved via plasmid-mediated gene transfer, our first *in vivo* experiments were conducted over just 1 week. It was, subsequently, hypothesised that a longer time period might be required to achieve maximum secretion of the protein from muscle. We, therefore, re-assessed electrotransfer of p.CAG.ApoE3 over 4 weeks and at the same time directly compared this plasmid with the ssAAV2/7.CAG.ApoE3 vector. Despite local expression in the muscle, ApoE3 remained undetectable in the plasma of p.CAG.ApoE3-treated animals, 4 weeks post-injection (Figure 4-4) and their plasma cholesterol levels remained unchanged. Furthermore, a direct comparison of 1 week muscle lysates, from animals previously injected with p.CAG.ApoE3, with the 4 week muscle lysates, clearly demonstrated a decline in the levels of ApoE3; suggesting that there had been plasmid loss or possibly silencing of gene expression. We can therefore infer that plasmid-mediated ApoE3 transfer in skeletal muscle is not sustainable and that active secretion of the expressed protein will not be maintained over a prolonged period.

Fortunately, the complete opposite was observed in animals treated with the ssAAV2/7.CAG.ApoE3 vector; ApoE3 was readily detected in the plasma as early as one week post-injection and the level steadily increased overtime (Figure 4-4). This ultimately reinforces the high tropism of serotype 7 for skeletal muscle, since a previous study failed to detect ApoE3 in the plasma of $ApoE^{-/-}$ mice that had received i.m injections of a rAAV-serotype 2 vector [316]. The basis for this improved efficiency, however, is unclear since essential information such as primary attachment receptors, co-receptors and trafficking properties to the nucleus remains unknown for serotype 7. A pseudotyped AAV2/7 vector has been shown to transduce skeletal muscle as efficiently as AAV1 [191], which is the serotype that confers the highest level of transduction in skeletal muscle of the primate AAVs tested to date. It could therefore be inferred that these two serotypes share the same properties required for efficient transduction in muscle. The advantage, however, of using AAV7 over AAV1, is that 7 is immunologically distinct and sera from humans show less neutralising antibodies to this serotype compared with AAV1 [191]. Furthermore, AAV DNA has been identified in 17% of normal human muscles [361] which emphasises the importance of using novel AAV serotypes isolated from non-human primates for skeletal muscle gene transfer.

Despite measurable levels of circulating ApoE3, plasma total cholesterol and lipoprotein profiles of ssAAV2/7.CAG.ApoE3-treated animals remained unchanged after 4 weeks (Figure 4-5). The concentration of ApoE reported to normalise plasma cholesterol is 2μg/ml [96], albeit endogenous mouse ApoE which is 6-fold more efficient than human ApoE3 in clearing remnant particles [137]. The concentrations (1.40±0.35μg/ml) of plasma ApoE3 reached in our mice were just below this threshold level, thus, we would not expect to observe a reduction in hypercholesterolaemia. Unexpectedly, we found local ApoE3 expression in the muscle of ssAAV2/7.CAG.ApoE3-treated animals to be lower than that observed in animals treated with the CAG-driven plasmid. We can only assume that this is because ApoE3 is being actively secreted into the plasma from ssAAV-injected muscle, whilst expression in plasmid-injected muscle is retained. It is possible that the ssAAV2/7 viral vector and plasmid are being taken-up by different cell-types within the TA muscle, which could consequently affect their ability to be secreted.

In parallel with the previous experiment, we directly compared the ssAAV2/7.CAG.ApoE3 vector with the CK6-driven scAAV2/7 vector in $ApoE^{-/-}$ mice. The main objective of this experiment was to see whether a scAAV vector could enhance expression from the less active muscle-specific promoter *in vivo*. Ultimately, it is desirable to use the lowest vector dose possible; hence, animals were injected with both high (1×10^{10} vg) and low (5×10^{9} vg) doses. Consistent with our previous experiment, mice that received intramuscular injections of ssAAV2/7.CAG.ApoE3 demonstrated detectable plasma ApoE3 levels, with the concentration reaching its highest at 4 and 8 weeks (Figure 4-6). Furthermore, ApoE3 was still detectable in the plasma at the 12 and 27 week time-points, albeit the levels having declined slightly, suggesting that there may have been a humoral immune response directed against either the vector or the transgene. Human ApoE is a neo-antigen to $ApoE^{-/-}$ mice, making it likely that antibodies against ApoE were produced. In addition, direct intramuscular injection *per se* induces a localised inflammatory immune response mediated by a mixed infiltrate of activated lymphocytes and macrophage/dendritic cells [362]. It was anticipated that such immune responses would be circumvented with our muscle-specific promoter-driven AAV vectors [254] and we would observe an increase in persistence of transduced muscle cells. However, failure to detect ApoE3 in the plasma and very low amounts in the muscle of scAAV2/7.CK6.ApoE3-treated animals (Figure 4-6), rendered this analysis impossible. We were able to confirm that this observed vector inefficiency was not due to the scAAV vector but a result of the weak activity of the muscle-specific promoter, since both the ssAAV2/7.CK6.ApoE3 and scAAV2/7.C512.ApoE3 vectors equally failed to produce ApoE3 *in vivo*.

Why is transduction efficiency in the skeletal muscle significantly lower with muscle-specific promoters? It might be that, while, the ubiquitous promoters drive a high level of expression in virtually all skeletal-muscle fibres, the CK6 promoter has been reported to favour only the fast-twitch fibres [363]. A similar expression pattern was also observed with both CK1 and CK7, their activity was demonstrated to be low and mosaic in predominantly slow muscles, such as the soleus [364]. The TA muscle, however, is predominantly made up of fast-twitch fibres [365], which should in theory favour expression from the CK6 promoter. Nevertheless, we can be encouraged by the development of novel, muscle-specific promoters with improved transduction efficiencies; these include a muscle creatine kinase/SV40 hybrid promoter which is reported to yield enhanced and long-term transgene expression [256], while a MHCK7

(α-myosin heavy-chain enhancer, creatine kinase 7) promoter was shown to direct high-level expression comparable to CMV and RSV (Rous sarcoma virus) promoters [364].

Although we are encouraged by our findings that skeletal muscle injected with ssAAV2/7.CAG.ApoE3 can secrete μg/ml quantities of ApoE3, further experiments are ultimately needed to determine why therapeutic levels and a reversal in hypercholesterolaemia were not achieved. By directly comparing the ssAAV2/7.CAG.ApoE3 vector with a scAAV2/7.CAG.ApoE3 vector, we might be able to delineate whether the poor outcome was due to the use of the less efficient ssAAV vector or the CAG promoter. Although the CAG promoter has been reported to direct high transgene expression in skeletal muscle [252], its potential to provoke an immune response is a limiting factor. Another important experiment is to assess liver versus muscle transduction. A comparison of plasma ApoE levels in animals injected either intravenously or intramuscularly with ssAAV2/7.CAG.ApoE3, will give a clear indication of whether inadequate secretion by muscle was the cause of low concentrations of circulating ApoE in our study. It would also be worthwhile to generate reporter gene constructs; the injection of both CAG-driven and muscle-specific promoter-driven ssAAV2/7 vectors expressing LacZ or GFP into skeletal muscle will allow us to accurately evaluate the activity of each promoter and determine whether they target different muscle cell types.

Chapter 5:

Comparison of ssAAV2/7, ssAAV2/8 and ssAAV2/9 Vectors Expressing ApoE3

5 COMPARISON OF ssAAV2/7, ssAAV2/8 AND ssAAV2/9 VECTORS EXPRESSING APOE3

5.1 Introduction

As discussed in previous chapters, ApoE has several anti-atherosclerotic properties, which are mediated by means that are both dependent [85-87;90] and independent [96;147;311] of plasma cholesterol homeostasis. This is corroborated by earlier studies using rAd vectors for liver-directed ApoE gene transfer, which resulted in the correction of hypercholesterolaemia and protection against atherosclerosis in ApoE-deficient mice [308;366]. The effect of these first generation rAd vectors, however, was transient due to an associated immune response, which cleared transduced hepatocytes. Nevertheless, vector modifications have since resulted in reduced toxicity and prolonged ApoE expression in treated animals [310;312;313]. The general safety issues associated with rAd vectors, however, have driven our group and others to use rAAV as an alternative. This viral vector has emerged as an attractive candidate for gene transfer, firstly because it does not appear to cause any human disease and secondly because it remains quiescent in the absence of helper virus. AAV has therefore been labelled as a safe and stable gene transfer vehicle and for these reasons has attracted the attention of many researchers.

The first AAV serotype to be identified and fully characterised was AAV2, which has therefore, been extensively investigated as a gene transfer vector. Although AAV2 is a promising vector *in vitro*, it is now well documented to perform less efficiently *in vivo*. Fortunately, eleven different serotypes (designated AAV1 to AAV11) and over one hundred genomic variants of AAV from human and non-human primate samples have now been identified [185;190;192;194]. Furthermore, pseudotyped rAAV2 vectors which have been cross-packaged into alternative AAV serotype capsids, exhibit serotype-specific tissue or cell-type tropism and/or strikingly improved transduction efficiency [190;194;367]. The success of AAV gene therapy is thus essentially dependent on finding the optimal AAV serotype for efficient transduction of specific target tissues. Gregorevic and colleagues were first to discover that genes could be delivered globally to target tissue(s) by systemic administration of pseudotyped rAAV vectors derived from alternative serotypes [260]. Nakai et al. and Wang et al, subsequently demonstrated that transduction of all hepatocytes, all the skeletal muscles

throughout the body and the entire myocardium in mice could be achieved by intravenous injection of CMV and EF1α-driven rAAV8 vectors [211;212]. Moreover, Inagaki and colleagues have recently discovered that AAV9 is as robust as AAV8 and can also cross vascular endothelial cell barriers very efficiently and transduce many nonhepatic tissues, especially the heart, following systemic administration [213;214].

AAV vectors for liver-directed ApoE gene transfer have demonstrated promising and encouraging results. Thus, intravenous injection of a pseudotyped AAV2/8 vector, expressing ApoE, produced normal human levels (50 to 80μg/ml) in the plasma of $ApoE^{-/-}$ mice [317], while AAV2/7 and AAV2/8 vectors lowered cholesterol levels for up to 1 year and completely prevented atherosclerosis [318].

Here, we have chosen skeletal muscle as the platform for AAV-mediated ApoE gene transfer, since it is a stable, post-mitotic tissue, which is highly vascularised and actively secretory [261;262]. Several studies have demonstrated sustained transgene expression over several weeks following intramuscular injection of rAAV vectors [263;264;347;368]. Xiao et al. in fact, observed maintained expression over 1.5 years with no evidence of an immune response directed against the vector or lacZ reporter gene [264]. Intramuscular, AAV-mediated ApoE gene transfer has previously been tested in $ApoE^{-/-}$ mice and, achieved a reduction in atherosclerotic plaque density, although plasma ApoE levels were low and did not ameliorate hypercholesterolaemia [316]. AAV serotype-2 was used in this study, which, as mentioned above, is less efficient *in vivo* and could explain poor secretion of ApoE protein. Furthermore, in chapter 4, I demonstrated that intramuscular injection of a CAG-driven AAV-serotype 7 vector in $ApoE^{-/-}$ mice results in detectable ApoE3 levels in the plasma. The ApoE concentration attained in the plasma, however, was below the anticipated threshold required to correct the hypercholesterolaemic phenotype. Nevertheless, this is still an improvement on the aforementioned study and, although, atherosclerotic plaque density was not assessed, we would predict that this would be reduced over time.

It was conclusive from the experiments described in chapter 4 that the activities of the two muscle-specific promoters were significantly weaker than that of the ubiquitous CAG promoter *in vivo*. Even with the aid of a scAAV vector, both CK6 and C512 performed inefficiently and failed to drive vigorously ApoE3 expression, as judged by local levels of ApoE3 protein in muscle and in plasma. It is, therefore, unlikely that in a

long-term experiment, these vectors would have an effect on atherosclerotic lesion development. Instead, I decided to pseudotype the ssAAV2.CAG.ApoE3 vector with the capsids of alternative serotypes and directly compare these with the ssAAV2/7.CAG.ApoE3 vector *in vivo*. The AAV serotypes 8 and 9 were selected for their aforementioned robustness with the main objective of this experiment to compare the abilities of all three vectors to ameliorate hypercholesterolaemia and inhibit progression of pre-existing early atherosclerotic lesions, following intramuscular injection into $ApoE^{-/-}$ mice.

5.2 Specific methodology - ELISA quantification of human ApoE3 in murine plasma samples

The ELISA, previously described in this thesis (section **2.2.4.2**) had only been used for the determination of ApoE3 concentrations in cell culture supernatants and muscle tissue lysates. Unfortunately, when this assay was used for analysis of human ApoE3 in murine plasma samples, an inhibitory effect was observed. The signal appeared to be quenched and it was assumed, therefore, that the capture antibody in this ELISA was binding additional proteins in the mouse plasma, which blocked human ApoE3 antigen binding. Semi-quantitative Western blot analysis had so far been employed to estimate ApoE3 levels in our plasma samples; however, for large-scale experiments this would be very time consuming. An alternative ELISA was, therefore, used which was optimised by Dr Patrick Rensen's group at Leiden University Medical Centre.

The following buffers were prepared prior to starting the ELISA:

- Wash buffer (1× PBS with 0.05% Tween-20 (v/v))
- Blocking buffer (1× PBS with 0.1% Casein)
- Secondary antibody buffer (Blocking buffer with 0.05% Tween-20 (v/v))

The ELISA plate was prepared by coating each well of a medium binding (Costar) immunoassay plate with 100μl of polyclonal goat anti-human ApoE primary antibody (Academy Biomedical Company; cat. 50A-G1b), diluted 1:1000 in PBS to give a final concentration of 1μg/ml. The plate was covered and incubated firstly for 1h at 37°C and then overnight at 4°C. The following day, the plate was washed 3 times with wash buffer and then blocked by the addition of 150μl/well of blocking buffer and incubating for 1h at 37°C. Meanwhile, a human ApoE3 standard (Academy Biomedical Company; cat. 50P-103) stock solution was first diluted with wild-type mouse serum to a

concentration of 0.1mg/ml and then 9 further dilutions were prepared in blocking buffer ranging from 10ng/ml – 0.03906ng/ml. After blocking, the plates were washed as before and 100μl of each sample and standard was added in triplicates to the appropriate wells and the plate was incubated for 2h at 37°C in a humidified incubator. The plate was then washed a further 3 times and 100μl of HRP-goat anti-human ApoE (Academy Biomedical Company; cat. 50H-G1b) detection antibody, diluted to a concentration of 2μg/ml in secondary antibody buffer was added to each well. The plate was incubated for 2h at room temperature and this was followed by a final washing step and the addition of 100μl of TMB substrate (equal volumes of 0.004% (v/v) H_2O_2 and TMB dye) to each well. The plate was wrapped in aluminium foil and incubated for 15min on a shaker at room temperature, after which the enzymatic reaction was stopped by the addition of 2M H_2SO_4 (100μl/well). The absorbance at 450nm was immediately measured using a Dynex microplate reader.

5.3 Results

5.3.1 Construction and characterisation of ssAAV2/8 and ssAAV2/9 vectors expressing the human ApoE3 transgene

Both the ssAAV2/8.CAG.ApoE3 and ssAAV2/9.CAG.ApoE3 vectors were generated as per the method described in chapter 2, section 2.2.3.1. Briefly, 293-T cells were transfected with an Ad helper plasmid, the pAAV2.CAG.ApoE3 expression plasmid, and a packaging plasmid containing the AAV-serotype 2 *Rep* and AAV-serotype 8 or 9 *Cap* genes at a ratio of 3:1:1, respectively. Cell lysates were prepared two days after transfection and rAAV particles purified by iodixanol step-gradient ultracentrifugation (section **2.2.3.2**). The virus particle titer was determined by DNA dot-blot hybridisation (section **2.2.3.3**) and verified by real-time quantitative PCR (Q-PCR) (section **2.2.1.4**). The two quantitative methods produced similar values for each viral preparation tested, as previously observed in chapter 4 (Table 5-1).

As before, the rAAV stocks were assessed for their quality and purity by electrophoresis of 1×10^9vg of each rAAV preparation on a NuPAGE® Novex 4-12% Bis-Tris polyacrylamide gel (see section **2.2.4.1** for details), which was then stained with silver nitrate using the PlusOne silver staining kit (see section **2.2.3.4**). The capsid proteins, VP1, VP2 and VP3, of both viral preparations were visible on the gel but not well defined, thus, it was difficult to confirm whether they were in accordance with the 1:1:10 stoichiometric ratio (Figure 5-1). Furthermore, both ssAAV2/8 and 9 viral

stocks exhibited the presence of additional protein bands, which was also apparent with the other AAV vectors described in chapter 4.

AAV vector	Dot-blot concentration (vg/ml)	Total yield (vg)	Q-PCR concentration (vg/ml)	Total yield (vg)
ssAAV2/8.CAG.ApoE3	2.98×10^{11}	5.96×10^{11}	1.57×10^{11}	3.14×10^{11}
ssAAV2/9.CAG.ApoE3	2.98×10^{12}	5.96×10^{12}	2.61×10^{12}	5.22×10^{12}

Table 5-1. A comparison of viral titers obtained by DNA dot-blot hybridisation analysis and real-time Q-PCR

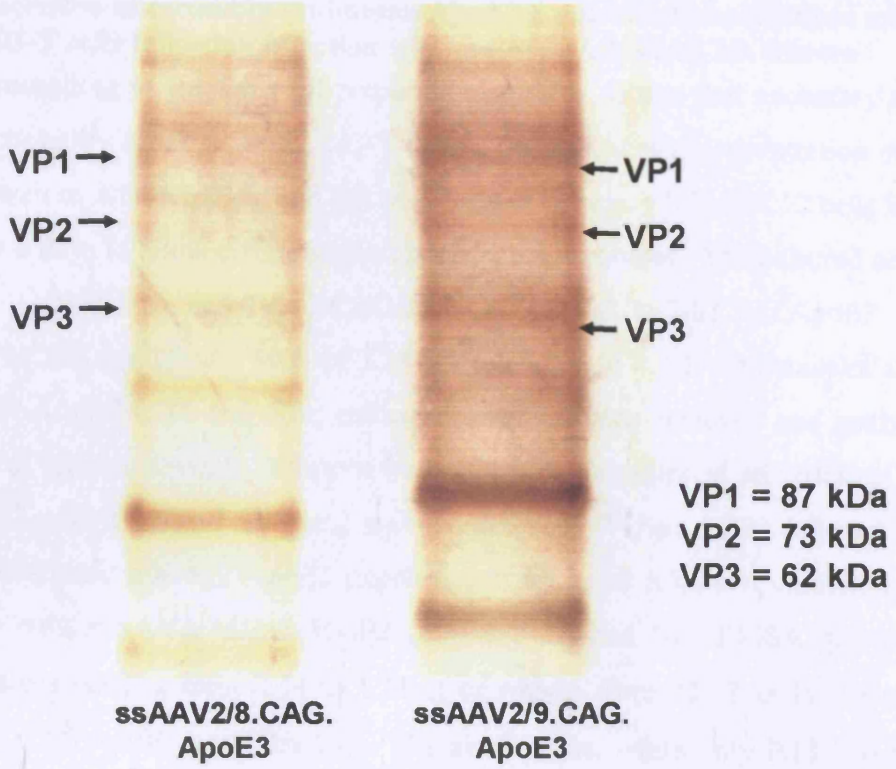

Figure 5-1. Purity profiles of the ssAAV2/8.CAG.ApoE3 and ssAAV2/9.CAG.ApoE3 vectors isolated by iodixanol step-gradient ultracentrifugation

The volume equivalent to 1× 10^9vg of each viral preparation was loaded onto a 4-12% Bis-Tris polyacrylamide gel and, following electrophoresis, stained with silver nitrate. The positions of the viral capsid proteins, VP1, VP2 and VP3, are indicated.

5.3.2 Secretion of recombinant human ApoE3 from cultured myotubes and HEK 293-T cells following infection with ssAAV2/7, 2/8 and 2/9 vectors

Before proceeding to test the viral preparations *in vivo*, it was first necessary to assess their functionality *in vitro*. HEK 293-T cells were seeded at a concentration of 5×10^5 cells per well of a 6-well plate and left overnight to adhere, while C2C12 cells had been grown for 6 days to allow differentiation into mature myotubes. The cultured cells were infected with ssAAV2/7.CAG.ApoE3, ssAAV2/8.CAG.ApoE3 and ssAAV2/9.CAG.ApoE3 at a MOI of 3.2×10^5 (see section 4.2.2. for details of infection protocol). After 24, 48 and 72h, culture supernatant was removed and analysed for secretion of human ApoE3. Western blot analysis demonstrated secretion of ApoE3 from 293-T cells (Figure 5-2A) and mature myotubes (Figure 5-2B) infected with all viral preparations, although ApoE3 expression was higher following infection of both cell types with ssAAV2/7.CAG.ApoE3 (Figure 5-2A and B). ELISA quantification yielded values ranging from 0.34 to 1.33μg of ApoE3 from 293-T cells infected with ssAAV2/7.CAG.ApoE3 over the 24 – 72h time-course, while only 0.13 – 0.4μg and 0.14 – 0.3μg of ApoE3 was secreted from cells transduced with ssAAV2/8.CAG.ApoE3 and ssAAV2/9.CAG.ApoE3 respectively (Figure 5-2A). Mature myotubes infected with ssAAV2/7, ssAAV2/8 and ssAAV2/9 vectors produced about 70, 20 and 35ng of ApoE3 per well, respectively, after 48h (Figure 5-2B).

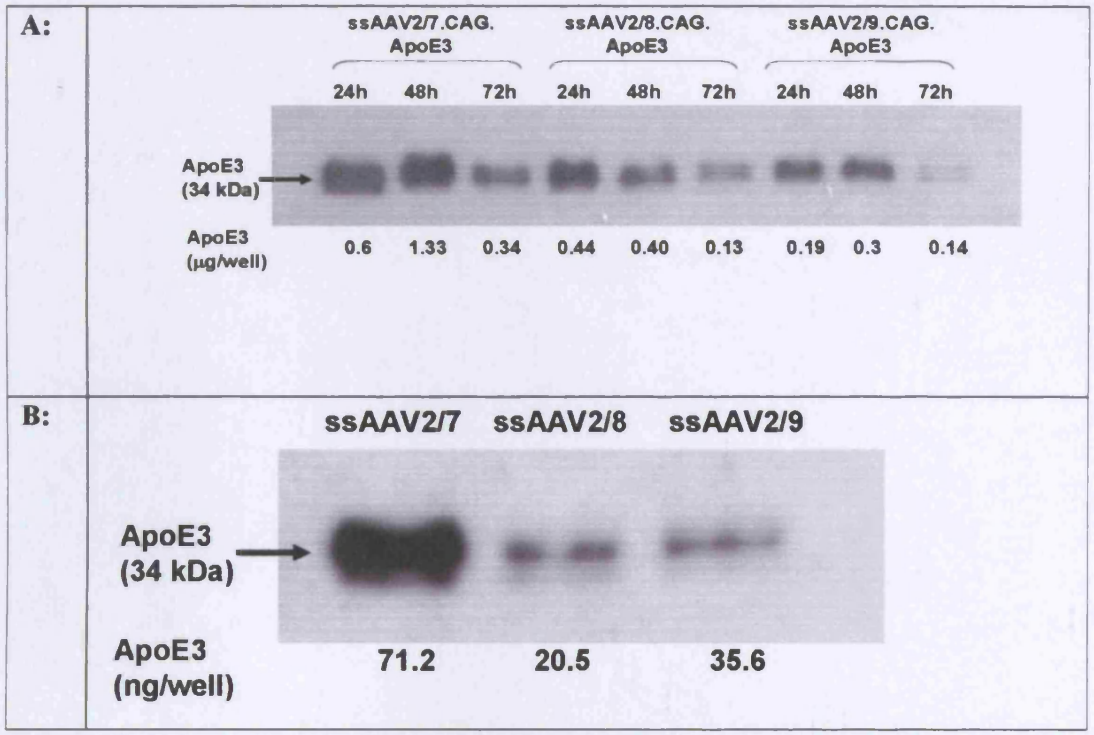

Figure 5-2. Secretion of recombinant human ApoE3 from cultured HEK 293-T cells and mature C2C12 myotubes following infection with ssAAV2/7, 2/8 and 2/9 vectors

Viral preparations were added to the cultured cells at a MOI of 3.2×10^5 and supernatant was collected at 24, 48 and 72h post infection. ApoE3 expression was assessed by Western Blot analysis and quantified by an ELISA assay. ***(A)*** *ApoE3 expression from HEK 293-T cells.* ***(B)*** *ApoE3 expression from mature C2C12 myotubes after 48h only.*

5.3.3 Human ApoE3 is detectable in the plasma of ApoE$^{-/-}$ mice following intramuscular administration of the CAG-driven ssAAV2/7, 2/8 and 2/9 vectors

Having verified that each vector was functional *in vitro*, I went on to conduct a side-by-side experiment with ssAAV2/7, 2/8 and 2/9 vectors delivered via the TA muscle of ApoE-deficient mice. Three groups of 6 week old, female mice (8 mice per group), were injected with ssAAV2/7.CAG.ApoE3, ssAAV2/8.CAG.ApoE3 and ssAAV2/9.CAG.ApoE3 at a dose of 1×10^{10} vg, while a fourth control group was uninjected. One week before treatment all animals were fed a high-fat diet and this continued throughout the duration of the experiment. Tail vein bleeds were taken prior to injection and at 1, 2, 4 and 13 weeks post-injection and plasma was assayed for human ApoE3 protein by Western blot analysis and ELISA (see section 5.2).

As expected no ApoE3 was found in the plasma of control animals at all time-points (Figure 5-3C), but it was clearly detectable in the plasma of mice treated with ssAAV2/7.CAG.ApoE3 and ssAAV2/8.CAG.ApoE3 as early as 1 week and levels were sustained for the 13 week time-course (Figure 5-3A and C). After 1 week, circulating ApoE3 in these two groups of animals reached comparable levels (1.9μg/ml±0.56 and 2.08μg/ml±0.43 respectively), however, at 2 weeks the concentration in ssAAV2/7-treated mice had markedly declined to 0.87μg/ml±0.47 (Figure 5-3B, C and D), which was significantly lower than that observed in the ssAAV2/8-treated mice (1.78±0.64μg/ml P = 0.03 Figure 5-3B, C and E). In fact, only 3 animals from the ssAAV2/8-injected group demonstrated a decline at 2 weeks, while there were 6 ssAAV2/7-treated mice that exhibited this trend (Figure 5-3G and H). This decrease is most likely due to ApoE3 being sequestered by the excess of remnant lipoproteins in the plasma and rapidly cleared by the liver via interaction with the LDL-R or LRP. Furthermore, different trends were observed in both groups after 2 weeks, plasma ApoE3 levels in animals injected with the ssAAV2/7 vector appeared to augment (Figure 5-3D), while levels declined in ssAAV2/8-treated mice (Figure 5-3E). Thus at termination the mean concentration in the ssAAV2/7 group of mice was slightly higher (1.4±0.41μg/ml), than that of the ssAAV2/8 group (1.28±0.2μg/ml). In contrast, the amount of ApoE3 protein detected in the plasma of ssAAV2/9-treated animals was markedly lower at each time-point (Figure 5-3C and F), with concentrations reaching only 0.49±0.18μg/ml and falling almost below the sensitivity limit of the Western blot (data not shown).

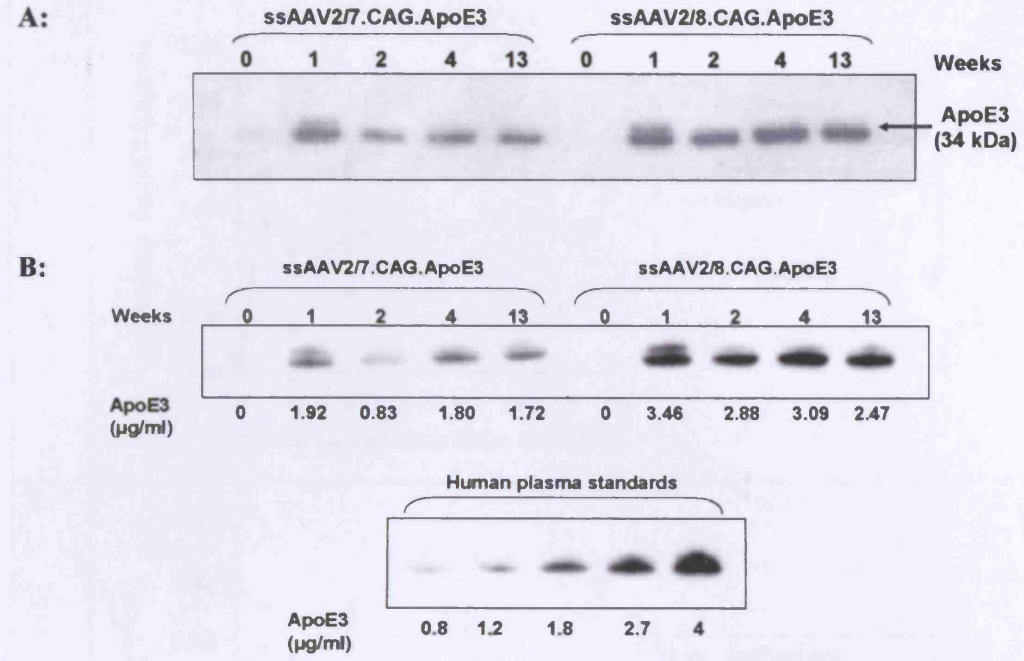
A:
ssAAV2/7.CAG.ApoE3
ssAAV2/8.CAG.ApoE3
0 1 2 4 13 0 1 2 4 13
Weeks
ApoE3
(34 kDa)
B:
ssAAV2/7.CAG.ApoE3
ssAAV2/8.CAG.ApoE3
Weeks
0 1 2 4 13 0 1 2 4 13
ApoE3
(µg/ml)
0 1.92 0.83 1.80 1.72 0 3.46 2.88 3.09 2.47
Human plasma standards
ApoE3
(µg/ml)
0.8 1.2 1.8 2.7 4
C:
ssAAV2/7.CAG.ApoE3
ssAAV2/8.CAG.ApoE3
ssAAV2/9.CAG.ApoE3
Negative control
Plasma ApoE3 (µg/ml)
2.5
2.0
1.5
1.0
0.5
0.0
0 2 4 6 8 10 12 14
Post-injection time (weeks)

D:

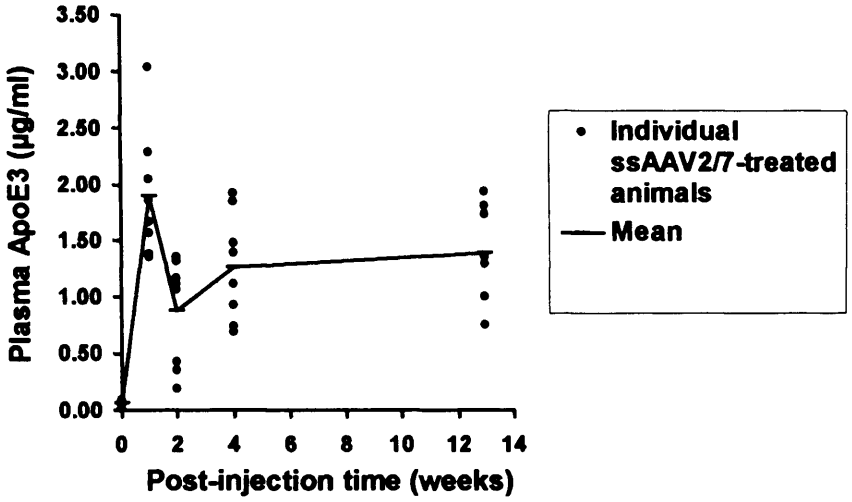
Plasma ApoE3 (µg/ml)
3.50
3.00
2.50
2.00
1.50
1.00
0.50
0.00
0
2
4
6
8
10
12
14
Post-injection time (weeks)
Individual ssAAV2/7-treated animals
Mean

E:

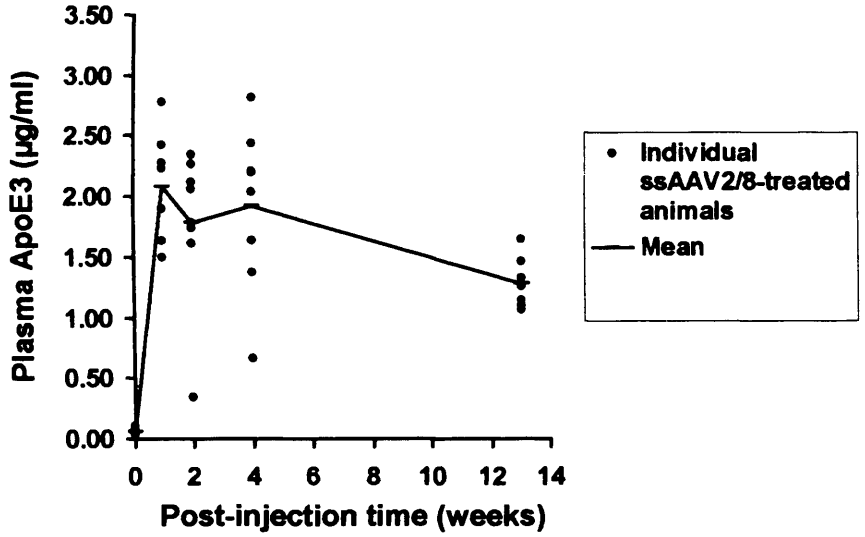
Plasma ApoE3 (µg/ml)
3.50
3.00
2.50
2.00
1.50
1.00
0.50
0.00
0
2
4
6
8
10
12
14
Post-injection time (weeks)
Individual ssAAV2/8-treated animals
Mean

F:

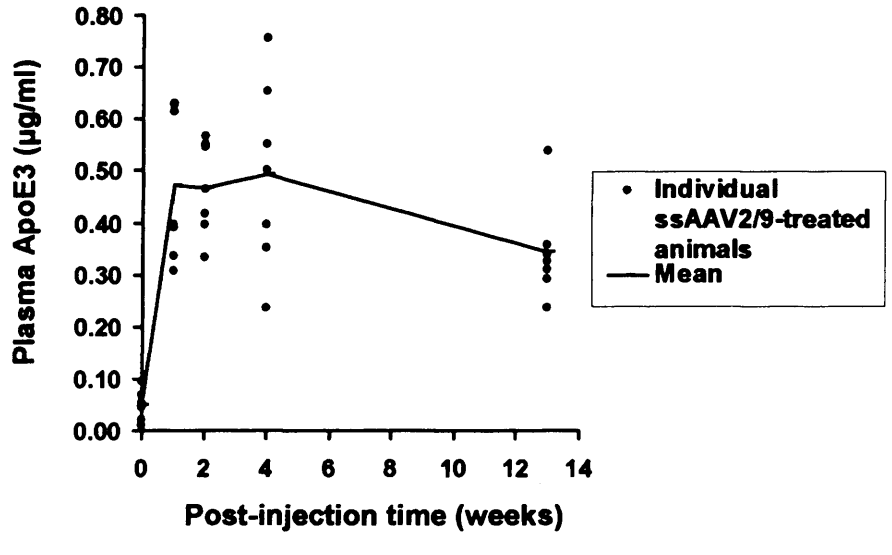
Plasma ApoE3 (µg/ml)
0.80
0.70
0.60
0.50
0.40
0.30
0.20
0.10
0.00
0
2
4
6
8
10
12
14
Post-injection time (weeks)
Individual ssAAV2/9-treated animals
Mean

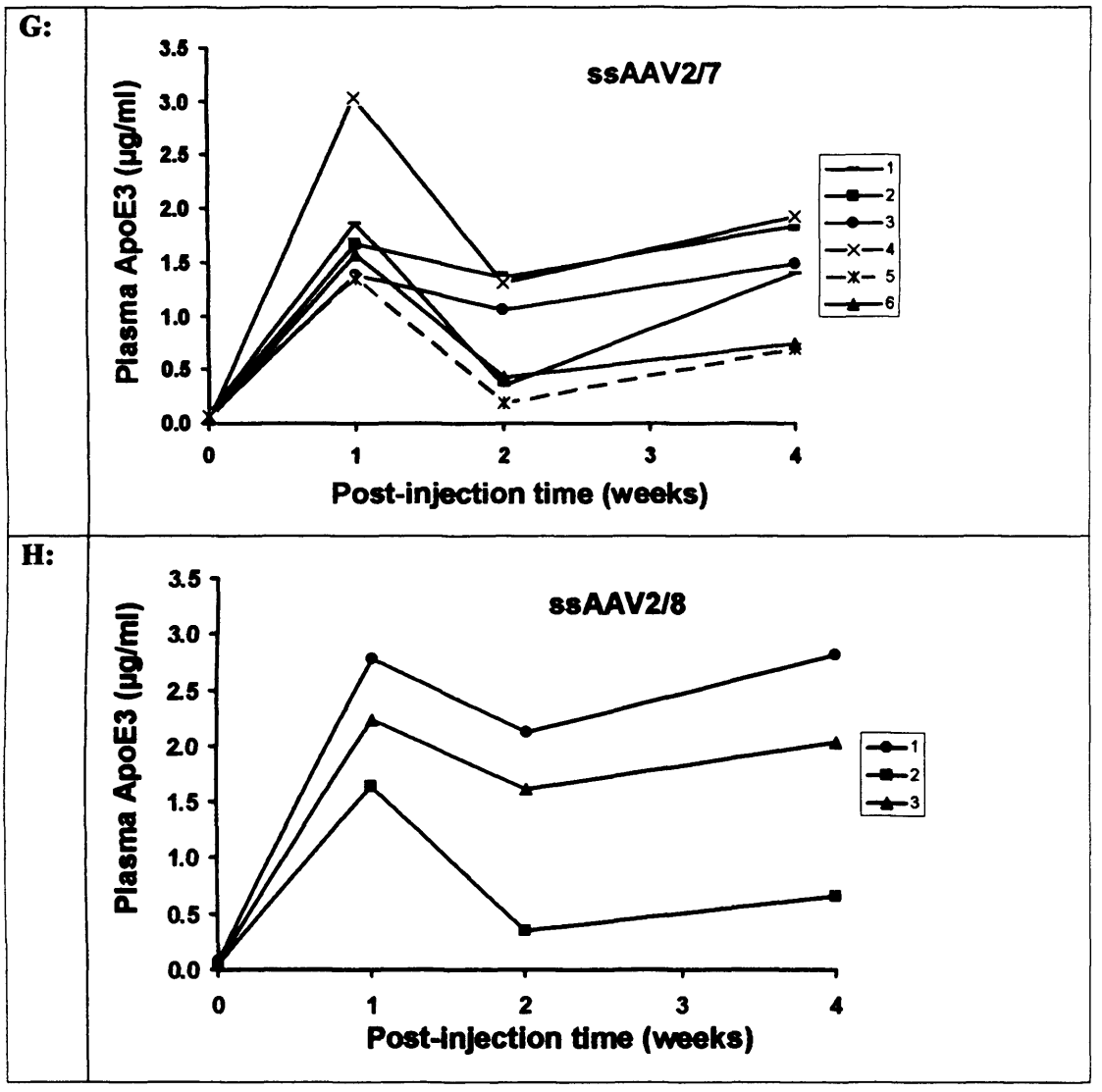

Figure 5-3. Plasma ApoE3 levels in ApoE$^{-/-}$ mice following intramuscular injections of ssAAV2/7, ssAAV2/8 and ssAAV2/9 vectors

Three groups of female mice were injected with 1× 10^{10}vg of either ssAAV2/7.CAG.ApoE3, ssAAV2/8.CAG.ApoE3 or ssAAV2/9.CAG.ApoE3, while a fourth control group was uninjected. Tail vein bleeds were taken prior to injection and at 1, 2, 4 and 13 weeks post-injection and plasma was assayed for human ApoE3 protein. ***(A)*** *A Western blot of pooled plasma samples from ssAAV2/7- and ssAAV2/8-treated mice over the 13 week time course.* ***(B)*** *Semi-quantitative Western blot analysis of plasma ApoE3 levels (µg/ml) in individual animals injected with ssAAV2/7 and ssAAV2/8.* ***(C)*** *ELISA quantification of circulating human ApoE3 concentrations (µg/ml), the graph represents the mean value at each time-point of all four groups.* ***(D-F)*** *Plasma ApoE3 levels in individual mice at each time-point is shown (•), with the solid line indicating the mean value for animals injected with ssAAV2/7* ***(D)****, ssAAV2/8* ***(E)*** *or ssAAV2/9* ***(F)****. Individual ssAAV2/7-* ***(G)*** *and ssAAV2/8-treated animals* ***(H)*** *demonstrating a decrease in plasma ApoE3 levels at 2 weeks and an increase at 4 weeks.*

5.3.4 The hyperlipidaemic profile of ApoE$^{-/-}$ mice treated with the CAG-driven ssAAV2/7, 2/8 and 2/9 vectors is not ameliorated

Plasma from individual AAV-treated and control animals was assayed for total cholesterol. Plasma total cholesterol from the control animals rose 2-fold between 0 (7.7±2mmol/L) and 2 weeks (14±1.6mmol/L) and then sharply declined at 4 weeks (10.9±2mmol/L), but by the final 13 week time-point the level had augmented again (13.4±2.9mmol/L) (Figure 5-4A). A similar pattern was also observed with ssAAV2/8- and ssAAV2/9-treated mice (Figure 5-4A); however, a different trend was displayed with animals from the ssAAV2/7 group. These mice demonstrated a steep increase in total cholesterol level between the 0 and 2 week time-points, however, the level continued to gradually rise thereafter and at 4 weeks (13.9±1.5mmol/L) was significantly ($P<0.05$) different from the negative control group (Figure 5-4A). The initial rise in total cholesterol exhibited in all 32 animals within the first two weeks was most likely due to the high-fat diet, which was commenced only one week before treatment. Nevertheless, none of the treated groups exhibited a normalisation in cholesterol level after 13 weeks or a reduction when compared with baseline levels. It is important to emphasise, however, that the increase in total cholesterol observed between 4 and 13 weeks might also be due to the ageing of the mice.

Figure 5-4B represents a comparison of total cholesterol at 2 and 13 weeks in each group. Interestingly, the ssAAV2/7- and ssAAV2/8-treated animals demonstrate lower levels at 2 weeks, while ssAAV2/9-treated mice, which displayed very low circulating ApoE3 concentrations, and negative control animals show very little difference between these two time-points. Direct comparisons were also made between total cholesterol and plasma ApoE3 levels over time for three individual mice treated with ssAAV2/7 (Figure 5-4C, D and E) or ssAAV2/8 (Figure 5-4F, G and H). Animals with the highest and lowest mean plasma ApoE level over the time-course were selected for comparison and two trends were clearly observed. When ApoE3 concentrations were high in these two treated groups, the decrease in total cholesterol, which was observed at 4 weeks in control mice, was inhibited and the level appeared to reach either a plateau or decline after 13 weeks (Figure 5-4C, D, F and G). In contrast, when ApoE3 levels were much lower, a marked increase in total cholesterol was observed at termination (Figure 5-4E and H).

To determine whether the abnormal lipoprotein profile of high atherogenic VLDL/IDL/LDL, and low anti-atherogenic HDL, had improved in treated-animals, pooled plasma samples from the individual mice in each group were subjected to agarose gel electrophoresis. The separated lipoproteins were stained with Sudan black and analysed by densitometry to determine the relative proportions of lipoprotein classes. Plasma from wild-type C57BL/6 mice exhibit high levels of HDL and a relatively low proportion of clearly separated VLDL and LDL; hence their HDL to total lipoprotein ratio was greater than 1 (Figure 5-5A, B, C and D). In contrast, the plasma of the negative control ApoE$^{-/-}$ mice demonstrated mostly VLDL/IDL/LDL lipoprotein particles, and a profile was displayed that clearly reflected their total cholesterol levels over the time-course. As expected, the high-fat diet resulted in an increase at 1 week in the absolute amounts of HDL and VLDL/IDL/LDL particles; furthermore, between baseline and 1 week the HDL to total lipoprotein ratio had increased from 0.05 to 0.09 (Figure 5-5A and E). At 2 weeks, each individual lipoprotein fraction had markedly decreased, but by 13 weeks, VLDL/IDL/LDL levels had risen again, while HDL remained low. The HDL to total lipoprotein ratio at termination was, thus, significantly lower (0.02) than that observed at 0 and 1 weeks. This lipoprotein profile was also exhibited in mice treated with ssAAV2/7, 2/8 and 2/9 vectors (Figure 5-5B, C, D and E), however, the 2, 4 and 13 week HDL to total lipoprotein ratios do not appear as suppressed (relative to 0 and 1 weeks) in these animals (Figure 5-5E). Although no amelioration in the hyperlipidaemic phenotype was observed after 13 weeks, the ApoE in the plasma of treated animals appears to counteract the effect of prolonged fat feeding or ageing, especially at 2 and 4 weeks.

A:

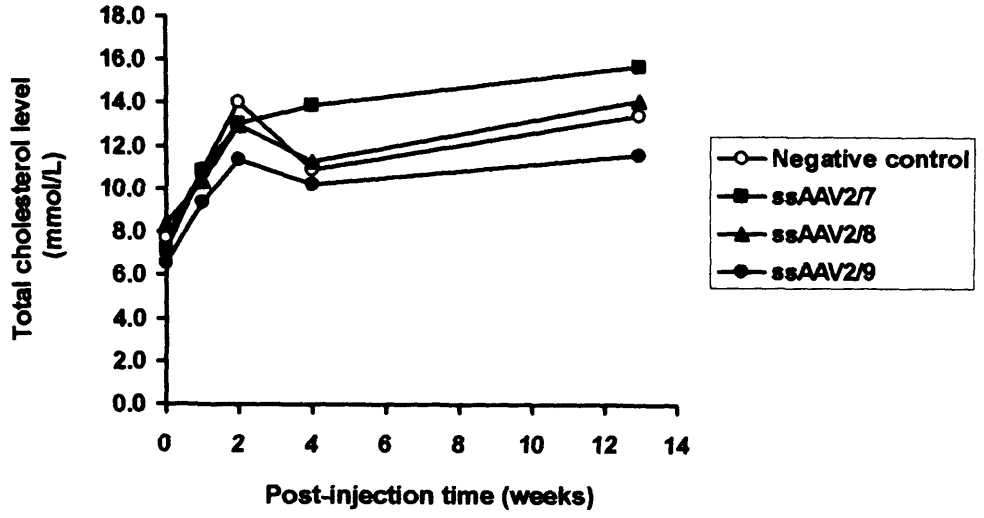
Total cholesterol level (mmol/L)
18.0
16.0
14.0
12.0
10.0
8.0
6.0
4.0
2.0
0.0
0
2
4
6
8
10
12
14
Post-injection time (weeks)
Negative control
ssAAV2/7
ssAAV2/8
ssAAV2/9

B:

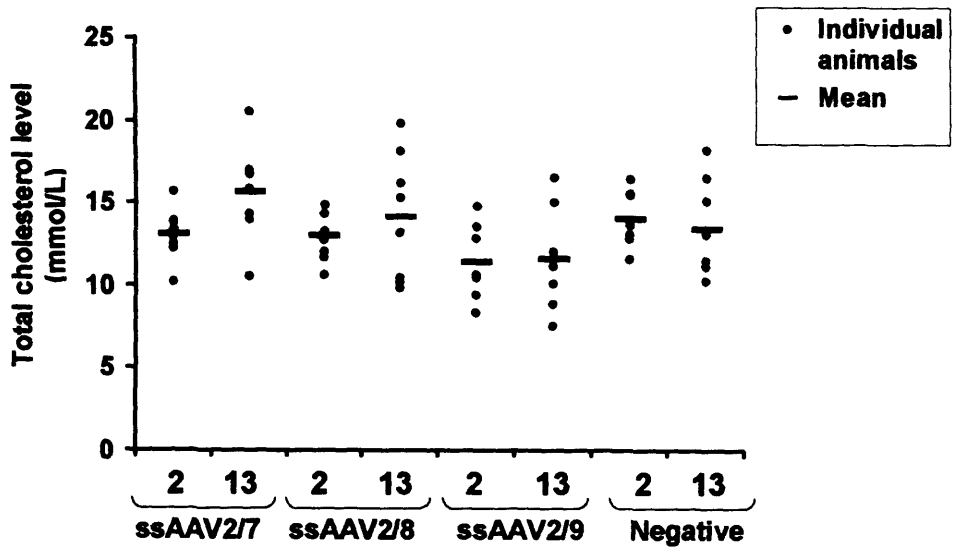
Total cholesterol level (mmol/L)
25
20
15
10
5
0
2
13
2
13
2
13
2
13
ssAAV2/7
ssAAV2/8
ssAAV2/9
Negative
Individual animals
Mean

C:

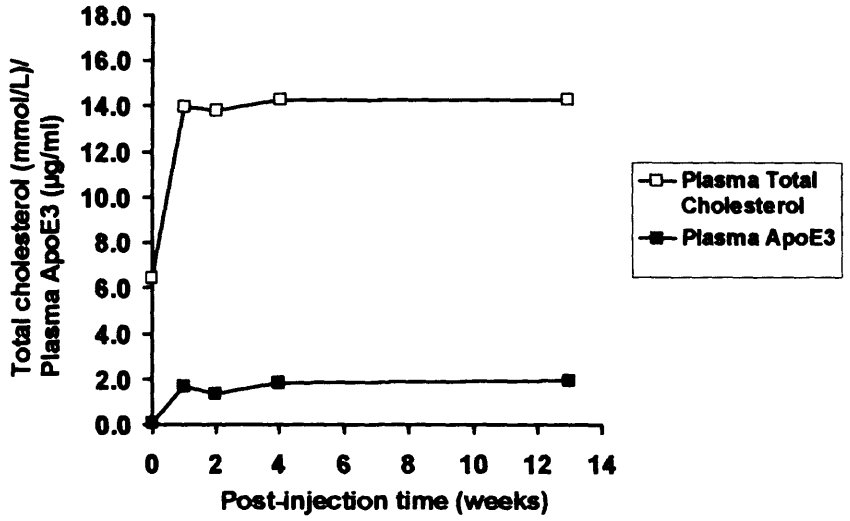
Total cholesterol (mmol/L)/
Plasma ApoE3 (µg/ml)
18.0
16.0
14.0
12.0
10.0
8.0
6.0
4.0
2.0
0.0
0 2 4 6 8 10 12 14
Post-injection time (weeks)
Plasma Total Cholesterol
Plasma ApoE3

D:

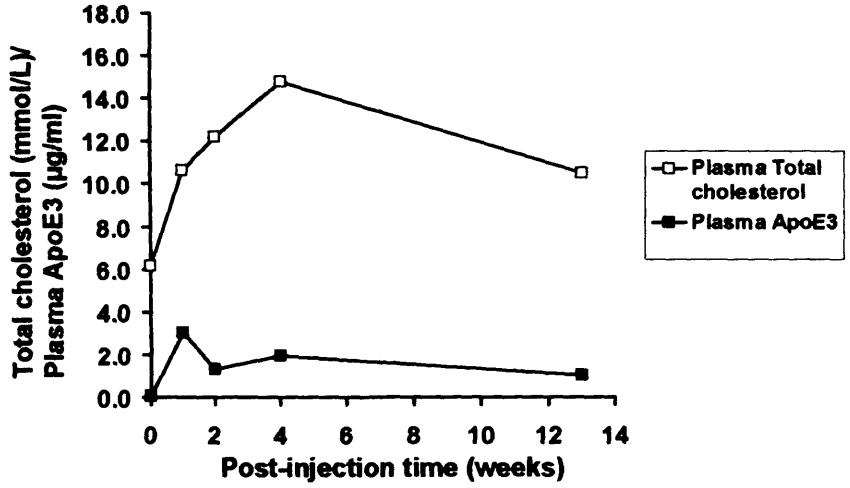
Total cholesterol (mmol/L)/
Plasma ApoE3 (µg/ml)
18.0
16.0
14.0
12.0
10.0
8.0
6.0
4.0
2.0
0.0
0 2 4 6 8 10 12 14
Post-injection time (weeks)
Plasma Total cholesterol
Plasma ApoE3

E:

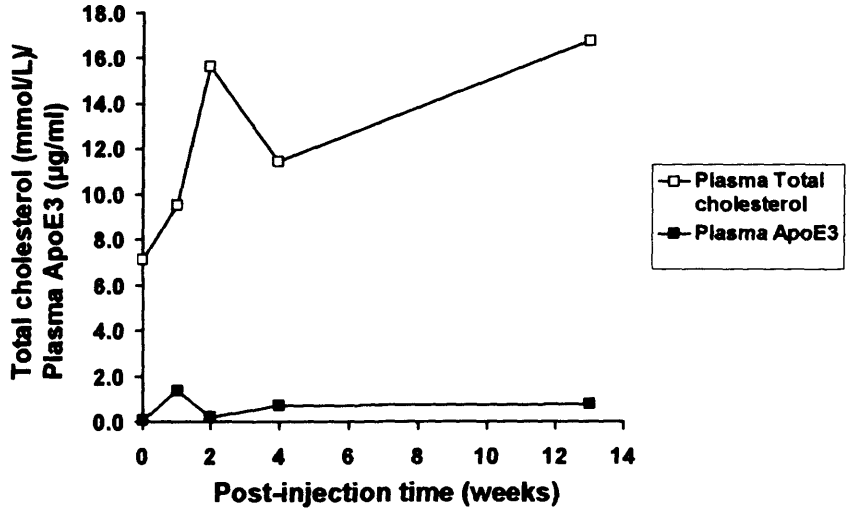
Total cholesterol (mmol/L)/
Plasma ApoE3 (µg/ml)
18.0
16.0
14.0
12.0
10.0
8.0
6.0
4.0
2.0
0.0
0 2 4 6 8 10 12 14
Post-injection time (weeks)
Plasma Total cholesterol
Plasma ApoE3

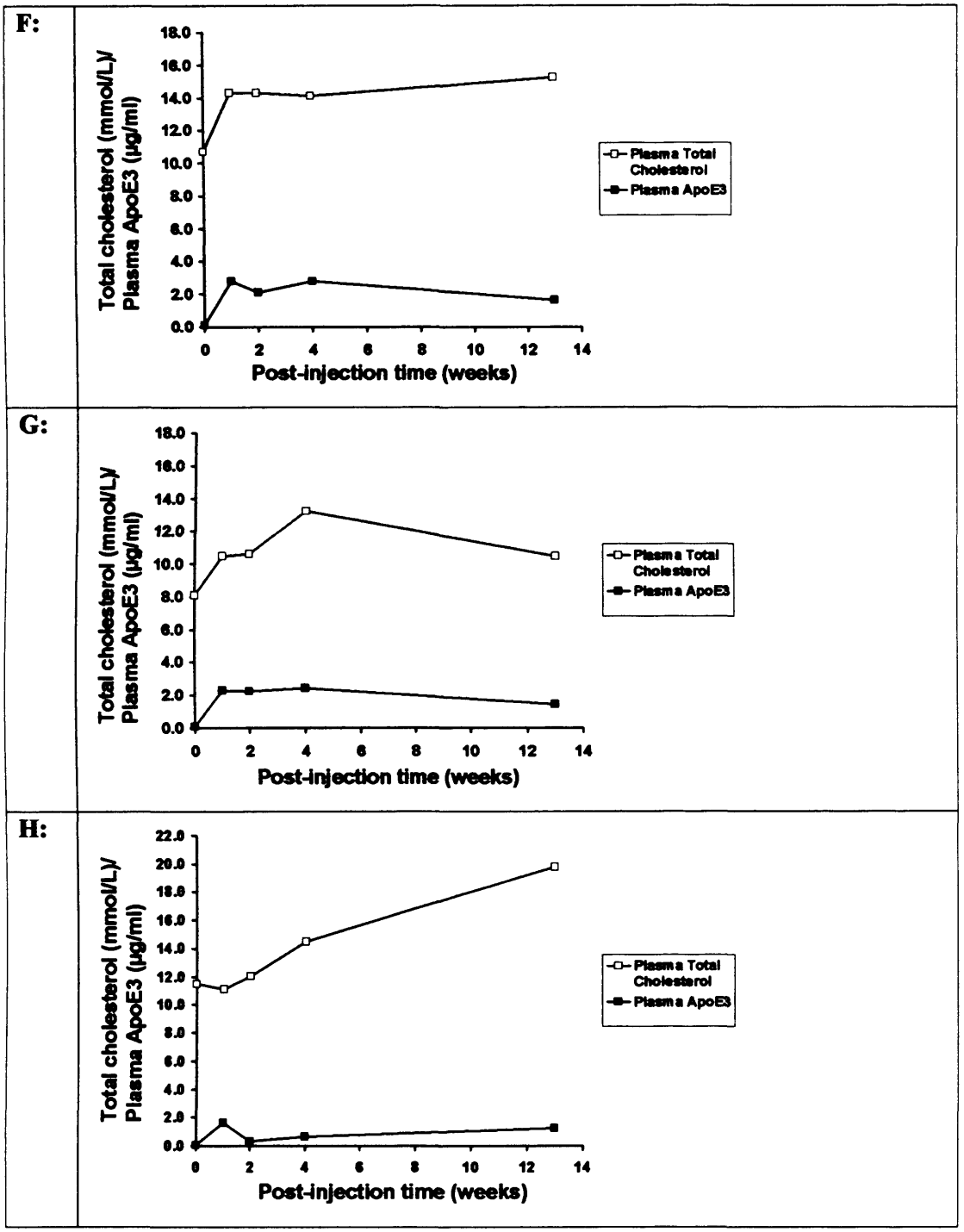

Figure 5-4. Total plasma cholesterol levels in ApoE$^{-/-}$ mice treated with ssAAV2/7, ssAAV2/8 and ssAAV2/9 vectors expressing human ApoE3

Total plasma cholesterol levels (mmol/L) were determined for individual control animals and animals that received intramuscular injections of either ssAAV2/7.CAG.ApoE3, ssAAV2/8.CAG.ApoE3, or ssAAV2/9.CAG.ApoE3. ***(A)*** *Represents the mean total cholesterol level (mmol/L) of all 8 animals in each group at each time-point.* ***(B)*** *Represents the total cholesterol levels of individual mice (•) in each group at 2 and 13 weeks, with the solid line (-) indicating the mean values. Total cholesterol vs plasma ApoE3 concentrations over time for individual animals treated with ssAAV2/7* ***(C,D and E)*** *and ssAAV2/8* ***(F, G and H)****.*

A:

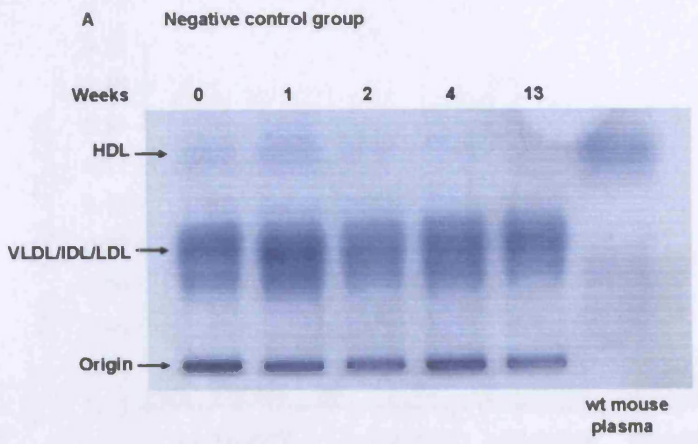
A
Negative control group
Weeks
0
1
2
4
13
HDL
VLDL/IDL/LDL
Origin
wt mouse plasma

B:

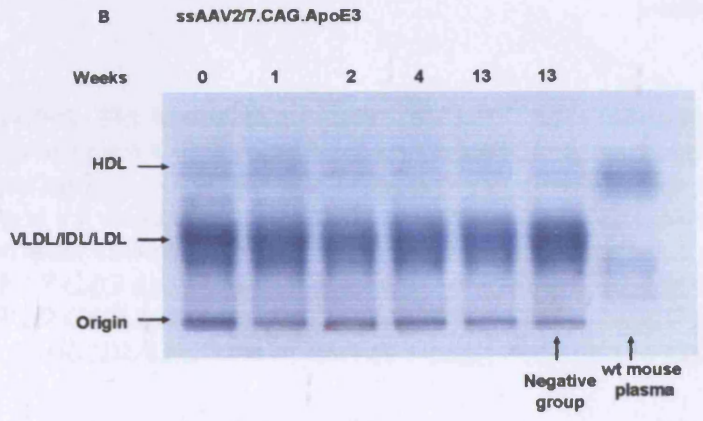
B
ssAAV2/7.CAG.ApoE3
Weeks
0
1
2
4
13
13
HDL
VLDL/IDL/LDL
Origin
Negative group
wt mouse plasma

C:

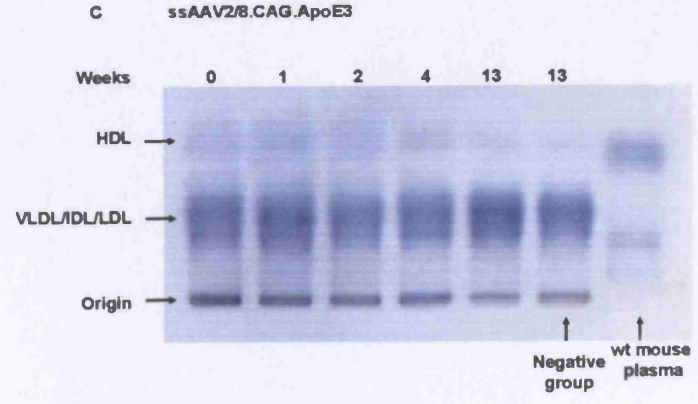
C
ssAAV2/8.CAG.ApoE3
Weeks
0
1
2
4
13
13
HDL
VLDL/IDL/LDL
Origin
Negative group
wt mouse plasma

D:

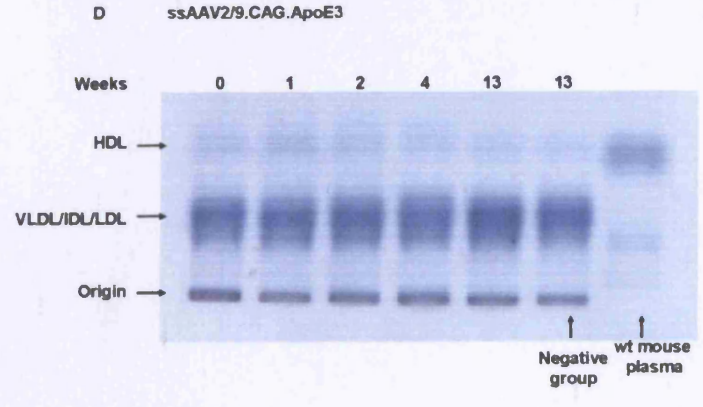
D
ssAAV2/9.CAG.ApoE3
Weeks
0
1
2
4
13
13
HDL
VLDL/IDL/LDL
Origin
Negative group
wt mouse plasma

E:

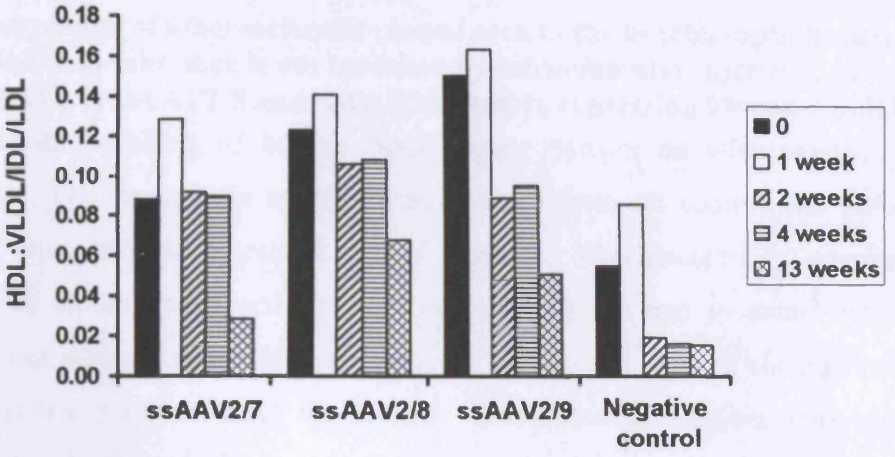

Figure 5-5. The lipoprotein profiles of ApoE$^{-/-}$ mice following intramuscular injections of ssAAV2/7, ssAAV2/8 and ssAAV2/9 vectors expressing human ApoE3
For each group, pooled plasma samples from individual mice at each time-point (0, 1, 2, 4 and 13 weeks) were subjected to agarose gel electrophoresis and the separated lipoproteins stained with Sudan black. Lipoprotein profiles of control animals ***(A)****, ssAAV2/7.CAG.ApoE3-treated mice* ***(B)****, ssAAV2/8.CAG.ApoE3-treated mice* ***(C)*** *and ssAAV2/9.CAG.ApoE3-treated mice* ***(D)****. Graphical representation of the HDL:VLDL/IDL/LDL ratio at each time-point, in all groups* ***(E)****.*

5.3.5 Progression of atherosclerotic plaque area in the brachiocephalic artery of ApoE-deficient mice is not inhibited by intramuscular injections of ssAAV2/7, ssAAV2/8 and ssAAV2/9 vectors expressing human ApoE3

To investigate the effect of human ApoE3 gene transfer on atherosclerotic lesion development, brachiocephalic arteries were excised from all control and ssAAV2/7, ssAAV2/8 and ssAAV2/9-treated $ApoE^{-/-}$ mice. Brachiocephalic arteries were embedded in paraffin and sections were cut every 30μm and mounted onto slides. Serial sections were stained with hematoxylin and eosin and Miller's elastin/van Gieson stain (EVG) (see section **2.2.5.4** for details). Elastin-stained sections were visualised under a microscope and plaque morphometry was performed with a computerised image-analysis program (Image Pro-Plus). The internal and external elasticae perimeters were recorded and used to derive the media area, which was assumed to be the circumference of a perfect circle. The plaque area was measured and the true lumen size was determined by subtracting the plaque area from the area enclosed by the internal elastic lamina (see Figure 2-5 for details). Plaques were also inspected for the presence of buried fibrous caps and their lipid content was quantified.

Plaque sizes varied considerably within each group; some brachiocephalic arteries contained very large and unstable plaques (Figure 5-9), while others had very small lesions (Figure 5-7B) or none at all (Figure 5-7A). All arteries containing plaques had undergone expansive remodelling of the arterial wall in an attempt to preserve blood flow down the lumen. Unfortunately, 3 of the 8 brachiocephalic arteries from the negative control group and 1 from both the ssAAV2/7 and ssAAV2/8-treated groups could not be analysed due to technical problems during processing. Unexpectedly, 2 of the 5 elastin-stained sections from the control group were free of plaques, whereas only 3 of the 21 arteries from the treated groups were "clean". For these reasons and with the anticipation that ssAAV2/9-treated animals might exhibit more plaque area due to their very low levels of circulating ApoE, comparisons have only been made between the three treated groups.

The plaque area did not differ significantly between ssAAV2/7, ssAAV2/8 and ssAAV2/9-treated animals ($68.9\pm69.9\times10^3\mu m^2$, $72.7\pm41.5\times10^3\mu m^2$ and $91.5\pm20.8\times10^3\mu m^2$ respectively) (Figure 5-6A), although it is important to emphasise here that there were plaque-free arteries in ssAAV2/7 and ssAAV2/8-injected mice, while this was not observed in animals treated with the ssAAV2/9 vector (Table 5-2). Although

the mean vessel, lumen and media areas appeared to be generally lower in ssAAV2/7-treated animals, the differences were not significant (Figure 5-6A). The plaque lipid content was also quantified for individual animals in each group (Figure 5-6B). The mean percentage in the brachiocephalic arteries of mice treated with ssAAV2/9 was ~ 50% higher, although this was not statistically significantly different compared with the ssAAV2/7- or ssAAV2/8-injected animals (P>0.05).

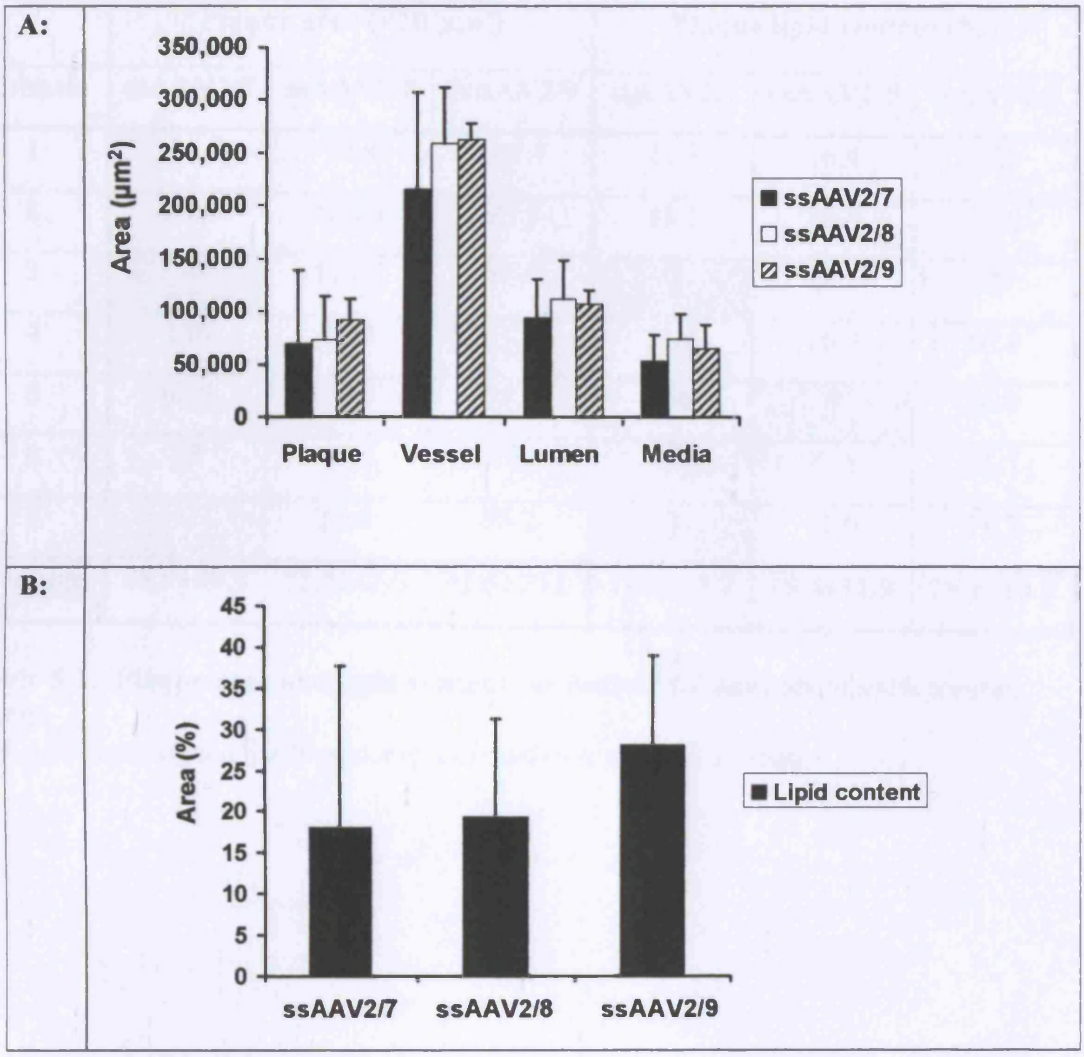

Figure 5-6. The brachiocephalic artery morphometry of ApoE$^{-/-}$ mice treated with ssAAV2/7, ssAAV2/8 and ssAAV2/9 vectors expressing human ApoE3

*Elastin-stained brachiocephalic artery sections were visualised under a microscope and plaque morphometry was performed with a computerised image-analysis program (Image Pro-Plus). The plaque, vessel, true lumen and media area were determined for individual animals and the mean of each ssAAV2/7, ssAAV2/8 and ssAAV2/9-treated group was calculated **(A)**. The plaque lipid content was also quantified for individual animals with the average values for each group represented in the graph **(B)**.*

	Plaque area ($\times 10^3 \mu m^2$)			Plaque lipid content (%)		
Animals	**ssAAV2/7**	**ssAAV2/8**	**ssAAV2/9**	**ssAAV2/7**	**ssAAV2/8**	**ssAAV2/9**
1	124.3	72.9	101.7	21.5	16.4	29.3
2	90.4	122.5	97.8	35.1	38.8	11.6
3	**0**	119.4	51.7	**0**	18.1	29
4	186	71.4	77.3	51.6	16.9	40.4
5	63.9	**0**	98.8	2.6	**0**	26.2
6	18	69	115.2	15.4	27.8	41.7
7	**0**	53.8	98.2	**0**	17.6	18.3
Average	**68.9±69.9**	**72.7±41.5**	**91.5±20.8**	**18.0±19.7**	**19.4±11.9**	**28.1±10.9**

Table 5-2. Plaque area and lipid content for individual animals in each treated group
N.B A 0 was assigned for brachiocephalic arteries without a plaque

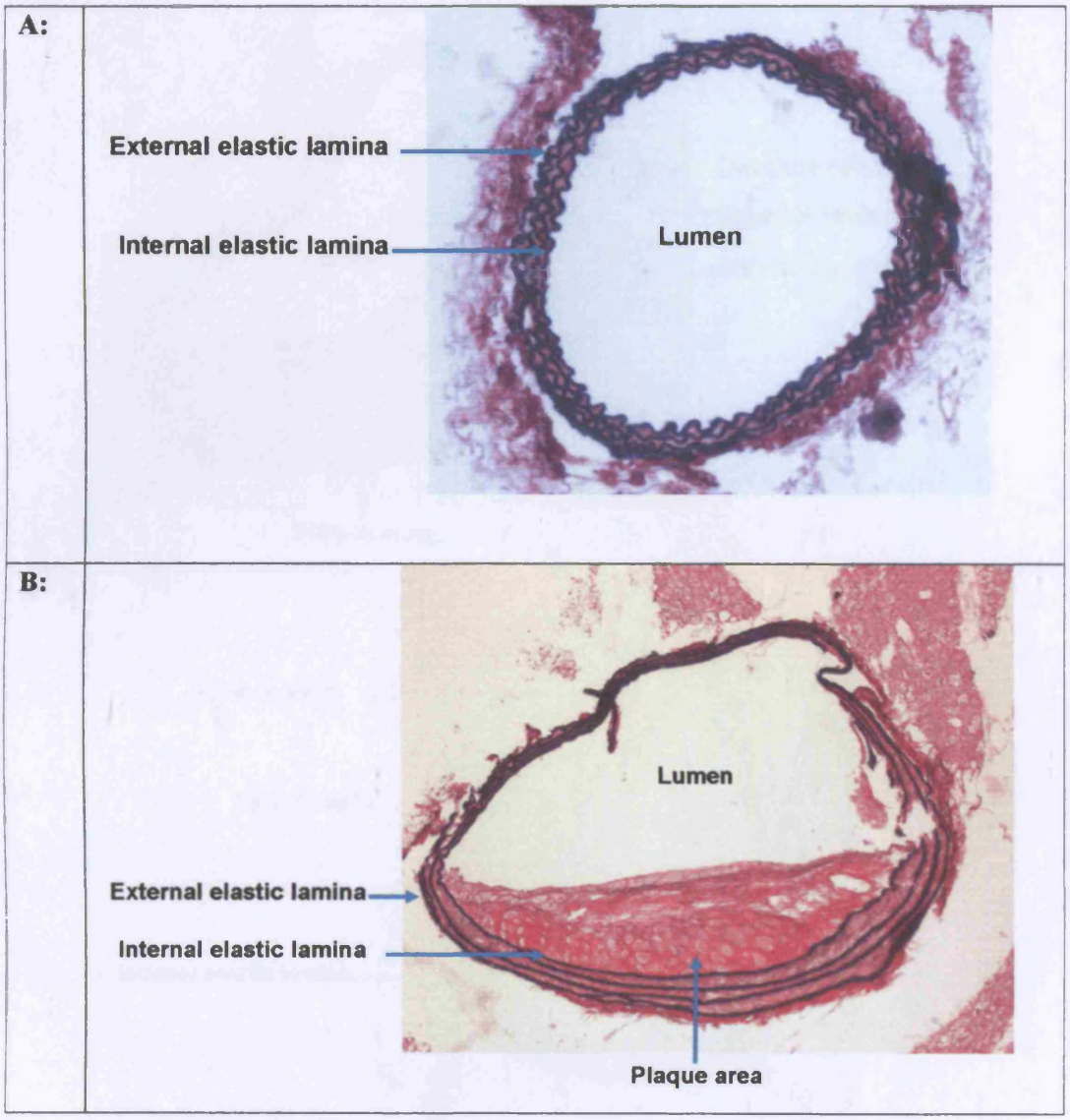

Figure 5-7. EVG stained sections of brachiocephalic arteries (10× magnification) ***(A)*** *A 30μm section from a brachiocephalic artery with no visible plaque. The artery was excised from a mouse treated with ssAAV2/7.CAG.ApoE3.* ***(B)*** *A 120μm section with a small, stable plaque. The artery was from an animal treated with ssAAV2/8.CAG.ApoE3.*

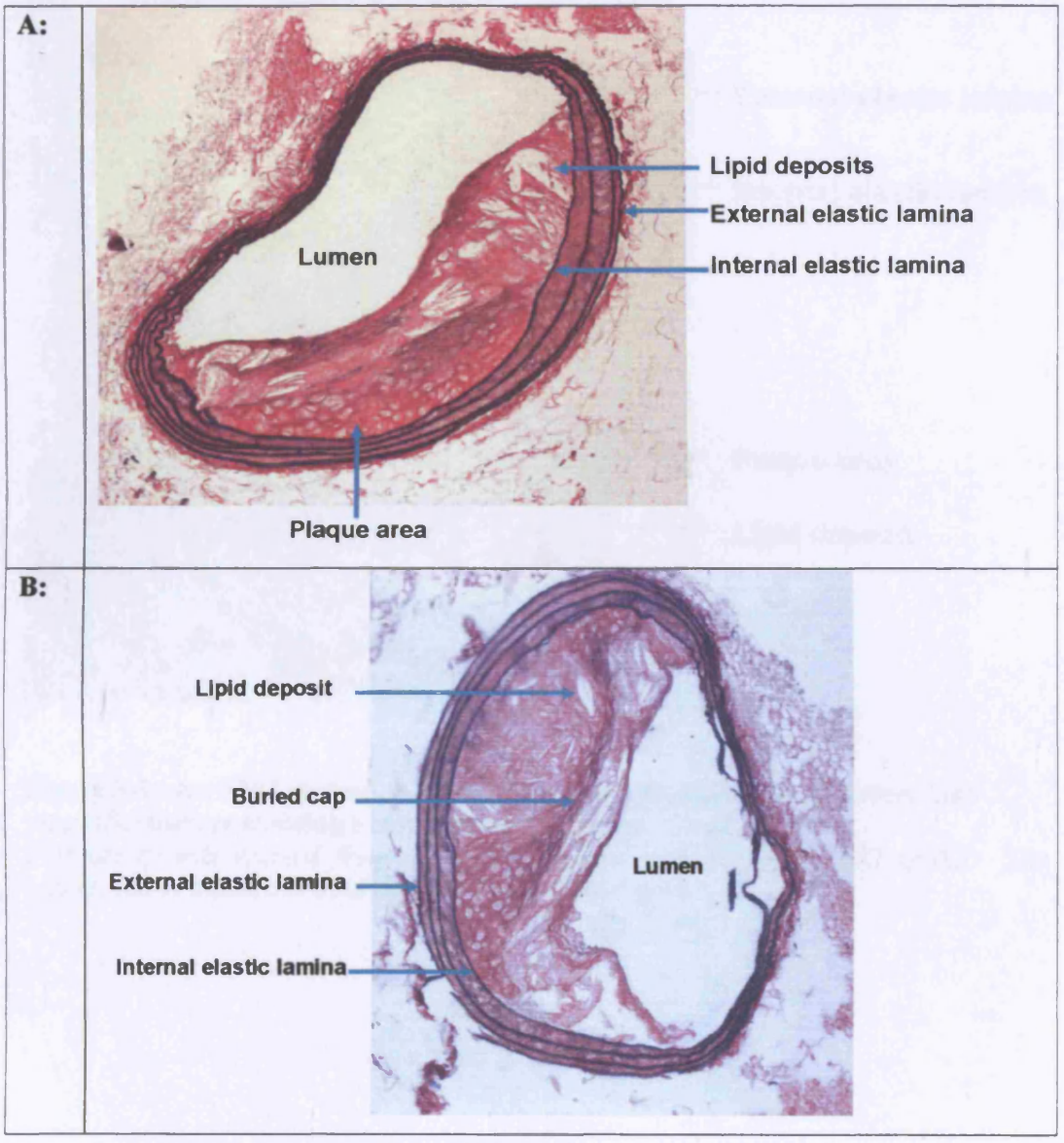

Figure 5-8. EVG stained sections of brachiocephalic arteries (10× magnification) *(A) A 120μm section showing an intermediate, stable plaque with small lipid deposits. This artery was excised from an animal treated with ssAAV2/9.CAG.ApoE3.* ***(B)*** *A 120μm section showing an intermediate, unstable plaque with visible buried fibrous caps and lipid deposits. The artery was taken from an animal injected with ssAAV2/8.CAG.ApoE3.*

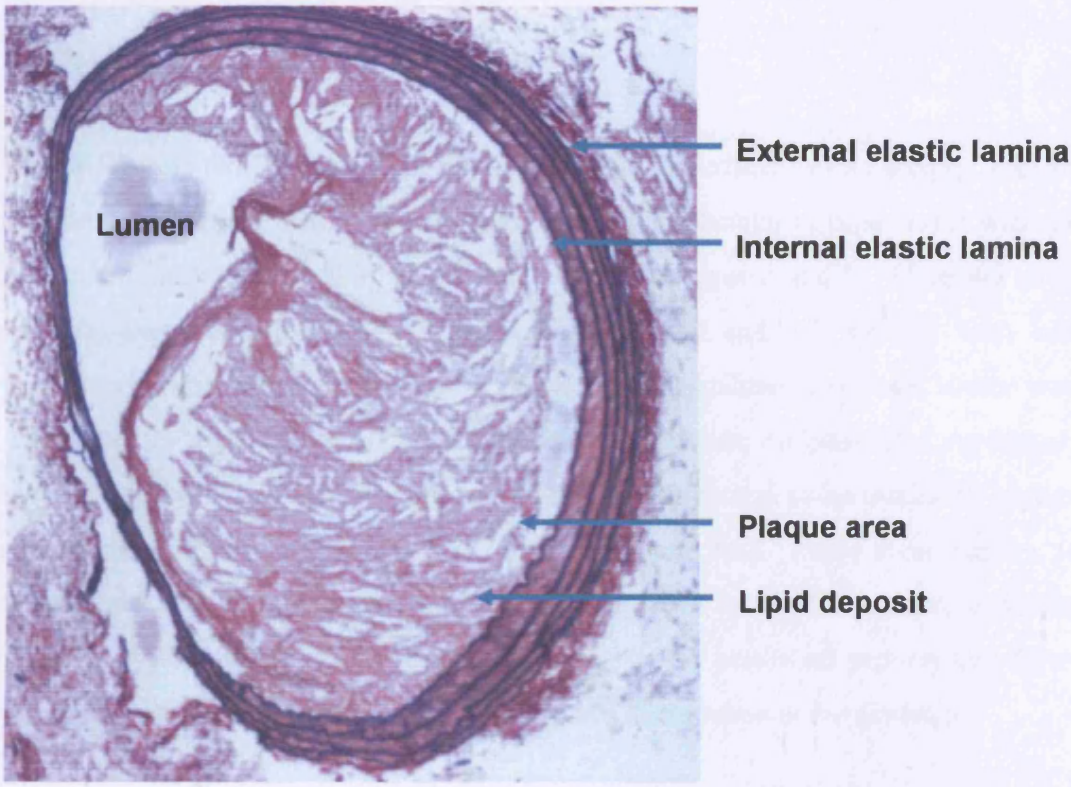

Figure 5-9. An EVG stained section (150μm) of a brachiocephalic artery (10× magnification) containing a large, unstable plaque.
This artery was excised from an animal treated with ssAAV2/7.CAG.ApoE3. The section shows numerous lipid deposits in the plaque area.

5.4 Discussion

The overall aim of the large-scale *in vivo* experiment described in this chapter was to identify the AAV capsid best suited for gene delivery to skeletal muscle and it was for the aforementioned qualities that we selected AAV serotypes 8 and 9. Here we have directly compared pseudotyped, CAG-driven ssAAV2/8 and 2/9 vectors with our previously tested ssAAV2/7.CAG.ApoE3 vector. The functionality of each vector was first confirmed *in vitro*, in both HEK 293-T cells and mature, differentiated myotubes. Secretion of human ApoE3 from both cell-types was discovered to be markedly higher following infection with ssAAV2/7.CAG.ApoE3 (Figure 5-2). From these results, it can be inferred that *in vitro* gene transfer to muscle cells by AAV7 is more efficient than that by AAV8 and AAV9. Currently there are no published reports that have carried out the same comparisons *in vitro*, which could corroborate our findings.

Having verified that all three vectors function efficiently *in vitro*, we then went on to perform a head-to-head comparison of each vector *in vivo*, injecting the TA muscle of $ApoE^{-/-}$ mice. These mice are a valuable model of human atherosclerosis. The animals become grossly hypercholesterolaemic on normal chow, exhibit spontaneous xanthoma formation and develop atheroma in coronary arteries from 2 months [117;133]. For the purpose of this experiment, the mice were fed a high-fat diet which has been shown to advance the progression of atherosclerosis by at least 6 weeks with lesions developing more rapidly throughout the vascular tree [121]. Our 13 week experiment was designed to evaluate the hypolipidaemic effects of each vector and also their ability to inhibit the progression of early atherosclerotic lesion development.

Human ApoE3 was detected in the plasma of all animals treated with both ssAAV2/7.CAG.ApoE3 and ssAAV2/8.CAG.ApoE3 as early as 1 week post-injection (Figure 5-3A) and levels were sustained for the entire 13 week period. After the first week levels had reached 2μg/ml and above in both groups. However, at 2 weeks the level had fallen, possibly suggesting secreted ApoE3 had been sequestered by the excess of remnant lipoproteins in the plasma and rapidly cleared by the liver. Interestingly, mean circulating concentrations had significantly declined in ssAAV2/7-treated animals (1.9±0.56μg/ml to 0.87±0.47μg/ml $p < 0.005$), but the decrease was much less in mice that had received ssAAV2/8 injections. This ultimately highlights differences in vector efficiency, as ssAAV2/8 must be producing more ApoE3 to

compensate for its rapid removal. Nevertheless, by 13 weeks, plasma ApoE3 levels had declined in ssAAV2/8 animals, whereas in ssAAV2/7-treated mice concentrations had augmented compared with the 2 and 4 week time-points (Figure 5-3C). From these findings, it could be speculated that both vectors function differently over time; it is possible that ssAAV2/8 transduces skeletal muscle more rapidly, while transduction is slower with ssAAV2/7, with peak expression occurring later on. Gao et al. have previously used AAV7 and AAV8 for skeletal muscle gene transfer and directly compared and evaluated their relative performances [191]. Both serotypes were discovered to transduce the muscle with a high efficiency, although AAV7 performed slightly better and demonstrated efficiencies of transgene expression equivalent to that observed with AAV1. These findings were confirmed in a subsequent study, which quantitatively compared the transduction efficiencies of pseudotyped AAV vectors in both slow and fast muscle fibres. Here, however, the performance of AAV2/8 was also comparable to that of AAV2/1 [207].

Unfortunately, plasma ApoE3 levels in mice injected with ssAAV2/9.CAG.ApoE3 were very low and fell below the detection limit of the Western blot. This was disappointing, however, as it was predicted that this vector would function relatively well; substantial transduction of AAV9 in skeletal muscle has previously been reported following systemic delivery [213]. Nevertheless, our knowledge of the biology of AAV9 *in vivo* is currently limited and there are no studies so far that have assessed transgene expression following direct injection of AAV9 into skeletal muscle.

Total plasma cholesterol in ssAAV2/7-, ssAAV2/8- and ssAAV2/9-treated mice was not reduced after 13 weeks, despite there being detectable circulating levels of ApoE3 in these animals. Due to the high-fat diet, plasma total cholesterol from both control and treated animals significantly augmented between 0 and 2 weeks; this was followed by a sharp decline at 4 weeks in all animals apart from those that were treated with ssAAV2/7.CAG.ApoE3. In $ApoE^{-/-}$ mice, ApoB100 naturally becomes the principle ligand mediating hepatic remnant clearance through the LDL-R; as a result plasma from these mice normally has only traces of ApoB100-VLDL, but contains very high levels of the binding-defective ApoB48-VLDL [129]. The sudden decrease in total cholesterol observed at 4 weeks suggests that alternative mechanisms for the hepatic uptake of remnant lipoproteins were initiated in response to their excessive accumulation in the plasma. It has been hypothesised that lipoprotein lipase and hepatic lipase, when

present on the surface of VLDL, IDL and LDL, can act as ligands for the LDL-R and LRP and, thus, mediate the endocytosis of these lipoprotein particles [369]. The HDL receptor, SR-BI, is also believed to mediate the hepatic removal of ApoB48-carrying lipoproteins in the absence of ApoE [370]. It is possible that SR-BI binds to anionic phospholipids, for which it has high affinity, on the surface of cholesterol-rich lipoproteins. Furthermore, inhibition of SR-BI expression in the liver of ApoE-deficient mice results in accumulation of remnants in the plasma and this can be reversed by the restoration of hepatic SR-BI [371]. Interestingly, chylomicrons and VLDL in the plasma of $ApoE^{-/-}$ are also enriched in ApoAI, which could also mediate their removal via the SR-BI receptor [372]. Initiation of such mechanisms, however, might not occur when a certain level of ApoE in the plasma is restored; indeed, in wild-type mice lipoproteins are readily cleared from the circulation even when their hepatic SR-BI is absent [373]. It is also speculated that SR-BI does not bind remnants until their concentration in the plasma becomes sufficiently high to efficiently compete with other lipoproteins that also bind to this receptor [371]. Two trends were observed in our study that are consistent with these reports; high levels of ApoE3 in ssAAV2/7 and ssAAV2/8-treated animals appeared to prevent the decline in total cholesterol at 4 weeks, and suppress any further increase at 13 weeks, while low circulating concentrations resulted in a marked increase in total cholesterol at termination (Figure 5-4C to H). It is possible to speculate, therefore, that the small amount of ApoE3 secreted in the plasma of ssAAV2/7 and ssAAV2/8-treated animals was sufficient to inhibit the induction of alternative mechanisms that clear remnant lipoproteins, but insufficient to mediate effective clearance via LRP.

In accordance with the observed decrease in total cholesterol at 4 weeks in control, ssAAV2/8- and ssAAV2/9-treated mice, there was also a visible reduction in both the HDL and VLDL/IDL/LDL fractions (Figure 5-5). By 13 weeks, however, the absolute amount of VLDL/IDL/LDL had augmented and reached levels equivalent to that observed at 0 and 1 week; thus there was no amelioration in the hyperlipidaemic phenotype of treated animals after 13 weeks. Interestingly, the suppression of the HDL to total lipoprotein ratio at 2, 4 and 13 weeks was much less in treated compared with control animals (Figure 5-5E). It could therefore, be speculated that the presence of ApoE3 in the plasma counteracted the effect of prolonged fat feeding or ageing in these mice, especially at 2 and 4 weeks post-treatment. The concentration of ApoE reported to normalise plasma cholesterol is 2μg/ml [96], however, this threshold level was

derived from a study using mouse and not human ApoE. Mouse ApoE is in fact 6-fold more efficient than human ApoE3 in clearing remnant particles and transgenic mice expressing the human ApoE isoform in place of the mouse protein are more susceptible to diet-induced hypercholesterolaemia and atherosclerosis [137]. Furthermore, in a study comparing hypomorphic mice, which express reduced levels of Arg-61 ApoE (an isoform resembling human ApoE4), with $ApoE^{-/-}$ mice expressing similar levels of Arg-61 ApoE after bone marrow transplantation, hepatocyte ApoE was demonstrated to be more efficient than extrahepatic ApoE in promoting clearance of remnant lipoproteins [374]. Although this contradicts findings by Thorngate et al. whom demonstrated that only low levels of ApoE expressed specifically in the adrenal gland of ApoE-/- was sufficient to inhibit atherosclerosis [96]. Nevertheless, the aforementioned factors along with increased plasma total cholesterol, induced by a high-fat diet, might explain why the circulating ApoE in our treated mice could not prevent the accumulation of VLDL–size lipoproteins of abnormal conformation and enriched in unesterified cholesterol.

The brachiocephalic artery, which is the first branch from the aortic arch, is a well-defined area in which to study plaque stability and rupture. The lesion characteristics in this artery of a fat-fed $ApoE^{-/-}$ mouse are similar to those associated with plaque instability in humans and it was for this reason that we selected this site to investigate the anti-atherosclerotic effect of ectopically expressed human ApoE. $ApoE^{-/-}$ mice, when fed a high-fat diet for only 8 weeks, exhibit a high frequency of plaque rupture in these arteries and at later times buried fibrous layers within the plaque can be seen, which may represent previous healed ruptures [125]. The layered appearance of the brachiocephalic artery plaques has also been observed in human coronary arteries [375;376]. Consistent with these reports, our mice, which had also been fed a high-fat diet for a short period of 13 weeks, demonstrated unstable plaques with visible buried fibrous caps. Plaque sizes, however, varied considerably within each group; some arteries contained very large and unstable plaques, while in others the lesions were very small and less developed. Surprisingly, two of our control animals had arteries that were "clean", the reason for this, however, cannot be explained. Plaque progression in the brachiocephalic artery, however, was not attenuated in ssAAV2/7, 2/8 and 2/9-treated animals and no significant reductions in lumen and media size were observed. An increase in lipid core size has been linked to vulnerability of human plaques [376], which is also true in mouse brachiocephalic arteries; Williams et al. reported ruptured plaques to have a much greater lipid content than intact plaques [125]. We, therefore,

measured the plaque lipid content in our treated animals, and although the lesions from mice injected with ssAAV2/9 demonstrated a higher percentage, consistent with their lower levels of plasma ApoE3, the difference was not significant.

Previous deliveries of ApoE3 by intramuscular plasmid [325] and AAV injection [316] have demonstrated reductions in atherosclerotic aortic plaques despite a failure to detect ApoE3 in plasma. Given that in this study we have detected circulating levels of human ApoE3, we considered an inhibition in atherosclerotic lesion development highly feasible. The failure to observe such inhibition, however, was not due to the AAV serotypes used since liver-directed ApoE gene transfer mediated by AAV2/7 and AAV2/8 vectors completely prevented atherosclerosis in ApoE deficient mice [318]. The method previously used for plaque quantification, *en face* lipid staining, could be considered as more sensitive, although plaque lipid content in the brachiocephalic artery demonstrated a trend towards a reduction in ssAAV2/7- and ssAAV2/8-treated animals. It is possible that differences in aortic and brachiocephalic artery plaque development could be responsible. In the aortic sinus the lesions remain as fatty streaks for an extended period, and it is months before a fibrous cap can be discerned, while lesions develop rapidly in the brachiocephalic artery, especially under conditions of high-fat feeding, when advanced plaques are present after as little as 5 weeks [126]. It is conceivable that the small amount of ectopically expressed ApoE becomes limiting in the face of the challenge of such rapidly growing lesions in the brachiocephalic artery and a much higher level of circulating ApoE is required to inhibit their development. Furthermore, ApoE has been shown to inhibit progression, rather than reverse established atherosclerotic plaques. Based on these findings, it would be more advantageous to carry out the experiment for a longer period without feeding the animals a high-fat diet, and in order to reinforce plaque quantification, *en-face* lipid staining of the aorta should be performed.

Chapter 6:

General Discussion

6 GENERAL DISCUSSION

Atherosclerosis, the leading cause of death in industrialised countries, is increasingly recognised as an inflammatory disease [2] and has multiple genetic and environmental contributions [10]. Atherosclerosis is characterised by the accumulation of lipids and foam cells in the artery wall and the eventual development of a fibrous plaque. ApoE is a 34-kDa circulating glycoprotein synthesised in liver and macrophages, which has been demonstrated to be highly anti-atherogenic. This is evidently displayed in ApoE-deficient mice which develop severe hypercholesterolaemia and atherosclerosis on a normal chow diet [117;118]. ApoE was initially described to play a major role in plasma lipoprotein metabolism and cholesterol homeostasis, specifically its ability to facilitate the removal of remnant lipoproteins in the liver. There is now, however, a substantial amount of evidence suggesting that ApoE has anti-atherosclerotic properties that are independent of lipid lowering [96;97;147;311]. These include anti-oxidant [110], anti-platelet [99] and anti-inflammatory [103-105] actions that are all unrelated to lipid transport and metabolism and contribute to the anti-atherogenic effect.

Circulating proteins are attractive targets for genetic manipulation and, unsurprisingly, ApoE has emerged as a strong candidate for treating hypercholesterolaemia and cardiovascular disease. Indeed, viral ApoE gene transfer studies have shown some encouraging results. In particular, liver-directed adenoviral gene transfer of ApoE ameliorates hyperlipidaemia and inhibits atherogenesis in ApoE-deficient mice [310;312;313;366]. Nevertheless, safety considerations and the option of repeat administrations have prompted renewed interest in alternative vectors, including non-viral (plasmid or "naked DNA") constructs [338] and rAAV [239]. Two studies have reported systemic delivery and long-term biological effects of ApoE following intramuscular injection of plasmid DNA containing the cytomegalovirus (CMV) promoter to drive human ApoE expression. One study noted a decrease in plasma cholesterol despite very low levels of plasma ApoE [324], while the other found reduced atherosclerotic plaque and xanthoma formation after 9 months [325]. Similarly, a rAAV vector derived from serotype-2 inhibited the development of atherosclerosis in $ApoE^{-/-}$ mice, although their hyperlipidaemia was unchanged [316]. These aforementioned studies have all used skeletal muscle as an alternative therapeutic target to liver, since it is a stable post-mitotic tissue with little nuclear turnover, which is highly vascularised and actively secretory [261;262].

The main objective of this study was to assess the potential of muscle-based expression of the human ApoE3 gene for ameliorating hypercholesterolaemia and preventing atherosclerosis in the ApoE$^{-/-}$ mouse, by plasmid and AAV-mediated delivery. With the aim to improve on previous studies, plasmids were injected via electrotransfer, which is a technique that has been demonstrated to significantly enhance uptake of naked DNA by skeletal muscle [336;337]. Furthermore, our plasmids contained muscle-specific promoters, which, unlike viral promoters, avoid cellular shutdown by DNA methyltransferases and, importantly, prevent transgene expression in antigen-presenting cells. Although rAAV vectors derived from serotype-2 have underperformed, alternative serotypes are showing great promise and markedly improve transduction efficiency *in vivo*. Here, we have used AAV serotypes 7 [194;207], 8 and 9 [212-215] which are all reported to have a high tropism for skeletal muscle. In addition, we also constructed scAAV vectors, which obviate the need for viral second-strand DNA synthesis and are, therefore, more efficient than the contemporary ssAAV vector [285;286]. Hence, it was anticipated that these alterations to plasmid and AAV-mediated delivery would improve intramuscular gene transfer of human ApoE3, with the ultimate goal to reverse hypercholesterolaemia and protect against atherosclerosis.

6.1 Hyperlipidaemia in ApoE-deficient mice is not reversed following intramuscular electrotransfer of plasmids expressing human Apolipoprotein E3

Chapter 3 described the construction and evaluation of single-stranded and self-complementary AAV expression plasmids harbouring the human ApoE3 gene, driven by the ubiquitous CAG promoter [250] and two muscle-specific promoters, CK6 [257] and C512 [258]. Each plasmid construct was first tested *in vitro* in murine C2C12 myoblasts and myotubes and then injected via electrotransfer into the *T. anterior* muscles of ApoE$^{-/-}$ mice. I demonstrated that cultured mouse C2C12 muscle cells transfected with each expression plasmid efficiently synthesise and secrete recombinant human ApoE3, albeit plasmids driven by the muscle-specific promoters failed to produce ApoE3 until after 24h, when the myoblasts had differentiated into myotubes. This, however, could be explained as, similar to the endogenous muscle creatine kinase gene [257;340], both the CK6 and C512 promoters are transcriptionally inactive in myoblasts and only become activated when myoblasts commit to terminal differentiation into myotubes [258;340]. Significantly, less ApoE3 was secreted from

cell cultures transfected with muscle-specific promoter-driven plasmids, which clearly implied that they were less active than the CAG promoter.

All ssAAV plasmids were then injected with or without electrotransfer into TA muscles of $ApoE^{-/-}$ mice. Unfortunately, after 1 week our assay methods did not detect ApoE3 in plasma of mice injected with p.CAG.ApoE3 or with the muscle-specific plasmids, p.CK6.ApoE3 and p.C512.ApoE3. In agreement, we found no evidence for reduced total cholesterol or for normalisation of the lipoprotein profile in mice 7 days after treatment with any of the ApoE3 expression plasmids. Though disappointing, these results were consistent with studies in $ApoE^{-/-}$ mice [325] and Yoshida Wistar rats [341] receiving non-electroporated intramuscular injections of naked plasmids expressing human ApoE2 or ApoE3. In both of these studies, the binding-defective ApoE2, but not ApoE3, was detected in plasma, although local expression of recombinant ApoE3 was measurable in the muscle. Likewise, we were able to measure local expression of human ApoE3 in excised muscles and this was markedly increased (50-fold) by electroporation, confirming previous reports that this technique significantly enhances plasmid transfer [342]. In agreement with our findings *in vitro*, the two plasmid vectors driven by the C512 and CK6 muscle-specific promoters appeared to produce much less ApoE3 protein (~ 0.5μg per muscle) than the CAG-driven plasmid (6-25μg).

These first *in vivo* experiments were conducted over just 1 week and it was, subsequently, hypothesised that a longer time period might be required to achieve maximum secretion of the protein from muscle. In chapter 4, we re-assessed electrotransfer of p.CAG.ApoE3 over a one month period; however, despite local expression in the muscle, ApoE3 remained undetectable in the plasma of treated animals. Furthermore, a direct comparison of 1 week muscle lysates, from animals previously injected with p.CAG.ApoE3, with the 4 week muscle lysates, clearly demonstrated a decline in the levels of ApoE3, suggesting that there had been plasmid loss or possibly silencing of gene expression. It was therefore concluded that plasmid-mediated ApoE3 transfer in skeletal muscle, is not sustainable and active secretion of the expressed protein will not be maintained over a prolonged period.

It was speculated that human ApoE3 secreted into plasma is rapidly cleared by the liver due to the excess of remnant lipoproteins in the plasma of $ApoE^{-/-}$ mice, which has previously been suggested following injection of ApoE3 protein [327;345].

Alternatively, recombinant ApoE3 could be successfully expressed by muscle, but the protein be inefficiently secreted, although this is unlikely as we readily measured ApoE3 protein in myotube culture medium following *in vitro* transfections, while *in vivo* skeletal muscle transduced with an ApoE3-expressing rAd vector secreted ApoE3 into plasma [312]. Nevertheless, failure to detect circulating levels of ApoE3 does not exclude long-term therapeutic benefits, as previous deliveries of ApoE3 by intramuscular plasmid injection [325] or by a cell-based platform [326] have demonstrated reductions in atherosclerotic aortic plaques, without measurable levels of ApoE3 in the plasma. However, the aim was to attain full therapeutic levels of plasma ApoE3 in order to achieve a reduction in total cholesterol, hence, we went on to try rAAV-mediated ApoE gene transfer.

6.2 Detectable levels of human ApoE3 in the plasma of ApoE$^{-/-}$ mice following intramuscular injection of the ssAAV2/7.CAG.ApoE3 vector

Chapter 4 described the construction, characterisation and the *in vitro* and *in vivo* evaluation of both ssAAV2/7 and scAAV2/7 vectors expressing human ApoE3. Western blot analysis demonstrated secretion of human ApoE3 into the medium of cultured myotubes infected with each viral preparation; thus, their functionality was verified. It was also evident from an ELISA that the ssAAV2/7.CAG.ApoE3 vector was more efficient *in vitro* than both ss and scAAV2/7 vectors driven by the muscle-specific promoters. This corroborated our previous findings (Chapter 3) for the C512 and CK6-driven plasmids, both of which produced markedly less ApoE3 *in vitro* and *in vivo*.

We next went on to inject the TA muscles of ApoE$^{-/-}$ mice with the ssAAV2/7.CAG.ApoE3 vector. Fortunately, in distinct contrast to the previous *in vivo* plasmid injections, ApoE3 was readily detected in the plasma as early as one week post-injection and the level steadily increased over time. This begs the question as to why ApoE3 is secreted from skeletal muscle following AAV, but not plasmid-mediated delivery? ApoE interacts strongly with glycosaminoglycans (GAGs) in cell-surface membranes and extracellular matrix [346], and it is conceivable that a threshold level of ApoE3 expression is needed to saturate such binding sites before efficient secretion occurs. Nevertheless, we have, ultimately, reinforced evidence showing the high tropism of serotype-7 for skeletal muscle, since an earlier study failed to detect ApoE3

in the plasma of ApoE$^{-/-}$ mice that had received i.m. injections of a rAAV serotype-2 vector [316]. Unfortunately, we did not observe a hypocholesterolaemic effect in our treated animals since the concentrations of circulating ApoE3 attained were just below the reported threshold level required to normalise plasma cholesterol. Nevertheless, our finding that skeletal muscle injected with ssAAV2/7.CAG.ApoE3 can secrete μg/ml quantities of ApoE3 is very encouraging and offers hope that an optimised rAAV vector will reverse hyperlipidaemia.

Chapter 4 also describes a direct comparison of the ssAAV2/7.CAG.ApoE3 vector with the CK6-driven scAAV2/7 vector in ApoE$^{-/-}$ mice. As before, mice that received intramuscular injections of ssAAV2/7.CAG.ApoE3 demonstrated detectable plasma ApoE3 levels, which were sustained in the plasma for 27 weeks. Levels, however, had declined slightly, suggesting that there may have been a humoral immune response directed against either the vector or the transgene. Unfortunately, we failed to detect ApoE3 in the plasma of scAAV2/7.CK6.ApoE3-treated animals and expression in muscle was very low. We were able to confirm that this observed vector inefficiency was not due to the scAAV vector but a result of the weak activity of the muscle-specific promoter, since both the ssAAV2/7.CK6.ApoE3 and scAAV2/7.C512.ApoE3 vectors equally failed to produce ApoE3 *in vivo*.

6.3 The transduction efficiencies of the ssAAV2/7 and ssAAV2/8 vectors in skeletal muscle show different patterns over time.

Chapter 5 describes a large-scale *in vivo* experiment directly comparing pseudotyped, CAG-driven ssAAV2/8 and 2/9 vectors with our previously tested ssAAV2/7.CAG.ApoE3 vector. The functionality of each vector was first confirmed *in vitro*, in both HEK 293-T cells and mature, differentiated myotubes. Secretion of human ApoE3 from both cell-types was discovered to be markedly higher following infection with ssAAV2/7.CAG.ApoE3. It was therefore inferred that *in vitro* gene transfer to muscle cells by AAV7 is more efficient than that by AAV8 and AAV9.

In vivo human ApoE3 was detected in the plasma of animals treated with each ssAAV vector, however, significantly lower levels were exhibited in ssAAV2/9.CAG.ApoE3-treated mice. In animals injected with ssAAV2/7.CAG.ApoE3 and ssAAV2/8.CAG.ApoE3, circulating ApoE3 was detected as early as 1 week and was sustained for the entire 13 week period. By 2 weeks, levels had markedly declined in

ssAAV2/7-treated mice, which was most likely due to ApoE3 being sequestered by the excess of remnant lipoproteins in the plasma and rapidly cleared by the liver. By contrast, the ssAAV2/8 vector appeared to be functioning much more efficiently at this early time-point as high ApoE3 levels were sustained, thus counteracting its rapid removal. The ssAAV2/7 vector, however, outperformed ssAAV2/8 at the later 13 week time-point; it was, therefore, speculated that transduction of the former vector in skeletal muscle is much slower.

Total plasma cholesterol and the atherosclerotic VLDL/IDL/LDL lipoproteins in ssAAV2/7-, ssAAV2/8- and ssAAV2/9-treated mice were not reduced after 13 weeks, despite there being detectable circulating levels of ApoE3 in these animals. A sharp decline in total cholesterol was observed at 4 weeks in the control and ssAAV2/8 and ssAAV2/9-treated animals, which suggests that alternative mechanisms for the hepatic uptake of remnant lipoproteins were initiated in response to their excessive accumulation in the plasma. However, when plasma ApoE3 levels in ssAAV2/7 and ssAAV2/8 animals were high, this decrease was prevented and total cholesterol appeared to either plateau or decline at 13 weeks. By contrast, low ApoE3 resulted in a marked increase in total cholesterol at termination. Although the small amount of ApoE3 secreted into the plasma of ssAAV2/7- and ssAAV2/8-treated animals was sufficient to inhibit the induction of SR-B1-mediated removal of remnant lipoproteins, it was insufficient to mediate effective clearance via LRP.

Plaque progression in the brachiocephalic artery was not attenuated in ssAAV2/7, 2/8 and 2/9-treated animals and no significant reductions in lumen and media size were observed. It was speculated that the rapid development of lesions in the brachiocephalic artery, under conditions of high-fat feeding, might be responsible for this outcome. ApoE has been shown to inhibit progression, rather than reverse established atherosclerotic plaques; therefore, it is conceivable that the small amount of ectopically expressed ApoE is overwhelmed by the challenge of such rapidly growing lesions.

6.4 Conclusions and future considerations

In summary, we have shown that plasmid-mediated ApoE3 gene transfer in skeletal muscle of $ApoE^{-/-}$ mice is not sustainable and active secretion of the expressed protein is unlikely to be maintained over a prolonged period. We concluded that a more efficient delivery vehicle is needed to exploit the benefits of ApoE3 gene therapeutics fully and

that although non-viral gene therapy has made substantial progress it still struggles to mimic the efficiency of recombinant viruses. We, therefore, went on to investigate rAAV-mediated ApoE3 gene transfer and found that by utilising serotypes with a high tropism for skeletal muscle (AAV7 and AAV8), we could enhance transduction efficiency and obtain measurable circulating levels. The concentration attained in the plasma, however, was not sufficient to ameliorate hypercholesterolaemia, thus we have clearly demonstrated that more than 2μg/ml of human ApoE3 is required to reduce total cholesterol. Plaque quantification by aortic *en face* lipid staining has previously shown that very low amounts of circulating ApoE can inhibit atherosclerotic lesion development. In our study, despite, observing higher plasma levels, we failed to see the same effect in the brachiocephalic artery. It could be speculated that lesion quantifiation in the brachiocephalic artery is less sensitive, however, plaque lipid content at this atherosclerotic site demonstrated a trend towards a reduction in ssAAV2/7- and ssAAV2/8-treated animals Our findings are somewhat negative in terms of treating hyperlipidaemia and atherosclerosis, however for the first time we have reported μg levels of circulating human ApoE3 following intramuscular injection of rAAV. This has given us the confidence that a further optimised AAV vector for muscle-based delivery would undoubtedly have long-term therapeutic effects.

There are several aspects of this current study that could be changed which may improve the results of future studies and there are ways in which the AAV vector itself could be modified to enhance ApoE3 gene transfer to the skeletal muscle. It is perhaps unadvisable to use $ApoE^{-/-}$ mice that have been fed a high-fat diet for only a short period before the start of the experiment, since this clearly masked the effects of plasma ApoE3 during the early stages of treatment. Rapid development of lesions in the brachiocephalic artery is also a consequence of this diet, thus we were unlikely to see an effect with low levels of circulating ApoE3. Ideally, we would carry out the experiment for a longer period, thus a high-fat diet would not be required. Although we must bear in mind that towards the end of the 13 week *in vivo* experiment plasma ApoE3 in ssAAV2/8-treated animals had significantly declined, suggesting that there may have been a humoral immune response directed against either the vector or the transgene. This could have been assessed by screening the plasma for antibodies against human ApoE and rAAV capsid proteins, and in future studies this should be a routine procedure. The possibility of an immune response ultimately highlights the importance of using muscle-specific promoters; sustained transgene expression may have been

achieved with our CK6 and C512-driven AAV vectors, had they proven to be more active in our preliminary *in vivo* experiments. Fortunately, novel, muscle-specific promoters with improved transduction efficiencies have recently been developed; these include the muscle creatine kinase/SV40 hybrid promoter which is reported to yield enhanced and long-term transgene expression [256], while a MHCK7 (α-myosin heavy-chain enhancer, creatine kinase 7) promoter was shown to direct high-level expression comparable to CMV and RSV (Rous sarcoma virus) promoters [364].

Another means by which we could improve ApoE expression in the skeletal muscle is by using the full-length human ApoE gene (5.8-kb, including 5'- and 3'-flanking regions) or a mini-gene in which introns 2 and 3 are deleted (3.4-kb); genomic-based transgenes are substantially more effective than cDNA-based vectors [377]. Unfortunately, in this study we were unable to take full advantage of the scAAV vector, due to the inefficiencies of our muscle-specific promoters. However, the new AAV serotypes 7 and 8 and a scAAV vector driven by either MHCK7 or MCK/SV40 appears an optimum combination to achieve sustained therapeutic levels of ApoE.

The general safety issues associated with other viral vectors, e.g. rAd, have driven our group and others to use rAAV as an alternative. This viral vector has emerged as an attractive candidate for gene transfer; firstly, because it does not appear to cause any human disease and, secondly, because it remains quiescent in the absence of helper virus. AAV is, thus, considered a safe and stable gene transfer vehicle and for these reasons continues to attract considerable interest. Our choice of using skeletal muscle as a platform for ApoE gene transfer is, however, more questionable since ApoE is naturally synthesised and secreted by the liver. Indeed, the majority of ApoE gene therapy studies have targeted the liver (Table 1-2). Nevertheless, there is clear evidence for the ability of muscle to secrete recombinant therapeutic proteins and this fully justifies the long-term goal of the current investigation: a single intramuscular injection as a safe, non-invasive and effective gene therapy protocol to supply atheroprotective plasma ApoE. Indirect support includes the efficient secretion of FIX [266], IL-12 [297], TIMP-4 [298], and IL-1Ra [299] proteins to therapeutic plasma levels, in some cases sustained for weeks, following either viral vector delivery to muscle or electrotransfer-mediated plasmid injections. There is also direct support that muscle is able to secrete ApoE, since injection of a rAd vector into the skeletal muscle of $ApoE^{-/-}$ mice produced measurable levels of human ApoE3 in the plasma [312].

Emerging evidence also suggests that ectopic expression of ApoE via the skeletal muscle is a safer option than liver-directed gene transfer. Muscle represents a non-invasive route for vector delivery, with only a single injection needed, and chromosomal integration of rAAV has not been detected following transduction of muscle, albeit only one study has yet assessed this possibility [181]. By contrast, in liver rAAV integration has been reported with a preference for transcriptionally active genes, although this occurs at a low frequency compared with episomal retention [180]. On the other hand, the sustained systemic expression of several therapeutic proteins after intramuscular administration of rAAV, has been limited by a neutralising antibody response. Examples include FIX [368], α_1-antitrypsin [378] and erythropoietin [347] and these responses were typically observed if a neo-antigen was expressed, such as a human protein in a mouse or a species-specific transgene product harbouring a mutation.

Further investigation revealed the generation of a local inflammatory immune response in AAV transduced muscle fibre. The response was specific to the transgene product and characterised by the activation of transgene-specific T-helper cells in the draining lymph nodes of the muscle. This was followed by an inflammatory immune response and clearance of transgene-expressing muscle fibres by $CD8^+$ T-cells [243]. More importantly, the inflammatory response was discovered to be vector dose-specific, which is consistent with a previous study in haemophilia dogs that suggested T- and B-cell activation at high levels of local FIX production in skeletal muscle [379]. This highlights the necessity for highly-efficient AAV vectors that produce adequate levels of secreted protein, as these abrogate the need for high vector doses. Notwithstanding, very high levels of systemic FIX transgene expression achieved by intramuscular injection of high-dose AAV1 vector is reported not to cause an immune response [205;380]. As with the liver, which promotes tolerance induction and sustained systemic transgene expression, it is possible that tolerogenic antigen presentation at sites outside the transduced muscle could be a factor for the observed stable expression.

A recent report has shown that hepatic AAV-mediated gene transfer in humans induces a $CD8^+$ T cell immune response directed against the AAV capsid, which is not observed in animals [381]. Capsid-derived peptides are presented by MHC class I molecules that then become targets for lysis by AAV capsid-specific $CD8^+$ T cells. Fortunately, the

muscle expresses only discreet levels of MHC class I molecules, while in the liver they are highly expressed, suggesting that AAV-mediated delivery to liver will be more toxic than to muscle. It may, however, be viewed that the benefits attained from the higher efficacy following AAV administration to the liver outweighs the disadvantage of increased toxicity. If the same efficiency could be achieved via the muscle, then the risks associated with the liver would appear higher and this would allow us to confidently advocate the muscle as a safer tissue to target for gene therapy.

Although the effectiveness of AAV vectors for muscle-based ApoE gene transfer can undoubtedly be improved, as I have discussed above, the results from liver-directed administration are most promising and encouraging; recent reports demonstrate sustained therapeutic levels of ApoE3 in plasma, which normalised the lipoprotein profile in $ApoE^{-/-}$ mice and completely prevented atherosclerosis after one year [318]. Alternative animal models, other than the $ApoE^{-/-}$ mouse, however are required to assess whether ApoE gene augmentation can be a generic treatment for hyperlipidaemia and atherosclerosis. Such models might include the $LDLR^{-/-}$ mouse, fat-fed hamsters or the Watanabe heritable-hyperlipidaemic rabbit, all of which could help evaluate treatment regimes. In some cases, for example, only low but sustained levels of plasma ApoE3 may be required in patients at an early age to protect against atherosclerosis and reverse hypercholesterolaemia, while high levels are possibly needed to regress established lesions. ApoE3 gene transfer might also be used as a short-term treatment to complement surgical procedures, such as coronary angioplasty for preventing restenosis and carotid endarterectomy for removing harmful plaque. A relatively narrow therapeutic range of plasma ApoE3, however, is required to achieve normolipidaemia, since very low levels will fail to ameliorate hyperlipidaemia, but supraphysiological concentrations promote hypertriglyceridaemia [152]. Ultimately, further research is needed to obtain optimal vectors for ApoE delivery, whether intramuscular or liver-targeted; however, in terms of bringing ApoE gene therapeutics into the clinic, we are now closer than ever.

References

[1] Murray,C.J. & Lopez,A.D. (1997) Global mortality, disability, and the contribution of risk factors: Global Burden of Disease Study. *Lancet*, **349,** 1436-1442.

[2] Ross,R. (1999) Atherosclerosis--an inflammatory disease. *N. Engl. J. Med.*, **340,** 115-126.

[3] Elkind,M.S. (2006) Inflammation, atherosclerosis, and stroke. *Neurologist.*, **12,** 140-148.

[4] Navab,M., Berliner,J.A., Watson,A.D., Hama,S.Y., Territo,M.C., Lusis,A.J., Shih,D.M., Van Lenten,B.J., Frank,J.S., Demer,L.L., Edwards,P.A., & Fogelman,A.M. (1996) The Yin and Yang of oxidation in the development of the fatty streak. A review based on the 1994 George Lyman Duff Memorial Lecture. *Arterioscler. Thromb. Vasc. Biol.*, **16,** 831-842.

[5] Cybulsky,M.I. & Gimbrone,M.A., Jr. (1991) Endothelial expression of a mononuclear leukocyte adhesion molecule during atherogenesis. *Science*, **251,** 788-791.

[6] Boring,L., Gosling,J., Cleary,M., & Charo,I.F. (1998) Decreased lesion formation in CCR2-/- mice reveals a role for chemokines in the initiation of atherosclerosis. *Nature*, **394,** 894-897.

[7] Qiao,J.H., Tripathi,J., Mishra,N.K., Cai,Y., Tripathi,S., Wang,X.P., Imes,S., Fishbein,M.C., Clinton,S.K., Libby,P., Lusis,A.J., & Rajavashisth,T.B. (1997) Role of macrophage colony-stimulating factor in atherosclerosis: studies of osteopetrotic mice. *Am. J. Pathol.*, **150,** 1687-1699.

[8] Glass,C.K. & Witztum,J.L. (2001) Atherosclerosis. the road ahead. *Cell*, **104,** 503-516.

[9] Nicholson,A.C. & Hajjar,D.P. (2004) CD36, oxidized LDL and PPAR gamma: pathological interactions in macrophages and atherosclerosis. *Vascul. Pharmacol.*, **41,** 139-146.

[10] Lusis,A.J., Mar,R., & Pajukanta,P. (2004) Genetics of atherosclerosis. *Annu. Rev. Genomics Hum. Genet.*, **5,** 189-218.

[11] Tabas,I. (2005) Consequences and therapeutic implications of macrophage apoptosis in atherosclerosis: the importance of lesion stage and phagocytic efficiency. *Arterioscler. Thromb. Vasc. Biol.*, **25,** 2255-2264.

[12] Boullier,A., Li,Y., Quehenberger,O., Palinski,W., Tabas,I., Witztum,J.L., & Miller,Y.I. (2006) Minimally oxidized LDL offsets the apoptotic effects of extensively oxidized LDL and free cholesterol in macrophages. *Arterioscler. Thromb. Vasc. Biol.*, **26,** 1169-1176.

[13] Kim,C.J., Khoo,J.C., Gillotte-Taylor,K., Li,A., Palinski,W., Glass,C.K., & Steinberg,D. (2000) Polymerase chain reaction-based method for quantifying recruitment of monocytes to mouse atherosclerotic lesions in vivo: enhancement by tumor necrosis factor-alpha and interleukin-1 beta. *Arterioscler. Thromb. Vasc. Biol.*, **20,** 1976-1982.

[14] Ohta,H., Wada,H., Niwa,T., Kirii,H., Iwamoto,N., Fujii,H., Saito,K., Sekikawa,K., & Seishima,M. (2005) Disruption of tumor necrosis factor-alpha gene diminishes the development of atherosclerosis in ApoE-deficient mice. *Atherosclerosis*, **180,** 11-17.

[15] Pinderski,L.J., Fischbein,M.P., Subbanagounder,G., Fishbein,M.C., Kubo,N., Cheroutre,H., Curtiss,L.K., Berliner,J.A., & Boisvert,W.A. (2002) Overexpression of interleukin-10 by activated T lymphocytes inhibits atherosclerosis in LDL receptor-deficient Mice by altering lymphocyte and macrophage phenotypes. *Circ. Res.*, **90,** 1064-1071.

[16] Robertson,A.K., Rudling,M., Zhou,X., Gorelik,L., Flavell,R.A., & Hansson,G.K. (2003) Disruption of TGF-beta signaling in T cells accelerates atherosclerosis. *J. Clin. Invest*, **112,** 1342-1350.

[17] Fazio,S. & Linton,M.F. (2001) The inflamed plaque: cytokine production and cellular cholesterol balance in the vessel wall. *Am. J. Cardiol.*, **88,** 12E-15E.

[18] Newby,A.C. (2005) Dual role of matrix metalloproteinases (matrixins) in intimal thickening and atherosclerotic plaque rupture. *Physiol Rev.*, **85,** 1-31.

[19] Johnson,J.L., Baker,A.H., Oka,K., Chan,L., Newby,A.C., Jackson,C.L., & George,S.J. (2006) Suppression of atherosclerotic plaque progression and instability by tissue inhibitor of metalloproteinase-2: involvement of macrophage migration and apoptosis. *Circulation*, **113,** 2435-2444.

[20] Lemaitre,V., O'Byrne,T.K., Borczuk,A.C., Okada,Y., Tall,A.R., & D'Armiento,J. (2001) ApoE knockout mice expressing human matrix metalloproteinase-1 in macrophages have less advanced atherosclerosis. *J. Clin. Invest*, **107,** 1227-1234.

[21] Cohn,E.J., Strong,L.E., Hughes,W.L., Mulford,D.J., Ashworth,J.N., Melin,M., & Taylor,H.L. (1946) Preparation and properties of serum and plasma proteins: IV. System for separation into fractions of protein and lipoprotein components of biological tissues and fluids. *J. Am. Chem. Soc.*, **68,** 459-475.

[22] Blix,G., Tiselius,A., & Svensson,H. (1941) Lipids and polysaccharides in electrophoretically separated blood serum proteins. *J. Biol. Chemistry*, **137,** 485-494.

[23] Gofman,J., Lindgren,F., & Elliot,H. (1949) Ultracentrifugal studies of lipoproteins of human serum. *J. Biol. Chem.*, **179,** 973-978.

[24] Brown,M.S. & Goldstein,J.L. (1986) A receptor-mediated pathway for cholesterol homeostasis. *Science*, **232,** 34-47.

[25] Innerarity,T.L. & Mahley,R.W. (1978) Enhanced binding by cultured human fibroblasts of apo-E-containing lipoproteins as compared with low density lipoproteins. *Biochemistry*, **17,** 1440-1447.

[26] Herz,J., Qiu,S.Q., Oesterle,A., DeSilva,H.V., Shafi,S., & Havel,R.J. (1995) Initial hepatic removal of chylomicron remnants is unaffected but endocytosis is delayed in mice lacking the low density lipoprotein receptor. *Proc. Natl. Acad. Sci. U. S. A*, **92,** 4611-4615.

[27] Utermann,G. (1989) The mysteries of lipoprotein(a). *Science*, **246,** 904-910.

[28] Wild,S.H., Fortmann,S.P., & Marcovina,S.M. (1997) A prospective case-control study of lipoprotein(a) levels and apo(a) size and risk of coronary heart disease in Stanford Five-City Project participants. *Arterioscler. Thromb. Vasc. Biol.*, **17,** 239-245.

[29] Green,P.H., Tall,A.R., & Glickman,R.M. (1978) Rat intestine secretes discoid high density lipoprotein. *J. Clin. Invest*, **61,** 528-534.

[30] Gordon,D.J. & Rifkind,B.M. (1989) High-density lipoprotein--the clinical implications of recent studies. *N. Engl. J. Med.*, **321,** 1311-1316.

[31] Brousseau,M.E. & Hoeg,J.M. (1999) Transgenic rabbits as models for atherosclerosis research. *J. Lipid Res.*, **40,** 365-375.

[32] Van Lenten,B.J., Navab,M., Shih,D., Fogelman,A.M., & Lusis,A.J. (2001) The role of high-density lipoproteins in oxidation and inflammation. *Trends Cardiovasc. Med.*, **11,** 155-161.

[33] Navab,M., Ananthramaiah,G.M., Reddy,S.T., Van Lenten,B.J., Ansell,B.J., Fonarow,G.C., Vahabzadeh,K., Hama,S., Hough,G., Kamranpour,N., Berliner,J.A., Lusis,A.J., & Fogelman,A.M. (2004) The oxidation hypothesis of atherogenesis: the role of oxidized phospholipids and HDL. *J. Lipid Res.*, **45,** 993-1007.

[34] Wang,N., Lan,D., Chen,W., Matsuura,F., & Tall,A.R. (2004) ATP-binding cassette transporters G1 and G4 mediate cellular cholesterol efflux to high-density lipoproteins. *Proc. Natl. Acad. Sci. U. S. A*, **101,** 9774-9779.

[35] Moore,R.E., Navab,M., Millar,J.S., Zimetti,F., Hama,S., Rothblat,G.H., & Rader,D.J. (2005) Increased atherosclerosis in mice lacking apolipoprotein A-I attributable to both impaired reverse cholesterol transport and increased inflammation. *Circ. Res.*, **97,** 763-771.

[36] Goldstein,J.L. & Brown,M.S. (1985) Familial hypercholesterolemia: a genetic receptor disease. *Hosp. Pract. (Off Ed)*, **20,** 35-36.

[37] Innerarity,T.L., Mahley,R.W., Weisgraber,K.H., Bersot,T.P., Krauss,R.M., Vega,G.L., Grundy,S.M., Friedl,W., Davignon,J., & McCarthy,B.J. (1990) Familial defective apolipoprotein B-100: a mutation of apolipoprotein B that causes hypercholesterolemia. *J. Lipid Res.*, **31,** 1337-1349.

[38] Pajukanta,P., Lilja,H.E., Sinsheimer,J.S., Cantor,R.M., Lusis,A.J., Gentile,M., Duan,X.J., Soro-Paavonen,A., Naukkarinen,J., Saarela,J., Laakso,M., Ehnholm,C., Taskinen,M.R., & Peltonen,L. (2004) Familial combined hyperlipidemia is associated with upstream transcription factor 1 (USF1). *Nat. Genet.*, **36,** 371-376.

[39] Sing,C.F. & Davignon,J. (1985) Role of the apolipoprotein E polymorphism in determining normal plasma lipid and lipoprotein variation. *Am. J. Hum. Genet.*, **37,** 268-285.

[40] Shore,V.G. & Shore,B. (1973) Heterogeneity of human plasma very low density lipoproteins. Separation of species differing in protein components. *Biochemistry*, **12,** 502-507.

[41] Elshourbagy,N.A., Liao,W.S., Mahley,R.W., & Taylor,J.M. (1985) Apolipoprotein E mRNA is abundant in the brain and adrenals, as well as in the liver, and is present in other peripheral tissues of rats and marmosets. *Proc. Natl. Acad. Sci. U. S. A*, **82,** 203-207.

[42] Myklebost,O. & Rogne,S. (1988) A physical map of the apolipoprotein gene cluster on human chromosome 19. *Hum. Genet.*, **78,** 244-247.

[43] Zannis,V.I., McPherson,J., Goldberger,G., Karathanasis,S.K., & Breslow,J.L. (1984) Synthesis, intracellular processing, and signal peptide of human apolipoprotein E. *J. Biol. Chem.*, **259,** 5495-5499.

[44] Zanni,E.E., Kouvatsi,A., Hadzopoulou-Cladaras,M., Krieger,M., & Zannis,V.I. (1989) Expression of ApoE gene in Chinese hamster cells with a reversible defect in O-glycosylation. Glycosylation is not required for apoE secretion. *J. Biol. Chem.*, **264,** 9137-9140.

[45] Auwerx,J.H., Deeb,S., Brunzell,J.D., Peng,R., & Chait,A. (1988) Transcriptional activation of the lipoprotein lipase and apolipoprotein E genes accompanies differentiation in some human macrophage-like cell lines. *Biochemistry*, **27,** 2651-2655.

[46] Basheeruddin,K., Rechtoris,C., & Mazzone,T. (1994) Evaluation of the role of Ap1-like proteins in the enhanced apolipoprotein E gene transcription accompanying phorbol ester induced macrophage differentiation. *Biochim. Biophys. Acta*, **1218,** 235-241.

[47] Duan,H., Gu,D., & Mazzone,T. (2000) Sterols and inhibitors of sterol transport modulate the degradation and secretion of macrophage ApoE: requirement for the C-terminal domain. *Biochim. Biophys. Acta*, **1484,** 142-150.

[48] Duan,H., Li,Z., & Mazzone,T. (1995) Tumor necrosis factor-alpha modulates monocyte/macrophage apoprotein E gene expression. *J. Clin. Invest*, **96,** 915-922.

[49] Zuckerman,S.H. & O'Neal,L. (1994) Endotoxin and GM-CSF-mediated down-regulation of macrophage apo E secretion is inhibited by a TNF-specific monoclonal antibody. *J. Leukoc. Biol.*, **55,** 743-748.

[50] Berg,D.T., Calnek,D.S., & Grinnell,B.W. (1996) Trans-repressor BEF-1 phosphorylation. A potential control mechanism for human ApoE gene regulation. *J. Biol. Chem.*, **271,** 4589-4592.

[51] Brand,K., Mackman,N., & Curtiss,L.K. (1993) Interferon-gamma inhibits macrophage apolipoprotein E production by posttranslational mechanisms. *J. Clin. Invest*, **91,** 2031-2039.

[52] Andreani-Mangeney,M., Vandenbrouck,Y., Janvier,B., Girlich,D., & Bereziat,G. (1996) Transcriptional regulation of apolipoprotein E expression by cyclic AMP. *FEBS Lett.*, **397,** 155-158.

[53] Artiga,M.J., Bullido,M.J., Sastre,I., Recuero,M., Garcia,M.A., Aldudo,J., Vazquez,J., & Valdivieso,F. (1998) Allelic polymorphisms in the transcriptional regulatory region of apolipoprotein E gene. *FEBS Lett.*, **421,** 105-108.

[54] Lambert,J.C., Brousseau,T., Defosse,V., Evans,A., Arveiler,D., Ruidavets,J.B., Haas,B., Cambou,J.P., Luc,G., Ducimetiere,P., Cambien,F., Chartier-Harlin,M.C., & Amouyel,P. (2000) Independent association of an APOE gene promoter polymorphism with increased risk of myocardial infarction and decreased APOE plasma concentrations-the ECTIM study. *Hum. Mol. Genet.*, **9,** 57-61.

[55] Allan,C.M., Taylor,S., & Taylor,J.M. (1997) Two hepatic enhancers, HCR.1 and HCR.2, coordinate the liver expression of the entire human apolipoprotein E/C-I/C-IV/C-II gene cluster. *J. Biol. Chem.*, **272,** 29113-29119.

[56] Shih,S.J., Allan,C., Grehan,S., Tse,E., Moran,C., & Taylor,J.M. (2000) Duplicated downstream enhancers control expression of the human apolipoprotein E gene in macrophages and adipose tissue. *J. Biol. Chem.*, **275,** 31567-31572.

[57] Laffitte,B.A., Repa,J.J., Joseph,S.B., Wilpitz,D.C., Kast,H.R., Mangelsdorf,D.J., & Tontonoz,P. (2001) LXRs control lipid-inducible expression of the apolipoprotein E gene in macrophages and adipocytes. *Proc. Natl. Acad. Sci. U. S. A*, **98,** 507-512.

[58] Deng,J., Rudick,V., & Dory,L. (1995) Lysosomal degradation and sorting of apolipoprotein E in macrophages. *J. Lipid Res.*, **36,** 2129-2140.

[59] Mazzone,T., Pustelnikas,L., & Reardon,C.A. (1992) Post-translational regulation of macrophage apoprotein E production. *J. Biol. Chem.*, **267,** 1081-1087.

[60] von Eckardstein,A., Langer,C., Engel,T., Schaukal,I., Cignarella,A., Reinhardt,J., Lorkowski,S., Li,Z., Zhou,X., Cullen,P., & Assmann,G. (2001) ATP binding cassette transporter ABCA1 modulates the secretion of apolipoprotein E from human monocyte-derived macrophages. *FASEB J.*, **15,** 1555-1561.

[61] Dory,L. (1991) Regulation of apolipoprotein E secretion by high density lipoprotein 3 in mouse macrophages. *J. Lipid Res.*, **32,** 783-792.

[62] Kockx,M., Rye,K.A., Gaus,K., Quinn,C.M., Wright,J., Sloane,T., Sviridov,D., Fu,Y., Sullivan,D., Burnett,J.R., Rust,S., Assmann,G., Anantharamaiah,G.M., Palgunachari,M.N., Katz,S.L., Phillips,M.C., Dean,R.T., Jessup,W., & Kritharides,L. (2004) Apolipoprotein A-I-stimulated apolipoprotein E secretion from human macrophages is independent of cholesterol efflux. *J. Biol. Chem.*, **279,** 25966-25977.

[63] Huang,Z.H., Gu,D., & Mazzone,T. (2004) Oleic acid modulates the post-translational glycosylation of macrophage ApoE to increase its secretion. *J. Biol. Chem.*, **279,** 29195-29201.

[64] Rensen,P.C., Jong,M.C., van Vark,L.C., van der,B.H., Hendriks,W.L., van Berkel,T.J., Biessen,E.A., & Havekes,L.M. (2000) Apolipoprotein E is resistant to intracellular degradation in vitro and in vivo. Evidence for retroendocytosis. *J. Biol. Chem.*, **275,** 8564-8571.

[65] Heeren,J., Weber,W., & Beisiegel,U. (1999) Intracellular processing of endocytosed triglyceride-rich lipoproteins comprises both recycling and degradation. *J. Cell Sci.*, **112 (Pt 3),** 349-359.

[66] Heeren,J., Grewal,T., Laatsch,A., Rottke,D., Rinninger,F., Enrich,C., & Beisiegel,U. (2003) Recycling of apoprotein E is associated with cholesterol efflux and high density lipoprotein internalization. *J. Biol. Chem.*, **278,** 14370-14378.

[67] Wilson,C., Wardell,M.R., Weisgraber,K.H., Mahley,R.W., & Agard,D.A. (1991) Three-dimensional structure of the LDL receptor-binding domain of human apolipoprotein E. *Science*, **252,** 1817-1822.

[68] Weisgraber,K.H., Rall,S.C., Jr., Mahley,R.W., Milne,R.W., Marcel,Y.L., & Sparrow,J.T. (1986) Human apolipoprotein E. Determination of the heparin binding sites of apolipoprotein E3. *J. Biol. Chem.*, **261,** 2068-2076.

[69] Thuahnai,S.T., Lund-Katz,S., Anantharamaiah,G.M., Williams,D.L., & Phillips,M.C. (2003) A quantitative analysis of apolipoprotein binding to SR-BI: multiple binding sites for lipid-free and lipid-associated apolipoproteins. *J. Lipid Res.*, **44,** 1132-1142.

[70] Segrest,J.P., Jones,M.K., De Loof,H., Brouillette,C.G., Venkatachalapathi,Y.V., & Anantharamaiah,G.M. (1992) The amphipathic helix in the exchangeable apolipoproteins: a review of secondary structure and function. *J. Lipid Res.*, **33,** 141-166.

[71] Raussens,V., Drury,J., Forte,T.M., Choy,N., Goormaghtigh,E., Ruysschaert,J.M., & Narayanaswami,V. (2005) Orientation and mode of lipid-binding interaction of human apolipoprotein E C-terminal domain. *Biochem. J.*, **387,** 747-754.

[72] Zannis,V.I., Just,P.W., & Breslow,J.L. (1981) Human apolipoprotein E isoprotein subclasses are genetically determined. *Am. J. Hum. Genet.*, **33,** 11-24.

[73] Weisgraber,K.H., Innerarity,T.L., & Mahley,R.W. (1982) Abnormal lipoprotein receptor-binding activity of the human E apoprotein due to cysteine-arginine interchange at a single site. *J. Biol. Chem.*, **257,** 2518-2521.

[74] Saito,H., Dhanasekaran,P., Baldwin,F., Weisgraber,K.H., Phillips,M.C., & Lund-Katz,S. (2003) Effects of polymorphism on the lipid interaction of human apolipoprotein E. *J. Biol. Chem.*, **278,** 40723-40729.

[75] Dong,L.M., Wilson,C., Wardell,M.R., Simmons,T., Mahley,R.W., Weisgraber,K.H., & Agard,D.A. (1994) Human apolipoprotein E. Role of arginine 61 in mediating the lipoprotein preferences of the E3 and E4 isoforms. *J. Biol. Chem.*, **269,** 22358-22365.

[76] Mahley,R.W. & Rall,S.C., Jr. (2000) Apolipoprotein E: far more than a lipid transport protein. *Annu. Rev. Genomics Hum. Genet.*, **1,** 507-537.

[77] Stengard,J.H., Weiss,K.M., & Sing,C.F. (1998) An ecological study of association between coronary heart disease mortality rates in men and the relative frequencies of common allelic variations in the gene coding for apolipoprotein E. *Hum. Genet.*, **103,** 234-241.

[78] Song,Y., Stampfer,M.J., & Liu,S. (2004) Meta-analysis: apolipoprotein E genotypes and risk for coronary heart disease. *Ann. Intern. Med.*, **141,** 137-147.

[79] Saunders,A.M., Strittmatter,W.J., Schmechel,D., George-Hyslop,P.H., Pericak-Vance,M.A., Joo,S.H., Rosi,B.L., Gusella,J.F., Crapper-MacLachlan,D.R., Alberts,M.J., & . (1993) Association of apolipoprotein E allele epsilon 4 with late-onset familial and sporadic Alzheimer's disease. *Neurology*, **43,** 1467-1472.

[80] Chou,C.Y., Lin,Y.L., Huang,Y.C., Sheu,S.Y., Lin,T.H., Tsay,H.J., Chang,G.G., & Shiao,M.S. (2004) Structural Variation in Human Apolipoprotein E3 and E4: Secondary Structure, Tertiary Structure, and Size Distribution. *Biophys. J.*.

[81] Mahley,R.W. & Ji,Z.S. (1999) Remnant lipoprotein metabolism: key pathways involving cell-surface heparan sulfate proteoglycans and apolipoprotein E. *J. Lipid Res.*, **40,** 1-16.

[82] Kuipers,F., Jong,M.C., Lin,Y., Eck,M., Havinga,R., Bloks,V., Verkade,H.J., Hofker,M.H., Moshage,H., Berkel,T.J., Vonk,R.J., & Havekes,L.M. (1997) Impaired secretion of very low density lipoprotein-triglycerides by apolipoprotein E- deficient mouse hepatocytes. *J. Clin. Invest*, **100**, 2915-2922.

[83] De Pauw,M., Vanloo,B., Weisgraber,K., & Rosseneu,M. (1995) Comparison of lipid-binding and lecithin:cholesterol acyltransferase activation of the amino- and carboxyl-terminal domains of human apolipoprotein E3. *Biochemistry*, **34**, 10953-10966.

[84] Kinoshita,M., Arai,H., Fukasawa,M., Watanabe,T., Tsukamoto,K., Hashimoto,Y., Inoue,K., Kurokawa,K., & Teramoto,T. (1993) Apolipoprotein E enhances lipid exchange between lipoproteins mediated by cholesteryl ester transfer protein. *J. Lipid Res.*, **34**, 261-268.

[85] Thuren,T., Weisgraber,K.H., Sisson,P., & Waite,M. (1992) Role of apolipoprotein E in hepatic lipase catalyzed hydrolysis of phospholipid in high-density lipoproteins. *Biochemistry*, **31**, 2332-2338.

[86] Huang,Y., von Eckardstein,A., Wu,S., Maeda,N., & Assmann,G. (1994) A plasma lipoprotein containing only apolipoprotein E and with gamma mobility on electrophoresis releases cholesterol from cells. *Proc. Natl. Acad. Sci. U. S. A*, **91**, 1834-1838.

[87] Hayek,T., Oiknine,J., Brook,J.G., & Aviram,M. (1994) Role of HDL apolipoprotein E in cellular cholesterol efflux: studies in apo E knockout transgenic mice. *Biochem. Biophys. Res. Commun.*, **205**, 1072-1078.

[88] Cullen,P., Cignarella,A., Brennhausen,B., Mohr,S., Assmann,G., & von Eckardstein,A. (1998) Phenotype-dependent differences in apolipoprotein E metabolism and in cholesterol homeostasis in human monocyte-derived macrophages. *J. Clin. Invest*, **101**, 1670-1677.

[89] Mazzone,T. & Reardon,C. (1994) Expression of heterologous human apolipoprotein E by J774 macrophages enhances cholesterol efflux to HDL3. *J. Lipid Res.*, **35**, 1345-1353.

[90] Krimbou,L., Denis,M., Haidar,B., Carrier,M., Marcil,M., & Genest,J., Jr. (2004) Molecular interactions between apoE and ABCA1: impact on apoE lipidation. *J. Lipid Res.*, **45**, 839-848.

[91] Lin,C.Y., Huang,Z.H., & Mazzone,T. (2001) Interaction with proteoglycans enhances the sterol efflux produced by endogenous expression of macrophage apoE. *J. Lipid Res.*, **42**, 1125-1133.

[92] Huang,Z.H., Lin,C.Y., Oram,J.F., & Mazzone,T. (2001) Sterol efflux mediated by endogenous macrophage ApoE expression is independent of ABCA1. *Arterioscler. Thromb. Vasc. Biol.*, **21**, 2019-2025.

[93] Huang,Z.H., Fitzgerald,M.L., & Mazzone,T. (2006) Distinct cellular loci for the ABCA1-dependent and ABCA1-independent lipid efflux mediated by endogenous apolipoprotein E expression. *Arterioscler. Thromb. Vasc. Biol.*, **26**, 157-162.

[94] Curtiss,L.K., Valenta,D.T., Hime,N.J., & Rye,K.A. (2006) What is so special about apolipoprotein AI in reverse cholesterol transport? *Arterioscler. Thromb. Vasc. Biol.*, **26**, 12-19.

[95] Shimano,H., Ohsuga,J., Shimada,M., Namba,Y., Gotoda,T., Harada,K., Katsuki,M., Yazaki,Y., & Yamada,N. (1995) Inhibition of diet-induced atheroma formation in transgenic mice expressing apolipoprotein E in the arterial wall. *J. Clin. Invest*, **95**, 469-476.

[96] Thorngate,F.E., Rudel,L.L., Walzem,R.L., & Williams,D.L. (2000) Low levels of extrahepatic nonmacrophage ApoE inhibit atherosclerosis without correcting hypercholesterolemia in ApoE-deficient mice. *Arterioscler. Thromb. Vasc. Biol.*, **20**, 1939-1945.

[97] Raffai,R.L., Loeb,S.M., & Weisgraber,K.H. (2005) Apolipoprotein E promotes the regression of atherosclerosis independently of lowering plasma cholesterol levels. *Arterioscler. Thromb. Vasc. Biol.*, **25**, 436-441.

[98] Rosenfeld,M.E., Butler,S., Ord,V.A., Lipton,B.A., Dyer,C.A., Curtiss,L.K., Palinski,W., & Witztum,J.L. (1993) Abundant expression of apoprotein E by macrophages in human and rabbit atherosclerotic lesions. *Arterioscler. Thromb.*, **13,** 1382-1389.

[99] Desai,K., Bruckdorfer,K.R., Hutton,R.A., & Owen,J.S. (1989) Binding of apoE-rich high density lipoprotein particles by saturable sites on human blood platelets inhibits agonist-induced platelet aggregation. *J. Lipid Res.*, **30,** 831-840.

[100] Desai,K., Mistry,P., Bagget,C., Burroughs,A.K., Bellamy,M.F., & Owen,J.S. (1989) Inhibition of platelet aggregation by abnormal high density lipoprotein particles in plasma from patients with hepatic cirrhosis. *Lancet*, **1,** 693-695.

[101] Riddell,D.R., Graham,A., & Owen,J.S. (1997) Apolipoprotein E inhibits platelet aggregation through the L-arginine:nitric oxide pathway. Implications for vascular disease. *J. Biol. Chem.*, **272,** 89-95.

[102] Riddell,D.R., Vinogradov,D.V., Stannard,A.K., Chadwick,N., & Owen,J.S. (1999) Identification and characterization of LRP8 (apoER2) in human blood platelets. *J. Lipid Res.*, **40,** 1925-1930.

[103] Stannard,A.K., Riddell,D.R., Sacre,S.M., Tagalakis,A.D., Langer,C., von Eckardstein,A., Cullen,P., Athanasopoulos,T., Dickson,G., & Owen,J.S. (2001) Cell-derived apolipoprotein E (ApoE) particles inhibit vascular cell adhesion molecule-1 (VCAM-1) expression in human endothelial cells. *J. Biol. Chem.*, **276,** 46011-46016.

[104] Ali,K., Middleton,M., Pure,E., & Rader,D.J. (2005) Apolipoprotein E suppresses the type I inflammatory response in vivo. *Circ. Res.*, **97,** 922-927.

[105] van den,E.P., Garg,S., Leon,L., Brigl,M., Leadbetter,E.A., Gumperz,J.E., Dascher,C.C., Cheng,T.Y., Sacks,F.M., Illarionov,P.A., Besra,G.S., Kent,S.C., Moody,D.B., & Brenner,M.B. (2005) Apolipoprotein-mediated pathways of lipid antigen presentation. *Nature*, **437,** 906-910.

[106] Swertfeger,D.K., Bu,G., & Hui,D.Y. (2002) Low density lipoprotein receptor-related protein mediates apolipoprotein E inhibition of smooth muscle cell migration. *J. Biol. Chem.*, **277,** 4141-4146.

[107] Zhu,Y. & Hui,D.Y. (2003) Apolipoprotein E binding to low density lipoprotein receptor-related protein-1 inhibits cell migration via activation of cAMP-dependent protein kinase A. *J. Biol. Chem.*, **278,** 36257-36263.

[108] Swertfeger,D.K. & Hui,D.Y. (2001) Apolipoprotein E receptor binding versus heparan sulfate proteoglycan binding in its regulation of smooth muscle cell migration and proliferation. *J. Biol. Chem.*, **276,** 25043-25048.

[109] Ishigami,M., Swertfeger,D.K., Hui,M.S., Granholm,N.A., & Hui,D.Y. (2000) Apolipoprotein E inhibition of vascular smooth muscle cell proliferation but not the inhibition of migration is mediated through activation of inducible nitric oxide synthase. *Arterioscler. Thromb. Vasc. Biol.*, **20,** 1020-1026.

[110] Miyata,M. & Smith,J.D. (1996) Apolipoprotein E allele-specific antioxidant activity and effects on cytotoxicity by oxidative insults and beta-amyloid peptides. *Nat. Genet.*, **14,** 55-61.

[111] Pham,T., Kodvawala,A., & Hui,D.Y. (2005) The receptor binding domain of apolipoprotein E is responsible for its antioxidant activity. *Biochemistry*, **44,** 7577-7582.

[112] Grainger,D.J., Reckless,J., & McKilligin,E. (2004) Apolipoprotein E modulates clearance of apoptotic bodies in vitro and in vivo, resulting in a systemic proinflammatory state in apolipoprotein E-deficient mice. *J. Immunol.*, **173,** 6366-6375.

[113] Chen,Y.C., Pohl,G., Wang,T.L., Morin,P.J., Risberg,B., Kristensen,G.B., Yu,A., Davidson,B., & Shih,I. (2005) Apolipoprotein E is required for cell proliferation and survival in ovarian cancer. *Cancer Res.*, **65,** 331-337.

[114] Saxena,U., Ferguson,E., & Bisgaier,C.L. (1993) Apolipoprotein E modulates low density lipoprotein retention by lipoprotein lipase anchored to the subendothelial matrix. *J. Biol. Chem.*, **268,** 14812-14819.

[115] Skalen,K., Gustafsson,M., Rydberg,E.K., Hulten,L.M., Wiklund,O., Innerarity,T.L., & Boren,J. (2002) Subendothelial retention of atherogenic lipoproteins in early atherosclerosis. *Nature*, **417,** 750-754.

[116] Lusis,A.J. (1988) Genetic factors affecting blood lipoproteins: the candidate gene approach. *J. Lipid Res.*, **29,** 397-429.

[117] Piedrahita,J.A., Zhang,S.H., Hagaman,J.R., Oliver,P.M., & Maeda,N. (1992) Generation of mice carrying a mutant apolipoprotein E gene inactivated by gene targeting in embryonic stem cells. *Proc. Natl. Acad. Sci. U. S. A*, **89,** 4471-4475.

[118] Plump,A.S., Smith,J.D., Hayek,T., Aalto-Setala,K., Walsh,A., Verstuyft,J.G., Rubin,E.M., & Breslow,J.L. (1992) Severe hypercholesterolemia and atherosclerosis in apolipoprotein E-deficient mice created by homologous recombination in ES cells. *Cell*, **71,** 343-353.

[119] Schaefer,E.J., Gregg,R.E., Ghiselli,G., Forte,T.M., Ordovas,J.M., Zech,L.A., & Brewer,H.B., Jr. (1986) Familial apolipoprotein E deficiency. *J. Clin. Invest*, **78,** 1206-1219.

[120] Reddick,R.L., Zhang,S.H., & Maeda,N. (1994) Atherosclerosis in mice lacking apo E. Evaluation of lesional development and progression. *Arterioscler. Thromb.*, **14,** 141-147.

[121] Getz,G.S. & Reardon,C.A. (2006) Diet and murine atherosclerosis. *Arterioscler. Thromb. Vasc. Biol.*, **26,** 242-249.

[122] Nakashima,Y., Plump,A.S., Raines,E.W., Breslow,J.L., & Ross,R. (1994) ApoE-deficient mice develop lesions of all phases of atherosclerosis throughout the arterial tree. *Arterioscler. Thromb.*, **14,** 133-140.

[123] Johnson,J.L. & Jackson,C.L. (2001) Atherosclerotic plaque rupture in the apolipoprotein E knockout mouse. *Atherosclerosis*, **154,** 399-406.

[124] Calara,F., Silvestre,M., Casanada,F., Yuan,N., Napoli,C., & Palinski,W. (2001) Spontaneous plaque rupture and secondary thrombosis in apolipoprotein E-deficient and LDL receptor-deficient mice. *J. Pathol.*, **195,** 257-263.

[125] Williams,H., Johnson,J.L., Carson,K.G., & Jackson,C.L. (2002) Characteristics of intact and ruptured atherosclerotic plaques in brachiocephalic arteries of apolipoprotein E knockout mice. *Arterioscler. Thromb. Vasc. Biol.*, **22,** 788-792.

[126] Johnson,J., Carson,K., Williams,H., Karanam,S., Newby,A., Angelini,G., George,S., & Jackson,C. (2005) Plaque rupture after short periods of fat feeding in the apolipoprotein E-knockout mouse: model characterization and effects of pravastatin treatment. *Circulation*, **111,** 1422-1430.

[127] Anant,S., Blanc,V., & Davidson,N.O. (2003) Molecular regulation, evolutionary, and functional adaptations associated with C to U editing of mammalian apolipoproteinB mRNA. *Prog. Nucleic Acid Res. Mol. Biol.*, **75,** 1-41.

[128] Greeve,J., Altkemper,I., Dieterich,J.H., Greten,H., & Windler,E. (1993) Apolipoprotein B mRNA editing in 12 different mammalian species: hepatic expression is reflected in low concentrations of apoB-containing plasma lipoproteins. *J. Lipid Res.*, **34,** 1367-1383.

[129] Hofker,M.H., van Vlijmen,B.J., & Havekes,L.M. (1998) Transgenic mouse models to study the role of APOE in hyperlipidemia and atherosclerosis. *Atherosclerosis*, **137,** 1-11.

[130] Veniant,M.M., Pierotti,V., Newland,D., Cham,C.M., Sanan,D.A., Walzem,R.L., & Young,S.G. (1997) Susceptibility to atherosclerosis in mice expressing exclusively apolipoprotein B48 or apolipoprotein B100. *J. Clin. Invest*, **100,** 180-188.

[131] Itskovich,V.V., Choudhury,R.P., Aguinaldo,J.G., Fallon,J.T., Omerhodzic,S., Fisher,E.A., & Fayad,Z.A. (2003) Characterization of aortic root atherosclerosis in ApoE knockout mice: high-resolution in vivo and ex vivo MRM with histological correlation. *Magn Reson. Med.*, **49,** 381-385.

[132] Lutgens,E., Faber,B., Schapira,K., Evelo,C.T., van Haaften,R., Heeneman,S., Cleutjens,K.B., Bijnens,A.P., Beckers,L., Porter,J.G., Mackay,C.R., Rennert,P., Bailly,V., Jarpe,M., Dolinski,B., Koteliansky,V., de Fougerolles,T., & Daemen,M.J. (2005) Gene profiling in atherosclerosis reveals a key role for small inducible cytokines: validation using a novel monocyte chemoattractant protein monoclonal antibody. *Circulation*, **111,** 3443-3452.

[133] Meir,K.S. & Leitersdorf,E. (2004) Atherosclerosis in the apolipoprotein E-deficient mouse: a decade of progress. *Arterioscler. Thromb. Vasc. Biol.*, **24,** 1006-1014.

[134] van den Maagdenberg,A.M., Hofker,M.H., Krimpenfort,P.J., de,B., I, van Vlijmen,B., van der,B.H., Havekes,L.M., & Frants,R.R. (1993) Transgenic mice carrying the apolipoprotein E3-Leiden gene exhibit hyperlipoproteinemia. *J. Biol. Chem.*, **268,** 10540-10545.

[135] van Vlijmen,B.J., van den Maagdenberg,A.M., Gijbels,M.J., van der,B.H., HogenEsch,H., Frants,R.R., Hofker,M.H., & Havekes,L.M. (1994) Diet-induced hyperlipoproteinemia and atherosclerosis in apolipoprotein E3-Leiden transgenic mice. *J. Clin. Invest*, **93,** 1403-1410.

[136] Knouff,C., Hinsdale,M.E., Mezdour,H., Altenburg,M.K., Watanabe,M., Quarfordt,S.H., Sullivan,P.M., & Maeda,N. (1999) Apo E structure determines VLDL clearance and atherosclerosis risk in mice. *J. Clin. Invest*, **103,** 1579-1586.

[137] Sullivan,P.M., Mezdour,H., Aratani,Y., Knouff,C., Najib,J., Reddick,R.L., Quarfordt,S.H., & Maeda,N. (1997) Targeted replacement of the mouse apolipoprotein E gene with the common human APOE3 allele enhances diet-induced hypercholesterolemia and atherosclerosis. *J. Biol. Chem.*, **272,** 17972-17980.

[138] Sullivan,P.M., Mezdour,H., Quarfordt,S.H., & Maeda,N. (1998) Type III hyperlipoproteinemia and spontaneous atherosclerosis in mice resulting from gene replacement of mouse Apoe with human Apoe*2. *J. Clin. Invest*, **102,** 130-135.

[139] Hinsdale,M.E., Sullivan,P.M., Mezdour,H., & Maeda,N. (2002) ApoB-48 and apoB-100 differentially influence the expression of type-III hyperlipoproteinemia in APOE*2 mice. *J. Lipid Res.*, **43,** 1520-1528.

[140] Knouff,C., Malloy,S., Wilder,J., Altenburg,M.K., & Maeda,N. (2001) Doubling expression of the low density lipoprotein receptor by truncation of the 3'-untranslated region sequence ameliorates type iii hyperlipoproteinemia in mice expressing the human apoe2 isoform. *J. Biol. Chem.*, **276,** 3856-3862.

[141] Havel,R.J. & Hamilton,R.L. (2004) Hepatic catabolism of remnant lipoproteins: where the action is. *Arterioscler. Thromb. Vasc. Biol.*, **24,** 213-215.

[142] Yamada,N., Inoue,I., Kawamura,M., Harada,K., Watanabe,Y., Shimano,H., Gotoda,T., Shimada,M., Kohzaki,K., Tsukada,T., & . (1992) Apolipoprotein E prevents the progression of atherosclerosis in Watanabe heritable hyperlipidemic rabbits. *J. Clin. Invest*, **89,** 706-711.

[143] Shimano,H., Yamada,N., Katsuki,M., Shimada,M., Gotoda,T., Harada,K., Murase,T., Fukazawa,C., Takaku,F., & Yazaki,Y. (1992) Overexpression of apolipoprotein E in transgenic mice: marked reduction in plasma lipoproteins except high density lipoprotein and resistance against diet-induced hypercholesterolemia. *Proc. Natl. Acad. Sci. U. S. A*, **89,** 1750-1754.

[144] Yamamoto,K., Shimano,H., Shimada,M., Kawamura,M., Gotoda,T., Harada,K., Ohsuga,J., Yazaki,Y., & Yamada,N. (1995) Overexpression of apolipoprotein E prevents development of diabetic hyperlipidemia in transgenic mice. *Diabetes*, **44,** 580-585.

[145] Nikoulin,I.R. & Curtiss,L.K. (1998) An apolipoprotein E synthetic peptide targets to lipoproteins in plasma and mediates both cellular lipoprotein interactions in vitro and acute clearance of cholesterol-rich lipoproteins in vivo. *J. Clin. Invest*, **101**, 223-234.

[146] Gupta,H., White,C.R., Handattu,S., Garber,D.W., Datta,G., Chaddha,M., Dai,L., Gianturco,S.H., Bradley,W.A., & Anantharamaiah,G.M. (2005) Apolipoprotein E mimetic Peptide dramatically lowers plasma cholesterol and restores endothelial function in watanabe heritable hyperlipidemic rabbits. *Circulation*, **111**, 3112-3118.

[147] Bellosta,S., Mahley,R.W., Sanan,D.A., Murata,J., Newland,D.L., Taylor,J.M., & Pitas,R.E. (1995) Macrophage-specific expression of human apolipoprotein E reduces atherosclerosis in hypercholesterolemic apolipoprotein E-null mice. *J. Clin. Invest*, **96**, 2170-2179.

[148] Linton,M.F., Atkinson,J.B., & Fazio,S. (1995) Prevention of atherosclerosis in apolipoprotein E-deficient mice by bone marrow transplantation. *Science*, **267**, 1034-1037.

[149] Shi,W., Wang,X., Wang,N.J., McBride,W.H., & Lusis,A.J. (2000) Effect of macrophage-derived apolipoprotein E on established atherosclerosis in apolipoprotein E-deficient mice. *Arterioscler. Thromb. Vasc. Biol.*, **20**, 2261-2266.

[150] Huang,Y., Liu,X.Q., Rall,S.C., Jr., Taylor,J.M., von Eckardstein,A., Assmann,G., & Mahley,R.W. (1998) Overexpression and accumulation of apolipoprotein E as a cause of hypertriglyceridemia. *J. Biol. Chem.*, **273**, 26388-26393.

[151] Kypreos,K.E., Teusink,B., Van Dijk,K.W., Havekes,L.M., & Zannis,V.I. (2001) Analysis of the structure and function relationship of the human apolipoprotein E in vivo, using adenovirus-mediated gene transfer. *FASEB J.*, **15**, 1598-1600.

[152] Kypreos,K.E., van Dijk,K.W., Havekes,L.M., & Zannis,V.I. (2005) Generation of a Recombinant Apolipoprotein E Variant with Improved Biological Functions: HYDROPHOBIC RESIDUES (LEU-261, TRP-264, PHE-265, LEU-268, VAL-269) OF apoE CAN ACCOUNT FOR THE apoE-INDUCED HYPERTRIGLYCERIDEMIA. *J. Biol. Chem.*, **280**, 6276-6284.

[153] Kypreos,K.E. & Zannis,V.I. (2006) LDL receptor deficiency or apoE mutations prevent remnant clearance and induce hypertriglyceridemia in mice. *J. Lipid Res.*, **47**, 521-529.

[154] Kay,M.A., Glorioso,J.C., & Naldini,L. (2001) Viral vectors for gene therapy: the art of turning infectious agents into vehicles of therapeutics. *Nat. Med.*, **7**, 33-40.

[155] Thomas,C.E., Ehrhardt,A., & Kay,M.A. (2003) Progress and problems with the use of viral vectors for gene therapy. *Nat. Rev. Genet.*, **4**, 346-358.

[156] Hacein-Bey-Abina,S., Le Deist,F., Carlier,F., Bouneaud,C., Hue,C., De Villartay,J.P., Thrasher,A.J., Wulffraat,N., Sorensen,R., Dupuis-Girod,S., Fischer,A., Davies,E.G., Kuis,W., Leiva,L., & Cavazzana-Calvo,M. (2002) Sustained correction of X-linked severe combined immunodeficiency by ex vivo gene therapy. *N. Engl. J. Med.*, **346**, 1185-1193.

[157] Hacein-Bey-Abina,S., von Kalle,C., Schmidt,M., Le Deist,F., Wulffraat,N., McIntyre,E., Radford,I., Villeval,J.L., Fraser,C.C., Cavazzana-Calvo,M., & Fischer,A. (2003) A serious adverse event after successful gene therapy for X-linked severe combined immunodeficiency. *N. Engl. J. Med.*, **348**, 255-256.

[158] Hacein-Bey-Abina,S., von Kalle,C., Schmidt,M., McCormack,M.P., Wulffraat,N., Leboulch,P., Lim,A., Osborne,C.S., Pawliuk,R., Morillon,E., Sorensen,R., Forster,A., Fraser,P., Cohen,J.I., de Saint,B.G., Alexander,I., Wintergerst,U., Frebourg,T., Aurias,A., Stoppa-Lyonnet,D., Romana,S., Radford-Weiss,I., Gross,F., Valensi,F., Delabesse,E., Macintyre,E., Sigaux,F., Soulier,J., Leiva,L.E., Wissler,M., Prinz,C., Rabbitts,T.H., Le Deist,F., Fischer,A., & Cavazzana-Calvo,M. (2003) LMO2-associated clonal T cell proliferation in two patients after gene therapy for SCID-X1. *Science*, **302**, 415-419.

[159] Blesch,A. (2004) Lentiviral and MLV based retroviral vectors for ex vivo and in vivo gene transfer. *Methods*, **33,** 164-172.

[160] Carlotti,F., Bazuine,M., Kekarainen,T., Seppen,J., Pognonec,P., Maassen,J.A., & Hoeben,R.C. (2004) Lentiviral vectors efficiently transduce quiescent mature 3T3-L1 adipocytes. *Mol. Ther.*, **9,** 209-217.

[161] Kordower,J.H., Emborg,M.E., Bloch,J., Ma,S.Y., Chu,Y., Leventhal,L., McBride,J., Chen,E.Y., Palfi,S., Roitberg,B.Z., Brown,W.D., Holden,J.E., Pyzalski,R., Taylor,M.D., Carvey,P., Ling,Z., Trono,D., Hantraye,P., Deglon,N., & Aebischer,P. (2000) Neurodegeneration prevented by lentiviral vector delivery of GDNF in primate models of Parkinson's disease. *Science*, **290,** 767-773.

[162] Kobinger,G.P., Louboutin,J.P., Barton,E.R., Sweeney,H.L., & Wilson,J.M. (2003) Correction of the dystrophic phenotype by in vivo targeting of muscle progenitor cells. *Hum. Gene Ther.*, **14,** 1441-1449.

[163] Kobayashi,H., Carbonaro,D., Pepper,K., Petersen,D., Ge,S., Jackson,H., Shimada,H., Moats,R., & Kohn,D.B. (2005) Neonatal gene therapy of MPS I mice by intravenous injection of a lentiviral vector. *Mol. Ther.*, **11,** 776-789.

[164] Dodart,J.C., Marr,R.A., Koistinaho,M., Gregersen,B.M., Malkani,S., Verma,I.M., & Paul,S.M. (2005) Gene delivery of human apolipoprotein E alters brain Abeta burden in a mouse model of Alzheimer's disease. *Proc. Natl. Acad. Sci. U. S. A*, **102,** 1211-1216.

[165] Shen,Y. & Nemunaitis,J. (2006) Herpes simplex virus 1 (HSV-1) for cancer treatment. *Cancer Gene Ther.*, **13,** 975-992.

[166] Burton,E.A., Fink,D.J., & Glorioso,J.C. (2002) Gene delivery using herpes simplex virus vectors. *DNA Cell Biol.*, **21,** 915-936.

[167] Palmer,J.A., Branston,R.H., Lilley,C.E., Robinson,M.J., Groutsi,F., Smith,J., Latchman,D.S., & Coffin,R.S. (2000) Development and optimization of herpes simplex virus vectors for multiple long-term gene delivery to the peripheral nervous system. *J. Virol.*, **74,** 5604-5618.

[168] Wakimoto,H., Johnson,P.R., Knipe,D.M., & Chiocca,E.A. (2003) Effects of innate immunity on herpes simplex virus and its ability to kill tumor cells. *Gene Ther.*, **10,** 983-990.

[169] Wood,M.J., Byrnes,A.P., Rabkin,S.D., Pfaff,D.W., & Charlton,H.M. (1994) Immunological consequences of HSV-1-mediated gene transfer into the CNS. *Gene Ther.*, **1 Suppl 1,** S82.

[170] Amalfitano,A., Hauser,M.A., Hu,H., Serra,D., Begy,C.R., & Chamberlain,J.S. (1998) Production and characterization of improved adenovirus vectors with the E1, E2b, and E3 genes deleted. *J. Virol.*, **72,** 926-933.

[171] Hu,H., Serra,D., & Amalfitano,A. (1999) Persistence of an [E1-, polymerase-] adenovirus vector despite transduction of a neoantigen into immune-competent mice. *Hum. Gene Ther.*, **10,** 355-364.

[172] Alba,R., Bosch,A., & Chillon,M. (2005) Gutless adenovirus: last-generation adenovirus for gene therapy. *Gene Ther.*, **12 Suppl 1,** S18-S27.

[173] Kim,I.H., Jozkowicz,A., Piedra,P.A., Oka,K., & Chan,L. (2001) Lifetime correction of genetic deficiency in mice with a single injection of helper-dependent adenoviral vector. *Proc. Natl. Acad. Sci. U. S. A*, **98,** 13282-13287.

[174] Schiedner,G., Morral,N., Parks,R.J., Wu,Y., Koopmans,S.C., Langston,C., Graham,F.L., Beaudet,A.L., & Kochanek,S. (1998) Genomic DNA transfer with a high-capacity adenovirus vector results in improved in vivo gene expression and decreased toxicity. *Nat. Genet.*, **18,** 180-183.

[175] Schiedner,G., Hertel,S., Johnston,M., Biermann,V., Dries,V., & Kochanek,S. (2002) Variables affecting in vivo performance of high-capacity adenovirus vectors. *J. Virol.*, **76,** 1600-1609.

[176] Samulski,R.J., Zhu,X., Xiao,X., Brook,J.D., Housman,D.E., Epstein,N., & Hunter,L.A. (1991) Targeted integration of adeno-associated virus (AAV) into human chromosome 19. *EMBO J.*, **10,** 3941-3950.

[177] Duan,D., Sharma,P., Yang,J., Yue,Y., Dudus,L., Zhang,Y., Fisher,K.J., & Engelhardt,J.F. (1998) Circular intermediates of recombinant adeno-associated virus have defined structural characteristics responsible for long-term episomal persistence in muscle tissue. *J. Virol.*, **72,** 8568-8577.

[178] Nakai,H., Yant,S.R., Storm,T.A., Fuess,S., Meuse,L., & Kay,M.A. (2001) Extrachromosomal recombinant adeno-associated virus vector genomes are primarily responsible for stable liver transduction in vivo. *J. Virol.*, **75,** 6969-6976.

[179] Nakai,H., Montini,E., Fuess,S., Storm,T.A., Grompe,M., & Kay,M.A. (2003) AAV serotype 2 vectors preferentially integrate into active genes in mice. *Nat. Genet.*, **34,** 297-302.

[180] Nakai,H., Wu,X., Fuess,S., Storm,T.A., Munroe,D., Montini,E., Burgess,S.M., Grompe,M., & Kay,M.A. (2005) Large-scale molecular characterization of adeno-associated virus vector integration in mouse liver. *J. Virol.*, **79,** 3606-3614.

[181] Schnepp,B.C., Clark,K.R., Klemanski,D.L., Pacak,C.A., & Johnson,P.R. (2003) Genetic fate of recombinant adeno-associated virus vector genomes in muscle. *J. Virol.*, **77,** 3495-3504.

[182] Jang,M.Y., Yarborough,O.H., III, Conyers,G.B., McPhie,P., & Owens,R.A. (2005) Stable secondary structure near the nicking site for adeno-associated virus type 2 Rep proteins on human chromosome 19. *J. Virol.*, **79,** 3544-3556.

[183] Girod,A., Wobus,C.E., Zadori,Z., Ried,M., Leike,K., Tijssen,P., Kleinschmidt,J.A., & Hallek,M. (2002) The VP1 capsid protein of adeno-associated virus type 2 is carrying a phospholipase A2 domain required for virus infectivity. *J. Gen. Virol.*, **83,** 973-978.

[184] Grieger,J.C. & Samulski,R.J. (2005) Adeno-associated virus as a gene therapy vector: vector development, production and clinical applications. *Adv. Biochem. Eng Biotechnol.*, **99,** 119-145.

[185] Gao,G., Vandenberghe,L.H., & Wilson,J.M. (2005) New recombinant serotypes of AAV vectors. *Curr. Gene Ther.*, **5,** 285-297.

[186] Bantel-Schaal,U. & zur,H.H. (1984) Characterization of the DNA of a defective human parvovirus isolated from a genital site. *Virology*, **134,** 52-63.

[187] Erles,K., Sebokova,P., & Schlehofer,J.R. (1999) Update on the prevalence of serum antibodies (IgG and IgM) to adeno-associated virus (AAV). *J. Med. Virol.*, **59,** 406-411.

[188] Parks,W.P., Boucher,D.W., Melnick,J.L., Taber,L.H., & Yow,M.D. (1970) Seroepidemiological and Ecological Studies of the Adenovirus-Associated Satellite Viruses. *Infect. Immun.*, **2,** 716-722.

[189] Xiao,W., Chirmule,N., Berta,S.C., McCullough,B., Gao,G., & Wilson,J.M. (1999) Gene therapy vectors based on adeno-associated virus type 1. *J. Virol.*, **73,** 3994-4003.

[190] Gao,G., Vandenberghe,L.H., Alvira,M.R., Lu,Y., Calcedo,R., Zhou,X., & Wilson,J.M. (2004) Clades of Adeno-associated viruses are widely disseminated in human tissues. *J. Virol.*, **78,** 6381-6388.

[191] Gao,G.P., Alvira,M.R., Wang,L., Calcedo,R., Johnston,J., & Wilson,J.M. (2002) Novel adeno-associated viruses from rhesus monkeys as vectors for human gene therapy. *Proc. Natl. Acad. Sci. U. S. A*, **99,** 11854-11859.

[192] Mori,S., Wang,L., Takeuchi,T., & Kanda,T. (2004) Two novel adeno-associated viruses from cynomolgus monkey: pseudotyping characterization of capsid protein. *Virology*, **330,** 375-383.

[193] Rabinowitz,J.E. & Samulski,R.J. (2000) Building a better vector: the manipulation of AAV virions. *Virology*, **278,** 301-308.

[194] Gao,G.P., Alvira,M.R., Wang,L., Calcedo,R., Johnston,J., & Wilson,J.M. (2002) Novel adeno-associated viruses from rhesus monkeys as vectors for human gene therapy. *Proc. Natl. Acad. Sci. U. S. A*, **99,** 11854-11859.

[195] Ferrari,F.K., Samulski,T., Shenk,T., & Samulski,R.J. (1996) Second-strand synthesis is a rate-limiting step for efficient transduction by recombinant adeno-associated virus vectors. *J. Virol.*, **70,** 3227-3234.

[196] Xiao,X., Li,J., & Samulski,R.J. (1998) Production of high-titer recombinant adeno-associated virus vectors in the absence of helper adenovirus. *J. Virol.*, **72,** 2224-2232.

[197] Gao,G.P., Lu,F., Sanmiguel,J.C., Tran,P.T., Abbas,Z., Lynd,K.S., Marsh,J., Spinner,N.B., & Wilson,J.M. (2002) Rep/Cap gene amplification and high-yield production of AAV in an A549 cell line expressing Rep/Cap. *Mol. Ther.*, **5,** 644-649.

[198] Urabe,M., Ding,C., & Kotin,R.M. (2002) Insect cells as a factory to produce adeno-associated virus type 2 vectors. *Hum. Gene Ther.*, **13,** 1935-1943.

[199] Kohlbrenner,E., Aslanidi,G., Nash,K., Shklyaev,S., Campbell-Thompson,M., Byrne,B.J., Snyder,R.O., Muzyczka,N., Warrington,K.H., Jr., & Zolotukhin,S. (2005) Successful production of pseudotyped rAAV vectors using a modified baculovirus expression system. *Mol. Ther.*, **12,** 1217-1225.

[200] Rabinowitz,J.E., Rolling,F., Li,C., Conrath,H., Xiao,W., Xiao,X., & Samulski,R.J. (2002) Cross-packaging of a single adeno-associated virus (AAV) type 2 vector genome into multiple AAV serotypes enables transduction with broad specificity. *J. Virol.*, **76,** 791-801.

[201] Zolotukhin,S., Byrne,B.J., Mason,E., Zolotukhin,I., Potter,M., Chesnut,K., Summerford,C., Samulski,R.J., & Muzyczka,N. (1999) Recombinant adeno-associated virus purification using novel methods improves infectious titer and yield. *Gene Ther.*, **6,** 973-985.

[202] Davidoff,A.M., Ng,C.Y., Sleep,S., Gray,J., Azam,S., Zhao,Y., McIntosh,J.H., Karimipoor,M., & Nathwani,A.C. (2004) Purification of recombinant adeno-associated virus type 8 vectors by ion exchange chromatography generates clinical grade vector stock. *J. Virol. Methods*, **121,** 209-215.

[203] Zolotukhin,S., Potter,M., Zolotukhin,I., Sakai,Y., Loiler,S., Fraites,T.J., Jr., Chiodo,V.A., Phillipsberg,T., Muzyczka,N., Hauswirth,W.W., Flotte,T.R., Byrne,B.J., & Snyder,R.O. (2002) Production and purification of serotype 1, 2, and 5 recombinant adeno-associated viral vectors. *Methods*, **28,** 158-167.

[204] Manno,C.S., Chew,A.J., Hutchison,S., Larson,P.J., Herzog,R.W., Arruda,V.R., Tai,S.J., Ragni,M.V., Thompson,A., Ozelo,M., Couto,L.B., Leonard,D.G., Johnson,F.A., McClelland,A., Scallan,C., Skarsgard,E., Flake,A.W., Kay,M.A., High,K.A., & Glader,B. (2003) AAV-mediated factor IX gene transfer to skeletal muscle in patients with severe hemophilia B. *Blood*, **101,** 2963-2972.

[205] Chao,H., Monahan,P.E., Liu,Y., Samulski,R.J., & Walsh,C.E. (2001) Sustained and complete phenotype correction of hemophilia B mice following intramuscular injection of AAV1 serotype vectors. *Mol. Ther.*, **4,** 217-222.

[206] Blankinship,M.J., Gregorevic,P., Allen,J.M., Harper,S.Q., Harper,H., Halbert,C.L., Miller,D.A., & Chamberlain,J.S. (2004) Efficient transduction of skeletal muscle using vectors based on adeno-associated virus serotype 6. *Mol. Ther.*, **10,** 671-678.

[207] Louboutin,J.P., Wang,L., & Wilson,J.M. (2004) Gene transfer into skeletal muscle using novel AAV serotypes. *J. Gene Med.*.

[208] Riviere,C., Danos,O., & Douar,A.M. (2006) Long-term expression and repeated administration of AAV type 1, 2 and 5 vectors in skeletal muscle of immunocompetent adult mice. *Gene Ther.*, **13,** 1300-1308.

[209] Davidoff,A.M., Gray,J.T., Ng,C.Y., Zhang,Y., Zhou,J., Spence,Y., Bakar,Y., & Nathwani,A.C. (2005) Comparison of the ability of adeno-associated viral vectors pseudotyped with serotype 2, 5, and 8 capsid proteins to mediate efficient transduction of the liver in murine and nonhuman primate models. *Mol. Ther.*, **11,** 875-888.

[210] Lebherz,C., Gao,G., Louboutin,J.P., Millar,J., Rader,D., & Wilson,J.M. (2004) Gene therapy with novel adeno-associated virus vectors substantially diminishes atherosclerosis in a murine model of familial hypercholesterolemia. *J. Gene Med.*, **6,** 663-672.

[211] Nakai,H., Fuess,S., Storm,T.A., Muramatsu,S., Nara,Y., & Kay,M.A. (2005) Unrestricted hepatocyte transduction with adeno-associated virus serotype 8 vectors in mice. *J. Virol.*, **79,** 214-224.

[212] Wang,Z., Zhu,T., Qiao,C., Zhou,L., Wang,B., Zhang,J., Chen,C., Li,J., & Xiao,X. (2005) Adeno-associated virus serotype 8 efficiently delivers genes to muscle and heart. *Nat. Biotechnol.*, **23,** 321-328.

[213] Inagaki,K., Fuess,S., Storm,T.A., Gibson,G.A., Mctiernan,C.F., Kay,M.A., & Nakai,H. (2006) Robust systemic transduction with AAV9 vectors in mice: efficient global cardiac gene transfer superior to that of AAV8. *Mol. Ther.*, **14,** 45-53.

[214] Pacak,C.A., Mah,C.S., Thattaliyath,B.D., Conlon,T.J., Lewis,M.A., Cloutier,D.E., Zolotukhin,I., Tarantal,A.F., & Byrne,B.J. (2006) Recombinant adeno-associated virus serotype 9 leads to preferential cardiac transduction in vivo. *Circ. Res.*, **99,** e3-e9.

[215] Vandendriessche,T., Thorrez,L., Acosta-Sanchez,A., Petrus,I., Wang,L., Ma,L., De Waele,L., Iwasaki,Y., Gillijns,V., Wilson,J.M., Collen,D., & Chuah,M.K. (2006) Efficacy and safety of adeno-associated viral vectors based on serotype 8 and 9 versus lentiviral vectors for hemophilia B gene therapy. *J. Thromb. Haemost.*.

[216] Thomas,C.E., Storm,T.A., Huang,Z., & Kay,M.A. (2004) Rapid uncoating of vector genomes is the key to efficient liver transduction with pseudotyped adeno-associated virus vectors. *J. Virol.*, **78,** 3110-3122.

[217] Akache,B., Grimm,D., Shen,X., Fuess,S., Yant,S.R., Glazer,D.S., Park,J., & Kay,M.A. (2007) A Two-hybrid Screen Identifies Cathepsins B and L as Uncoating Factors for Adeno-associated Virus 2 and 8. *Mol. Ther.*, **15,** 330-339.

[218] Summerford,C. & Samulski,R.J. (1998) Membrane-associated heparan sulfate proteoglycan is a receptor for adeno-associated virus type 2 virions. *J. Virol.*, **72,** 1438-1445.

[219] Qing,K., Mah,C., Hansen,J., Zhou,S., Dwarki,V., & Srivastava,A. (1999) Human fibroblast growth factor receptor 1 is a co-receptor for infection by adeno-associated virus 2. *Nat. Med.*, **5,** 71-77.

[220] Kashiwakura,Y., Tamayose,K., Iwabuchi,K., Hirai,Y., Shimada,T., Matsumoto,K., Nakamura,T., Watanabe,M., Oshimi,K., & Daida,H. (2005) Hepatocyte growth factor receptor is a coreceptor for adeno-associated virus type 2 infection. *J. Virol.*, **79,** 609-614.

[221] Summerford,C., Bartlett,J.S., & Samulski,R.J. (1999) AlphaVbeta5 integrin: a co-receptor for adeno-associated virus type 2 infection. *Nat. Med.*, **5,** 78-82.

[222] Opie,S.R., Warrington,K.H., Jr., Agbandje-McKenna,M., Zolotukhin,S., & Muzyczka,N. (2003) Identification of amino acid residues in the capsid proteins of adeno-associated virus type 2 that contribute to heparan sulfate proteoglycan binding. *J. Virol.*, **77,** 6995-7006.

[223] Blackburn,S.D., Steadman,R.A., & Johnson,F.B. (2006) Attachment of adeno-associated virus type 3H to fibroblast growth factor receptor 1. *Arch. Virol.*, **151,** 617-623.

[224] Di Pasquale,G., Davidson,B.L., Stein,C.S., Martins,I., Scudiero,D., Monks,A., & Chiorini,J.A. (2003) Identification of PDGFR as a receptor for AAV-5 transduction. *Nat. Med.*, **9,** 1306-1312.

[225] Kaludov,N., Brown,K.E., Walters,R.W., Zabner,J., & Chiorini,J.A. (2001) Adeno-associated virus serotype 4 (AAV4) and AAV5 both require sialic acid binding for hemagglutination and efficient transduction but differ in sialic acid linkage specificity. *J. Virol.*, **75,** 6884-6893.

[226] Chen,S., Kapturczak,M., Loiler,S.A., Zolotukhin,S., Glushakova,O.Y., Madsen,K.M., Samulski,R.J., Hauswirth,W.W., Campbell-Thompson,M., Berns,K.I., Flotte,T.R., Atkinson,M.A., Tisher,C.C., & Agarwal,A. (2005) Efficient transduction of vascular endothelial cells with recombinant adeno-associated virus serotype 1 and 5 vectors. *Hum. Gene Ther.*, **16,** 235-247.

[227] Seiler,M.P., Miller,A.D., Zabner,J., & Halbert,C.L. (2006) Adeno-associated virus types 5 and 6 use distinct receptors for cell entry. *Hum. Gene Ther.*, **17,** 10-19.

[228] Wu,Z., Miller,E., Agbandje-McKenna,M., & Samulski,R.J. (2006) Alpha2,3 and alpha2,6 N-linked sialic acids facilitate efficient binding and transduction by adeno-associated virus types 1 and 6. *J. Virol.*, **80,** 9093-9103.

[229] Akache,B., Grimm,D., Pandey,K., Yant,S.R., Xu,H., & Kay,M.A. (2006) The 37/67-kilodalton laminin receptor is a receptor for adeno-associated virus serotypes 8, 2, 3, and 9. *J. Virol.*, **80,** 9831-9836.

[230] Xiao,W., Chirmule,N., Berta,S.C., McCullough,B., Gao,G., & Wilson,J.M. (1999) Gene therapy vectors based on adeno-associated virus type 1. *J. Virol.*, **73,** 3994-4003.

[231] Halbert,C.L., Miller,A.D., McNamara,S., Emerson,J., Gibson,R.L., Ramsey,B., & Aitken,M.L. (2006) Prevalence of neutralizing antibodies against adeno-associated virus (AAV) types 2, 5, and 6 in cystic fibrosis and normal populations: Implications for gene therapy using AAV vectors. *Hum. Gene Ther.*, **17,** 440-447.

[232] Hildinger,M., Auricchio,A., Gao,G., Wang,L., Chirmule,N., & Wilson,J.M. (2001) Hybrid vectors based on adeno-associated virus serotypes 2 and 5 for muscle-directed gene transfer. *J. Virol.*, **75,** 6199-6203.

[233] Halbert,C.L., Standaert,T.A., Aitken,M.L., Alexander,I.E., Russell,D.W., & Miller,A.D. (1997) Transduction by adeno-associated virus vectors in the rabbit airway: efficiency, persistence, and readministration. *J. Virol.*, **71,** 5932-5941.

[234] Moskalenko,M., Chen,L., van Roey,M., Donahue,B.A., Snyder,R.O., McArthur,J.G., & Patel,S.D. (2000) Epitope mapping of human anti-adeno-associated virus type 2 neutralizing antibodies: implications for gene therapy and virus structure. *J. Virol.*, **74,** 1761-1766.

[235] Mack,C.A., Song,W.R., Carpenter,H., Wickham,T.J., Kovesdi,I., Harvey,B.G., Magovern,C.J., Isom,O.W., Rosengart,T., Falck-Pedersen,E., Hackett,N.R., Crystal,R.G., & Mastrangeli,A. (1997) Circumvention of anti-adenovirus neutralizing immunity by administration of an adenoviral vector of an alternate serotype. *Hum. Gene Ther.*, **8,** 99-109.

[236] Mastrangeli,A., Harvey,B.G., Yao,J., Wolff,G., Kovesdi,I., Crystal,R.G., & Falck-Pedersen,E. (1996) "Sero-switch" adenovirus-mediated in vivo gene transfer: circumvention of anti-adenovirus humoral immune defenses against repeat adenovirus vector administration by changing the adenovirus serotype. *Hum. Gene Ther.*, **7,** 79-87.

[237] Halbert,C.L., Rutledge,E.A., Allen,J.M., Russell,D.W., & Miller,A.D. (2000) Repeat transduction in the mouse lung by using adeno-associated virus vectors with different serotypes. *J. Virol.*, **74,** 1524-1532.

[238] Wang,L., Calcedo,R., Nichols,T.C., Bellinger,D.A., Dillow,A., Verma,I.M., & Wilson,J.M. (2005) Sustained correction of disease in naive and AAV2-pretreated hemophilia B dogs: AAV2/8-mediated, liver-directed gene therapy. *Blood*, **105,** 3079-3086.

[239] Wu,Z., Asokan,A., & Samulski,R.J. (2006) Adeno-associated virus serotypes: vector toolkit for human gene therapy. *Mol. Ther.*, **14,** 316-327.

[240] De,B.P., Heguy,A., Hackett,N.R., Ferris,B., Leopold,P.L., Lee,J., Pierre,L., Gao,G., Wilson,J.M., & Crystal,R.G. (2006) High levels of persistent expression of alpha1-antitrypsin mediated by the nonhuman primate serotype rh.10 adeno-associated virus despite preexisting immunity to common human adeno-associated viruses. *Mol. Ther.*, **13,** 67-76.

[241] Limberis,M.P. & Wilson,J.M. (2006) Adeno-associated virus serotype 9 vectors transduce murine alveolar and nasal epithelia and can be readministered. *Proc. Natl. Acad. Sci. U. S. A*, **103,** 12993-12998.

[242] Brockstedt,D.G., Podsakoff,G.M., Fong,L., Kurtzman,G., Mueller-Ruchholtz,W., & Engleman,E.G. (1999) Induction of immunity to antigens expressed by recombinant adeno-associated virus depends on the route of administration. *Clin. Immunol.*, **92,** 67-75.

[243] Wang,L., Dobrzynski,E., Schlachterman,A., Cao,O., & Herzog,R.W. (2005) Systemic protein delivery by muscle-gene transfer is limited by a local immune response. *Blood*, **105,** 4226-4234.

[244] Wang,L., Cao,O., Swalm,B., Dobrzynski,E., Mingozzi,F., & Herzog,R.W. (2005) Major role of local immune responses in antibody formation to factor IX in AAV gene transfer. *Gene Ther.*, **12,** 1453-1464.

[245] Mingozzi,F., Liu,Y.L., Dobrzynski,E., Kaufhold,A., Liu,J.H., Wang,Y., Arruda,V.R., High,K.A., & Herzog,R.W. (2003) Induction of immune tolerance to coagulation factor IX antigen by in vivo hepatic gene transfer. *J. Clin. Invest*, **111,** 1347-1356.

[246] Gao,G., Lebherz,C., Weiner,D.J., Grant,R., Calcedo,R., McCullough,B., Bagg,A., Zhang,Y., & Wilson,J.M. (2004) Erythropoietin gene therapy leads to autoimmune anemia in macaques. *Blood*, **103,** 3300-3302.

[247] Ritter,T., Brandt,C., Prosch,S., Vergopoulos,A., Vogt,K., Kolls,J., & Volk,H.D. (2000) Stimulatory and inhibitory action of cytokines on the regulation of hCMV-IE promoter activity in human endothelial cells. *Cytokine*, **12,** 1163-1170.

[248] Everett,R.S., Evans,H.K., Hodges,B.L., Ding,E.Y., Serra,D.M., & Amalfitano,A. (2004) Strain-specific rate of shutdown of CMV enhancer activity in murine liver confirmed by use of persistent [E1(-), E2b(-)] adenoviral vectors. *Virology*, **325,** 96-105.

[249] Prosch,S., Stein,J., Staak,K., Liebenthal,C., Volk,H.D., & Kruger,D.H. (1996) Inactivation of the very strong HCMV immediate early promoter by DNA CpG methylation in vitro. *Biol. Chem. Hoppe Seyler*, **377,** 195-201.

[250] Xu,L., Daly,T., Gao,C., Flotte,T.R., Song,S., Byrne,B.J., Sands,M.S., & Parker,P.K. (2001) CMV-beta-actin promoter directs higher expression from an adeno-associated viral vector in the liver than the cytomegalovirus or elongation factor 1 alpha promoter and results in therapeutic levels of human factor X in mice. *Hum. Gene Ther.*, **12,** 563-573.

[251] Sirninger,J., Muller,C., Braag,S., Tang,Q., Yue,H., Detrisac,C., Ferkol,T., Guggino,W.B., & Flotte,T.R. (2004) Functional characterization of a recombinant adeno-associated virus 5-pseudotyped cystic fibrosis transmembrane conductance regulator vector. *Hum. Gene Ther.*, **15,** 832-841.

[252] Yue,Y. & Dongsheng,D. (2002) Development of multiple cloning site cis-vectors for recombinant adeno-associated virus production. *Biotechniques*, **33,** 672, 674, 676-672, 674, 678.

[253] Franco,L.M., Sun,B., Yang,X., Bird,A., Zhang,H., Schneider,A., Brown,T., Young,S.P., Clay,T.M., Amalfitano,A., Chen,Y.T., & Koeberl,D.D. (2005) Evasion of immune responses to introduced human acid alpha-glucosidase by liver-restricted expression in glycogen storage disease type II. *Mol. Ther.*, **12,** 876-884.

[254] Cordier,L., Gao,G.P., Hack,A.A., McNally,E.M., Wilson,J.M., Chirmule,N., & Sweeney,H.L. (2001) Muscle-specific promoters may be necessary for adeno-associated virus-mediated gene transfer in the treatment of muscular dystrophies. *Hum. Gene Ther.*, **12,** 205-215.

[255] Sun,B., Zhang,H., Franco,L.M., Brown,T., Bird,A., Schneider,A., & Koeberl,D.D. (2005) Correction of glycogen storage disease type II by an adeno-associated virus vector containing a muscle-specific promoter. *Mol. Ther.*, **11,** 889-898.

[256] Takeshita,F., Takase,K., Tozuka,M., Saha,S., Okuda,K., Ishii,N., & Sasaki,S. (2007) Muscle creatine kinase/SV40 hybrid promoter for muscle-targeted long-term transgene expression. *Int. J. Mol. Med.*, **19,** 309-315.

[257] Hauser,M.A., Robinson,A., Hartigan-O'Connor,D., Williams-Gregory,D.A., Buskin,J.N., Apone,S., Kirk,C.J., Hardy,S., Hauschka,S.D., & Chamberlain,J.S. (2000) Analysis of muscle creatine kinase regulatory elements in recombinant adenoviral vectors. *Mol. Ther.*, **2,** 16-25.

[258] Li,X., Eastman,E.M., Schwartz,R.J., & Draghia-Akli,R. (1999) Synthetic muscle promoters: activities exceeding naturally occurring regulatory sequences. *Nat. Biotechnol.*, **17,** 241-245.

[259] Liu,Y.L., Mingozzi,F., Rodriguez-Colon,S.M., Joseph,S., Dobrzynski,E., Suzuki,T., High,K.A., & Herzog,R.W. (2004) Therapeutic levels of factor IX expression using a muscle-specific promoter and adeno-associated virus serotype 1 vector. *Hum. Gene Ther.*, **15,** 783-792.

[260] Gregorevic,P., Blankinship,M.J., Allen,J.M., Crawford,R.W., Meuse,L., Miller,D.G., Russell,D.W., & Chamberlain,J.S. (2004) Systemic delivery of genes to striated muscles using adeno-associated viral vectors. *Nat. Med.*, **10,** 828-834.

[261] Lu,Q.L., Bou-Gharios,G., & Partridge,T.A. (2003) Non-viral gene delivery in skeletal muscle: a protein factory. *Gene Ther*, **10,** 131-142.

[262] Wells,D.J. (2006) Viral and non-viral methods for gene transfer into skeletal muscle. *Curr. Opin. Drug Discov. Devel.*, **9,** 163-168.

[263] Fisher,K.J., Jooss,K., Alston,J., Yang,Y., Haecker,S.E., High,K., Pathak,R., Raper,S.E., & Wilson,J.M. (1997) Recombinant adeno-associated virus for muscle directed gene therapy. *Nat. Med.*, **3,** 306-312.

[264] Xiao,X., Li,J., & Samulski,R.J. (1996) Efficient long-term gene transfer into muscle tissue of immunocompetent mice by adeno-associated virus vector. *J. Virol.*, **70,** 8098-8108.

[265] Chao,H., Samulski,R., Bellinger,D., Monahan,P., Nichols,T., & Walsh,C. (1999) Persistent expression of canine factor IX in hemophilia B canines. *Gene Ther.*, **6,** 1695-1704.

[266] Herzog,R.W., Yang,E.Y., Couto,L.B., Hagstrom,J.N., Elwell,D., Fields,P.A., Burton,M., Bellinger,D.A., Read,M.S., Brinkhous,K.M., Podsakoff,G.M., Nichols,T.C., Kurtzman,G.J., & High,K.A. (1999) Long-term correction of canine hemophilia B by gene transfer of blood coagulation factor IX mediated by adeno-associated viral vector. *Nat. Med.*, **5,** 56-63.

[267] Greelish,J.P., Su,L.T., Lankford,E.B., Burkman,J.M., Chen,H., Konig,S.K., Mercier,I.M., Desjardins,P.R., Mitchell,M.A., Zheng,X.G., Leferovich,J., Gao,G.P., Balice-Gordon,R.J., Wilson,J.M., & Stedman,H.H. (1999) Stable restoration of the sarcoglycan complex in dystrophic muscle perfused with histamine and a recombinant adeno-associated viral vector. *Nat. Med.*, **5,** 439-443.

[268] Pacak,C.A., Walter,G.A., Gaidosh,G., Bryant,N., Lewis,M.A., Germain,S., Mah,C.S., Campbell,K.P., & Byrne,B.J. (2007) Long-term Skeletal Muscle Protection After Gene Transfer in a Mouse Model of LGMD-2D. *Mol. Ther.*.

[269] Xiao,X., Li,J., Tsao,Y.P., Dressman,D., Hoffman,E.P., & Watchko,J.F. (2000) Full functional rescue of a complete muscle (TA) in dystrophic hamsters by adeno-associated virus vector-directed gene therapy. *J. Virol.*, **74**, 1436-1442.

[270] Wang,Z., Kuhr,C.S., Allen,J.M., Blankinship,M., Gregorevic,P., Chamberlain,J.S., Tapscott,S.J., & Storb,R. (2007) Sustained AAV-mediated dystrophin expression in a canine model of Duchenne muscular dystrophy with a brief course of immunosuppression. *Mol. Ther.*, **15**, 1160-1166.

[271] Duan,D., Yue,Y., & Engelhardt,J.F. (2001) Expanding AAV packaging capacity with trans-splicing or overlapping vectors: a quantitative comparison. *Mol. Ther.*, **4**, 383-391.

[272] Smith-Arica,J.R., Thomson,A.J., Ansell,R., Chiorini,J., Davidson,B., & McWhir,J. (2003) Infection efficiency of human and mouse embryonic stem cells using adenoviral and adeno-associated viral vectors. *Cloning Stem Cells*, **5**, 51-62.

[273] Hauck,B., Chen,L., & Xiao,W. (2003) Generation and characterization of chimeric recombinant AAV vectors. *Mol. Ther.*, **7**, 419-425.

[274] Rabinowitz,J.E., Bowles,D.E., Faust,S.M., Ledford,J.G., Cunningham,S.E., & Samulski,R.J. (2004) Cross-dressing the virion: the transcapsidation of adeno-associated virus serotypes functionally defines subgroups. *J. Virol.*, **78**, 4421-4432.

[275] Hauck,B., Xu,R.R., Xie,J., Wu,W., Ding,Q., Sipler,M., Wang,H., Chen,L., Wright,J.F., & Xiao,W. (2006) Efficient AAV1-AAV2 hybrid vector for gene therapy of hemophilia. *Hum. Gene Ther.*, **17**, 46-54.

[276] May,O., Nguyen,P.T., & Arnold,F.H. (2000) Inverting enantioselectivity by directed evolution of hydantoinase for improved production of L-methionine. *Nat. Biotechnol.*, **18**, 317-320.

[277] Soong,N.W., Nomura,L., Pekrun,K., Reed,M., Sheppard,L., Dawes,G., & Stemmer,W.P. (2000) Molecular breeding of viruses. *Nat. Genet.*, **25**, 436-439.

[278] Maheshri,N., Koerber,J.T., Kaspar,B.K., & Schaffer,D.V. (2006) Directed evolution of adeno-associated virus yields enhanced gene delivery vectors. *Nat. Biotechnol.*, **24**, 198-204.

[279] Girod,A., Ried,M., Wobus,C., Lahm,H., Leike,K., Kleinschmidt,J., Deleage,G., & Hallek,M. (1999) Genetic capsid modifications allow efficient re-targeting of adeno-associated virus type 2. *Nat. Med.*, **5**, 1052-1056.

[280] White,S.J., Nicklin,S.A., Buning,H., Brosnan,M.J., Leike,K., Papadakis,E.D., Hallek,M., & Baker,A.H. (2004) Targeted gene delivery to vascular tissue in vivo by tropism-modified adeno-associated virus vectors. *Circulation*, **109**, 513-519.

[281] Arnold,G.S., Sasser,A.K., Stachler,M.D., & Bartlett,J.S. (2006) Metabolic biotinylation provides a unique platform for the purification and targeting of multiple AAV vector serotypes. *Mol. Ther.*, **14**, 97-106.

[282] Liu,M., Yue,Y., Harper,S.Q., Grange,R.W., Chamberlain,J.S., & Duan,D. (2005) Adeno-Associated virus-mediated microdystrophin expression protects young mdx muscle from contraction-induced injury. *Mol. Ther.*, **11**, 245-256.

[283] Ghosh,A., Yue,Y., & Duan,D. (2006) Viral serotype and the transgene sequence influence overlapping adeno-associated viral (AAV) vector-mediated gene transfer in skeletal muscle. *J. Gene Med.*, **8**, 298-305.

[284] Hirata,R.K. & Russell,D.W. (2000) Design and packaging of adeno-associated virus gene targeting vectors. *J. Virol.*, **74**, 4612-4620.

[285] McCarty,D.M., Monahan,P.E., & Samulski,R.J. (2001) Self-complementary recombinant adeno-associated virus (scAAV) vectors promote efficient transduction independently of DNA synthesis. *Gene Ther.*, **8,** 1248-1254.

[286] McCarty,D.M., Fu,H., Monahan,P.E., Toulson,C.E., Naik,P., & Samulski,R.J. (2003) Adeno-associated virus terminal repeat (TR) mutant generates self-complementary vectors to overcome the rate-limiting step to transduction in vivo. *Gene Ther.*, **10,** 2112-2118.

[287] Ren,C., Kumar,S., Shaw,D.R., & Ponnazhagan,S. (2005) Genomic stability of self-complementary adeno-associated virus 2 during early stages of transduction in mouse muscle in vivo. *Hum. Gene Ther.*, **16,** 1047-1057.

[288] Nathwani,A.C., Gray,J.T., Ng,C.Y., Zhou,J., Spence,Y., Waddington,S.N., Tuddenham,E.G., Kemball-Cook,G., McIntosh,J., Boon-Spijker,M., Mertens,K., & Davidoff,A.M. (2005) Self complementary adeno-associated virus vectors containing a novel liver-specific human factor IX expression cassette enable highly efficient transduction of murine and nonhuman primate liver. *Blood.*

[289] Matsui,H., Johnson,L.G., Randell,S.H., & Boucher,R.C. (1997) Loss of binding and entry of liposome-DNA complexes decreases transfection efficiency in differentiated airway epithelial cells. *J. Biol. Chem.*, **272,** 1117-1126.

[290] Chan,C.K. & Jans,D.A. (2001) Enhancement of MSH receptor- and GAL4-mediated gene transfer by switching the nuclear import pathway. *Gene Ther.*, **8,** 166-171.

[291] Kircheis,R., Wightman,L., Schreiber,A., Robitza,B., Rossler,V., Kursa,M., & Wagner,E. (2001) Polyethylenimine/DNA complexes shielded by transferrin target gene expression to tumors after systemic application. *Gene Ther.*, **8,** 28-40.

[292] Olivares,E.C., Hollis,R.P., Chalberg,T.W., Meuse,L., Kay,M.A., & Calos,M.P. (2002) Site-specific genomic integration produces therapeutic Factor IX levels in mice. *Nat. Biotechnol.*, **20,** 1124-1128.

[293] Telenius,H., Szeles,A., Kereso,J., Csonka,E., Praznovszky,T., Imreh,S., Maxwell,A., Perez,C.F., Drayer,J.I., & Hadlaczky,G. (1999) Stability of a functional murine satellite DNA-based artificial chromosome across mammalian species. *Chromosome. Res.*, **7,** 3-7.

[294] Heller,R., Jaroszeski,M., Atkin,A., Moradpour,D., Gilbert,R., Wands,J., & Nicolau,C. (1996) In vivo gene electroinjection and expression in rat liver. *FEBS Lett.*, **389,** 225-228.

[295] Neumann,E., Schaefer-Ridder,M., Wang,Y., & Hofschneider,P.H. (1982) Gene transfer into mouse lyoma cells by electroporation in high electric fields. *EMBO J.*, **1,** 841-845.

[296] Gollins,H., McMahon,J., Wells,K.E., & Wells,D.J. (2003) High-efficiency plasmid gene transfer into dystrophic muscle. *Gene Ther.*, **10,** 504-512.

[297] Lee,S.C., Wu,C.J., Wu,P.Y., Huang,Y.L., Wu,C.W., & Tao,M.H. (2003) Inhibition of established subcutaneous and metastatic murine tumors by intramuscular electroporation of the interleukin-12 gene. *J. Biomed. Sci.*, **10,** 73-86.

[298] Celiker,M.Y., Wang,M., Atsidaftos,E., Liu,X., Liu,Y.E., Jiang,Y., Valderrama,E., Goldberg,I.D., & Shi,Y.E. (2001) Inhibition of Wilms' tumor growth by intramuscular administration of tissue inhibitor of metalloproteinases-4 plasmid DNA. *Oncogene*, **20,** 4337-4343.

[299] Jeong,J.G., Kim,J.M., Ho,S.H., Hahn,W., Yu,S.S., & Kim,S. (2004) Electrotransfer of human IL-1Ra into skeletal muscles reduces the incidence of murine collagen-induced arthritis. *J. Gene Med.*, **6,** 1125-1133.

[300] Satkauskas,S., Bureau,M.F., Puc,M., Mahfoudi,A., Scherman,D., Miklavcic,D., & Mir,L.M. (2002) Mechanisms of in vivo DNA electrotransfer: respective contributions of cell electropermeabilization and DNA electrophoresis. *Mol. Ther.*, **5,** 133-140.

[301] Satkauskas,S., Bureau,M.F., Mahfoudi,A., & Mir,L.M. (2001) Slow accumulation of plasmid in muscle cells: supporting evidence for a mechanism of DNA uptake by receptor-mediated endocytosis. *Mol. Ther.*, **4,** 317-323.

[302] Peng,B., Zhao,Y., Lu,H., Pang,W., & Xu,Y. (2005) In vivo plasmid DNA electroporation resulted in transfection of satellite cells and lasting transgene expression in regenerated muscle fibers. *Biochem. Biophys. Res. Commun.*, **338,** 1490-1498.

[303] Piechaczek,C., Fetzer,C., Baiker,A., Bode,J., & Lipps,H.J. (1999) A vector based on the SV40 origin of replication and chromosomal S/MARs replicates episomally in CHO cells. *Nucleic Acids Res.*, **27,** 426-428.

[304] Schaarschmidt,D., Baltin,J., Stehle,I.M., Lipps,H.J., & Knippers,R. (2004) An episomal mammalian replicon: sequence-independent binding of the origin recognition complex. *EMBO J.*, **23,** 191-201.

[305] Jenke,B.H., Fetzer,C.P., Stehle,I.M., Jonsson,F., Fackelmayer,F.O., Conradt,H., Bode,J., & Lipps,H.J. (2002) An episomally replicating vector binds to the nuclear matrix protein SAF-A in vivo. *EMBO Rep.*, **3,** 349-354.

[306] Jenke,A.C., Scinteie,M.F., Stehle,I.M., & Lipps,H.J. (2004) Expression of a transgene encoded on a non-viral episomal vector is not subject to epigenetic silencing by cytosine methylation. *Mol. Biol. Rep.*, **31,** 85-90.

[307] Riu,E., Grimm,D., Huang,Z., & Kay,M.A. (2005) Increased maintenance and persistence of transgenes by excision of expression cassettes from plasmid sequences in vivo. *Hum. Gene Ther*, **16,** 558-570.

[308] Kashyap,V.S., Santamarina-Fojo,S., Brown,D.R., Parrott,C.L., Applebaum-Bowden,D., Meyn,S., Talley,G., Paigen,B., Maeda,N., & Brewer,H.B., Jr. (1995) Apolipoprotein E deficiency in mice: gene replacement and prevention of atherosclerosis using adenovirus vectors. *J. Clin. Invest*, **96,** 1612-1620.

[309] Desurmont,C., Caillaud,J.M., Emmanuel,F., Benoit,P., Fruchart,J.C., Castro,G., Branellec,D., Heard,J.M., & Duverger,N. (2000) Complete atherosclerosis regression after human ApoE gene transfer in ApoE-deficient/nude mice. *Arterioscler. Thromb. Vasc. Biol.*, **20,** 435-442.

[310] Tsukamoto,K., Tangirala,R., Chun,S.H., Pure,E., & Rader,D.J. (1999) Rapid regression of atherosclerosis induced by liver-directed gene transfer of ApoE in ApoE-deficient mice. *Arterioscler. Thromb. Vasc. Biol.*, **19,** 2162-2170.

[311] Tangirala,R.K., Pratico,D., FitzGerald,G.A., Chun,S., Tsukamoto,K., Maugeais,C., Usher,D.C., Pure,E., & Rader,D.J. (2001) Reduction of isoprostanes and regression of advanced atherosclerosis by apolipoprotein E. *J. Biol. Chem.*, **276,** 261-266.

[312] Harris,J.D., Graham,I.R., Schepelmann,S., Stannard,A.K., Roberts,M.L., Hodges,B.L., Hill,V., Amalfitano,A., Hassall,D.G., Owen,J.S., & Dickson,G. (2002) Acute regression of advanced and retardation of early aortic atheroma in immunocompetent apolipoprotein-E (apoE) deficient mice by administration of a second generation [E1(-), E3(-), polymerase(-)] adenovirus vector expressing human apoE. *Hum. Mol. Genet.*, **11,** 43-58.

[313] Harris,J.D., Graham,I.R., Amalfitano,A., Owen,J.S., & Dickson,G. (2006) Delivery of human apoE to liver by an [E1$^-$, E3$^-$, polymerase$^-$, pTP$^-$] adenovirus vector containing a liver-specific promoter inhibits atherogenesis in immunocompetent apoE-deficient mice. *Gene Ther Mol Biol*, **10,** 17-30.

[314] Harris,J.D., Graham,I.R., & Dickson G (2005) Retardation of atherosclerosis in immunocompetent apolipoprotein (apo) E-deficient mice following liver-directed administration of a (E1$^-$, E3$^-$, polymerase$^-$) adenovirus vector containing the elongation factor-1α promoter driving expression of human apoE cDNA . *Gene Ther Mol Biol*, **9,** 23-32.

[315] Kim,I.H., Jozkowicz,A., Piedra,P.A., Oka,K., & Chan,L. (2001) Lifetime correction of genetic deficiency in mice with a single injection of helper-dependent adenoviral vector. *Proc. Natl. Acad. Sci. U. S. A*, **98,** 13282-13287.

[316] Harris,J.D., Schepelmann,S., Athanasopoulos,T., Graham,I.R., Stannard,A.K., Mohri,Z., Hill,V., Hassall,D.G., Owen,J.S., & Dickson,G. (2002) Inhibition of atherosclerosis in apolipoprotein-E-deficient mice following muscle transduction with adeno-associated virus vectors encoding human apolipoprotein-E. *Gene Ther.*, **9,** 21-29.

[317] Ali,K., Middleton,M., Pure,E., & Rader,D.J. (2005) Apolipoprotein E suppresses the type I inflammatory response in vivo. *Circ. Res.*, **97,** 922-927.

[318] Kitajima,K., Marchadier,D.H., Miller,G.C., Gao,G.P., Wilson,J.M., & Rader,D.J. (2006) Complete prevention of atherosclerosis in apoE-deficient mice by hepatic human apoE gene transfer with adeno-associated virus serotypes 7 and 8. *Arterioscler. Thromb. Vasc. Biol.*, **26,** 1852-1857.

[319] Hasty,A.H., Linton,M.F., Swift,L.L., & Fazio,S. (1999) Determination of the lower threshold of apolipoprotein E resulting in remnant lipoprotein clearance. *J. Lipid Res.*, **40,** 1529-1538.

[320] Hasty,A.H., Linton,M.F., Brandt,S.J., Babaev,V.R., Gleaves,L.A., & Fazio,S. (1999) Retroviral gene therapy in ApoE-deficient mice: ApoE expression in the artery wall reduces early foam cell lesion formation. *Circulation*, **99,** 2571-2576.

[321] Yoshida,H., Hasty,A.H., Major,A.S., Ishiguro,H., Su,Y.R., Gleaves,L.A., Babaev,V.R., Linton,M.F., & Fazio,S. (2001) Isoform-specific effects of apolipoprotein E on atherogenesis: gene transduction studies in mice. *Circulation*, **104,** 2820-2825.

[322] Gough,P.J. & Raines,E.W. (2003) Gene therapy of apolipoprotein E-deficient mice using a novel macrophage-specific retroviral vector. *Blood*, **101,** 485-491.

[323] Wientgen,H., Thorngate,F.E., Omerhodzic,S., Rolnitzky,L., Fallon,J.T., Williams,D.L., & Fisher,E.A. (2004) Subphysiologic apolipoprotein E (ApoE) plasma levels inhibit neointimal formation after arterial injury in ApoE-deficient mice. *Arterioscler. Thromb. Vasc. Biol.*, **24,** 1460-1465.

[324] Rinaldi,M., Catapano,A.L., Parrella,P., Ciafre,S.A., Signori,E., Seripa,D., Uboldi,P., Antonini,R., Ricci,G., Farace,M.G., & Fazio,V.M. (2000) Treatment of severe hypercholesterolemia in apolipoprotein E-deficient mice by intramuscular injection of plasmid DNA. *Gene Ther.*, **7,** 1795-1801.

[325] Athanasopoulos,T., Owen,J.S., Hassall,D., Dunckley,M.G., Drew,J., Goodman,J., Tagalakis,A.D., Riddell,D.R., & Dickson,G. (2000) Intramuscular injection of a plasmid vector expressing human apolipoprotein E limits progression of xanthoma and aortic atheroma in apoE-deficient mice. *Hum. Mol. Genet.*, **9,** 2545-2551.

[326] Cioffi,L., Sturtz,F.G., Wittmer,S., Barut,B., Smith-Gbur,J., Moore,V., Zupancic,T., Gilligan,B., Auerbach,R., Gomez,F., Chauvin,F., Antczak,M., Platika,D., & Snodgrass,H.R. (1999) A novel endothelial cell-based gene therapy platform for the in vivo delivery of apolipoprotein E. *Gene Ther.*, **6,** 1153-1159.

[327] Tagalakis,A.D., Diakonov,I.A., Graham,I.R., Heald,K.A., Harris,J.D., Mulcahy,J.V., Dickson,G., & Owen,J.S. (2005) Apolipoprotein E delivery by peritoneal implantation of encapsulated recombinant cells improves the hyperlipidaemic profile in apoE-deficient mice. *Biochim. Biophys. Acta*, **1686 3,** 190-199.

[328] Piedrahita,J.A., Zhang,S.H., Hagaman,J.R., Oliver,P.M., & Maeda,N. (1992) Generation of mice carrying a mutant apolipoprotein E gene inactivated by gene targeting in embryonic stem cells. *Proc. Natl. Acad. Sci. U. S. A*, **89,** 4471-4475.

[329] Mullis,K., Faloona,F., Scharf,S., Saiki,R., Horn,G., & Erlich,H. (1986) Specific enzymatic amplification of DNA in vitro: the polymerase chain reaction. *Cold Spring Harb. Symp. Quant. Biol.*, **51 Pt 1,** 263-273.

[330] Mullis,K.B. & Faloona,F.A. (1987) Specific synthesis of DNA in vitro via a polymerase-catalyzed chain reaction. *Methods Enzymol.*, **155,** 335-350.

[331] Hanahan,D. (1983) Studies on transformation of Escherichia coli with plasmids. *J. Mol. Biol.*, **166,** 557-580.

[332] DuBridge,R.B., Tang,P., Hsia,H.C., Leong,P.M., Miller,J.H., & Calos,M.P. (1987) Analysis of mutation in human cells by using an Epstein-Barr virus shuttle system. *Mol. Cell Biol.*, **7,** 379-387.

[333] Bradford,M.M. (1976) A rapid and sensitive method for the quantitation of microgram quantities of protein utilizing the principle of protein-dye binding. *Anal. Biochem.*, **72,** 248-254.

[334] Grimm,D., Kern,A., Rittner,K., & Kleinschmidt,J.A. (1998) Novel tools for production and purification of recombinant adenoassociated virus vectors. *Hum. Gene Ther.*, **9,** 2745-2760.

[335] Matsushita,T., Elliger,S., Elliger,C., Podsakoff,G., Villarreal,L., Kurtzman,G.J., Iwaki,Y., & Colosi,P. (1998) Adeno-associated virus vectors can be efficiently produced without helper virus. *Gene Ther.*, **5,** 938-945.

[336] McMahon,J.M., Signori,E., Wells,K.E., Fazio,V.M., & Wells,D.J. (2001) Optimisation of electrotransfer of plasmid into skeletal muscle by pretreatment with hyaluronidase -- increased expression with reduced muscle damage. *Gene Ther.*, **8,** 1264-1270.

[337] Mennuni,C., Calvaruso,F., Zampaglione,I., Rizzuto,G., Rinaudo,D., Dammassa,E., Ciliberto,G., Fattori,E., & La Monica,N. (2002) Hyaluronidase increases electrogene transfer efficiency in skeletal muscle. *Hum. Gene Ther.*, **13,** 355-365.

[338] Glover,D.J., Lipps,H.J., & Jans,D.A. (2005) Towards safe, non-viral therapeutic gene expression in humans. *Nat. Rev. Genet.*, **6,** 299-310.

[339] Davis,H.L., Whalen,R.G., & Demeneix,B.A. (1993) Direct gene transfer into skeletal muscle in vivo: factors affecting efficiency of transfer and stability of expression. *Hum. Gene Ther.*, **4,** 151-159.

[340] Chamberlain,J.S., Jaynes,J.B., & Hauschka,S.D. (1985) Regulation of creatine kinase induction in differentiating mouse myoblasts. *Mol. Cell Biol.*, **5,** 484-492.

[341] Fazio,V.M., Fazio,S., Rinaldi,M., Catani,M.V., Zotti,S., Ciafre,S.A., Seripa,D., Ricci,G., & Farace,M.G. (1994) Accumulation of human apolipoprotein-E in rat plasma after in vivo intramuscular injection of naked DNA. *Biochem. Biophys. Res. Commun.*, **200,** 298-305.

[342] Aihara,H. & Miyazaki,J. (1998) Gene transfer into muscle by electroporation in vivo. *Nat. Biotechnol.*, **16,** 867-870.

[343] Somiari,S., Glasspool-Malone,J., Drabick,J.J., Gilbert,R.A., Heller,R., Jaroszeski,M.J., & Malone,R.W. (2000) Theory and in vivo application of electroporative gene delivery. *Mol. Ther.*, **2,** 178-187.

[344] Mahley,R.W., Huang,Y., & Rall,S.C., Jr. (1999) Pathogenesis of type III hyperlipoproteinemia (dysbetalipoproteinemia). Questions, quandaries, and paradoxes. *J. Lipid Res.*, **40,** 1933-1949.

[345] Wu,G., Yuan,J., & Hunninghake,D.B. (1998) Effect of human apolipoprotein E isoforms on plasma lipids, lipoproteins and apolipoproteins in apolipoprotein E-deficient mice. *Atherosclerosis*, **141,** 287-296.

[346] Burgess,J.W., Liang,P., Vaidyanath,C., & Marcel,Y.L. (1999) ApoE of the HepG2 cell surface includes a major pool associated with chondroitin sulfate proteoglycans. *Biochemistry*, **38,** 524-531.

[347] Kessler,P.D., Podsakoff,G.M., Chen,X., McQuiston,S.A., Colosi,P.C., Matelis,L.A., Kurtzman,G.J., & Byrne,B.J. (1996) Gene delivery to skeletal muscle results in sustained expression and systemic delivery of a therapeutic protein. *Proc. Natl. Acad. Sci. U. S. A*, **93,** 14082-14087.

[348] Bohl,D., Bosch,A., Cardona,A., Salvetti,A., & Heard,J.M. (2000) Improvement of erythropoiesis in beta-thalassemic mice by continuous erythropoietin delivery from muscle. *Blood*, **95,** 2793-2798.

[349] Chao,H., Liu,Y., Rabinowitz,J., Li,C., Samulski,R.J., & Walsh,C.E. (2000) Several log increase in therapeutic transgene delivery by distinct adeno-associated viral serotype vectors. *Mol. Ther.*, **2,** 619-623.

[350] Hagstrom,J.N., Couto,L.B., Scallan,C., Burton,M., McCleland,M.L., Fields,P.A., Arruda,V.R., Herzog,R.W., & High,K.A. (2000) Improved muscle-derived expression of human coagulation factor IX from a skeletal actin/CMV hybrid enhancer/promoter. *Blood*, **95,** 2536-2542.

[351] Dong,J.Y., Fan,P.D., & Frizzell,R.A. (1996) Quantitative analysis of the packaging capacity of recombinant adeno-associated virus. *Hum. Gene Ther.*, **7,** 2101-2112.

[352] Grieger,J.C. & Samulski,R.J. (2005) Packaging capacity of adeno-associated virus serotypes: impact of larger genomes on infectivity and postentry steps. *J. Virol.*, **79,** 9933-9944.

[353] Wu,J., Zhao,W., Zhong,L., Han,Z., Li,B., Ma,W., Weigel-Kelley,K.A., Warrington,K.H., & Srivastava,A. (2007) Self-Complementary Recombinant Adeno-Associated Viral Vectors: Packaging Capacity And The Role of Rep Proteins in Vector Purity. *Hum. Gene Ther.*.

[354] Timpe,J., Bevington,J., Casper,J., Dignam,J.D., & Trempe,J.P. (2005) Mechanisms of adeno-associated virus genome encapsidation. *Curr. Gene Ther.*, **5,** 273-284.

[355] Wang,Z., Ma,H.I., Li,J., Sun,L., Zhang,J., & Xiao,X. (2003) Rapid and highly efficient transduction by double-stranded adeno-associated virus vectors in vitro and in vivo. *Gene Ther.*, **10,** 2105-2111.

[356] Alexander,I.E., Russell,D.W., & Miller,A.D. (1997) Transfer of contaminants in adeno-associated virus vector stocks can mimic transduction and lead to artifactual results. *Hum. Gene Ther.*, **8,** 1911-1920.

[357] Walsh,K. & Perlman,H. (1997) Cell cycle exit upon myogenic differentiation. *Curr. Opin. Genet. Dev.*, **7,** 597-602.

[358] Duan,D., Yan,Z., Yue,Y., Ding,W., & Engelhardt,J.F. (2001) Enhancement of muscle gene delivery with pseudotyped adeno-associated virus type 5 correlates with myoblast differentiation. *J. Virol.*, **75,** 7662-7671.

[359] Zhong,L., Chen,L., Li,Y., Qing,K., Weigel-Kelley,K.A., Chan,R.J., Yoder,M.C., & Srivastava,A. (2004) Self-complementary adeno-associated virus 2 (AAV)-T cell protein tyrosine phosphatase vectors as helper viruses to improve transduction efficiency of conventional single-stranded AAV vectors in vitro and in vivo. *Mol. Ther.*, **10,** 950-957.

[360] Zhong,L., Li,W., Li,Y., Zhao,W., Wu,J., Li,B., Maina,N., Bischof,D., Qing,K., Weigel-Kelley,K.A., Zolotukhin,I., Warrington,K.H., Jr., Li,X., Slayton,W.B., Yoder,M.C., & Srivastava,A. (2006) Evaluation of primitive murine hematopoietic stem and progenitor cell transduction in vitro and in vivo by recombinant adeno-associated virus vector serotypes 1 through 5. *Hum. Gene Ther.*, **17,** 321-333.

[361] Tezak,Z., Nagaraju,K., Plotz,P., & Hoffman,E.P. (2000) Adeno-associated virus in normal and myositis human skeletal muscle. *Neurology*, **55,** 1913-1917.

[362] Jooss,K., Yang,Y., Fisher,K.J., & Wilson,J.M. (1998) Transduction of dendritic cells by DNA viral vectors directs the immune response to transgene products in muscle fibers. *J. Virol.*, **72,** 4212-4223.

[363] Bartoli,M., Roudaut,C., Martin,S., Fougerousse,F., Suel,L., Poupiot,J., Gicquel,E., Noulet,F., Danos,O., & Richard,I. (2006) Safety and efficacy of AAV-mediated calpain 3 gene transfer in a mouse model of limb-girdle muscular dystrophy type 2A. *Mol. Ther.*, **13,** 250-259.

[364] Salva,M.Z., Himeda,C.L., Tai,P.W., Nishiuchi,E., Gregorevic,P., Allen,J.M., Finn,E.E., Nguyen,Q.G., Blankinship,M.J., Meuse,L., Chamberlain,J.S., & Hauschka,S.D. (2007) Design of tissue-specific regulatory cassettes for high-level rAAV-mediated expression in skeletal and cardiac muscle. *Mol. Ther.*, **15,** 320-329.

[365] Dunant,P., Larochelle,N., Thirion,C., Stucka,R., Ursu,D., Petrof,B.J., Wolf,E., & Lochmuller,H. (2003) Expression of dystrophin driven by the 1.35-kb MCK promoter ameliorates muscular dystrophy in fast, but not in slow muscles of transgenic mdx mice. *Mol. Ther.*, **8,** 80-89.

[366] Stevenson,S.C., Marshall-Neff,J., Teng,B., Lee,C.B., Roy,S., & McClelland,A. (1995) Phenotypic correction of hypercholesterolemia in apoE-deficient mice by adenovirus-mediated in vivo gene transfer. *Arterioscler. Thromb. Vasc. Biol.*, **15,** 479-484.

[367] Grimm,D. & Kay,M.A. (2003) From virus evolution to vector revolution: use of naturally occurring serotypes of adeno-associated virus (AAV) as novel vectors for human gene therapy. *Curr. Gene Ther.*, **3,** 281-304.

[368] Herzog,R.W., Hagstrom,J.N., Kung,S.H., Tai,S.J., Wilson,J.M., Fisher,K.J., & High,K.A. (1997) Stable gene transfer and expression of human blood coagulation factor IX after intramuscular injection of recombinant adeno-associated virus. *Proc. Natl. Acad. Sci. U. S. A*, **94,** 5804-5809.

[369] Cooper,A.D. (1997) Hepatic uptake of chylomicron remnants. *J. Lipid Res.*, **38,** 2173-2192.

[370] Crawford,S.E. & Borensztajn,J. (1999) Plasma clearance and liver uptake of chylomicron remnants generated by hepatic lipase lipolysis: evidence for a lactoferrin-sensitive and apolipoprotein E-independent pathway. *J. Lipid Res.*, **40,** 797-805.

[371] Fu,T., Kozarsky,K.F., & Borensztajn,J. (2003) Overexpression of SR-BI by adenoviral vector reverses the fibrateinduced hypercholesterolemia of apolipoprotein E-deficient mice. *J. Biol. Chem.*, **278,** 52559-52563.

[372] Zhang,S.H., Reddick,R.L., Piedrahita,J.A., & Maeda,N. (1992) Spontaneous hypercholesterolemia and arterial lesions in mice lacking apolipoprotein E. *Science*, **258,** 468-471.

[373] Fu,T., Kashireddy,P., & Borensztajn,J. (2003) The peroxisome-proliferator-activated receptor alpha agonist ciprofibrate severely aggravates hypercholesterolaemia and accelerates the development of atherosclerosis in mice lacking apolipoprotein E. *Biochem. J.*, **373,** 941-947.

[374] Raffai,R.L., Hasty,A.H., Wang,Y., Mettler,S.E., Sanan,D.A., Linton,M.F., Fazio,S., & Weisgraber,K.H. (2003) Hepatocyte-derived ApoE is more effective than non-hepatocyte-derived ApoE in remnant lipoprotein clearance. *J. Biol. Chem.*, **278,** 11670-11675.

[375] Burke,A.P., Kolodgie,F.D., Farb,A., Weber,D.K., Malcom,G.T., Smialek,J., & Virmani,R. (2001) Healed plaque ruptures and sudden coronary death: evidence that subclinical rupture has a role in plaque progression. *Circulation*, **103,** 934-940.

[376] Virmani,R., Kolodgie,F.D., Burke,A.P., Farb,A., & Schwartz,S.M. (2000) Lessons from sudden coronary death: a comprehensive morphological classification scheme for atherosclerotic lesions. *Arterioscler. Thromb. Vasc. Biol.*, **20,** 1262-1275.

[377] Morral,N., Parks,R.J., Zhou,H., Langston,C., Schiedner,G., Quinones,J., Graham,F.L., Kochanek,S., & Beaudet,A.L. (1998) High doses of a helper-dependent adenoviral vector yield supraphysiological levels of alpha1-antitrypsin with negligible toxicity. *Hum. Gene Ther.*, **9**, 2709-2716.

[378] Song,S., Morgan,M., Ellis,T., Poirier,A., Chesnut,K., Wang,J., Brantly,M., Muzyczka,N., Byrne,B.J., Atkinson,M., & Flotte,T.R. (1998) Sustained secretion of human alpha-1-antitrypsin from murine muscle transduced with adeno-associated virus vectors. *Proc. Natl. Acad. Sci. U. S. A*, **95**, 14384-14388.

[379] Herzog,R.W., Fields,P.A., Arruda,V.R., Brubaker,J.O., Armstrong,E., McClintock,D., Bellinger,D.A., Couto,L.B., Nichols,T.C., & High,K.A. (2002) Influence of vector dose on factor IX-specific T and B cell responses in muscle-directed gene therapy. *Hum. Gene Ther.*, **13**, 1281-1291.

[380] Arruda,V.R., Schuettrumpf,J., Herzog,R.W., Nichols,T.C., Robinson,N., Lotfi,Y., Mingozzi,F., Xiao,W., Couto,L.B., & High,K.A. (2004) Safety and efficacy of factor IX gene transfer to skeletal muscle in murine and canine hemophilia B models by adeno-associated viral vector serotype 1. *Blood*, **103**, 85-92.

[381] Mingozzi,F., Maus,M.V., Hui,D.J., Sabatino,D.E., Murphy,S.L., Rasko,J.E., Ragni,M.V., Manno,C.S., Sommer,J., Jiang,H., Pierce,G.F., Ertl,H.C., & High,K.A. (2007) CD8(+) T-cell responses to adeno-associated virus capsid in humans. *Nat. Med.*, **13**, 419-422.